

Bangor University

DOCTOR OF PHILOSOPHY

Methanogenic ether lipids in acoustically turbid and gas-free marine sediments

Smith, Geoff C.

Award date:
1997

Awarding institution:
University of Wales, Bangor

[Link to publication](#)

General rights

Copyright and moral rights for the publications made accessible in the public portal are retained by the authors and/or other copyright owners and it is a condition of accessing publications that users recognise and abide by the legal requirements associated with these rights.

- Users may download and print one copy of any publication from the public portal for the purpose of private study or research.
- You may not further distribute the material or use it for any profit-making activity or commercial gain
- You may freely distribute the URL identifying the publication in the public portal ?

Take down policy

If you believe that this document breaches copyright please contact us providing details, and we will remove access to the work immediately and investigate your claim.

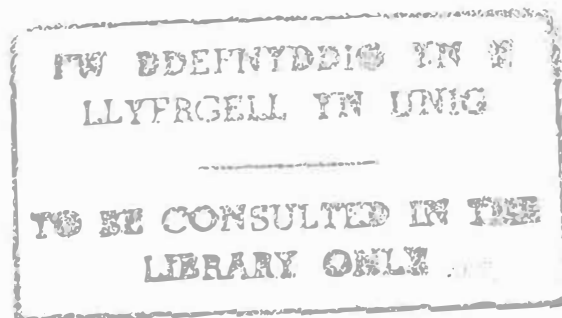
Methanogenic Ether Lipids in Acoustically Turbid and Gas-Free Marine Sediments.

A thesis submitted to the University of Wales

by

Geoff C. Smith

In candidature for the degree of Doctor of Philosophy.



University College of Wales, Bangor
School of Ocean Sciences
Menai Bridge
Anglesey
Gwynedd
North Wales



March 1997

ACKNOWLEDGMENTS

I wish to extend my thanks to my supervisor Dr G.D. Floodgate for his advise and correction of the manuscript. I am also extremely grateful to Dr P. Intriago for his unrelenting help with various microbiological techniques and also for his continual encouragement over the beginning of my research period. I would also like to thank Dr S. Mudge for his useful comments and manuscript corrections who together with Mr J. East provided much of the mass spectral analyses. I would also like to thank Mr J. Rowlands, Mrs V. Ellis and Mr J. East for their expertise and technical assistance, and also the crew of the R.V. Prince Madog for the sampling of Holyhead Harbour, and Dr D. Watson for help during the intertidal sampling. To Miss F. Couper I owe many thanks for her support and understanding over this period.

The Chemistry Dept. (UCNW) and the SERC Mass Spectral Dept. (Swansea) also provided some of the mass spectral information. The methanogenic monocultures were supplied by Dr M. Blaut (Gottingen, Germany), Dr K. Sowers (UCLA, USA). Lipid standards and also invaluable comments with respect to their quantification were supplied by Dr M. Kates, Dr E.S. Van Vleet, Dr M. Nishihara and Dr A. Gambacorta. Mr J. Cave (Holyhead Historian) and Mr D. Roberts (Anglesey Aluminium Ltd) provided invaluable information on the Holyhead area. I extend my sincere thanks to all.

This work was supported by the Science and Engineering Research Council (SERC) (grant no. GR/E/9746.3) and was also a case studentship award with ESSO Petroleum Company (Leatherhead).

ABSTRACT

The generation of methane in marine sediments by methanogenic bacteria has been shown, in certain areas, to form undissolved gas voids and to provide a characteristic geoaoustic signature known as acoustic turbidity. The ether linked membrane lipids in the marine sediments of Holyhead Harbour and an intertidal site, are expected to primarily reflect methanogenic bacteria. The concentration of ether lipids was shown to be a good criterion for the determination of methanogenic biomass in pure cultures, since it correlated well with other biomass determinants, including the cell dry weight of the organism. Alkane derivatives of the larger diether and acyclic and cyclic tetraethers gave the best reproducibility over the long analytical procedure. The preparation of a halogenated derivative of the diether offers an improved sensitivity by electron capture detection. An uncharacterised ether lipid derivative was shown to be an isomer of a three-cyclopentyl ring tetraether derivative. It is hypothesised that the high concentration of cyclic ether lipids in the sediments are formed by known methanogenic bacteria as a result of changing conditions in the sediment and are expected to occur soon after deposition. The concentration of methane below the sulphate reduction zone (SRZ) in Holyhead Harbour was shown to increase significantly and was calculated to exceed the solubility limit of the pore water and form gas voids, which was also corroborated by sound velocity and X-ray measurements. Modelling of the methane distributions suggested that a methane removal term was necessary which may reflect anaerobic methane oxidation in the SRZ of the Holyhead sediments. Conversion factors of methane produced per ether lipid synthesised were calculated from pure cultures. Application of these conversion factors to the ether lipid data in the sediments of this study and an artificially prepared core revealed some interesting results. The concentration of ether lipids in the surface sediments was comparable to the deeper sediments, which was in contrast to the counts of viable methanogens and the methane concentration. Also, contrary to the literature the ether lipids did not show a consistent increase below the SRZ. Due to the limited ether lipid data for near-shore marine sediments it is not known whether these results are typical or just reflect a variable depositional input to the sediments of Holyhead Harbour.

CONTENTS

CHAPTER 1. INTRODUCTION AND LITERATURE REVIEW.

Introduction	1
Literature Review	2
1.1. Methane in the Environment	2
1.2. Shallow Gas in Marine Sediments	2
1.3. Thermogenic Origin of Methane in Marine Sediments	5
1.4. Biogenic Origin of Methane	6
1.5. Biogenic Methane Produced in Marine Sediments	7
1.6. Methods of Quantifying Methanogenic Biomass	9
1.6.1. Most Probable Number Technique	9
1.6.2. Immunoassay	11
1.6.3. Coenzymes	11
1.6.4. Isopranyl Ether Lipids	12
1.6.4.1. Ether Lipids in Methanogens	14
1.6.4.2. Ether Lipids in the Environment	18
1.6.4.3. Sources of Methanogens and Ether Lipids to the Sediments	19
• From Deeper Sediment Horizons	19
• Water Column Input: Zooplankton and Faecal Waste	20
• Water Column Input: River Run-off	21
• Water Column Input: Sewage	22

CHAPTER 2. MATERIALS AND METHODS.

2.1. Anaerobic Culture Preparation	23
2.1.1. Anaerobic Cabinet	23
2.1.2. Media Preparation	23
2.1.3. Isolation of Methanogenic Bacteria	25
2.2. Growth Culture Experiments	26
2.2.1. Culturing of Methanogens	26
• <i>Methanosarcina acetivorans</i>	27
• <i>Methanococcoides methylutens</i>	27
• <i>Methanlobus tindarius</i>	27
2.2.2. Turbidity Measurements	27
2.2.3. Bacterial Direct Counts	28
2.2.4. Ether Lipid Degradation Experiment	28
2.3. Sediment Sampling	29
2.3.1. Coring of Holyhead Harbour Sediments	29

2.3.2. Coring of Intertidal Sediment	30
2.3.3. Bathymetry Surveys of Holyhead Harbour	30
2.4. Methane Sampling	31
2.4.1. From Sediment Cores	31
2.4.2. From Growth Culture Tubes	31
2.4.3. Methane Analysis	31
2.4.4. Packing of a Wide Bore Column	31
2.4.5. Methane Calibration	32
2.5. Most Probable Number (MPN) Determination	32
2.6. Water Content Determination	33
2.7. Measurement of the Sound Velocity Across the Sediment Core Sections	34
2.7.1. Sound Velocities Measured Across Holyhead Core Sections	34
2.8. X-ray Analysis of Core Sections	34
2.9. Preparation of an Artificially Consolidated Acoustically Turbid Sediment Core	34
2.10. Sediment Pore Water Extraction	36
2.11. Determination of Sulphate in Sediment Pore Waters	36
2.12. Determination of Sulphide in Sediment Pore Water	37
2.13. Ether Lipid Determination	37
2.13.1. Lipid Extraction: Sediment Samples	37
2.13.2. Lipid Extraction: Cultured Methanogens	40
2.13.3. Acid Methanolysis of Polar lipids	40
2.13.4. Silicic Acid Column Purification of Glycerol Diether and Tetraether Derivatives	41
2.13.5. Dihydrophytol Determination	42
2.13.6. Cleavage and Substitution of Ether Lipids	42
• Using Hydriodic Acid	42
• Using Boron Trichloride	42
2.13.7. Reduction of Iodo- Group to Alkanes Using Lithium Aluminium Hydride	43
2.13.8. Substitution of the Halogenated derivative for an Acetate Ester Functional Group	44
2.13.9. Purification of the Alkyl Acetates	44
2.13.10. Preparation of the Phytanyl Acetate Standard	44
2.13.11. Preparation of the Penta-Fluoro Propionyl Derivative for Analysis by GC/ECD	44
2.14. Gas Chromatography	45
2.15. Phospholipid Phosphate Determination	46
2.16. Infra-Red Spectrophotometry	47
2.17. Mass Spectrometry	47

CHAPTER 3. QUANTIFICATION OF THE METHANOGENIC ETHER LIPIDS.

3.1. Introduction	49
3.2. Reproducibility of Ether Lipid Extraction from Sediments	52
3.2.1. Selection of an Internal Standard	52
3.3. Characterisation and Quantification of Ether Lipids	53
3.3.1. Infra-Red Determination of Intact Glycerol Ethers	53
3.3.2. Quantitative Determination of Ether Lipid Derivatives by GC/FID	55
3.3.2.1. Analysis of Alkyl-Halogen Derivatives	55
3.3.2.2. Analysis of Acetate Derivatives	60
3.3.2.3. Analysis of Alkane Derivatives	63
3.3.3. Alkane Derivatives Isolated from Marine Sediments	71
3.3.3.1. Mass Spectral Analysis of Uncharacterised Ether Lipid Derivative	71
3.4. Production of a Derivative for Electron Capture Detection (GC/ECD)	75
3.4.1. Introduction	75
3.4.2. Production of ECD Sensitive Derivatives	75
3.4.2.1. Penta-Fluoro Propionyl Derivatives	76
3.5. Summary	78

CHAPTER 4. COMPARISON OF ETHER LIPID CONCENTRATIONS WITH METHANOGENIC BIOMASS AND METHANE PRODUCTION IN AXENIC CULTURE EXPERIMENTS, AND ETHER LIPID DEGRADATION STUDIES.

4.1. Introduction	79
RESULTS AND DISCUSSION	
4.2. Results of Growth Experiment Using <i>Methanosarcina acetivorans</i>	83
4.2.1. Comparison of the DPGE Lipid Concentration with the Biomass Related Parameters for <i>Methanosarcina acetivorans</i>	83
4.2.2. DPGE Lipid-Methane Ratios for <i>Methanosarcina acetivorans</i>	89
4.3. Results of Growth Experiment Using <i>Methanococcoides methylutens</i>	90
4.3.1. Comparison of the DPGE Lipid Concentration With the Biomass Related Parameters for <i>Methanococcoides methylutens</i>	90
4.3.2. Methane - DPGE Lipid Ratios for <i>Methanococcoides methylutens</i>	90
4.4. Results of Growth Experiment Using <i>Methanobrevibacter smithii</i>	91
4.5. Mean Ratios of Methane Produced per Ether Lipid Synthesised	93
4.6. Ether Lipid Degradation Experiment	94
4.7. Summary	96

CHAPTER 5. ANALYSIS OF THE FACTORS ASSOCIATED WITH THE BIOLOGICAL PRODUCTION, DISTRIBUTION AND FATE OF METHANE IN ACOUSTICALLY TURBID AND GAS-FREE MARINE SEDIMENTS.

5.1. Introduction.	98
5.2. Description of the Study Areas	99
5.2.1. Holyhead Harbour	99
5.2.2. Intertidal Area	99
5.3. Bathymetry of Holyhead Harbour and Sedimentation Rate	101
5.4. Distribution of Sulphate and Methane with Depth in the Sediment Cores	105
5.4.1. Holyhead Harbour	106
5.4.2. Intertidal Site	111
5.5. Evidence and Extent of Acoustic Turbidity in the Holyhead Cores	113
5.5.1. Acoustic Turbidity - Sound Velocity	114
5.5.2. Acoustic Turbidity - Calculated Volume of Undissolved Methane in the Sediment	114
5.5.2.1. Correlation of Undissolved Methane and Sound Velocity Measurements	116
5.5.3. Acoustic Turbidity - X-ray Analysis	119
5.6. Physical Factors Influencing Methane Distributions in the SRZ of the Holyhead Cores	125
5.6.1. Determination of the Sediment Porosity and Diffusion Coefficients	125
5.6.2. Which Model Best Describes the Methane Profiles of Holyhead Harbour	127
5.7. Ether Lipid - Methane Comparisons	136
5.7.1. Ether Lipid/Methane Comparisons - Holyhead Harbour	136
5.7.2. Ether Lipid/Methane Comparisons - Intertidal	138
5.8. MPN - Methane Comparisons	139
5.8.1. MPN/Methane Comparisons - Holyhead Harbour	139
5.8.2. MPN/Methane Comparisons - Intertidal	141
5.9. Ether Lipid - MPN Comparison	142
5.9.1. Estimated Proportion of Ether Lipids in the Sediment that can be Accounted for by the Viable Methanogens Determined by the MPN Technique	142
5.9.2. Comparison of Ether Lipid with Phospholipid Phosphate Concentration	147
5.10. Estimated Total Methane Produced from Concentrations of Ether Lipid Present	151
5.11. Observation of Trends in the Isopranyl Ether Lipids	154
5.11.1. Trends in the Concentration of the Ether Lipids with Depth	154
5.11.2. Changes in the Proportions of Ether Lipids	

with Increasing Sediment Depth	155
5.11.3. Significant Proportions of Cyclic Tetraether Lipids	156
5.11.4. Correlation of Ether Lipid Species	159
5.12. The Ether Lipid Concentration Anomaly; A Possible Explanation	160
5.13. Conclusions	166
CHAPTER 6. ARTIFICIALLY PREPARED CONSOLIDATED SEDIMENTS USING METHANOGENIC BACTERIA TO CREATE ACOUSTIC TURBIDITY	
6.1. Introduction	169
6.2. Results and Discussion	172
6.2.1. Sediment Parameters Determined During the Consolidation Experiment	172
6.2.2. Sediment Parameters Determined at the End of the Consolidation Experiment	176
6.3 Summary	182
CHAPTER 7. CONCLUSIONS AND SUGGESTIONS FOR FURTHER RESEARCH	184
REFERENCES	189
APPENDICIES	
Appendix I Methanogenic Media	211
Appendix II Peak Area <i>versus</i> Peak Height	214
Appendix III Statistical Equations	215
Appendix IV Sound Velocity Output	216
Appendix V Phosphate, Sulphate and Sulphide Calibrations	217
Appendix VI Raw Ether Lipid Data	220
Appendix VII Ether Lipid Calculation	247
Appendix VIII Summary of Ether Lipid Data	251
Appendix IX Smith & Floodgate (1992) Publication	254
Appendix X Bathymetry Surveys	264
Appendix XI Holyhead Harbour Raw Sediment Data	267

CHAPTER 1. INTRODUCTION AND LITERATURE REVIEW.

INTRODUCTION

Methane in the environment is important for a number of reasons. It is, for example, a greenhouse gas, an important by-product of waste disposal and is produced in the digestive system of ruminants. Methane is generated either thermogenically deep within the earth's crust or biogenically as a direct product from all energy producing reactions in methanogenic bacteria. In a marine context methane is of interest to bacteriologists, geochemists, geophysicists, geologists, geotechnical engineers and marine chemists and biologists, and has been the subject of three international symposia; the proceedings of the first have been published (Davis, 1992).

The object of the research reported in this thesis was to explore the relationship between the methanogenic bacteria, using specific biomass related measurements, and the methane content of marine sediments, especially in areas showing acoustic turbidity. Section 1.6 reviews the various biological, biochemical and chemical methods that have been employed in methanogen biomass studies. In this work greatest attention was paid to using and developing the chemical method because (a) it seemed to be most likely to give precise and accurate results and (b) to provide the most appropriate training for the author.

The work comprised of four sections. The first, dealt with in chapter 3, was the development of a chemical method that could be used to detect and quantify the membrane lipids that are unique to methanogens. The second section (chapter 4) compared the concentrations of the membrane lipids with other biomass related parameters in controlled growth experiments of three species of methanogenic bacteria. The third section (chapter 5) was concerned with field studies in acoustically turbid (Holyhead Harbour) and gas-free marine sediments. The final section (chapter 6) involved using methanogenic bacteria to recreate acoustic turbidity in artificially consolidated sediments in a consolidation apparatus.

Many of the materials and methods used are common to all sections. It was therefore decided to place all of them, together with some comments, in chapter 2 to avoid repetition. Each subsequent chapter therefore briefly refers back to chapter 2.

Each chapter carries its own results and discussion section and a summary of the conclusions made, and the final conclusions and suggestions for further research are given in chapter 7.

1. LITERATURE REVIEW

1.1. Methane in the Environment

The process of biological methane formation is of considerable current interest since methane emitted to the atmosphere may affect the earth's climate (Burke & Sackett, 1986). The concentration of atmospheric methane has been calculated to be increasing by approximately 1 % per year (Blake *et al.*, 1982; Rasmussen & Khalil, 1984). The methane molecule, which absorbs radiation between 700 and 1400 cm^{-1} , is a "greenhouse gas" and as such is directly related to global warming. The contribution of methane has been calculated to be approximately 20-40 % of the effect attributed to atmospheric carbon dioxide (Craig & Chou, 1982; Lacis *et al.*, 1981).

More than 80 % of the earth's annual output of atmospheric methane is produced biologically in anaerobic environments by bacteria. Most of the methane originates from the enteric fermentations of animals, paddy fields, swamps and marshes (Archer & Harris, 1986). Biogenic and thermogenic deposits of methane hydrates have been observed in marine sediments, usually below sea water depths of 300 m (Rice & Claypool, 1981). Hydrates in sediments or seawater that are close to the critical temperature and pressure stability threshold could provide a positive feedback loop for increased global warming if sea water temperatures rose significantly (Cranston, 1992).

However, not all the effects of biologically produced methane are detrimental to mankind. The biogenesis of methane under controlled conditions in anaerobic sewage sludge digesters has the potential to become a significant source of renewable energy. The synthesis of diesel oil from methane (Stat-Oil Newsletter, 1989) only acts to emphasise the future benefits of biogenic methane.

1.2. Shallow Gas in Marine Sediments

Methane is the only gas that is found in considerable quantity in marine sediments. When it is in an undissolved state and present at depths of less than 1000 m into the seabed it is commonly referred to as "shallow gas". Shallow gas is acknowledged to have a significant effect on the engineering and acoustic behavior of the sediments, because it causes an increase in the compressibility of the sediment, a reduction in the undrained shear strength, and also reduces the sound wave velocity (Sills & Wheeler, 1992). A general overview of the various effects of undissolved gas on the geotechnical behaviour of fine-grained sediments is given in Sills *et al.* (1991). For these reasons, shallow gas poses a potential hazard for the offshore construction and development industry (Hovland & Judd, 1988). Blowouts during drilling operations have recently been attributed to shallow gas (Judd, 1991; Stat-Oil Newsletter,

1989). In extreme cases shallow gas could cause the collapse of an offshore structure due to undermining of the foundation (Wheeler *et al.*, 1991).

Shallow gas has been detected in many continental shelf, slope and abyssal regions of the world (Hovland & Judd, 1988). Shallow gas was first encountered in 1865 in the Kattegat region of Denmark and has since been exploited as an energy supply for the local community (Jørgensen *et al.*, 1990). The areas of gassy sediment generally range from 150 to 2500 m in horizontal extent and the distance from the tops of the gassy sediment to the sea floor can vary from zero to the nominal 1000 m, with an average distance of less than 100 m (Anderson & Bryant, 1990; Hovland & Judd, 1988).

The presence of shallow gas can be determined remotely from geophysical surveys of the buried sediment horizons, and also from features on the surface of the seabed which are associated with shallow gas. Direct observational evidence as well as geochemical analysis of retrieved core samples can also provide useful information.

Geophysical surveys of the buried sediment horizons are usually carried out by high resolution seismic profiling, and certain anomalies found in the profiling record are interpreted as indicators for shallow gas. Buried undissolved gas significantly reduces the velocity of sound waves passing through the sediment, and can also cause the incident sound to be scattered (Hovland & Judd, 1988; Anderson & Bryant, 1990). The result is a loss of the acoustic signal from underlying reflectors and a "turbid" appearance on the record. The sediments are then said to be "acoustically turbid." Seismic profiling can also detect columnar disturbances such as chimneys or mud diapirs. These are formed due to the upward migration of pore fluids which disturb the normal layering of the sediment (Hovland & Judd, 1988). Gas charged sediments detected by acoustic methods often form a sharp boundary with the surrounding material. Such enhanced reflections that are observed on a seismic profile signify a "gas front" which usually occurs where migrating gas is trapped by an overlying relatively impermeable sediment.

Plumes of escaping methane rising up from the seabed are another indicator of shallow gas. These methane seeps have been observed above marine sediments containing shallow gas by the use of remotely operated vehicles and divers, and also from echo-sounders, side-scan sonar and high resolution seismic records (Judd & Hovland, 1992).

Pockmarks, which can also be identified by geophysical techniques or visual observations, are commonly observed in areas of shallow gas and are seabed depressions caused by the removal of sediment due to escaping gas. Pockmarks in the northern North Sea are believed to have been formed by rapid expulsion of gas and liquid through the seabed, displacing fine-grained

sediment and forming characteristic craters (Hovland & Judd, 1988). This rapid expulsion theory has been endorsed by Dando *et al.*, (1991) because of the numerous fish otoliths found within such craters, which implied that substantial winnowing of the sediment had taken place. Pockmarks vary in size according to the nature of the seabed sediment and are generally between a few metres and a few hundred metres in diameter, and from less than one metre to twenty metres deep (Judd & Hovland, 1992).

Seabed domes are thought to be formed by gas displacing water in the pore spaces of the upper sediments causing a local volume increase. Domes have been found to range from 1-2 m high with diameters of over 100 m. It is also suspected that seabed domes may be an initial stage of pockmark formation (Hovland & Judd, 1988; Judd & Hovland, 1992). Mud diapirs, which can be detected below the sediment surface in geophysical surveys, can also penetrate the seabed surface, and in areas such as the Adriatic Sea, Caspian Sea and Arabian Gulf have been observed to be actively venting (Judd & Hovland, 1992).

Carbonate precipitates are also features that are sometimes found on the surface of the seabed above areas of shallow gas (Hovland *et al.*, 1987). Early diagenetic carbonates can be formed via two processes. Firstly, when carbon dioxide is removed from the dissolved bicarbonate reservoir of the pore waters by reduction and formation of methane, the pH can rise, therefore causing the precipitation of authigenic carbonates in the anoxic sediment. The second, and most dominant mechanism for carbonate precipitation, is by bacterial methane oxidation which indirectly forms bicarbonate, which is then available for precipitation to form a carbonate cement (Rice & Claypool, 1981). Carbonate precipitates have been observed to cement the normal seabed sediments together to form a hard rock-like material (Jørgensen 1976; 1992), and can also form chimney-like structures (Kulm & Suess, 1990). This phenomenon is known from a large number of gas seepages in shallow seas, and also from many localities of venting pore fluid in the deep oceans (Hovland & Judd, 1988).

Dando *et al.*, (1991) observed greater densities than expected of fauna within some pockmarks. They found that the carbon associated with methane seeping from the pockmark does not contribute to the carbon of the surrounding animals on a significant scale, and concluded that the increase was partly due to the carbonate structures providing a hard substrate habitat, in an area of predominantly soft sediments. Such a habitat would encourage colonisation by anthozoans and bryozoans. Furthermore, resuspension of the bottom sediments by escaping gas was thought to provide additional food for filter feeders (Dando *et al.*, 1991).

1.3. Thermogenic Origin of Methane in Marine Sediments

Shallow gas can comprise of methane of either biogenic or thermogenic origin, and an increasing number of natural gas occurrences have been shown to consist of mixtures of both types of gas (MacDonald, 1983). Thermogenic hydrocarbons are generated from organic matter disseminated in fine-grained sedimentary rocks by a series of complex chemical reactions at depths greater than 1000 m. The quantity and molecular size of hydrocarbons generated are influenced by the concentration and type of organic matter preserved in the source rock, and also by the stage of thermochemical alteration (Rice & Claypool, 1981). Upward migration of thermogenic gas can accumulate at shallow depths beneath the sea floor which can then mix with the shallower biogenic sources. Pure biogenic or thermogenic gas can be differentiated using analytical experimental techniques.

Thermogenic hydrocarbon gases contain predominantly methane as well as significant amounts of higher order gases such as ethane, propane, butane and pentane. Biogenically produced gas however contains only trace amounts of the higher order alkanes *i.e.* <0.05 % (Oremland 1988; Rice & Claypool, 1981; Davis & Squires, 1954). The isotopic signature of the carbon atom can also differentiate thermogenic from biogenic sources of gas. Biogenic gas is typically more enriched in the ^{12}C carbon isotope and therefore values of $\delta^{13}\text{C}$ range from -60 to -80 ppt (relative to the Peedee Belemnite (PDB) standard reference). A full description of the determination and significance of isotopic signatures is given in MacDonald (1983). The variation in the isotopic composition of biogenic methane is controlled by the $\delta^{13}\text{C}$ of the original carbon substrate (Rice & Claypool, 1981; Jørgensen *et al.*, 1990). Gas of thermogenic origin is more enriched in the ^{13}C carbon isotope than the ^{12}C isotope when compared to biogenic gases, and therefore has $\delta^{13}\text{C}$ values ranging from -25 to -40 ppt PDB (Rice & Claypool, 1981). Biogenic and thermogenic sources can also be differentiated by the hydrogen ($\delta^2\text{H}_{\text{CH}_4}$) and carbon ($\delta^{13}\text{C}_{\text{CH}_4}$) isotopic compositions (Whiticar *et al.*, 1986; Jørgensen *et al.*, 1990).

Shallow gas can often comprise of a mixture of both isotopically heavy thermogenic gas and isotopically light biogenic gas. Also subsequent chemical or biological oxidation of the methane gas can also confuse such signatures since isotopically light molecules will be oxidised more readily and will cause the proportion of isotopically heavy methane remaining to increase. These processes can cause difficulties when trying to identify the source of the gas (Hovland & Judd, 1988). These complicating factors therefore require that geological, chemical and isotopic evidence be considered together when attempting to interpret the origin of gas accumulations (Rice & Claypool, 1981).

1.4. Biogenic Origin of Methane.

This thesis is concerned with a diverse group of bacteria that are able to generate methane, and are known as methanogens. These together with certain thermoacidophilic and halophilic bacteria (Brock & Madigan, 1991) constitute a separate kingdom of bacteria known as the archaeobacteria; a distinction that depends on the possession of a number of unusual biochemical features that clearly differentiate the archaeobacteria from all known prokaryotic and eukaryotic life (Balch *et al.*, 1979). As the name would suggest the archaeobacteria are thought to have diverged from the other lines of descent at least by the time when the prokaryotic and eukaryotic groups became phylogenetically distinct kingdoms. This distinction has led to the renaming of the traditional prokaryotic kingdom into the eubacterial and archaeobacterial primary kingdoms.

Methanogens include mesophilic and thermophilic bacteria that exhibit extreme habitat diversity. The term mesophilic has been used to describe methanogens that inhabit environments which have a low temperature range (*i.e.* 3 - 40 °C). The term mesophilic has also been used to describe these types of habitats. Species of methanogens have been isolated from virtually every habitat in which the anaerobic biodegradation of organic compounds occurs. Such environments have a low redox potential and include; the guts of ruminant animals and termites (Smith & Hungate, 1958), some human guts (König & Stetter, 1989), paddy fields (Holzapfel-Pschorn & Seiler, 1986), swamps (Archer & Harris, 1986), marshes (Jones & Paynter, 1980), sewage digesters (Henson *et al.*, 1985), landfill sites (Rice & Claypool, 1981), and sediments from marine (Sowers *et al.*, 1984), freshwater (Pedersen & Sayler, 1980; Harris *et al.*, 1984), estuarine (Jones & Paynter, 1980), saltmarsh (Senior *et al.*, 1982), hydrothermal vents (Kurr *et al.*, 1991) and hot springs (Stetter *et al.*, 1982). Other sites have included methanogens as endosymbionts in marine ciliates (Bruggen *et al.*, 1986) and in faecal pellets (Sieburth *et al.*, 1993) and zooplankton (Bianchi *et al.*, 1992; Oremland, 1979) in the seawater. Hence any bioindicator technique must be flexible enough to function in a wide range of circumstances.

Methanogenic bacteria can utilize only a limited range of substrates for growth and methanogenesis (Smith *et al.*, 1980). These substrates are frequently products of previous oxidation reactions and have relatively little free energy available for ATP formation compared to other fermentation reactions which occur at much higher redox potentials. Therefore the methanogens are the terminal trophic group of organisms in the process of biological organic matter breakdown. The energy yields for the substrates typically available to methanogens are given in table 1.1. Typically about 90 % of the carbon dioxide utilized by methanogenic bacteria is reduced with hydrogen to methane, with accompanied ATP synthesis, and only 10 % is reduced to cell carbon (Fuchs & Stupperich, 1984).

Table 1.1. Energy yields for major methanogenic substrates (Oremland, 1988; Kirsop, 1984).

Reaction	ΔG (KJ mol ⁻¹ CH ₄)
Substrates out-competed by SRB:	
$4\text{H}_2 + \text{H}^+ + \text{HCO}_3^- \rightarrow \text{CH}_4 + 3\text{H}_2\text{O}$	-136
$\text{CH}_3\text{COO}^- + \text{H}_2\text{O} \rightarrow \text{CH}_4 + \text{HCO}_3^-$	-31
$\text{HCOO}^- + \text{H}^+ + 3\text{H}_2 \rightarrow \text{CH}_4 + 2\text{H}_2\text{O}$	-134
$\text{CH}_3\text{OH} + \text{H}_2 \rightarrow \text{CH}_4 + \text{H}_2\text{O}$	-113
Substrates not out-competed by SRB:	
$4\text{CH}_3\text{OH} \rightarrow 3\text{CH}_4 + \text{CO}_2 + 2\text{H}_2\text{O}$	-103
$4\text{CH}_3\overset{+}{\text{N}}\text{H}_3 + 2\text{H}_2\text{O} + 4\text{H}^+ \rightarrow 3\text{CH}_4 + \text{CO}_2 + 4\text{NH}_4^+$	-75
$2(\text{CH}_3)_2\overset{+}{\text{N}}\text{H}_2 + 2\text{H}_2\text{O} + 4\text{H}^+ \rightarrow 3\text{CH}_4 + \text{CO}_2 + 4\text{NH}_4^+$	-73
$4(\text{CH}_3)_3\overset{+}{\text{N}}\text{H} + 9\text{H}_2\text{O} \rightarrow 9\text{CH}_4 + 3\text{HCO}_3^- + 4\text{NH}_4^+ + 3\text{H}^+$	-74
$2(\text{CH}_3)_2\text{S} + 2\text{H}_2\text{O} \rightarrow 3\text{CH}_4 + \text{CO}_2 + 2\text{H}_2\text{S}$	-111

1.5. Biogenic Methane Produced in Marine Sediments

The various types of metabolism in marine sediment are, to some degree, stratified on the basis of competition rates for common substrates. Methanogenic bacteria and sulphate reducing bacteria play a key role in the consumption of metabolic products produced by organisms at preceding stages of the aerobic and anaerobic decomposition process.

In anoxic marine sediments the vertical profiles of methane and sulphate generally showing two distinct zonations. An upper zone in which methane concentrations are low and sulphate is rapidly depleted with increasing depth and a lower zone where sulphate has diminished to limiting concentrations for the SRB and methane concentrations increase rapidly with increasing depth (Ward & Winfrey, 1985).

Although the methanogenic bacteria and sulphate reducing bacteria have a similar role towards the mineralisation of organic matter, there is a dominance of sulphate reduction over methanogenesis when sulphate concentrations are high due to the competition for common substrates (*i.e.* electrons) (Oremland & Taylor, 1978). Sulphate reducing bacteria (SRB) can utilize hydrogen as an electron donor (Robinson & Tiedje, 1984) and acetate as a substrate (Schonheit *et al.*, 1982) at much lower concentrations (*i.e.* lower K_m values) than methanogens. The substrates given in the first four equations of table 1.1 will therefore be

metabolised by SRB and not methanogens when the sulphate concentration is not limited. The metabolism of substrates such as bicarbonate, acetate and formate by the SRB before the methanogens in sediments is part of the reason why the rates of sulphate reduction are several orders of magnitude greater than the rates of methanogenesis (Senior *et al.*, 1982).

However, there are substrates which methanogens can metabolise that are not out-competed for by the SRB when sulphate concentrations are high. It can be noted from bottom four equations of table 1.1 that methanogens can also metabolise methylamine, dimethylamine, trimethylamine, methanol and dimethyl sulphide. Other substrates such as methylmercaptan and dimethyl disulphide can also be metabolised but their contribution to methanogenesis in marine sediments is not expected to be significant (Oremland, 1988). Methanol can be metabolised by certain methanogens but for some species diatomic hydrogen is required which would therefore be out-competed for by SRB (König & Stetter, 1989). Dimethyl sulphide has also been found to be a methanogenic substrate that is not competed for by SRB (Kiene *et al.*, 1986).

Trimethylamine is produced from the decomposition of choline and glycine betaine. Choline is present in the membrane lipids of most organisms (Fiebig & Gottschalk, 1983), and glycine betaine is a common osmoregulator in bacteria, plants and animals (Yancey *et al.*, 1982). Both choline and glycine betaine can be fermented to trimethylamine and acetate, therefore providing substrates for both methanogens and SRB (King, 1984). Methylamines are also present in industrial waste from tanning and industrial food waste from decaying fish.

Methanogenesis has therefore been shown to exist within the SRZ of an intertidal sediment with trimethylamine accounting for 35 to 61 % of the total methanogenesis and methanol and monomethylamine accounting for less than 2.4 % (King *et al.*, 1983). Low rates of methanogenesis have also been detected in the SRZ from substrates that are competed for by the SRB (*i.e.* acetate, bicarbonate and formate) (Sansome & Martens, 1981; Winfrey *et al.*, 1981; Kosiur & Warford, 1979), and substrates that are not competed by the SRB (*i.e.* trimethylamine, other methylamines and methanol) (King *et al.*, 1983).

The rates of methane production within the deeper methanogenesis dominated zone have been reported to be significantly greater than in the SRZ via substrates such as acetate and bicarbonate by factors of ; 80 (Sansome & Martens, 1981), 140 (Winfrey *et al.*, 1981), and 2-8 (Kosiur & Warford, 1979). There is very little information on the rates of methanogenesis measured simultaneously from all substrates potentially available to methanogens over a marine profile encompassing sulphate and methane containing depths. However, from the information available the rate of methanogenesis is expected to show a significant increase across the sulphate - methane transition.

Another factor which contributes towards the distinct zonation of the methane and sulphate concentrations is the subsequent oxidation of methane produced within, and diffusing into, the SRZ. Elevated rates of anaerobic methane oxidation and sulphate reduction have been detected at the sulphate - methane transition of acoustically turbid marine sediments (Iversen & Jørgensen, 1985). This depth has also been shown to coincide with elevated concentrations of sulphide (Devol *et al.*, 1984), probably from the reaction given in equation 1 (Reeburgh, 1980; Martens & Berner, 1974).



EQUATION 1

The oxidation of methane has been detected at very low rates in axenic cultures of SRB (Davis & Yarborough, 1966), and has also been shown to occur simultaneously with methane production in laboratory experiments of methanogenic bacteria (Zehnder & Brock, 1980). However, the organism primarily responsible for methane oxidation in natural marine sediments has yet to be determined.

The information in the literature suggests that sulphate is the oxidising agent for methane oxidation though it is still not clear whether sulphate reduction is involved in the process (Iversen & Jørgensen, 1985; Alperin & Reeburgh, 1985). As well as the publications of radiotracer techniques to determine the presence of anaerobic methane oxidation some of the strongest evidence has originated from geochemical models of methane distributions in marine sediments (Devol *et al.*, 1984; Martens & Berner, 1977; Bernard, 1977). A methane consumption term has often been required to model the concave-up-wards methane profiles found in many marine sediments.

1.6. Methods of Quantifying Methanogenic Biomass

As stated on page 1 the object of this research was to relate the biomass of methanogens to the gas content of marine sediments. Early studies have not satisfactorily solved the problem of estimating methanogen biomass, although several different approaches have been made. The major methods reported in the literature are critically reviewed below.

1.6.1. Most Probable Number Technique

One of the most obvious indications of the presence of methanogenic bacteria in sediments is their ability to produce methane. Methane production is a process directly linked to energy generation in methanogens (Fuchs & Stupperich, 1984; Oremland, 1988). Active methanogenesis has been detected to 86 m (Parkes *et al.*, 1990) and to 167 m (Oremland, 1988). Methane synthesis is, however, not unique to methanogenic bacteria since some anaerobic eubacteria evolve small amounts of methane during their normal metabolism (Postgate, 1969). However this is not coupled to energy production and is not considered to be a major input of methane into the sedimentary system (Rudd & Taylor, 1980).

Because of the complexity of the marine environment, direct *in-vivo* quantification of methane present cannot be reliably taken as a measure of the methanogenic biomass. However, *in-vitro* culture under appropriate conditions can be adapted to provide a better indicator of the number of methanogenic organisms using the most probable (MPN) technique. The method involves serial dilution's of the sediment sample in a suitable liquid growth media to the point of extinction of the methanogenic bacteria. The point of extinction is realised by the lack of methane produced after dilution and upon incubation. From sample replication, dilution rates and statistical tables the number of methanogens can be calculated providing most of the species are stimulated, usually to well within an order of magnitude, depending on the dilution rates and replication (Rowe *et al.*, 1977).

Under estimation of the microbial population is, however, common using this method, which is an error encountered when the liquid growth media supplies the correct growth conditions for only a proportion of the bacterial population, so that only part of the population can grow (Jones, 1979). Information on the expected under estimates of the MPN technique for total viable population of methanogenic bacteria is not available in the literature. However, comparison of MPN counts with direct counts of other marine bacteria have shown that between 0.0001 and 10 % of the population are stimulated by the growth media (van Es & Meyer-Reil, 1982). Jørgensen (1978) calculated that for MPN determinations of SRB the true population density could be as much as three or more orders of magnitude under estimated. The confidence limits of the MPN method are therefore relatively wide and the statistical reliability is quite low. Notwithstanding these inherent shortcomings, the MPN method has been shown to provide an indication of the order of magnitude of viable bacteria in a particular sediment sample (Seyfried & Owen, 1978).

Typical numbers of methanogens have been determined at approximately 10^4 g^{-1} to 10^5 g^{-1} in saltmarsh sediments (Jones & Paynter, 1980), and for marine sediments at 10^5 g^{-1} to 10^6 g^{-1} (Jones & Paynter, 1980), up to $4 \times 10^3 \text{ g}^{-1}$ (Hines & Buck, 1982) and 10^4 per ml of sediment at a marine site receiving a significant input of raw sewage (Warford & Kosiur, 1979). The limited data for acoustically turbid sediments suggested maximum numbers of 4.3×10^3 per ml of sediment and showed few trends with increasing sediment depth (Peters, 1988). Although increases in the rate of methanogenesis have been observed at the base of the SRZ (Sansome & Martens, 1981; Winfrey *et al.*, 1981; Kosiur & Warford, 1979), an increase in the numbers of methanogens at the base of the SRZ has not been shown in near-shore sediments using MPN techniques (Hines & Buck, 1982). In contrast, increases in the numbers of methanogens have been found to coincide with an increase in methanogenic activity below a maximum in sulphate reduction in deep sea sediments (Parkes *et al.*, 1990).

1.6.2. Immunoassay

Woese (1981) using partial sequencing discovered that the 16S ribosomal RNA's of archaeobacteria were unique. Such features were instrumental in the formulation of the archaeobacterial kingdom since ribosomal RNA molecules appear to remain constant in function over great evolutionary periods. The use of monoclonal antibody probes has allowed precise quantification of individual species (Macario & Conway de Macario, 1985), to numbers as low as 4.6×10^6 and up to 6.8×10^{10} cells per gram (Ward & Frea, 1979). Interesting results taken from a study of a lake sediment compared fluorescent antibody probes, with a specificity for one species of methanogen, with MPN counts which contained media to potentially stimulate most of the methanogens present (Strayer & Tiedje, 1978). Results showed that the fluorescent antibody counts ranged from 3.1×10^6 to 1.4×10^7 per gram for one methanogen species whereas the highest MPN count of the total viable methanogens were at least an order of magnitude lower (Strayer & Tiedje, 1978). However, it should be noted that the fluorescent antibody technique will detect and count intact cells whether they are dead, dormant or viable.

1.6.3. Coenzymes

Methanogenic bacteria can be microscopically identified by their strong autofluorescence under oxidising conditions at ultra-violet wavelengths. The contributing components to this phenomenon are several unusual coenzymes that act as electron carriers and include coenzyme F420, F350, coenzyme M and some methanopterin derivatives (Moura *et al.*, 1983). Coenzyme F420, which shows the strongest fluorescence, is found in all methanogenic cells and has an absorption maximum at 420 nm with an associated emission fluorescence at 470 nm. It acts as a low potential electron carrier (Zeikus 1977) and has been shown to participate directly in the reduction of carbon dioxide to methane (Hartzell *et al.*, 1985).

Although tentative identification of methanogenic bacteria can be made using ultra violet microscopy, Doddema and Vogels (1978) found that fluorescence decreased with both the aging of cells and also by continued exposure to ultra-violet light. *Escherichia coli* and *Pseudomonas aeruginosa* have also been shown to weakly fluoresce at 420 nm, though the enzyme responsible is different in structure and no fluorescence is observed at 350 nm as with methanogens (Jones *et al.*, 1987). The F420 chromophore has recently been discovered in the light activated DNA repair enzyme of *Streptomyces griseus* which has led to the prediction that the biochemical involvement of coenzyme F420 is more widespread in nature than was previously suspected (Jones *et al.*, 1987). Although the microscopic enumeration of methanogenic bacteria using F420 would appear both difficult and not necessarily specific to the total methanogenic population in environmental samples, the fluorescence of coenzyme F420 has proved an important screening feature for new methanogenic isolates in addition to checking the purity of methanogenic monocultures (Edwards & McBride, 1974).

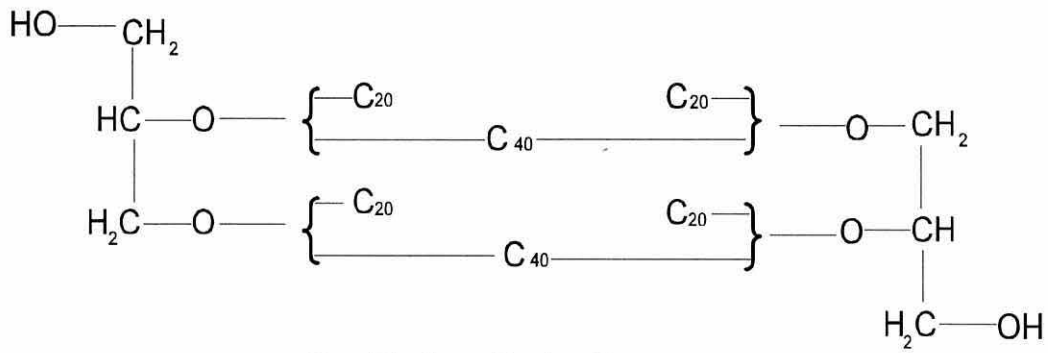
Attempts to quantitatively use concentrations of these unusual coenzymes as indicators of methanogenic biomass has been made, though not through microscopic means. Complicated extraction and chromatographic techniques performed under anaerobic conditions has led to the quantification of the amount of coenzyme F420 present in methanogenic cultures (Heine-Dobbernack *et al.*, 1988). Comparisons with cell protein, cell dry weight, optical density and specific methane production rates have shown that the intracellular F420 content approximately reflected the biomass of methanogenic bacteria in controlled growth experiments. However the influence of changing substrates, growth conditions, and methanogenic strains on the coenzyme F420 content was considerable (Heine-Dobbernack *et al.*, 1988).

1.6.4. Isopranyl Ether Lipids

Since the original definition of archaeobacteria by Woese (1977), a number of archaeobacterial traits have been catalogued. The structure of the membrane lipids are one such distinguishing feature. The structure of these molecules, and a range of isoprenoid derivatives found in archaeobacteria, are given in figure 1.1.

Archaeobacteria contain ether linked phospholipids whereas eubacteria contain ester linked phospholipids in the cell membranes. Ether linked membrane lipids have been found in a few eubacterial species, but they are not isoprenoid in nature (Langworthy *et al.*, 1983), and since such examples are rare they may be adaptive traits rather than representative constituents of early evolutionary bacterial lipids. Thermoacidophilic archaeobacteria, are found in what is believed to be a more extreme environment, and tend to possess a significant proportion of the stronger tetraether membrane lipids. Thermophile and thermoacidophile groups tend to contain predominantly the tetraether lipids in a monolayer membrane configuration. Woese *et al.*, (1978) postulated that such archaeobacteria are similar to those early life forms present when primordial earth was a hot, acidic, anaerobic environment. Halophiles occupy relatively less extreme environments and as a result contain mainly, if not all, diether phospholipid components (Jones *et al.*, 1987). Extreme halophiles and thermosulphotobacteria contain exclusively the diether-based membrane lipids. The habitats where methanogens are found are generally less extreme than the habitats of the thermoacidophiles. However, some methanogens have been isolated from more extreme environments, such as *Methanothermus fervidus*, which has an optimal growth temperature of 83°C (Stetter *et al.*, 1981).

The glycerol ether molecules given in figure 1.1 represent the hydrolysed forms of the lipids found in the membranes of the archaeobacteria. One glycerol molecule would normally be bonded to a hydrophilic, phosphate containing, polar head group which corresponds to the outer surface of the cell membrane. The other glycerol molecule, however, would normally be bonded to a hydrophobic, non-polar head group corresponding to the inner membrane surface.



C₂₀ Diether Derivative



C₄₀ Tetraether Derivatives

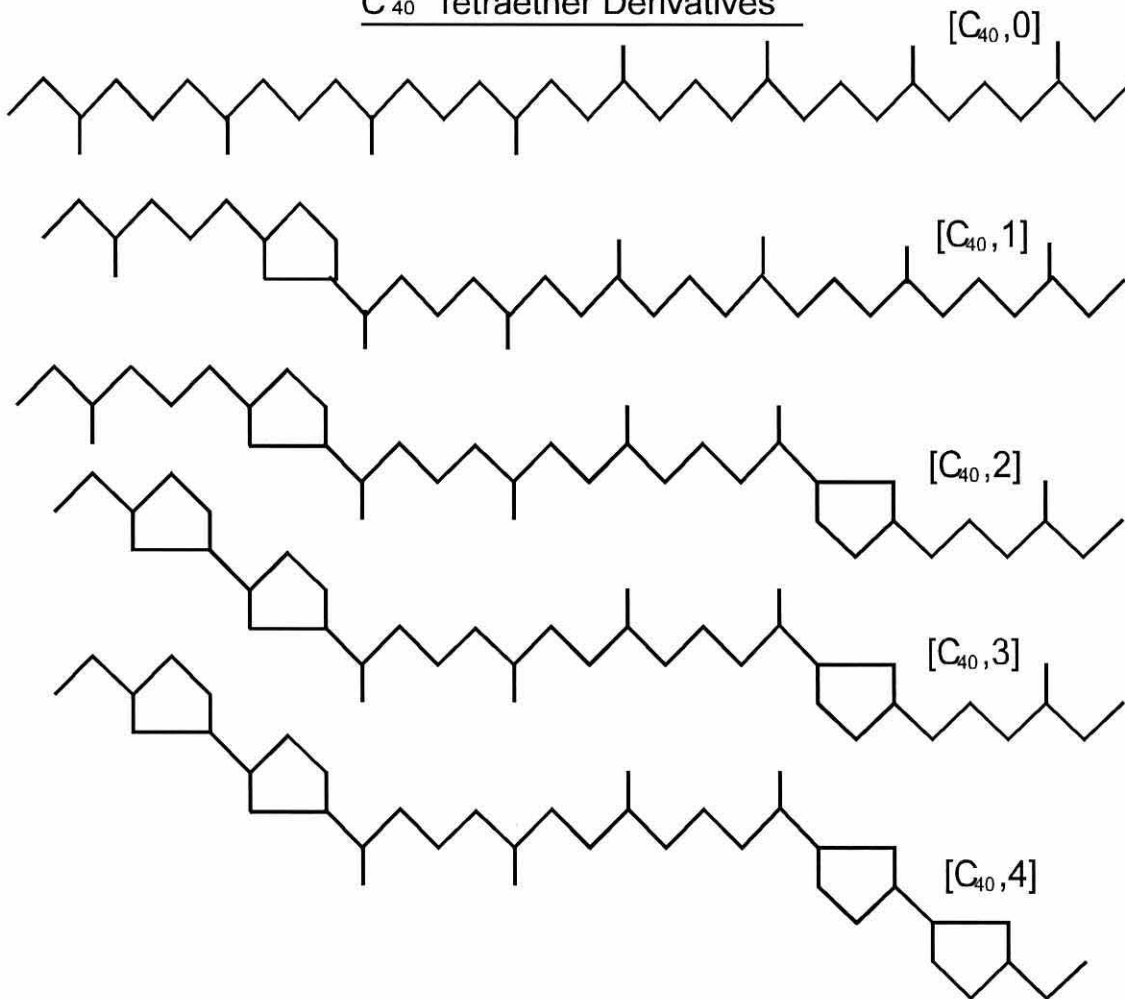


Figure 1.1. Diether and tetraether derivatives of the glycerol ether lipids found in the membranes of archaeobacteria.

Figure 1.1 shows how a single glycerol molecule bonds via two ether linkages to two C_{20} derivatives (diether) (*i.e.* di-*O*-phytanyl glycerol ether; DPGE). Two diether molecules are therefore required to form a single membrane unit bridging the inner and outer sides of the cell.

Figure 1.1 also shows how two C_{40} derivatives bond via four ether linkages (tetraether) to two glycerol molecules. Only one tetraether molecule is required to form a single membrane unit in the "monolayer" type membrane configuration (*i.e.* tetra-*O*-di (biphytanyl glycerol ether); biDPGE). The acyclic and cyclic C_{40} derivatives found in the tetraether molecules are also given in figure 1.1. Single tetraether molecules have been found to comprise of either similar or different C_{40} derivatives (De Rosa *et al.*, 1986b). The method of synthesis of the ether lipids is not completely understood, but several theories have been proposed by Jones *et al.* (1987) and Bu'Lock *et al.* (1983).

Greater chemical stability is given by the ether linkages of the alkyl chains to the glycerol molecules, when compared to the ester linked analogues of eubacterial membranes (Jones *et al.*, 1987). Archaeobacteria containing significant proportions of tetraether lipids which can form a rigid monolayer membrane, directly linking the outer membrane hydrophilic polar head group with inner membrane hydrophobic units (see figure 1.1). Monolayers can provide greater thermostability to the membrane (Jones *et al.*, 1987). A slightly positive membrane potential found in monolayer configurations may also be a form of passive proton exclusion in low pH conditions (De Rosa *et al.*, 1986a). Internal cyclisation, as shown in the C_{40} derivatives of figure 1.1, may also contribute towards greater membrane thermostability (De Rosa *et al.*, 1980). The branches in the alkyl chains are thought to provide fluidity to the membrane in a similar manner to unsaturated bonds in eubacterial membrane lipids.

1.6.4.1. Ether Lipids in Methanogens

Methanogenesis has been discovered in a wide range of anaerobic habitats in the environment as listed in section 1.4. These habitats are more diverse than the environments where thermoacidophiles and halophiles are found which is perhaps reflected in the greater variability in the ether lipids detected in methanogens.

All methanogens contain the diether (C_{20}) membrane lipids in proportions ranging from 11 to 100 %. The next most common ether lipid is generally acknowledged to be the acyclic tetraether lipid ($C_{40,0}$) which is present in proportions ranging from trace levels to 89 %. The proportions of these two lipids in most of the methanogens isolated to date is shown in table 1.2. Also included in this table is the types of habitats the methanogens have been isolated from, optimal growth temperatures and the substrates metabolised. It is evident from table 1.2 that the ether lipids of many of the methanogens isolated to date have yet to be published.

Table 1.2. Published diether and tetraether lipid compositions of methanogens with substrates utilised, mean optimal growth temperatures and habitats isolated.

Methanogen Species (with mean optimal growth temperature)	Ether Lipid ^a C ₂₀ (%) C ₄₀		Substrates ^b Metabolised	Habitat ^c Isolated
ORDER: METHANOBACTERIALES				
FAMILY: METHANOBACTERIACEAE				
<i>Methanobacterium</i> strain AZ (37°C)	38	62	H ₂ /CO ₂	Dig
<i>Methanobacterium bryantii</i> (MoH) (38°C)	44	56	H ₂ /CO ₂ , F	Dig, F+MSed
<i>M. thermoautotrophicum</i> (68°C)	BOTH ^d		H ₂ /CO ₂	Dig
<i>Methanobacterium formicicum</i> (42°C)	11	89	H ₂ /CO ₂ , F	Dig, FSed, R, Pro
<i>Methanobacterium thermoformicicum</i> (56°C)	BOTH		H ₂ /CO ₂ , F	Dig
<i>Methanobacterium thermalcaliphilum</i> (60°C)	BOTH		H ₂ /CO ₂	Dig
<i>Methanobacterium wolfei</i> (60°C)	BOTH		H ₂ /CO ₂	Dig, FSed
<i>Methanobacterium uliginosum</i> (37°C)	?		H ₂ /CO ₂	Marsh, Soil
<i>Methanobacterium alcaliphilum</i> (37°C)	?		H ₂ /CO ₂	Alkaline lake
<i>Methanobacterium thermoaggregans</i> (65°C)	?		H ₂ /CO ₂	Dig
<i>Methanobrevibacter smithii</i> P.S. (37°C)	45	55	H ₂ /CO ₂ , F	Human faeces
<i>Methanobrevibacter ruminantium</i> (37°C)	72	28	H ₂ /CO ₂ , F, A	Rumen (R)
<i>Methanobrevibacter arboriphilicus</i> A2(37°C)	BOTH		H ₂ /CO ₂	trees, Dig
<i>Methanobrevibacter arboriphilicus</i> DH1(37°C)	BOTH		H ₂ /CO ₂	trees, Dig
FAMILY: METHANOTHERMACEAE				
<i>Methanothermus fervidus</i> (88°C)	14	86 ⁱ	H ₂ /CO ₂	Hot spring
<i>Methanothermus sociabilis</i> (97°C)	?		H ₂ /CO ₂	Hot spring
FAMILY: UNDEFINED				
<i>Methanosphaera stadtmaniae</i> (37°C)	BOTH ^f		Me, H ₂ /CO ₂	R, Human faeces
<i>Methanopyrus kandleri</i> (98°C)	100	0	H ₂ /CO ₂	Hydrothermal
ORDER: METHANOCOCCALES				
FAMILY: METHANOCOCCACEAE				
<i>Methanococcus vaniellii</i> (37°C)	99.9 ^f	0.1	H ₂ /CO ₂ , F	Saltmarsh,
<i>Methanococcus voltae</i> (37°C)	100 ^f	0	H ₂ /CO ₂ , F	Estuarine, MSed
<i>Methanococcus aeolicus</i> (37°C)	?		H ₂ /CO ₂ , F	FSed
<i>Methanococcus deltae</i> (37°C)	?		H ₂ /CO ₂ , F	FSed
<i>Methanococcus maripaludis</i> (37°C)	100	0	H ₂ /CO ₂ , F	Saltmarsh
<i>Methanococcus thermolithotrophicus</i> (65°C)	BOTH ^f		H ₂ /CO ₂ , F	Hydrothermal
<i>Methanococcus igneus</i> (65°C)	BOTH ^h		H ₂ /CO ₂	Hydrothermal
<i>Methanococcus jannaschii</i> (85°C)	BOTH ^{d h}		H ₂ /CO ₂	Hydrothermal
ORDER: METHANOMICROBIALES				
FAMILY: METHANOSARCINACEAE				
<i>Methanosarcina barkeri</i> (35°C)	<100 ^f	trace ^e	H ₂ /CO ₂ , A, Me, Ma	Dig, F+MSed, R
<i>Methanosarcina mazei</i> (35°C)	100 ^f	0	Me Ma	Dig, Urban Soil
<i>Methanosarcina acetivorans</i> (35°C)	100	0	Me, Ma, A	MSed
<i>Methanosarcina alcaliphila</i> (37°C)	100 ^f	0	Me	MSed
<i>Methanosarcina vacuolata</i> (40°C)	?		H ₂ /CO ₂ , A, Me, Ma	Dig, FSed, Soil

(cont.)

Table 1.2 (continued).

Methanogen Species (with mean optimal growth temperature)	Ether Lipid ^a C ₂₀ (%) C ₄₀	Substrates ^b Metabolised	Habitat ^c Isolated
ORDER: METHANOMICROBIALES (cont.)			
FAMILY: METHANOSARCINACEAE (cont.)			
<i>Methanolobus tindarius</i> (25°C)	100 ^f 0	Me, Ma	MSed
<i>Methanolobus siciliae</i> (37°C)	?	Me, Ma	MSed
<i>Methanolobus vulcani</i> (37°C)	?	Me, Ma	MSed
<i>Methanolobus bombayensis B-1</i> (37°C)	?	Me, Ma, DMS	MSed
<i>Methanotherix thermoacetophila</i> (65°C)	BOTH	A	Dig
<i>Methanosarcina thermophila</i> (PT) (50°C)	?	Me, Ma, A	Dig
<i>Methanotherix concilii</i> (37°C)	100 ^f 0	A	Dig
<i>Methanotherix soehngeni</i> (37°C)	100 0	A	Dig
<i>Methanococcoides methylutens</i> (33°C)	100 0	Me, Ma	MSed
<i>Methanococcus halophilus</i> (31°C)	?	H ₂ , Me, Ma	Salt Lake
<i>Methanococcus frisius</i> (36°C)	BOTH	H ₂ , Me, Ma	MSed
<i>Methanococcoides burtonii</i> (33°C)	100 ^g 0	Me, Ma	Antarctic Sed
<i>Methanohalophilus mahii</i> (35°C)	100 ^f 0	Ma, Me	Salt Lake
<i>Methanohalophilus zhilinaceae</i> (37°C)	100 0	Ma, Me	Salt Lake
<i>Methanosalinarium flagellum</i> (37°C)	100 ^f 0	Ma	Salt Lake
FAMILY: METHANOMICROBIACEAE			
<i>Methanomicrobium mobile</i> (40°C)	BOTH	H ₂ /CO ₂ , F	Rumen
<i>Methanomicrobium paynteri</i> (40°C)	BOTH	H ₂ /CO ₂	MSed
<i>Methanospirillum hungatei</i> (37°C)	41 59	H ₂ /CO ₂ , F	Dig, F+MSed
<i>Methanospirillum</i> strain AZ (35°C)	38 62	H ₂ /CO ₂ , F	Dig
<i>Methanogenium cariaci</i> (23°C)	BOTH	H ₂ /CO ₂ , F, A	MSed
<i>Methanogenium marisnigri</i> (23°C)	BOTH	H ₂ /CO ₂ , F	Black Sea Sed.
<i>Methanogenium thermophilicum</i> (60°C)	BOTH	H ₂ /CO ₂ , F	Sed
<i>Methanogenium olentangyi</i> (37°C)	BOTH	H ₂ /CO ₂	FSed
<i>Methanogenium tationis</i> (40°C)	?	H ₂ /CO ₂ , A, F	Thermal mud
<i>Methanogenium frittonii</i> (57°C)	?	H ₂ /CO ₂ , A, F	F Sed, thermal
<i>Methanogenium aggregans</i> (37°C)	BOTH	H ₂ /CO ₂ , F, A	Dig
<i>Methanogenium bourgense</i> (37°C)	BOTH	H ₂ /CO ₂ , F, A	Dig
<i>Methanocullens oldenburgensis</i>	BOTH	H ₂ /CO ₂	Dig
FAMILY: METHANOCORPUSCULACEAE			
<i>Methanocorpusculum</i>	?	H ₂ /CO ₂ , F, Me	?
FAMILY: METHANOPLANACEAE			
<i>Methanoplanus endosymbiosus</i> (36°C)	?	H ₂ /CO ₂ , F	Marine ciliate
<i>Methanoplanus limicola</i> (40°C)	BOTH	H ₂ /CO ₂ , F, A	Swamp
ORDER: UNDEFINED			
<i>Methanopyrus kandleri</i> (98°C)	100 0	H ₂ /CO ₂	Hydrothermal

(cont.)

Table 1.2 (*continued*)

- a. Only the major lipid constituents are given, C20 is diether, C40 is tetraether (acyclic)
- b. Abbreviated metabolites include; hydrogen/carbon dioxide (H₂/CO₂), formate (F), acetate (A), methanol (Me), methyl amines (Ma) and dimethyl sulphide (DMS). Carbon monoxide and methylmercaptans and dimethyldisulphide have also been identified as substrates for some methanogens but are not shown in table 1.2.
- c. Abbreviated habitats isolated include; sewage digesters (Dig), freshwater (F) and marine (M) sediments (Sed), ruminant animals (R), protozoa (Pro) and thermal muds (thermal).
- d. Proportions of diether and tetraether shown to change with growth temperature (Sprott *et al.*, 1991) or growth phase (Morii & Koga, 1993).
- e. Cyclic tetraether lipids detected by De Rosa *et al.* (1986b) but disputed by Nishihara & Koga (1991).
- f. Various isomers of a diether with an hydroxyl group detected on the C3 carbon (Koga *et al.*, 1993b).
- g. Unsaturated C20 diether lipid detected (Nichols & Franzmann, 1992).
- h. Macrocyclic diether lipid detected (Koga *et al.*, 1993b; Comita & Gagosian, 1983).
- i. Cyclic tetraether lipids detected to 30 % (Pauly & Van Vleet, 1986b).

The information in table 1.2 was taken from the following references; Koga *et al.*, (1993a,b); Tornabene & Langworthy, (1978); Hedrick *et al.*, (1991a); Kadam *et al.*, (1994); De Rosa *et al.*, (1986b); Nishihara & Koga, (1987, 1991); Kurr *et al.*, (1991); König & Stetter, (1989); Bruggen *et al.*, (1986); Sowers *et al.*, (1984); Corder *et al.*, (1983); Jones *et al.*, (1987); Brock & Madigan, (1991); Nichols & Franzmann, 1992; Morii & Koga, (1993); Sprott *et al.*, (1991); Comita & Gagosian, (1983).

It is apparent from table 1.2 that the mesophilic methanogens of the *Methanosarcinaceae* family contain predominantly diether lipids and most are able to metabolise methylamines and methanol. The mesophilic methanogens of the *Methanococcus* genus (*Methanococcaceae* family) also contain predominantly diether lipids but can not metabolise methyl amine and methanol and are restricted to hydrogen/carbon dioxide and formate.

In addition, other types of ether lipids have been identified in certain methanogens but are not included in table 1.2. The presence of trace amounts of C40,2 and C40,3 lipids in *Methanosarcina barkeri* have been identified in one study (De Rosa *et al.*, 1986b), but this has since been disputed by Nishihara & Koga (1991). Proportions of cyclic tetraether lipids of up to 3 % have been found in other mesophilic methanogens (Pauly & Van Vleet, 1986b) and up to 30 % of C40,1 and C40,2 in the thermophile *Methanothermobacter feravidus* (Pauly & Van Vleet, 1986b). A macrocyclic diether is present in the thermophilic methanogen *Methanococcus jannaschii* (Comita & Gagosian, 1983) and two isomers of the diether lipid containing hydroxyl groups have been shown in some methanogens of the *Methanococcaceae* and *Methanosarcinaceae* families (Koga *et al.*, 1993b).

An unsaturated diether lipid has also been identified in the Antarctic methanogen *Methanococcoides burtonii* (Nichols & Franzmann, 1992), and the isoprenoid chain length of the diether membranes can also show some variation (Mancuso *et al.*, 1985).

The polar ether lipids of the methanogenic bacteria typically show much less structural diversity than, for instance, eubacterial ester linked, fatty acid lipids, being dominated by the diether (C20) and tetraether (C40,0) lipids. Although there are some variations in these lipids, as detailed above there is generally inadequate diversity to relate ether lipids to specific groups of mesophilic methanogens in ecological samples. In thermophilic methanogens it has been shown that the proportion of diether to tetraether lipids may change with different growth temperature (Sprott *et al.*, 1991), and changes in the growth phase (Morii & Koga (1993). This observation has yet to be made for mesophilic species of methanogens.

The information content of the methanogenic lipids can be increased, however, by determining the intact phospholipid and glycolipid headgroups attached to the ether lipid chains by supercritical fluid chromatography (Hedrick *et al.*, 1991a). Koga *et al.* (1993a,b) found that the presence of certain phospho- and glyco- ether lipid component parts, regardless of their arrangement, was characteristic of methanogenic taxonomic groups at a family or genus level. These lipids can now be used to infer the presence of methanogenic families in anaerobic sludge digesters (Nishihara *et al.*, 1995; Ohtsubo *et al.*, 1993).

1.6.4.2. Ether Lipids in the Environment

There have been only three extensive studies of ether lipids in environmental samples. These were in deep sea sediments (Pauly & Van Vleet, 1986b; Pease *et al.*, 1992) and freshwater sediments (Pauly & Van Vleet, 1986a). Also, a limited number of samples have also been analysed for their ether lipid content from estuarine, marine and freshwater sediments (Martz *et al.*, 1983; Guezennec & Fiala-Medioni, 1996; Teixidor & Grimalt, 1992), the water column of a hypersaline basin (Dickins & Van Vleet, 1992), geologically dated freshwater and marine sediments (Chappe *et al.*, 1982), and sewage digesters (Hedrick *et al.*, 1991b).

There have been some interesting observations of the ether lipids present in marine and freshwater sediments. The presence of C40,2 and the isomer C40,2' in sediments has also been shown to be an indicator of a marine depositional environment whereas C40,1', an isomer of C40,1 lipid shown in figure 1.1, has been shown to indicate a freshwater depositional environment (Pauly & Van Vleet, 1986b; Chappe *et al.*, 1982). Further research is required but it would appear that these cyclic ether lipids would serve as an excellent indicator of marine and freshwater depositional environments.

Interesting observations have been made in areas where methanogens represent the major archaeobacterial input. Pauly and Van Vleet (1986b) showed that cyclic tetraether lipids (C40,1 = 7%, C40,2 = 17 %, C40,2' = 17 %) constituted a large proportion of the total ether lipids in marine sediments compared to the acyclic tetraether (C40,0 = 53 %) and diether (C20 = 6 %) lipids. The chemical structure of the C40,2' lipid has yet to be determined but it has been

suggested in other geologically dated marine sediments to be an isomer of the C_{40,2} lipid described in figure 1.1 (Chappe *et al.*, 1982). The increased proportion of cyclic ether lipids to the total ether lipid content with increasing sediment depth in geologically dated sediments has been suggested as an indicator of a discriminatory diagenetic mechanism (Pauly & Van Vleet, 1986b), though further study is required. There have been very few reports of these cyclic ether lipids in laboratory cultured methanogens and when they have been detected their concentration compared with the other ether lipids has been small. Therefore the presence of large proportions of these cyclic ether lipids in deep sea sediments is unexpected. Their presence in near-shore marine sediments has yet to be determined.

As discussed in section 1.5 the rate of methanogenic activity can increase at the base of the SRZ due to the reduced competition for common substrates by the SRB. From the limited data given in Pauly & Van Vleet (1986b) it could be shown that increased concentrations of ether lipids were apparent at the base of the SRZ. Also, in more recent sediments a relationship between ether lipid and methane concentration, the product of all metabolic activity in methanogens, could be suggested to exist in the limited study of Martz *et al.* (1983). Harvey *et al.* (1986) has, however, shown that ether lipids degrade at a much slower rate in anaerobic sediments than fatty acid membrane lipids, which degrade 20 times faster, which may suggest that the proportions of ether lipids representing non viable methanogenic material (*i.e.* necromass) should increase with increasing sediment depth. This will, however, depend on the rate that the methanogenic cells become non viable and metabolically inactive.

1.6.4.3. Sources of Methanogens and Ether Lipid to the Sediments

The distribution of methanogens and methanogenic material to the sediments can be influenced by factors other than *in-situ* growth. Numbers of other marine bacteria in surface sediments have been shown to be largely controlled by the input of bacteria from the water column (Rheinheimer, 1991). The sources of ether lipids to the sediments also requires careful consideration because of their recalcitrant nature. It is not known whether the ether lipids of non-viable methanogenic material would degrade during transport in the water column. Therefore, ether lipids could reflect methanogenic growth and death (*i.e.* turnover) from many sources prior to deposition to the surface sediments.

The sources of methanogenic bacteria and ether lipids to the surface sediments are considered:

- **From Deeper Sediment Horizons**

Methanogens are expected to migrate through the sediment by depositional advection due to sediment consolidation causing methanogens to travel in the pore waters from deeper sediments, where methanogenesis is greater, towards the surface. There is little information in the literature on the transport of methanogenic bacteria in this way. The movement of pore water is expected to be significant in acoustically turbid sediments.

- **Water Column Input: Zooplankton and Faecal Waste**

Methane in near-shore waters (Lamontagne *et al.*, 1971) and open ocean surface waters (Scranton & Brewer, 1977), have been detected at concentrations that are greater than expected for the given partial pressure of methane in the atmosphere. In most cases the methane in the water column is due to *in-situ* production (Burke *et al.*, 1983).

Rudd and Taylor (1980) suggested two possible sources of excess methane; from the transport of near shore anoxic sediments, and also from *in-situ* production. Methane production observed during photosynthesis in aerobic algal cultures of *Thalassiosira pseudonana* and *Coccolithus huxleyi* (Scranton & Brewer, 1977) were considered to form insufficient densities in the open ocean to primarily account for this *in-situ* methane production (Rudd & Taylor, 1980). In some regions where active decomposition of organic material is occurring the methane detected in the water column is more likely to originate from the sediments (Rudd & Taylor, 1980). Much of the methane concentrations in the surface oceans are, however, thought to originate from *in-situ* methanogenic production in anoxic microniches such as the anaerobic guts of zooplankton and the intestines of pelagic fish (Oremland, 1979; Bianchi *et al.*, 1992; Karl & Tilbrook, 1994; Tilbrook & Karl, 1995).

Viable methanogens have been shown to be present in the guts of zooplankton (Oremland, 1979; Bianchi *et al.*, 1992) and particulate matter associated with faecal waste of zooplankton (Bianchi *et al.*, 1992). Methanogens of the *Methanosarcinaceae* family have been isolated from water samples of the open ocean (Cynar & Yayanos, 1991) and Angelis and Lee (1994) have shown that the concentrations of trimethylamine in the guts contents of zooplankton are sufficient to account for all of the methanogenesis in zooplankton samples. From table 1.2 it is evident that the methanogens which metabolise methylamine contain predominantly diether membrane ether lipids. Ether lipids associated with faecal particulate matter of a hyper saline marine basin were shown to be of diether origin, though the presence of tetraether lipids was not ascertained at this site (Dickins and Van Vleet, 1992).

The possibility of oxygen poisoning the methanogens when inside the actively maintained anaerobic gut of the organism would be minimal. But when some of the gut fauna is excreted in the form of faecal pellets, with typical diameters of approximately 100 μm , it would be expected that the rate of oxygen diffusing into the pellet would far exceed the rate of oxygen consumption on the surface of the pellet (Rudd & Taylor, 1980). It has been calculated that particles of a composition similar to faecal pellets suspended in air-equilibrated water would require a diameter of greater than 500 μm in order for the centre to have a redox potential low enough to support methanogenesis (Rudd and Taylor, 1980).

The development of spores or cysts that might be resistant to oxygen penetration has not been documented in the methanogens (König & Stetter, 1989). Some species of methanogens can form a protective coating encompassing clusters of cells when dormant (Robinson, 1986). Increased tolerance to oxygen has been observed in methanogens that were endosymbionts of sapropelic freshwater protozoa (Lloyd *et al.*, 1989). The methanogen *Methanoplanus endosymbiosus* has been found in a marine sapropelic ciliate (*Metopus contortus*) which inhabits sulphide containing environments (Bruggen *et al.*, 1986). Other endosymbiont species of methanogen have also been found free-living in marine sediments (Bruggen *et al.*, 1986).

- **Water Column Input: River Run-off**

Methanogenic biomass and necromass may also be associated with river run-off, which is expected to have a greater input to near-shore than deep sea marine sediments. Methanogenic material in the riverine input is expected to originate from sewage outflows, run-off from fields, erosion of freshwater sediments and freshwater zooplankton. Antibody probes have shown that new immunotype methanogenic strains of the family *Methanosarcinaceae* were present and viable within the oxygenated water column samples taken from Chesapeake Bay (Sieburth *et al.*, 1993). Viable methanogens were mainly associated with the particulate matter of the riverine input to the water column of Chesapeake Bay and numbers of up to 35 per litre via the MPN technique were reported (Sieburth *et al.*, 1993). Methanogens of the *Methanosarcinaceae* family may be more oxygen tolerant than other families (Pauly & Van Vleet, 1986b) and, as already stated, they are the only methanogens to metabolise methanol and methylamines and also contain predominantly diether membrane lipids (see table 1.2). From this information on the types of methanogens enriched from the water column it could suggest that diether membrane lipids would predominate in the water column and surface sediments.

Methanogens are known to be very concentrated in the rumen of cattle (König & Stetter, 1989) which may be a potential source of the ether lipids to the sediments from run-off from fields. Methanogens isolated from the rumen of cattle to have been found to contain notable amounts of tetraether lipids when in pure culture with proportions ranging up to 89 % tetraether lipids of the total ether lipid present. Studies using fluorescent antibody techniques have shown that numbers of *Methanobrevibacter ruminantium* in the sediment of an aquatic harbour were in excess of 1×10^{10} per dry gram but could not, however, be enriched by MPN techniques (Ward & Frea, 1979). Since such species have not been isolated from sediments (König & Stetter, 1989) it may suggest that they have been washed from the fields where cattle or sheep graze to the rivers and finally to the lake in this particular study. The concentration of methanogens in the rumen chamber of cattle and sheep are typically 10^{10} per ml and the turnover of bacteria including methanogens is can be significant (D Lloyd, *pers. comm.* 1996). Methanogen concentrations of this size could provide a large ether lipid input to the sediment. A study of the ether lipid content within the faecal matter to determine whether it increases with increasing turnover in the guts of ruminants would provide some interesting information in this area.

- **Water Column Input: Sewage**

Methanogenic biomass and necromass may also be associated with sewage, which like riverine inputs is expected to be greater in near-shore than deep sea marine sediments. Research into methanogens present in the human gut has shown that of the people who harbour methanogens *Methanobrevibacter smithii* is the most abundant and is typically enriched in the large bowel (Nottingham & Hungate, 1968, König & Stetter, 1989). *Methanobrevibacter smithii* has been shown to contain 55 % tetraether lipids (see table 1.2). Numbers of methanogens range from extremely low (a few cells per gram) to as high as 10^{10} per dry gram faecal weight and in some individuals can be equal to 10 % of the total concentration of viable anaerobic bacteria (König & Stetter, 1989). It was shown in a large survey that only one third of US citizens had methanogens in their faeces and the concentration was generally low (10^4 to 10^7 per dry gram) (D.C. White, *Pers. comm.*, 1994). Anaerobic sewage digesters are known to promote bacterial activity including methanogenesis to increase the rate of degradation of the organic matter (Hedrick *et al.*, 1991b,c). Significant concentrations of ether lipid at $8.9 \pm 4.5 \mu\text{g g}^{-1}$ DPGE (C20) have been reported in sewage sludge taken from a digester.

CHAPTER 2. MATERIALS AND METHODS.

2.1. Anaerobic Culture Preparation

2.1.1. Anaerobic Cabinet

All anaerobic culture work was performed in a Don Whitley Mk II anaerobic cabinet. The cabinet was supplied with an anaerobic gas mixture of 80:10:10 % nitrogen: hydrogen: carbon dioxide respectively (BOC) which was continually circulated through tubes of Anotox, silica gel and Deoxo 'D' catalyst. These removed hydrogen sulphide, volatile fatty acids, moisture and catalysed the removal of any traces of oxygen present in the cabinet atmosphere. The Anotox was replaced annually and the silica gel was changed as and when was required, usually every 3 to 4 weeks. Manipulations inside the cabinet were performed through heavy duty sealable glove ports which were evacuated and flushed three times with the anaerobic gas mixture before access through the glove ports and into the cabinet was permitted. A simple pump was used to bubble the cabinet atmosphere through the anaerobic indicator solution (Don Whitley, A038) which gave a colourimetric test for the presence of oxygen. This pump also doubled as a means of degassing media over long periods of time while the media cooled within the cabinet. The materials were transferred into the cabinet via a roof mounted interchange lock, at least one day before they were required for methanogenic culture work. The cabinet was equipped with a temperature controller for temperatures above ambient, but in order to maintain cooler temperatures comparable to *in-situ* sediment temperatures (3 °C) a refrigeration unit was fitted to the side of the cabinet.

2.1.2. Media Preparation

A variety of different methanogenic media were prepared over the experimental period, the compositions of these are given in appendix I.

Many of the media preparation methods reported in the literature for methanogenic bacteria recommend autoclaving the medium containing most of the constituents before aseptically adding the sodium sulphide and cysteine reducing solution, adjusting the pH, and aseptically dispensing into the growth culture tubes within the anaerobic cabinet (Balch *et al.*, 1979; Moore, 1966). This was the method adopted at first, but it was difficult to obtain a consistent pH between different batch media and also required the media to be dispensed under aseptic

conditions. This was laborious and not always safe from contamination in a confined anaerobic cabinet, especially when preparing hundreds of Hungate tubes.

An alternative method, not described in the literature, was therefore devised to overcome these problems. All chemicals listed for each medium (appendix I), except for methanol, sodium sulphide, l-cysteine and the antibiotics, were dissolved in distilled water and made up to the appropriate volume in a conical flask. The top of the flask was plugged with a lint bung. The pH at this stage was measured (Gallenkamp pH stick) and adjusted to the correct value using 1 M hydrochloric acid. The medium was heated to almost boiling while continually degassing with oxygen free nitrogen (OFN, BOC) through a 0.2 μm filter. The medium was allowed to cool to approximately 70 °C while continually degassing with OFN before it was transferred to the cabinet through the cabinet lock. The vacuum generated during the evacuation cycles of the lock meant that temperatures greater than this would lead to violent boiling of the media out of the flask. The pump located inside the cabinet was used to continually purge the media with anaerobic gasses for a period of at least 6 h.

All media preparations contained 0.0001 % (w/v) resazurin as the redox indicator of possible oxygen contamination. Resazurin generates a blue colour when initially added to the medium and its subsequent reduction goes through two stages. After boiling and degassing within the anaerobic cabinet the medium should have a strong pink colour (resorufin) otherwise the medium was discarded. The second stage of the reaction was colourless (dihydroresorufin) after the addition of approximately 5 ml of a stock reducing solution consisting of sodium sulphide and L-cysteine (0.5 g of each per 5 ml). The completion of these colour transformations ensured that the anaerobic growth of the methanogenic bacteria could commence after inoculation. This final reduction stage could be readily reversed to the pink colouration on contact with traces of oxygen (*i.e.* when the redox potential increased above $E^\circ = -0.042 \text{ V}$).

The reducing solution was prepared by weighing 5 g of sodium sulphide and 5 g of l-cysteine into individual universal bottles before quickly transferring them to the anaerobic chamber. The reducing compounds were transferred to a 50 ml quick fit measuring cylinder and dissolved in distilled water that had been previously degassed in the cabinet at least 24 h before required. The solution was made up to 50 ml and kept in the cabinet for subsequent media preparations.

Anaerobically purged methanol was also added to the media preparation at this stage, if required. Final adjustment of the pH of the medium was achieved using concentrated hydrochloric acid which was required before dispensing into suitable sealed growth culture containers. The sealed culture containers were removed from the anaerobic chamber and were

immediately autoclaved on a 45 minute purge, sterilisation and cooling cycle. Providing that no carbon dioxide was allowed to escape from the dissolved bicarbonate in the medium during autoclaving then the pH would remain constant. When cool any precipitate that formed could be re-dissolved upon shaking. Media showing a pink colouration were discarded at this stage.

Different types of growth culture containers were used depending on the volume of media and hence amount of methanogens required. The types of culture containers used are listed below:

(a) Hungate tubes (20 ml, Horwell and Arnold Ltd) fitted with butyl rubber inset seals with plastic autoclavable screw tops. These were used for the subculture of pure methanogenic species as well as for the Most Probable Number (MPN) determination of total methanogenic populations (section 2.5). Media were dispensed into the tubes within the anaerobic cabinet using a Zippette connected to a 1 litre flask.

(b) Culture tubes (50 ml) and medical flasks (250 ml) for growth culture experiments using methanogenic monocultures. The greater volumes were required to perform lipid, cell number and turbidity measurements.

(c) Quickfit 1 litre flasks fitted with Suba seals for lipid degradation experiments. Large volumes were required for the removal of numerous 10 ml subsamples.

2.1.3. Isolation of Methanogenic Bacteria

In order to determine how the ether lipids were related to the methanogenic biomass it was first necessary to work on pure cultures so that direct enumeration of the methanogenic cells could be made (section 2.2.3).

The isolation of a pure methanogenic culture began by enriching from anaerobic marine sediment taken from the Menai Strait. The procedure is outlined in section 2.1.2 and the media was based on medium No.3 of Balch *et al.* (1979) (section A1.1, appendix I). The presence of methanogenic growth was determined from methane concentrations (section 2.4), but the subsequent dilution in media failed to produce a pure methanogenic monoculture after incubation. Attempts were made to isolate methanogens on agar plates (1.5 % agar, wt/vol, Merck) prepared with medium No.3 of Balch *et al.* (1979), using the fluorescence of the coenzyme F420 as an indicator for the presence of methanogenic species. Bacteria were screened for F420 coenzyme fluorescence on a Leitz Laborlux microscope fitted with a mercury ultra-violet lamp with 10 x 90/1.15, oil immersion magnification. For excitation at 420 nm a Ploenopak filter system (BG3) was used with a barrier filter (K460) to allow light of the wavelength 470 nm to be emitted.

Since methanogenic colonies were not identified on the agar plates the procedure was repeated using agar that had been washed in distilled water in an attempt to eliminate possible impurities which are known to inhibit methanogenic growth (Jones *et al.*, 1983). Mesophilic methanogens are known to grow slowly on agar plates of 1.5 % agar, and even when as little as 1 % agar is used, which presents problems with using partially unset wet agar surfaces. Some strains still require incubation for up to 4 weeks to reach a suitable size even when under low agar compositions (Harris, 1985). Other pure gelling agents such as polyol and electrophoresis grade agarose gave similar negative results.

Periodic problems with oxygen contamination in the anaerobic cabinet meant that methanogenic growth on agar plates might have been inhibited due to the colonies on the agar surface having an increased exposure to the cabinet atmosphere where oxygen contamination occurred. Gas tight anaerobic culture jars (Difco) were therefore used in the cabinet to incubate agar plates and prevent such oxygen contamination. Also in order to stimulate more methanogenic species to grow anaerobic gas forming sachets (Difco) were used to provide an atmosphere of hydrogen and carbon dioxide (40:60).

For time reasons it was considered appropriate to obtain pre-isolated methanogenic monocultures. Dr M. Blaut (Germany) and Dr K. Sowers (UCLA, USA) kindly donated three methanogenic cultures. Experimental details of these bacteria are given in section 2.2.1 and the media preparation procedure used was given in this section.

2.2. Growth Culture Experiments

2.2.1. Culturing of Methanogens

Methanogen cultures were initially maintained at optimal growth temperatures for a period of days before cooling to 5 °C, subculture was made every 3 weeks in the anaerobic cabinet. Contamination was checked for in each batch by the detection of methanogen cell fluorescence using the microscope with the ultra-violet attachment. The cultures received included; *Methanlobus tindarius* (Dr M Blaut, DSM 2278) (König and Stetter, 1982), *Methanococcoides methylutens* (Dr K Sowers, DSM 2657) (Sowers *et al.*, 1984), and *Methanosarcina acetivorans* (Dr K Sowers, DSM 2834) (Sowers *et al.*, 1984). All species grew well with methyl amines and methanol, with cell growth visible in liquid media within 1 to 4 days after inoculation. None of the methanogens received could be grown on carbon dioxide and hydrogen. The media constituents for each species are given in appendix I.

The materials and methods specific to each growth experiment using the methanogenic cultures are given below, and the experimental aims and results are detailed in chapter 4.

- ***Methanosarcina acetivorans***

For the growth experiment using *Methanosarcina acetivorans* 40 ml Pyrex glass, high pressure tubes were used with a screw top over a butyl rubber recessed septum. Twenty tubes were prepared with 20 ml of media specific for growth of *Methanosarcina acetivorans* (appendix I, section A1.3) were prepared by the method detailed in section 2.1.2. Trimethylamine was the only carbon source included for growth in the medium. Each tube was aseptically inoculated with 1 ml of a 4 day old culture of *Methanosarcina acetivorans*. Ten of the tubes were also aseptically injected with 30 ml of oxygen free nitrogen into the 20 ml headspace using a 50 ml plastic syringe a 0.2 µm filter and 28 gauge sterile needle. The initial pressure in these tubes was 2.5 times atmospheric. The remaining ten tubes were left at atmospheric pressure and all tubes were incubated at 30 °C in a controlled environment incubation (New Brunswick Inc.) shaker to ensure sample homogeneity. Culture tubes were removed from the incubator in order to determine the cell number and cell volume (section 2.2.3), methane (section 2.4.2), turbidity (section 2.2.2), ether lipids (section 2.13) and phospholipid phosphate (section 2.15). Two tubes at each pressure were sampled at time zero and at 24 h intervals after an initial 42 h lag period.

- ***Methanococcoides methylutens***

The growth experiment with *Methanococcoides methylutens* used similar culture tubes to those of the *M. acetivorans* growth experiment. Twenty tubes were prepared with 20 ml of medium (appendix I, section A1.2) as detailed in section 2.1.2. and were inoculated with 1 ml of a 6 day old culture and incubated at 35 °C. Single culture tubes were removed from the incubator during the lag and stationary growth phase and duplicate tubes were taken during the exponential growth phase. Sampling times were at zero and at 12 h intervals over a period of 132 h. The cell counts for this growth experiment could not be made because the samples froze at the back of the refrigerator before the counts were made. The cells were shown to lose their integrity on freezing.

- ***Methanlobus tindarius***

The material and methods for the growth experiment using *M. tindarius* are given in the publication (Smith & Floodgate, 1992) which is included in appendix IX and the media is given in section A1.4 of appendix I. *M. tindarius* was grown on both methanol and trimethylamine.

2.2.2. Turbidity Measurements

Samples of methanogenic cultures were analysed for turbidity (optical density) using 1 cm path length cuvettes in a diode array spectrophotometer (Hewlett Packard Ltd, Vectra ES/12). Wavelengths were chosen in the 540 to 570 nm range.

2.2.3. Bacterial Direct Counts

All aqueous reagents used for the direct bacterial counts were made with filtered (0.2 μm) distilled water and stored at 3°C until use. If stored for more than one week each reagent was re-filtered through a Millipore (Nucleopore) 0.2 μm , 47 mm filter paper.

A deflocculent, tetrasodium pyrophosphate (*i.e.* 0.001 M) was added to a known volume of the growth culture and a sonic probe was used to gently disperse the cells (Velji & Albright, 1986). Higher concentrations of this dispersive agent (*i.e.* 0.01 M) caused severe cell elongation and swelling, as well as some clumping.

Using the method of Parsons *et al.* (1984) the bacteria were diluted in appropriate volumes of formalin (40 %) before staining with 0.4 ml of acridine orange (1.0 g l⁻¹) for 10 min, and filtered on to a nucleopore filter which had been pre-stained with Irglan black (2 g Irglan black per litre of 2 % acetic acid).

The microscope eye piece contained a square grid which was used to count approximately 30 to 200 cells per field, and at least 15 field counts were made to determine the average cell number. The small, young methanogenic cells stained a bright blue/green colour when viewed in UV light whereas the large, older cells were orange in appearance by this technique. The filter diameter and area was determined using the Vernier caliper scale located on the microscope stage. This was best achieved by using a filter with a high density of stained cells so that the exact diameter of the filter could be measured. The eye piece field area was calculated using a stage graticule. Enumeration was made with a Leitz (Ortholux, 8667-51) UV microscope using BG38 (transmittance above 350 nm) and BG12 (transmittance between 390 and 470 nm) excitation filters and a K510 eye piece barrier filter (transmittance above 490 nm) on setting No.2.

2.2.4 Ether Lipid Degradation Experiment

Seven 500 ml cultures of *Methanlobus tindarius* were prepared in 1 litre flasks according to the method detailed in section 2.2.1. and each flask was fitted with a single Suba seal sampling port. The cultures were incubated at 30 °C for 3 months and the methane produced was periodically purged from the flasks. After one month methane production was negligible and the following two month incubation period was required to ensure the methanogens were well into their stationary growth phase. The cells were viewed by microscopy to observe cell integrity and motility. Pre-combusted sand (~ 10 g) was added to all flasks to help homogenise the mixture when shaken. The cultures could have been purposefully killed at this stage by using a variety of reagents but the use of extended incubation times was thought to represent what occurs *in-situ* in the sediments, albeit at a rather accelerated rate with the incubation temperature used. Anaerobic marine sediment (~ 5 g) was added to certain flasks and aeration

ports were located through the sampling ports. The aerated samples were bubbled continuously with air at a rate of 20 ml min⁻¹ through a 0.2 µm filter. Each of the seven flasks were set-up in the following configuration:

1. Anaerobic / Methanogens / 7 °C
2. Anaerobic / Methanogens / Anaerobic marine sediment / 7 °C
3. Anaerobic / Methanogens / 25 °C
4. Anaerobic / Methanogens / Anaerobic marine sediment / 25 °C
5. Aerobic / Methanogens / 25 °C
6. Aerobic / Methanogens / Anaerobic marine sediment / 25 °C
7. Aerobic / Methanogens / Anaerobic marine sediment / 25 °C / Gluteraldehyde

Negligible lipid degradation occurred in the killed control samples of Harvey *et al.* (1986) therefore gluteraldehyde (1 ml of 10 % solution) was added to the replicate sample which was expected to give one of the fastest ether lipid degradation rates (*i.e.* aerobic with marine sediment at 25 °C). Flask numbers 1, 2 and 3, 4, and 5, 6 were designed to show the effect that the other bacteria in the anaerobic sediment might have on the degradation rates at different temperatures. Comparison of flasks 1, 3 and 2, 4 was expected to show the effect of temperature and flasks 3 and 5 were expected to show the effect of aeration on the lipid degradation rates. Flasks 5 and 6 were expected to show the effect of aerobically enriched bacterial consorts on the ether lipid degradation rate.

Three subsamples (10 ml each) were collected from each flask at the designated sampling times using a needle and syringe via the Suba seal port. Time zero was effectively 3 months after the cultures were initially inoculated and 1 hour after the conditions given in (1) to (7) were established. Subsamples were also taken at the following times of 1, 2, 3 and 4 months. Internal standard was added to each of the subsamples as detailed in section 2.13.2. A GC was not available over this period therefore the samples were extracted according to the method detailed in section 2.13.2 and stored under nitrogen at -20 °C. The samples were finally prepared using the methods detailed in sections 2.13.3, 2.13.6 and 2.13.10 before analysis of the phytanyl acetate product by GC in section 2.14.

2.3. Sediment Sampling

2.3.1 Coring of Holyhead Harbour Sediments

Cores were taken with a Cambridge gravity corer from the Prince Madog using strengthened PVC tubes, 9 cm in diameter and 3 m long. Holes of 1.5 cm diameter were drilled into the core barrel at 20 cm intervals, beginning at 10 cm up from the core bottom. Parcel tape was used to seal the holes for coring and the tape was replaced with Suba seals which were inserted after the immediate sampling had taken place (*i.e.* methane and MPN sampling).

The winch and 'A' frame was connected to a vane attached at the top of the corer and a stainless steel sediment cutter was connected to the bottom of the core barrel with an inset flexible steel retaining rose. The core was positioned over the stern of the vessel with the aid of the 'A' frame and lowered through the water column by free fall with the winch out of gear and without applying the brake.

Upon retrieval and after the immediate sampling had taken place the barrel was sectioned using a saw at the 20 cm hole positions and sealed at both ends using aluminium foil, hot wax and tape (Jones *et al.*, 1986). Cores were stored at 3°C until subsequent analysis.

2.3.2. Coring of the Intertidal Sediment

A 1.5 m length of the PVC strengthened core barrel that was used for the gravity coring was also used for the intertidal sediment sampling, with pre-drilled holes at 10 cm intervals. The stainless steel cutter and retaining rose was also fitted and sediment penetration was achieved using body weight and a heavy mallet. Methane sampling was performed immediately after coring through the pre-drilled sampling ports (section 2.4.1). Samples for the MPN and water content determinations (sections 2.5 and 2.6, respectively) were removed from the sampling ports on return to the laboratory. After removal of the cutter and retaining rose the sediment was extruded with a piston into an anaerobic glove bag supplied with oxygen free nitrogen. Sediment was sectioned in 12 cm intervals and placed in Reeburgh squeezer tubes for pore water extraction (Reeburgh, 1967) and the remaining sediment was frozen for lipid analysis.

2.3.3. Bathymetry Surveys of Holyhead Harbour

The initial bathymetry survey was performed in May-June 1985 by Dunkerley, Marine and Hydrographic Surveys Ltd, Southampton for Anglesey Aluminium and the most recent survey took place in January 1993 by Andrews Hydrographics Ltd, White Waltham, Berks for Stena Sealink. The positioning was made by DPGS (Differential Global Positioning Satellite) and the longitude and latitude positions were translated into distances using 1" = 18.5 m and 1" = 30.75 m, respectively. The depth soundings in each survey were reduced to chart datum using tidal observations made at the Admiralty Pier Tide Gauge. Chart datum was typically 3.05 m below ordnance datum (*i.e.* mean sea level, Newlyn). The error associated with the depth soundings was ± 0.1 m which would also be directly comparable to other surveys of the area (S. Squibb, *pers. comm.*). The area extracted from each bathymetry survey was 222 m in the longitude direction (4°37'14" to 4°37'02") and 92.25 m in the latitude direction (53°19'36" to 53°19'39") and was translated into X-Y coordinates using a transparent grid overlay. The sedimentation rate was calculated by measuring the difference in overlying water height over the sediment between the two surveys (see Appendix X). The sedimentation rate in Newhaven Harbour was determined for comparison with the Holyhead data and was calculated using

bathymetry surveys collected by Westminster Dredging Company for Newhaven Ports and Properties Ltd from November 1993 and October 1996.

2.4. Methane Sampling

2.4.1 From Sediment Cores

Cut off 5 ml disposable syringes were used to obtain approximately 5 ml of sediment from the pre-drilled sampling ports. The sediment was immediately extruded into 50 ml serum vials containing 10 ml of 8 % trichloroacetic acid in order to prevent further microbial activity and also to aid in the transfer of methane into the gas phase. Serum vials were immediately wiped around the seal area with a tissue and sealed with a butyl rubber stopper, an aluminium crimp and dipped into hot wax to ensure no gas leakage. In this condition negligible methane loss was recorded over a period of weeks, though samples were usually measured the same day. Sample vials were stored upside down at 10°C to cover the seal area until analysis.

2.4.2. From Growth Culture Tubes

Methane was sampled from the headspace of the growth culture tubes using 1 ml disposable syringes and needles, and injected directly into sealed 50 ml serum vials. The serum vials had been purged with oxygen free nitrogen rather than air before use in case traces of methane were present in the atmosphere.

2.4.3. Methane Analysis

Methane was analysed on a DANI (304) gas chromatograph equipped with splitless septum injection and a flame ionisation detector. A 1.5 m x 3.0 mm stainless steel column was used with Porapak 80-100 Q (Phase Separations Ltd, Queensferry) support which was packed by the method detailed in section 2.4.4. A carrier gas of oxygen free nitrogen (25 ml min⁻¹) was purified (puritube, Phase Separations Ltd.) and dried (silica gel) and had the last traces of oxygen removed on-line to less than 1 ppm (Oxy-Trap, Phase Separations Ltd.) before passing through the column. Detector gasses were air (300 ml min⁻¹) and hydrogen (30 ml min⁻¹). Isothermal temperatures for the oven, injector and detector were 70°C, 100°C and 150°C, respectively, and peaks were analysed on a Spectra Physics integrator (S4070).

2.4.4. Packing of a Wide-Bore Column

A 1.5 m stainless steel tube of approximately 3 mm bore was bent into such a shape to accommodate both injector and detector fittings of the GC. The column was first washed with acetone before drying in an oven at 100°C for 4 h. The column was held upright in a retort stand while resting on a vortex mixer. One end of the column had a small glass wool plug fitted and was connected to a vacuum line. The other end was fitted with a plastic funnel into which the Porapak Q 80-100 mesh was added. Good consistent column packing was achieved using both the vacuum and the vortex mixer. This method had been previously checked for

consistent packing using a glass wide bore column for practice. The column required overnight conditioning at 120°C before use.

2.4.5. Methane Calibration

Errors associated with gas analysis by gas chromatography can often arise from the injection technique used. Since gas is difficult to confine to a syringe, small amounts may be lost when transferring a sample to the injector port. When the concentration of methane in the headspace gas is high, only small volumes (*i.e.* <10 µl) can be injected, otherwise the column is overloaded. In these cases the losses from the syringe may be significant, therefore such samples were diluted before analysis in order to maintain a larger injection volume. Methane standards were prepared by injecting known amounts of methane (99 %, BOC Special Gases) into 50 ml serum vials previously purged with oxygen free nitrogen. Dilutions were made in a similar manner and 20 µl was the typical injection volume used.

Peak area values were found to give more reproducible results than were peak height values over the relatively high methane concentrations analysed (see appendix II). This was unusual for gas analysis but could possibly be attributed to the gas chromatograph having only a splitless injection option. Methane concentrations in the sediment samples were quoted with 95 % confidence intervals which were non-symmetrical about the mean and were calculated from the statistical equation in appendix III. A detection limit of approximately 1×10^{-17} moles of methane was calculated for the gas chromatograph (GC).

2.5. Most Probable Number (MPN) Determination

The medium used for the most probable number (MPN) was based on medium No.3 of Balch *et al.* (1979) (appendix I, section A1.5). Many methanogens even when in pure culture require certain undefined media constituents. Such undefined components are known to be found in extract of a thermoacidophile archaeobacterium and also in rumen fluid (König & Stetter, 1989). Rumen fluid was therefore added to all MPN media preparations. The prevention of sulphate reducing bacterial (SRB) growth was a very important factor to consider due to it outcompeting the methanogens for electron acceptors. Sodium molybdate (20 mM) was added to prevent growth of any SRB (Sorensen *et al.*, 1981). The method of preparation is given in section 2.1.2. and the constituents of the medium is given in section A1.5 of appendix I.

Sediment samples taken from the core barrels were retrieved using cut off 5 ml disposable syringes in such a way that air was excluded. The open end was sealed with a butyl rubber recessed septum. For the intertidal sediments such MPN samples were transferred into the anaerobic chamber within 1 hour of sampling. For the Holyhead Harbour sediments the sample syringes were placed into clear polythene bags, sealed, and placed at 3 °C until analysis.

When ready for the MPN preparation the sample syringes were put into the anaerobic chamber and approximately 1 cm³ of sediment was placed in a universal bottle containing 9 ml of sterile medium, sealed and removed from the cabinet. The sediment remaining was re-sealed in the syringe and stored at 3 °C for further MPN analyses, if required at a later date. Satisfactory mixing of the sediment in the 9 ml of medium was achieved using a vortex mixer for 3 minutes before returning the universal bottle to the anaerobic chamber to complete the dilutions required to determine the viable methanogenic population. The universal bottle provided better mixing of the sediment slurry than the Hungate tubes for this initial mixing of the sample. The first dilution of 1 ml taken from the universal tube sample was performed using a 1 ml autopipette with disposable tips. For this initial dilution the tops of the first four replicate Hungate tubes were removed in order to facilitate this transfer. The tubes were sealed and each shaken vigorously for 30 seconds before subsequent 1 ml sub-samples were removed into a second set of four replicate tubes. Sterile 1 ml disposable syringes and needles were used for this and all subsequent transfers so as to minimise contamination during transfer. This was repeated for each set of four replicate tubes until a total of 24 Hungate tubes were used per analysis *i.e.* 6 dilutions of the 10x dilution series.

During the dilutions the rubber septum of each tube was cleaned with methanol to prevent contamination during needle penetration. Blanks were performed periodically using tubes containing medium plus 5 % gluteraldehyde. Hungate tubes were placed into polythene bags (1 sample = 24 tubes) and incubated at 30 °C for approximately 6 weeks before the replicates could be tested for methane as detailed in section 2.4.2. Tubes containing methane were treated as positive scores. The MPN calculations were performed using a computer program developed by Christofi *et al.* (1986) which was designed to work on a BBC computer. The program required the input of the dilution factor at each level and the number of replicates at each dilution showing the positive methane result after incubation. Slurry samples (1 ml) were also taken from the initial universal tube and placed into pre-weighed vials and dried at 60 °C for 24 h to determine MPN counts per dry weight of sediment.

A problem was encountered with the culture tubes prepared for the MPN determination of the Holyhead samples. The autoclave was shown to be not heating above 60°C which led to methanogens contaminating the culture tubes due to the method of preparation detailed in section 2.1.2.

2.6. Water Content Determination

Sediment extruded from the cut off syringes was placed onto pre-weighed aluminium discs and dried in an oven at 60 °C for 3 days before determining the dry weights. Approximately 5 g of sediment was used per analysis. The water content was expressed as a percentage of the total weight of the sediment.

2.7. Measurement of Sound Velocity Across the Sediment Core Sections

The measurement of the sound wave velocity across the sediment sections was performed using a signal enhancement seismograph 'sonic viewer' (model 5217A, OYO Corporation, Tokyo, Japan). The optimum settings were; sample time 200 nsec; pulse rate 128 sec⁻¹; output gain 1; input gain max. 10 K; without the filter option. The transducers were attached across the diameter of the gravity core barrel or consolidation apparatus. This meant that the slowest sound velocity was limited to the time taken for the sound wave to pass around the core barrel material itself (*i.e.* gas charged sediments), whereas the fastest sound velocity was achieved directly across the core barrel and through the sediments (*i.e.* gas-free sediments). The greater the difference in sound velocities between acoustically turbid and gas-free sediments was desirable and was dependent on the frequency of the transducer used. The transducer which gave the greatest range of sound velocities from acoustically turbid to gas-free sediments was 5 cm in diameter and operated at 250 KHz. A minimal amount of petroleum jelly was also applied to the surface of the transducer to provide a good repeatable contact. Sound velocities are reported as metres per second (m sec⁻¹).

2.7.1. Sound Velocities Measured Across Holyhead Core Sections

The 250 KHz transducers were placed either side of the core barrel section approximately midway up each core section using a retort stand. Five replicate acoustic measurements were made for each core section while on the research vessel within approximately 4 h of coring. The range of extreme acoustic measurements were determined using an empty PVC tube section and one full of consolidated sediment to set the lower and upper acoustic limits.

2.8. X-ray Analysis of Core Sections.

It was important to prepare the sediment sections in a similar manner so that the gas voids observed in the X-ray photographs could be compared between samples with consistent unit depths. X-ray analysis of sediment sections was performed on the Hewlett Packard cabinet X-ray system (Fascitron series, model 43855B) under the auto-exposure mode. Negatives were developed by the photographic department (School of Ocean Sciences, Menai Bridge).

2.9. Preparation of an Artificially Consolidated, Acoustically Turbid Sediment Core.

The sediment used for the consolidation experiments was a silty-clay from Combwich, Somerset, which was readily available and had also been used for acoustic measurements of artificially prepared gas charged sediments (Sills & Wheeler, 1992). The sediment was placed in the anaerobic cabinet approximately 24 h before use. The medium for *M. tindarius* (section A1.4, appendix I) was prepared and slowly mixed with the sediment using a spatula, making sure not to include bubbles of gas during the process. Trimethylamine was the only carbon substrate added. Approximately 70 ml of a culture of *M. tindarius* in media was added to every Kg of sediment.

The consolidation tubes (5 cm diameter, 20 cm high) consisted of a clear acrylic barrel with a base and tightly fitting solid acrylic piston plunger to which the lead weights were attached to consolidate the sediment. A diagram of the consolidation apparatus is given in figure 2.1. The tightly fitting bases of the consolidation tubes were removed so that the tubes could be pressed into the sediment evenly to a depth of about 13 cm. The tube bases were then refitted and the piston heads inserted. Killed control sediments were prepared by adding a cocktail of antibiotics so that neither the *M. tindarius* species or the indigenous methanogens or other bacteria could grow. The antibiotics used were neomycin (250 $\mu\text{g ml}^{-1}$ of pore water), streptomycin (250 $\mu\text{g ml}^{-1}$ pore water) for eubacterial species and 50 mM of the methanogen inhibitor 2-bromoethane sulphonic acid (Gunsalus *et al.*, 1978). Consolidation tubes were loaded with lead weights and placed in incubators at 30 °C and 8 °C.

The consolidation apparatus was removed from the incubator at least 1 h before measuring the sound wave velocity across the sediment. This ensured that temperature effects were consistent for each determination at the time of analysis. The transducers for the sound velocity determination were attached to retort stands and were placed up against the consolidation apparatus tubes at fixed top (9 cm), bottom (3 cm) and mid (6 cm) marked distances. The changes in core length was also monitored over a period of weeks. After completion of all sound velocity measurements, cores were extruded and sectioned for the methane analysis (section 2.4.1) and X-ray photography (section 2.8) and water content (section 2.6). Each analysis followed a similar procedure to that for the Holyhead sediment samples.

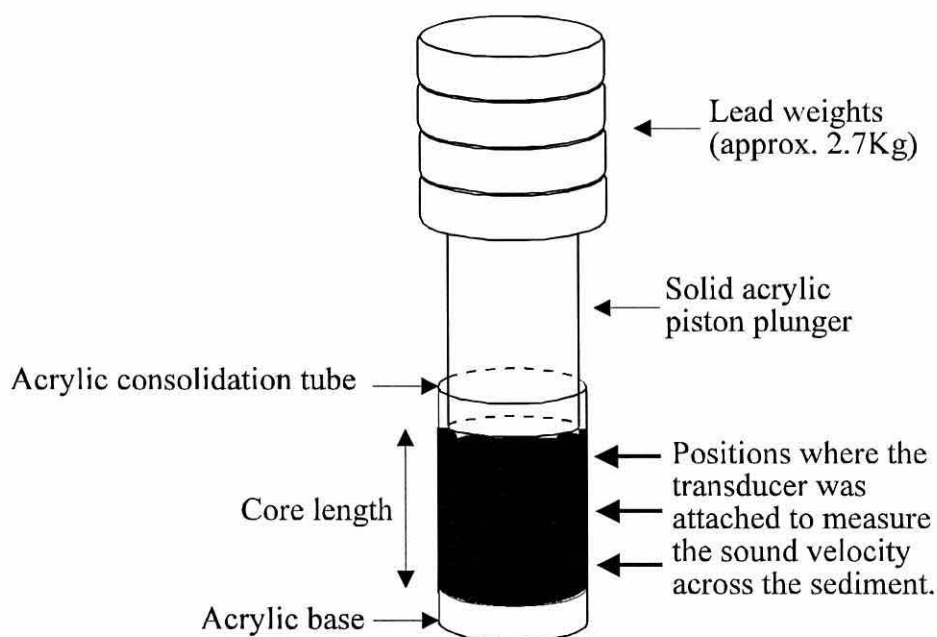


Figure 2.1. Diagram of the consolidation apparatus used when monitoring the sound wave velocity across the artificially prepared gas charged sediments.

2.10. Sediment Pore Water Extraction

Since the redox potential of chemicals in the pore water are oxygen sensitive, all manipulations of the sediment in air were kept to a minimum.

Pore waters were extruded from the intertidal core of Cadnant Creek, Menai Bridge using Reeburgh squeezers (Reeburgh, 1967). The squeezers were placed in the anaerobic cabinet thus keeping possible sample oxygenation to a minimum. The high gas pressure required to press against the dental dam rubber and cause pore water extraction was provided using a nitrogen cylinder which was plumbed through to the cabinet.

Operation of the Reeburgh squeezers proved to be time consuming (2 h per sample) so an alternative method of pore water extraction was utilised for extractions of Holyhead Harbour sediments. The Holyhead Harbour sediments were centrifuged at 3000 r.p.m. for 20 minutes to collect the pore water. Balancing of tubes was performed within the anaerobic cabinet and tubes were sealed with plastic stoppers before removal from the cabinet to the centrifuge. On return to the cabinet pore waters were divided into replicate vials for sulphate and sulphide determinations.

2.11. Determination of Sulphate in Sediment Pore Waters.

Pore water sulphate was determined by the method of Howarth (1978). The method is similar to the gravimetric barium sulphate method (Morris & Riley, 1966), except instead of weighing the barium sulphate precipitate on the filter paper it relies on dissolving the precipitate under alkaline conditions and chelating the barium with a known excess of EDTA. The remaining sites on the EDTA ligand are filled by titrating with magnesium ions. The end point is reached when all of the ligand sites in the EDTA are full and a sudden titration excess of magnesium ions is detected with Eirochrome black T which changes from a blue to a pink colouration.

Contamination from sulphide oxidation was prevented at the beginning of the analysis by precipitation with zinc acetate, and the zinc sulphide product was removed from the free sulphate ions by filtering through a 25 mm GF/C filter paper in a Swintex filter holder. Removal of the zinc sulphide precipitate, in this manner, was not completely necessary since the measured sulphide and sulphate levels in the sediment pore water differed by approximately three orders of magnitude.

A sulphate standard was prepared by dissolving 2.958 g of Na_2SO_4 (20.8 mM SO_4^{2-}) in 1 l of artificially prepared sulphate free sea water (Lyman & Fleming, 1940) which would allow for the possible interfering ions to be present and therefore simulate the method used on the pore waters. Standard concentrations of less than 20.8 mM were obtained by appropriately dilutions of the standard solution. The concentration of sulphate in the samples was calculated

directly from the standard calibration line. The calibration data is given in section A5.2 and table A5.2.1 of appendix V.

2.12. Determination of Sulphide in Sediment Pore Water

Sulphide was determined in the pore waters using the spectrophotometric method reported by Cline (1969). This method is applicable to natural waters containing between 1 and 1000 μg sulphur l^{-1} , is free of salt effects between 0-40 % and is not temperature dependent. The 3-40 μM sulphide concentration range was sufficient for the determinations of this study and the reagent comprised of 0.38 g of N,N-dimethyl-p-phenylenediamine oxalate and 0.75 g ferric chloride ($\text{FeCl}_3 \cdot 6\text{H}_2\text{O}$) which were dissolved in 125 ml of cool 50 % (v/v) hydrochloric acid. For greater sulphide concentration ranges the reagent concentrations are detailed in Cline (1969). The reagents were light sensitive but if stored refrigerated in an opaque bottle then the reagents were stable for several months. Absorbance at 670 nm was determined using a diode array spectrophotometer approximately 20 min after adding 80 μl of the 3-40 μM reagent to a 1 ml pore water sample in a 1 ml plastic cuvette.

Standard sulphide solutions were prepared by dissolving 0.96 g of dried sodium sulphide ($\text{Na}_2\text{S} \cdot 9\text{H}_2\text{O}$) into deoxygenated artificial sea water in the anaerobic cabinet, and made up to 100 ml in a volumetric flask. One ml of this standard solution contained 40 μM sulphide, lower concentrations were prepared by dilution with deoxygenated artificial sea water (Lyman & Fleming, 1940).

Calibration data is given in section A5.3 and table A5.3.1 of appendix V and the data showed that the error associated with each analysis increased as the sulphide concentration decreased. The 250-1000 μM calibration range gave a correlation coefficient, $r = 0.992$ ($n=15$, $p<0.001$); the 40-250 μM range $r = 0.979$ ($n=15$, $p<0.001$); and the 3-40 μM range $r = 0.954$ ($n=12$, $p<0.001$). The reagent for the 3-40 μM sulphide range was adequate for all pore water analyses of the Holyhead and intertidal sediments

2.13. Ether Lipid Determination

All glassware was washed overnight in Decon, dried and rinsed with chloroform before use. Lipid samples were stored in solvent at -20°C under oxygen free nitrogen and all solvent manipulations were performed in a fume cabinet. All chemicals were purchased from Sigma Chemicals unless otherwise stated.

2.13.1. Lipid Extraction : Sediment Samples

The lipid extraction method usually required at least 4 days to process a single batch of samples, and many extraction, derivatisation and purification stages were used. Therefore as

well as referring to the text of this section a flow diagram is also given in figure 2.2 as an overview of the entire lipid method for both sediment and laboratory culture experiments.

Sediment samples were kept frozen prior to lipid extraction for up to 3 months. Samples (approx. 250 g) were freeze dried for 3/4 days (Chemlab Instruments Ltd freeze dryer with Edwards pump model EF6) until dry and ground into a fine powder using a pestle and mortar. This gave a better sediment/solvent interaction for the more consolidated samples. Approximately 50 g of each sediment sample was weighed into a 500 ml round bottom flask and 200 ml of (2:1:0.8) methanol; chloroform and phosphate buffered (pH 7.4) distilled water was added (Bligh & Dyer, 1959). An addition of 315 µg internal standard 1,2-di-*O*-hexadecyl *rac* glycerol ensured that extraction losses were accounted for during sample clean-up and derivatisation. The mixture was refluxed at 90°C for 6 h and for two 15 min periods as detailed in Pauly and Van Vleet (1986a). Once cool to room temperature the supernatant was decanted and filtered under vacuum using a Buchner funnel and Whatman (No.4) 47 mm filters. The sediment was re-extracted twice using 50 ml volumes of methanol: chloroform: and phosphate buffered distilled water (2:1:0.8). Refluxing and sonication was again repeated for a further 1h before filtering the extract and pooling the supernatants.

Pauly and Van Vleet (1986a) report the necessity to use strong acid hydrolysis in order to extract 20 % additional isopranyl ether lipids from some semi-consolidated marine sediments of approximately 1 m depth. Therefore certain sediment samples (*i.e.* depths; 60-70 cm, 80-85 cm and 100-105 cm of Holyhead core C) were hydrolysed with acid following the three solvent extractions. Approximately 50 ml of 2 M HCl in methanol was added to the sediment residue and refluxed at 90 °C for 4 h. The extract was filtered (Whatman No.4) into a Quickfit 100 ml conical flask, to which was added 5 ml of petroleum ether and 30 ml of distilled water. After shaking, fractions of this mixture were centrifuged (Fisons Plc, Centaur 1 MSE) at 3000 r.p.m. for 5 minutes in 50 ml glass tubes. Each time the lower aqueous layer was discarded before repeating the addition. Once all of the acid hydrolysis extract had been centrifuged, the upper petroleum ether layer was removed using a Pasteur pipette, blown down under oxygen free nitrogen (OFN) and taken up in a minimum volume of chloroform. These extracts were not pooled with the rest of the extract from these samples but were prepared separately to determine whether the acid hydrolysis preferentially released greater proportions of certain ether lipid components from the pre-extracted samples.

The initial extracts in methanol, chloroform and water were filtered through a 47 mm, GF/C filter under vacuum to remove the fine silt particles from the cloudy extract. The volume of the pooled extract was measured and the appropriate volumes of chloroform and distilled water were added to make the two phase ratio of (1:1:0.9) methanol: chloroform: distilled water.

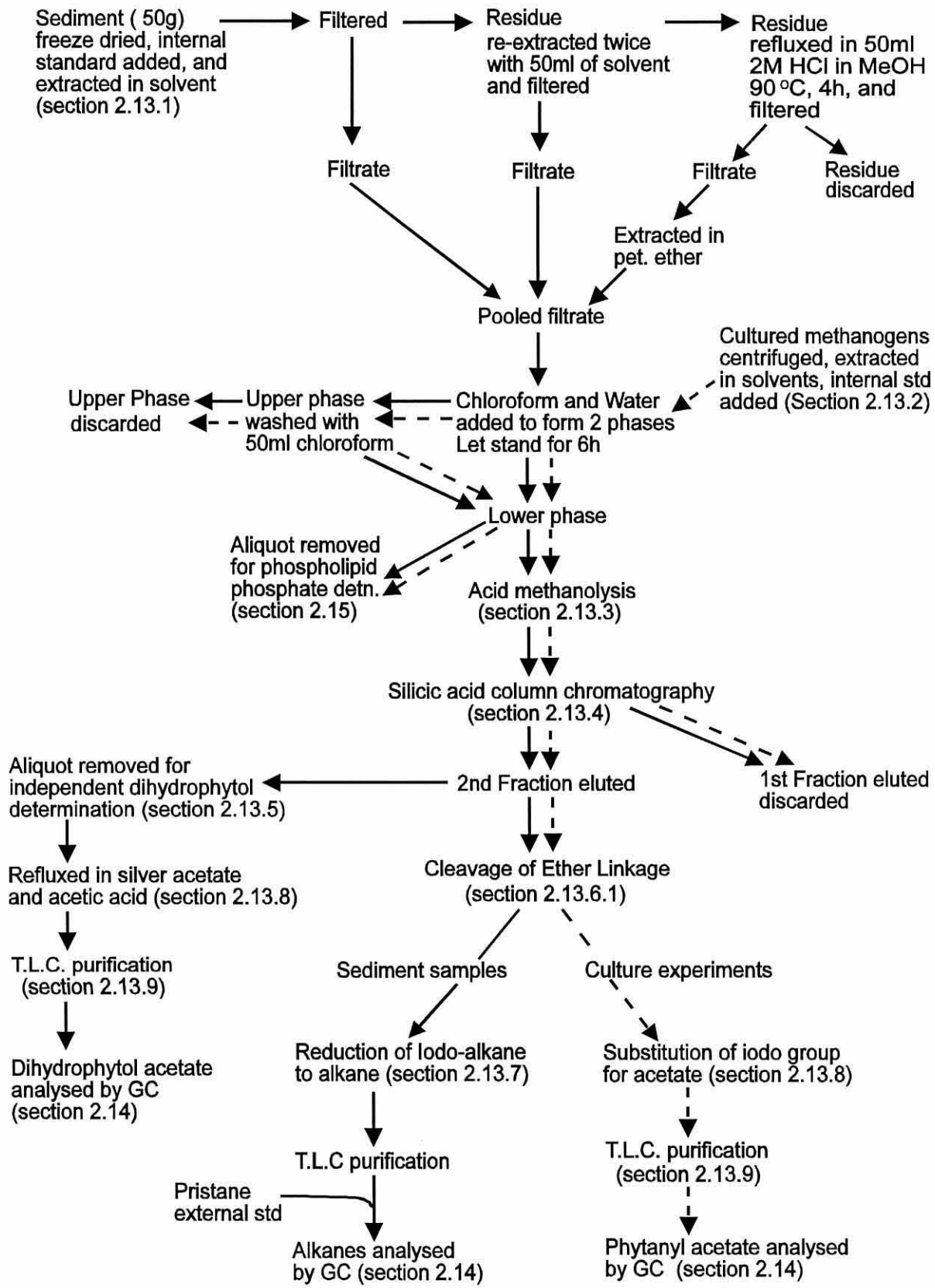


Figure 2.2. Flow diagram of experimental procedure for the determination of methanogenic ether lipids in sediments (—▶) and cultured methanogen samples (- - ▶).

The mixture was shaken in a separating funnel and allowed to settle for 6 h before the lower chloroform phase was removed. A further 50 ml of chloroform was added to the remaining aqueous phase and the mixture was again shaken to remove any lipids from the interface. The pooled chloroform extract was rotary evaporated (Orm Scientific, Buchii) down to 2 ml and either stored in a glass vial under nitrogen at -20 °C until use or transferred directly to a Reacti-vial for the next step of sample preparation. One twentieth (100 µl) of the total extract (2 ml) was removed using a glass micro-pipette and transferred to a 1 ml glass vial for phospholipid phosphate determination as detailed in section 2.15.

2.13.2. Lipid Extraction: Cultured Methanogens

After all prior methane, cell number and turbidity (*i.e.* optical density) analyses were made, the methanogenic cultures were centrifuged at 30,000 r.p.m. (10000 G) (Fisons Plc, MSE superspeed 65) for 20 minutes. The clear supernatant was discarded and the pellet of methanogenic cells was resuspended into a minimal amount of distilled water (4 ml), to which was added methanol (10 ml), chloroform (5 ml) (0.8:2:1) and 50 µg of 1,2 di-*O*-hexadecyl *rac* glycerol internal standard, and the mixture was shaken in a 50 ml separation flask and allowed to stand for 6 h. Addition of chloroform and distilled water (5 ml each) produced the two phases, and the mixture was shaken again and allowed to stand for a further 6 hours. The lower chloroform phase was removed and the upper phase washed with two 10 ml portions of chloroform to ensure good lipid removal from the interface. The total pooled chloroform phase was rotary evaporated almost to dryness, made up to 2 ml, and 200 µl was removed for phospholipid phosphate determination (*i.e.* 1/10th). At this stage lipid samples were either stored at -20°C overnight or continued to the next level of preparation (see figure 2.2).

2.13.3. Acid Methanolysis of Polar Lipids

Kates (1964) recommended using 2.5 % anhydrous methanolic HCl under reflux for 5 h to hydrolyse phosphate esters. This was due to phospholipids with hindered glycerol molecules (*i.e.* dialkyl glycerol ethers as opposed to mono-alkyl analogues) not reacting with hydrated methanolic HCl mixtures. This is the method adopted by Tornabene and Langworthy (1978) and also Pauly and Van Vleet (1986a).

Using the method of Kates (1964) the sample in 2 ml of chloroform was blown down under OFN until dry and 3 ml of the 2.5 % anhydrous methanolic HCl was added to the sample in the Reacti-vial (Phase Separations Ltd.) and refluxed in a Reacti-therm heater (Pierce Ltd) for 5 h.

The 2.5 % anhydrous methanolic HCl was prepared by bubbling HCl gas through re-distilled methanol and dried over anhydrous sodium sulphate ($d=0.796$) (Kates, 1972). The HCl gas was prepared on-line by adding concentrated sulphuric acid to sodium chloride, and letting the gas evolved to bubble through concentrated sulphuric acid. The correct concentration of HCl

gas was calculated by measuring the density of the HCl/Methanol mixture, once excess gas had bubbled (>1.5 l) into the methanol. The solvent was diluted with an appropriate volume of distilled methanol until a density of 0.821 g ml⁻¹ was determined using a balance (Gallenkamp, Mettler H20T) and 10 ml pipette.

Samples were allowed to cool before adding 0.5 ml of 7 M NaOH and refluxing was continued for a further 1 h before transferring the contents to a 20 ml Quickfit tube (Pauly & Van Vleet, 1986a). Approximately 4 ml of petroleum ether and 10 ml of distilled water was used to wash any organic residue from the Reacti-vial to the Quickfit tube. The tube was shaken and mixed on a vortex mixer for 2 minutes. The samples were centrifuged at 2000 r.p.m. (Fisons Plc, Centaur 1 MSE) for 5 minutes in order to partition the ether from the aqueous layer. The upper petroleum ether phase was transferred to a vial using a pipette, and the process repeated twice. The pooled petroleum ether fraction was blown down under nitrogen to a small volume and stored for up to 3 months in 0.5 ml of n-hexane.

2.13.4. Silicic Acid Column Purification of Glycerol Diether and Tetraether Derivatives

Silicic acid was activated by heating to 60°C overnight before the analysis. Columns consisted of 40 cm long, 1.2 cm internal diameter burettes each fitted with a Teflon stopcock and cleaned with chloroform before use. A small amount of solvent cleaned glasswool was used as a plug. A slurry of 8 g silicic acid in 20 ml n-hexane was poured into the burette by displacement of n-hexane (20 ml), while tapping the edges to dislodge any bubbles. After the column was washed with two column volumes of n-hexane the lipid sample was carefully applied to the top of the column (Kates, 1972). All subsequent solvent additions to the top of the column were washed through the original lipid containing vial to ensure that all of the sample was transferred to the column. The initial fraction of the sample was eluted from the column using 100 ml of n-hexane: diethyl ether (95:5).

Toluene was the recommended solvent for the initial fraction elution by Pauly and Van Vleet (1986a). The n-hexane: diethyl ether (95:5) solvent ratio gave similar results to a toluene mobile phase when chromatographing fatty acid methyl esters (FAME's), free bi-DPGE and 1,2-di-*O*-hexadecyl *rac* glycerol ether on TLC plates (Merck, 5x20 cm) and was therefore used as a less hazardous alternative.

The initial (95:5) elution removed the relatively less polar components such as hydrocarbons, FAME's and squalene. The second alcohol fraction (DPGE, bi-DPGE and free dihydrophytol) was eluted from the column using 50 ml n-hexane: ethyl acetate (50:50). Gas chromatography data showed that less than 0.1 % of 1,2 di-*O*-hexadecyl *rac* glycerol ether and 99 % of FAME's eluted with the first (95:5) fraction while 99 % of the ether internal standard and less

than 1 % of FAME's eluted with the second alcohol fraction. Although some of the initial fractions were kept for free phytane analyses by GC (section 2.14), most were discarded. The alcohol fractions were rotary evaporated almost to dryness in a 100 ml round bottomed flask and taken up in a minimum volume of chloroform in a vial.

2.13.5. Dihydrophytol Determination

During the preparation method of the alkane derivatives (section 2.13.7) of the methanogenic ether lipids it is possible that the final phytane derivative may arise from both the plant derivative dihydrophytol as well as from diphytanyl glycerol ether compounds. It was not possible to separate these compounds by column chromatography using dihydrophytol prepared in section 2.13.10. Therefore it was necessary to independently quantify the dihydrophytol as the acetate derivative and subtract this value from the total phytane determined after lithium aluminium hydride reduction. The latter comprised of both the dihydrophytol and diphytanyl glycerol ether lipids.

A sub-sample of the alcohol fraction (second elution of n-hexane: ethyl acetate, 50:50) obtained after column chromatography was taken and treated with acetic anhydride in a Reacti-vial to form the acetates (Pauly and Van Vleet, 1986a). This resulted in the free dihydrophytol acetate, DPGE acetate and bi-DPGE acetate. This reaction did not cleave the isopranyl ether linkages, and therefore resulted in the acetates forming on the free hydroxyl group of all intact glycerol ethers. The DPGE acetate was not volatile enough to be determined directly by GC alone. The dihydrophytol acetate was quantified by GC as detailed in section 2.14.

2.13.6. Cleavage and Substitution of the Ether Lipids

• Using Hydriodic Acid

Approximately 2.5 ml of 47 % hydriodic acid was added to each sample which had been blown down to dryness in a 10 ml Reacti-vial (Pierce Ltd) and refluxed for 12 h at 100°C with intermittent shaking. Each sample was transferred to a 20 ml Quickfit tube using deionised water (10 ml) and petroleum ether (40-60°C) (2 ml) to wash the lipids from the Reacti-vial. The stopper was fitted and the solution mixed thoroughly on a vortex mixer for 1 min. The upper ether phase containing the lipids was removed using a Pasteur pipette into a second Quickfit tube (10 ml). Addition of the 2 ml of petroleum ether was repeated twice and the upper organic phases combined into the 10 ml Quickfit tubes. The addition of deionised water facilitated the transfer of lipids into the organic ether upper phase. The petroleum ether phase was washed with a saturated solution of sodium thiosulphate to remove excess iodine before the upper ether phase was transferred to a separate container. The next derivatisation step depended on whether an acetate (section 2.13.8) or hydrocarbon (2.13.7) derivative was required for GC analysis. All growth experiment samples only required analysis of the diether

lipids present, and in these cases the acetate derivative was prepared for its simpler method of preparation. The determination of tetraether lipids in the sediment samples required that the hydrocarbon derivative should be used to give the best quantification, as detailed in chapter 3.

- **Using Boron Tri-chloride**

The chloro-alkane derivatives of the glycerol ether lipids were prepared by blowing down the ether lipid fraction of section 2.13.4 under OFN, in a Reacti-vial and adding an excess of boron trichloride in chloroform. The mixture was refluxed for 4 h and the products extracted using petroleum ether, as previously detailed.

2.13.7 Reduction of Iodo- Group to Alkanes

Using Lithium Aluminium Hydride

The alkyl iodide fractions that were to be reduced to hydrocarbons with lithium aluminium hydride were transferred to acid washed and chloroform rinsed 10 ml Hungate tubes fitted with Teflon lined plastic screw tops. The Hungate tubes were found to be the best to withstand the high pressures generated during this violent reaction. The solvent was blown down almost to dryness and 2 ml of diethyl ether: chloroform (9:1) was added. Solid lithium aluminium hydride (LiAlH_4) (Aldrich Chemicals) was stored in a desiccator under vacuum with silica gel present to remove any water vapour. All manipulations were made very carefully and within the safety regulations given for the compound. An excess of between 50 and 100 mg of LiAlH_4 was added to the Hungate tubes using a clean dry spatula and the screw tops were inserted immediately. The reaction tubes were placed in a water bath at 90 °C for 1 h and were shaken intermittently. The long reaction time was primarily required to reduce the C40 di-iodide derivatives whereas the C20 mono-iodides would be reduced much faster (Nishihara, pers. comm.). Reaction tubes were allowed to cool to room temperature and placed into an ice bath before the tops were removed and approximately 2-3 ml of distilled water was added dropwise down the edge of the tubes. The tubes were shaken well and centrifuged at 3000 r.p.m. (Fisons Plc, Centaur 1 MSE) for 2 min before the upper petroleum ether layer was removed using a glass Pasteur pipette into a 10 ml glass Quickfit tube. The extraction procedure was repeated twice with two further 2 ml volumes of both petroleum ether and distilled water. The extract was also washed with 2 ml of distilled water before transferring the petroleum ether extract to a clean glass vial (20 ml). The ether phase was blown down under nitrogen and taken up in 100 μl of chloroform before spotting onto a thin layer chromatography (TLC) plate in a similar manner to that of section 2.13.9, except in this case a mobile phase of 100 % n-hexane was used (Kates, 1972). Finally direct injection onto the gas chromatograph was performed from a total volume of approximately 300-500 μl n-hexane (section 2.14).

2.13.8. Substitution of the Halogenated Derivative for an Acetate Ester Functional Group

The DPGE determination of the laboratory grown methanogens required that the phytanyl ether group be substituted for an acetate ester functional group. The alkyl iodides were substituted for an acetate group by blowing down the ether phase in a Reacti-vial and adding 2.5 ml glacial acetic acid and an excess of silver acetate (>0.1 g). The mixture was refluxed at 100°C for 24 h with intermittent shaking (Guyer *et al.*, 1963). Lipid removal and clean up was again repeated with the addition of saturated sodium hydrogen carbonate solution to remove acid, followed by anhydrous sodium sulphate to dry the sample, in a similar manner as detailed in section 2.13.6.

2.13.9. Purification of the Alkyl Acetates

The sample was blown down under OFN and taken up in 100 µl of chloroform and spotted onto a TLC plate (Merck, 20x20 cm). A n-hexane/ether (95:5) mobile phase was used in a continuous co-elution tank for 50 min. Exposure of the phytanyl acetate standard to iodine vapour showed the location of the alkyl acetates which had been covered by another TLC plate during exposure to the degradative iodine vapours. The corresponding areas on the unexposed part of the TLC plate were scraped off (+/- 1 cm) using a scalpel, onto aluminium foil and the lipids were eluted with 5 ml chloroform through a 25 mm GF/F (Whatman) filter paper. The sample was blown down under nitrogen and taken up in 200 µl of n-hexane. The next step was injection onto the gas chromatograph is detailed in section 2.14.

2.13.10. Preparation of the Phytanyl Acetate Standard

Phytol was the starting compound in the preparation of the phytanyl acetate standard. Dihydrophytol derivative was prepared by bubbling hydrogen gas through a glass Pasteur pipette into a solution of phytol (100 mg), platinum dioxide (Adam's Catalyst) (50 mg) and methanol (50 ml) in a 100 ml pear shaped flask with a condenser fitted to the top (Guyer *et al.*, 1963). The dihydrophytol product was washed through a pre-washed silicic acid column (section 2.13.4) with chloroform to separate from the fine platinum powder. The acetate functional group was substituted for the alcohol group using the methods detailed in sections 2.13.6 and 2.13.8.

2.13.11. Preparation of Penta-Fluoro Propionyl Derivatives for Analysis By GC/ECD.

The preparation of pentafluoropropionyl derivatives of the iodoalkane derivatives (section 2.13.6) proceeded via the alcohol derivative. The alcohol derivatives were prepared by adding approximately 0.1 g silver nitrate and 2 ml industrial methylated spirit to the iodoalkane derivatives in a Reacti-vial and placing at 30 °C for 24 h. The products were extracted in petroleum ether after the addition of distilled water. Preparation of hexadecan-1-ol using 1-

iodo-hexadecane standard in this manner revealed approximately a 90 % yield using gas chromatography with flame ionisation detection.

The pentafluoropropionyl derivatives were prepared by blowing down the alcohol derivatives under OFN in a Reacti-vial and adding an excess of pentafluoropropionyl anhydride in pentafluoropropanol, and refluxing for 2 h. The products were extracted in several small quantities of petroleum ether after adding distilled water. The pooled ether extract was washed three times with distilled water to remove the last traces of reactants. The petroleum ether extract was blown down under OFN and taken up in n-hexane for analysis by gas chromatography using electron capture detection (section 2.14).

2.14. Gas Chromatography

The determination of the lipid concentrations was completed on a range of gas chromatographs, which depended both on the availability and whether the instrument was up and running. The GC's that are presented in this section include the instruments from which experimental results were presented. It should be noted, however, that two other GC's were also available and required significant time and effort to obtain meaningful information from them. But this proved unsuccessful and those GC's are not presented in this section. Overnight column conditioning was required when transferring capillary columns between instruments.

Phytanyl acetate derivatives of the di-phytanyl glycerol ether lipid from the *Methanobolus tindarius* growth experiment were analysed on a Carlo Erba (HRGC 5160) gas chromatograph.

Phytanyl acetate measurements for the *Methanococcoides methylutens* growth experiment were performed on a Carlo Erba (HRGC 3160) gas chromatograph with a Hewlett Packard Ltd integrator, model 3390A. A flame ionisation detector (FID) (350 °C) and an on-column injector were used with a 30 m column, 28 KPa nitrogen carrier, 20 KPa nitrogen (make-up), 50 KPa hydrogen, 100 KPa air, and an oven program 60 to 220 °C at 10 °C min⁻¹, 220 to 300 °C at 5 °C min⁻¹, and hold for 30 min.

For the growth experiment using *Methanosarcina acetivorans* the phytanyl acetate products were analysed on a Carlo Erba gas chromatograph (HRGC 4160) with a spectra physics S4070 integrator. An FID (350 °C) and an on-column injector with a 30 m SE30 column, 20 KPa hydrogen (carrier), 50 KPa hydrogen (detector), 100 KPa air and an oven program 60 to 220 °C at 10 °C min⁻¹ (hold for 5 min) 220 to 225 °C at 0.5 °C min⁻¹ and 225 to 300 °C at 10 °C min⁻¹ (hold for 10 min).

A significant amount of time (~ 6 months) was also spent trying to convert the DANI GC used for methane determinations (section 2.4.3) from the existing packed column set-up to a capillary column set-up in order to facilitate the ether lipid analyses. This proved unsuccessful.

For the Holyhead and intertidal sediment analyses phytane and dihydrophytol acetate determinations were performed on a Carlo Erba gas chromatograph (GC 6000, Vega series with ICU 600) with a S4070 Spectra Physics integrator. This GC could only be used out of regular working hours which required repeated transfer of capillary columns, short conditioning runs and standard calibration before analysis could commence. The instrument also had to be returned to its original set-up at the end of each experimental period. An FID (350°C) and an on-column injector with a 10 m SE30 column, 20 KPa hydrogen carrier, 50 KPa hydrogen detector, 100 KPa air. Pristane external standard (137.3 ng) was added to quantify the yield and hence dihydrophytol concentration.

DPGE acetate and bi-DPGE di-acetate were prepared simultaneously when producing the dihydrophytol acetate derivative of the sub-sample measured in section 2.13.6. Similar attempts to quantify the DPGE acetate directly by GC, as achieved by Pauly and Van Vleet (1986a), proved unsuccessful due to the very low volatility ($C_{45}O_4H_{92}$) of the derivative, as discussed in chapter 3.

Analysis of the ether lipid derivatives sensitive to electron capture detection, and initial phytanyl acetate determinations of the intertidal core were made on a gas chromatograph obtained from ESSO Chemicals Ltd (Abingdon, Oxfordshire). The instrument was a Pye Unicam GCV gas chromatograph with an FID. The ECD was purchased from Phillips Scientific and the on-column injector was taken from the DANI gas chromatograph which could only be used with the splitless injection port for methane analysis. A nitrogen make-up gas was separately installed to the base of the FID within the oven, using low volume stainless steel fittings (Phase Separations Ltd.). The nitrogen gas line was fitted with a puritube, silica gel filter and an oxy-trap (Phase Separations Ltd.). Gas pressures were: nitrogen carrier (2.0 ml min⁻¹); nitrogen make-up (FID) (28 ml min⁻¹); nitrogen make-up (quench) (33 ml min⁻¹); air (FID) (300 ml min⁻¹); hydrogen (FID) (33 ml min⁻¹).

2.15. Phospholipid Phosphate Determination

Concentrations of phospholipid phosphate were determined by the method of Findlay *et al.* (1989). 20 µl of the original 50 µl aliquot of sample set aside for the phosphate determination (section 2.13.3) was transferred to a 2 ml glass ampoule and blown down under OFN. To this was added 0.45 ml of a saturated solution of potassium persulphate in 0.36 N sulphuric acid, which under low pH acts as a strong oxidant. The ampoules were then flame sealed and kept at 95°C overnight. The phosphate released was determined by adding a solution of 0.1 ml

ammonium molybdate (2.5 % in 5.72 N sulphuric acid) which was allowed to stand for 10 min. To this was added 0.45 ml of a solution of malachite green and 100 % hydrolysed polyvinyl alcohol in water (Van Veldhoven & Mannaerts, 1987) and the solution was allowed to stand for a further 30 minutes.

The absorbance at 610 nm was determined for each sample relative to a deionised water blank on a diode array spectrophotometer (Hewlett Packard Ltd, Vectra ES/12). Between 1 and 20 nmol of phosphate was required to remain within the proportionality of Beer Lambert's Law, although standards revealed that proportionality was still maintained up to an absorbance greater than 1.5 units. The method was repeated if samples were above the 20 nmol limit by using appropriate dilutions of the remaining 30 μ l aliquot of sample. If all the phosphate concentrations were less than 1 to 2 nmol then the total aqueous phase from the acid methanolysis stage could be analysed (section 2.13.3), by evaporation at 60 °C, placing in an ampoule and preparing the sample as in the method detailed above for phosphate analysis. This was a slight difference to the method of Findlay *et al.* (1989) where intact phospholipids in chloroform were used, and had the advantage of not requiring part of the lipid sample when concentrations of the lipids and phospholipid phosphate were low. The results using this method were consistent with phospholipid phosphate determinations of intact glycerol ethers. All calibration data for the determination of phosphate from phospholipids, and acid methanolysis products of organic phospholipids, as well as comparison with inorganic phosphate concentrations are given in section A5.1 and table A5.1.1 of appendix V.

2.16. Infra-Red Spectrophotometry.

Lipid standards obtained from both cultured methanogens and as gifts from Dr M. Nishihara, Dr A. Gambacorta and Dr M. Kates required further purification by TLC before derivatisation and analysis by GC and GC/MS. Due to the parent lipids (DPGE and bi-DPGE) having a very low volatility, mass spectrometry proof of structure was only possible when the lipids were broken down into smaller derivatives. The only structural analyses that could be made on the parent lipid complexes was by infra-red spectrophotometry. The instrument used was a Perkin Elmer 1600 series Fourier Transform Infra-Red (FTIR) spectrophotometer. Lipid standards in carbon tetrachloride (CCl_4) were applied to potassium bromide discs using small glass capillaries. Concentration of the sample was made by allowing the CCl_4 to evaporate off before re-applying the next sample. Each sample was analysed using 16 scans with a sensitivity of 2 and a resolution of 4 wavenumbers.

2.17. Mass Spectrometry.

The mass spectrometer used for most of the analysis of environmental samples towards the end of the experimental period was a Finnigan MAT 4600 quadrupole system located at the School of Ocean Sciences, Menai Bridge. An ionisation voltage of 70 eV and temperature of 150 °C

was used for electron ionisation (EI) conditions and methane was the gas used for the chemical ionisation (CI) of the ether lipid derivatives. An INCOS data system was used to interpret and manipulate the data. Details of the MS at the Chemistry Dept, U.C. Wales; Bangor and the SERC facility at the Chemistry Dept, U.C. Wales; Swansea are given in the relevant method development sections of chapter 3.

CHAPTER 3. QUANTIFICATION OF THE METHANOGENIC ETHER LIPIDS.

3.1. Introduction.

Methanogenic membrane lipids are large, polar molecules that generally consist of two main structures; the diethers and tetraethers. The diethers consist of two phytane (C₂₀ isoprenoid) molecules bonded, via two ether linkages, to a glycerol backbone. The tetraethers consist of two biphytane (C₄₀ isoprenoid) molecules bonded, via four ether linkages at both ends of each chain, to two glycerol molecules. Other tetraether lipids detected in methanogens are similar but contain cyclopentyl ring structures within the alkyl chains. The structures of these archaeobacterial lipids have been given in figure 1.1 of chapter 1.

By determining the concentrations of these lipids it has been shown that it is possible to assess the biomass/necromass of methanogenic bacteria in sewage digester samples (Hedrick *et al.*, 1991b; Nichols *et al.*, 1987), marine sediments (Pauly & Van Vleet, 1986b; Pease *et al.*, 1992; Martz *et al.*, 1983) and also to differentiate terrestrial from marine depositional environments in geologically dated cores (Chappe *et al.*, 1982; Pauly & Van Vleet, 1986b).

A method that has been established for quantifying the intact diether and tetraether lipids from environmental samples uses high performance liquid chromatography (HPLC) (Martz *et al.*, 1983). HPLC is a technique which uses polar solvents to elute high molecular weight, nonvolatile compounds from a column. Martz *et al.* (1983) developed a method of analysing the intact diether and acyclic tetraether molecules as the *p*-nitrobenzoyl esters by HPLC. The determination of intact ether lipids by HPLC was not attempted in this study for the following reasons: (1) The determination of tetraethers containing cyclopentyl ring structures has yet to be demonstrated by HPLC (Nichols *et al.*, 1987), (2) The method of interfacing HPLC with mass spectrometry is a relatively recent science, hence very difficult to achieve, and was not available for this research. Therefore absolute confirmation of the identity of the peak would be difficult to confirm with comparisons of retention time alone and would also require pure standards for all compounds that would be studied. This would therefore be difficult for some of the cyclic tetraether lipids detected.

The tetraether lipid molecules are large and non-volatile and can not be measured directly by gas chromatography. Pauly and Van Vleet (1986a) reported that it was possible to quantify

concentrations of the intact diphytanyl glycerol diether once the polar hydroxyl group was substituted by an acetate derivative. However, such large molecules (*i.e.* C₄₅O₄H₈₈, Mw = 697) elute from the chromatography column as a much broader peak than components of lower boiling point. Components with larger peak widths will have a greater probability of not being fully resolved from other compounds of comparative retention, especially in environmental samples. The tetraether methanogen lipids (C₈₆O₆H₁₇₂, Mw = 1302) are much less volatile than the diether lipids and so would not elute from a gas chromatography column operating at its maximum temperature, due to the temperature limitations of the stationary phase.

The very low volatility of the intact glycerol ethers meant that in order to determine the concentration of archaeobacterial lipids by gas chromatography, it was necessary to prepare derivatives of the larger molecules which had a lower boiling point and higher volatility. The isoprenoid hydrocarbon chains are characteristic derivatives of the intact ether lipids of methanogenic bacteria. However, when analysing representative parts of the original intact molecule there is always a risk that the final derivative will resemble other non-methanogenic lipids. Fortunately, the isoprenoid chains of methanogenic bacteria are not commonly found in the analogue ester linked membrane material of eubacteria or eukaryotes. However, petroleum residues contain significant amounts of the isoprenoids phytane and biphytane, which are also bound to larger molecules as with the methanogenic lipids (Moldowan & Seifert, 1979; Chappe *et al.*, 1982). Such isoprenoids in the petroleum originate from diagenetically and catagenically altered lipids of ancient archaeobacterial populations (Moldowan & Seifert, 1979). Hence, for the purpose of this work any isoprenoids that were not bonded via ether linkages to glycerol molecules before derivatisation were considered not to represent recent populations of archaeobacteria. Therefore it was necessary to remove such non-bonded isoprenoids components from the sample before the ether linkages of the methanogenic bacteria were cleaved, *i.e.* during the sample purification steps (see section 2.13.4). After completion of these purifying steps, any remaining isoprenoid derivatives must have originated from the ether linked lipids of the archaeobacteria. More specifically, if the samples were collected from mesophilic marine sediments then the derivatives should represent the methanogenic class of archaeobacteria.

A number of different types of derivatives have been used when attempting to identify the isoprenoids by gas chromatography and GC/MS. These have included; alkyl iodides (De Rosa *et al.*, 1986b; Pauly & Van Vleet, 1986a) alkyl chlorides (De Rosa *et al.*, 1983; Nishihara & Koga, 1987, 1988), alkyl acetates (Pauly & Van Vleet, 1986a; Tornabene & Langworthy, 1978) and the reduced alkanes (Harvey *et al.* 1986; Vella & Holzer, 1990; Nishihara & Koga, 1988). However, when concentrations of the ether lipid derivatives need to be quantified in environmental samples, it is important to determine which derivative gives the most reliable

results. Clearly the quantification of the derivative chosen as the indicator must reflect as accurately and precisely as possible the amount of ether lipid, and hence methanogen biomass, in the sample. For these reasons, the aims of this chapter were to evaluate and develop derivatisation procedures as follows:

- (1) To provide a method that would monitor the variation in yield of the ether lipids due to inconsistent extraction and sample work-up procedures (section 3.2).
- (2) To provide a semi-qualitative proof of structure of the intact ether lipid molecules before derivatisation to smaller more volatile components (section 3.3.1).
- (3) To determine which isoprenoid derivative of the ether lipids give the most quantitative results with GC/FID, and to confirm with mass spectral proof of structure of lipid standards and lipids isolated from marine sediments (section 3.3.2).
- (4) To attempt to prepare a derivative sensitive to electron capture detection by gas chromatography in order to increase the sensitivity of the method (section 3.4).

3.2. Reproducibility of Ether Lipid Extraction from Sediments.

In order to ensure that the ether lipid concentrations can be compared in a quantitative manner between different samples and possibly also between other researchers, it is necessary to provide a reproducible method that is not sensitive to experimental inconsistencies.

3.2.1. Selection of an Internal Standard

The use of an internal standard to follow the organic components through the extraction, clean-up and derivatisation stages is important to monitor the reproducibility of the method. The internal standard should ideally experience the same proportional losses of the sample lipids, and if the final concentration of the internal standard is known, then losses of other lipids in the sample can be calculated. The choice of internal standard is therefore of prime consideration. The standard should be chemically similar to the lipid being quantified so that extraction yields are comparable, and also the standard should not be normally present in the sediment sample, otherwise only semi-quantitative results will be obtained.

Nichols and his colleagues (1987) showed that the most appropriate internal standard for the methanogenic ether lipids was 1,2 di-hexadecyl *rac* glycerol diether (Sigma Chemicals Ltd). The ether linkages of this internal standard resist the mild hydrolysis conditions used to separate the ester linked glycerides from the ether lipid fraction. The internal standard is chemically synthesised (Sigma Chemicals Ltd) and has not been detected naturally in the environment. The fact that the alkyl chain length of the standard is 4 carbons less than the phytanyl chain (diether) and 24 carbons less than the biphytane (tetraether) derivative might cause significant differences between the solubility and vapour pressures of the standard and sample lipids. Since larger ether lipid standards were not available it was considered necessary to minimise these solubility and vapour pressure effects by not completely evaporating the sample down to dryness, and also by washing any organic-aqueous partition at least three times with solvent.

The major difference between the internal standard and the sample ether lipids is the hydrophilic polar headgroup found on the methanogenic diether and tetraether lipids. Lipids containing polar phosphate headgroups have an interaction with various cations in the sediments. Since the internal standard is without polar headgroups, there is a danger of underestimating the true methanogenic lipid concentration. To minimise this possible cause of underestimation, sediment samples were thoroughly extracted with solvents (section 2.13.1) also using acid to increase yields from the pre-extracted sediment residue in some of the more consolidated sediments (section 2.13.1).

It was not possible during the analysis to separate the ether lipid components from a non-methanogenic lipid of plant origin (dihydrophytol), which interfered with the quantification of

the methanogenic diether lipid. It was therefore necessary to independently quantify the concentration of the dihydrophytol lipid and to subtract this from the total ether lipid derivative plus dihydrophytol determination (section 2.13.5). For this reason it was necessary to determine the yield of each extraction by using an external standard (pristane; C₁₉H₄₀) which was added to the lipid sample before injection onto the gas chromatograph.

3.3. Characterisation and Quantification of Ether Lipids.

Section 3.1 highlighted that due to the low volatility of the intact glycerol ethers it was not possible to analyse the whole tetraether lipids by gas chromatography, and therefore structural analysis by GC/MS is made very difficult. Direct insertion of TLC pure, tetraether lipids into the mass spectrometer, via the rapidly heating probe also did not reveal any structural information in this study.

3.3.1. Infra-red Determination of Intact Glycerol Ethers

Difficulties in analytically identifying such molecules can be partially overcome by obtaining at least a semi-qualitative determination of the identity of the component, before the molecules are broken up and the derivatives analysed more closely. This can be achieved by Fourier transform infra-red spectrometry (FTIR). Fourier transform infra-red spectrometry (FTIR) identifies the functional groups present in a molecule, providing it is in a pure state. Since a pure isolation of the ether lipids is difficult to achieve directly from extracted sediment samples the following infra-red spectra were obtained from the TLC pure ether lipids of cultured methanogens.

The details regarding to the FTIR spectrophotometer and the procedure used are given in section 2.16 of chapter 2. An infra-red spectrum of the hydrolysed, TLC pure, tetraether lipid which was a gift from M. Nishihara (Japan) is given in figure 3.1a. A spectrum of the diether extract isolated from *Methanlobus tindarius* and purified by TLC is given in figure 3.1b. Both infra-red spectra suggest the following functional groups: free -O-H (3583 cm⁻¹): C-H stretch of CH₂ and CH₃ (2926, 2868 cm⁻¹): C-H bend of CH₂- and CH₃- (1462, 1377 cm⁻¹), C-O stretch of ether (1113 cm⁻¹). The strong C-Cl stretch (783 cm⁻¹) of the carbon tetrachloride solvent probably masked the C-H bend at approximately 720 cm⁻¹. These spectra were indicative of isopranyl glycerol ethers and show similar absorbances to those reported by Kates *et al.* (1964) and Tornabene and Langworthy (1978). The spectra were also similar to the FTIR spectrum of the internal standard, 1,2-di-*O*-hexadecyl *rac* glycerol given in figure 3.1c, except that a small contamination peak of C=O stretch (1736 cm⁻¹) was observed with the internal standard, possibly an artifact from manufacture.

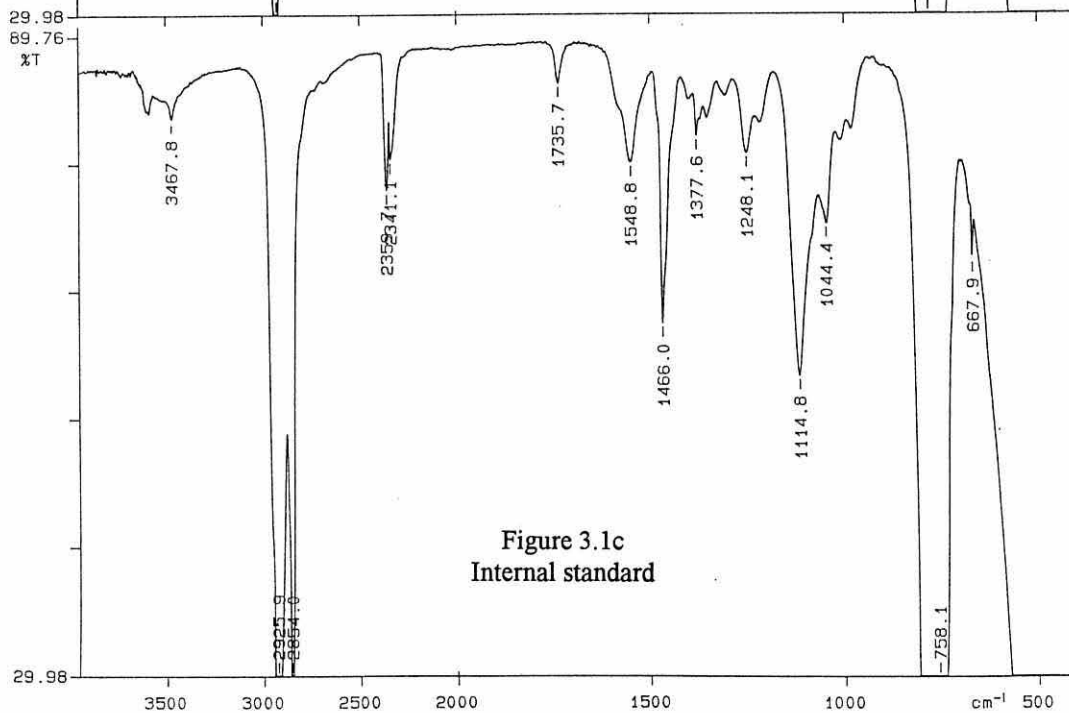
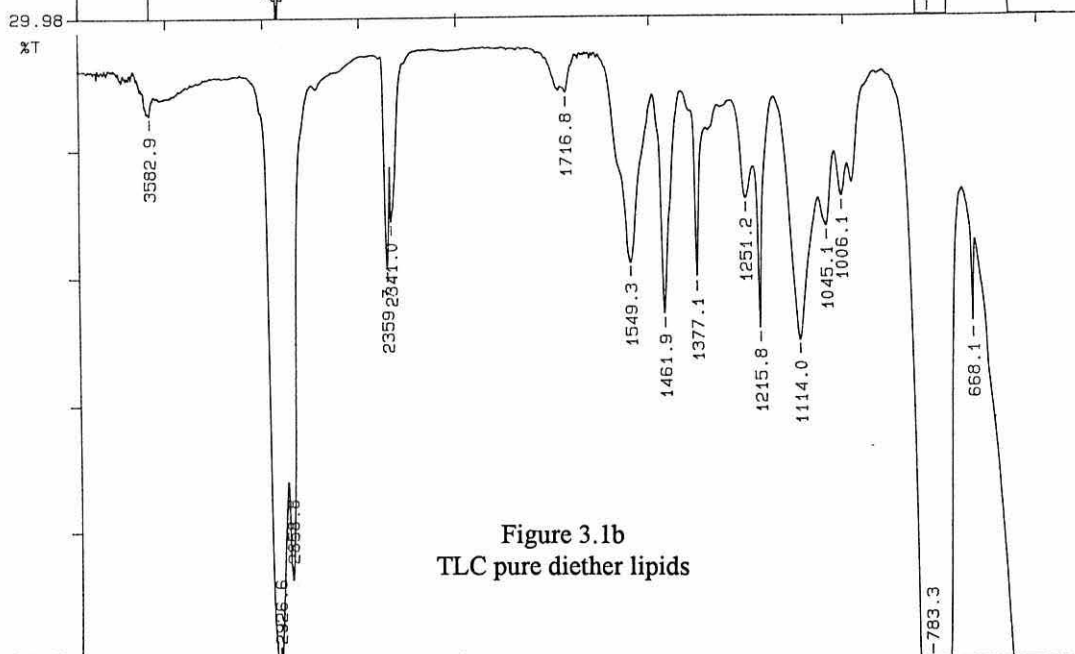
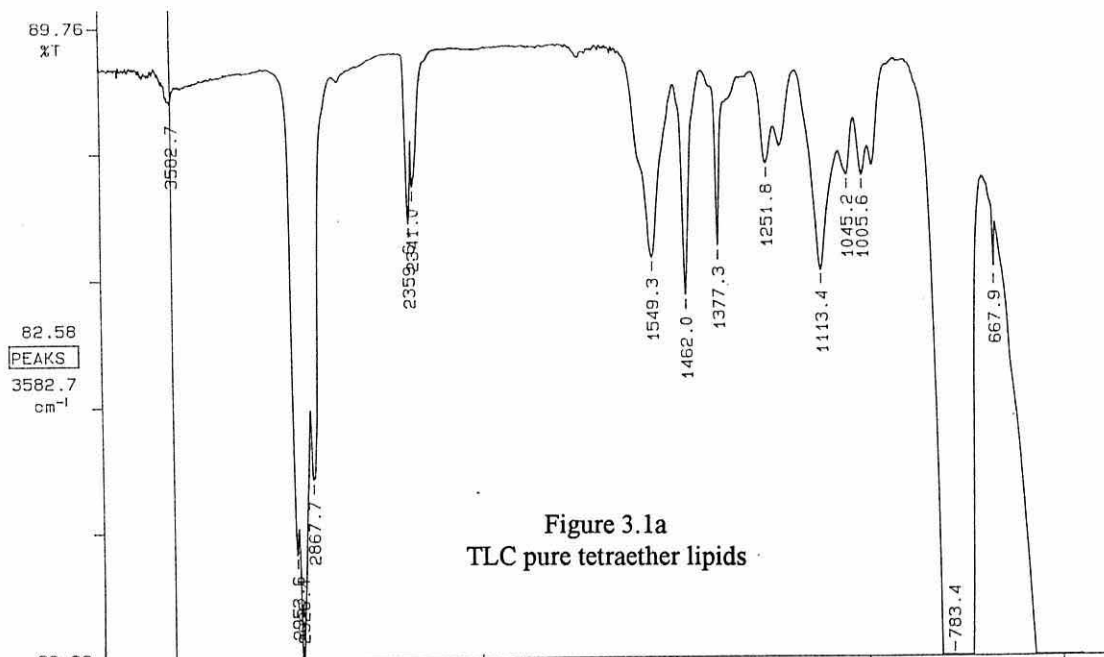


Figure 3.1. FTIR spectra of TLC pure tetraether lipids (figure 3.1a), diether lipid isolated from *M.tindarius* (figure 3.1b), and the internal standard 1,2-hexadecanyl *rac* glycerol ether (figure 3.1c).

3.3.2. Quantitative Determination of Ether Lipid Derivatives by GC/FID.

Initial work concentrated on determining which ether lipid derivative gave the most quantitative results by gas chromatography. The preparation of ether lipid derivatives were initially carried out on the internal standard material 1,2 di-*O*-hexadecyl *rac* glycerol diether due to its purity and the quantity available. If the derivative proved successful, with high yields and consistent elution on the gas chromatograph, then the methods were repeated using biogenic glycerol ether standards. The biogenic standards were either isolated from pure cultures of *Methanobolus tindarius* (diether) or received as gifts (tetraethers) from E. Van Vleet (Florida, USA), A. Gambacorta (Naples, Italy) and M. Nishihara (Kitakyushu, Japan).

3.3.2.1. Analysis of Alkyl-Halogen Derivatives

The ether linkages of diether and tetraether lipids are not as prone to nucleophilic attack as are the ester linked analogues and are not cleaved under the mild hydrolysis conditions that are commonly used to cleave ester linkages. The strong hydrolysing reagent used to break the ether linkages was hydriodic acid (section 2.13.6) (Guyer *et al.*, 1963). The determination of tetraether lipid concentrations using the C₄₀ di-iodide derivatives by gas chromatography has been reported (Pauly & Van Vleet, 1986a; De Rosa *et al.*, 1986b).

Analysis of the 1 iodo-hexadecane derivative of the internal standard by GC/MS (Electron Ionisation) showed a molecular ion of m/e 352 and a partially split RIC peak, as given in figure 3.2. Repetition of this procedure for the 1-iodophytane derivative did not give a molecular ion of m/e 408 by GC/MS (EI) on a number of runs, only the m/e 281 ion of the alkane. The production of a molecular ion by electron ionisation GC/MS can be difficult for a derivative containing an iodide group.

Therefore to determine whether the molecular ion was still complete on entering the mass spectrometer, milder ionisation MS procedures were used on the derivative as conducted by the SERC Chemistry Dept, U. C. Wales; Swansea. Analysis by both electron ionisation (figure 3.3A) and fast atom bombardment (FAB) did not show the m/e 408 molecular ion, but with low resolution chemical ionisation (NH₃) MS it was possible to detect the molecular ion of the 1-iodophytane derivative, as given in figure 3.3B.

Gas chromatography of this derivative was conducted after the mass spectral techniques had been performed due to the unavailability of a gas chromatograph. Subsequent gas chromatography demonstrated that the retention times of the 1-iodophytane derivative tended to vary for a constant temperature program and split peaks were also observed. This suggested that the iodide atom could become detached from the molecule within the capillary column of the gas chromatograph, which would be undesirable when relying on constant retention times to identify such peaks within environmental samples.

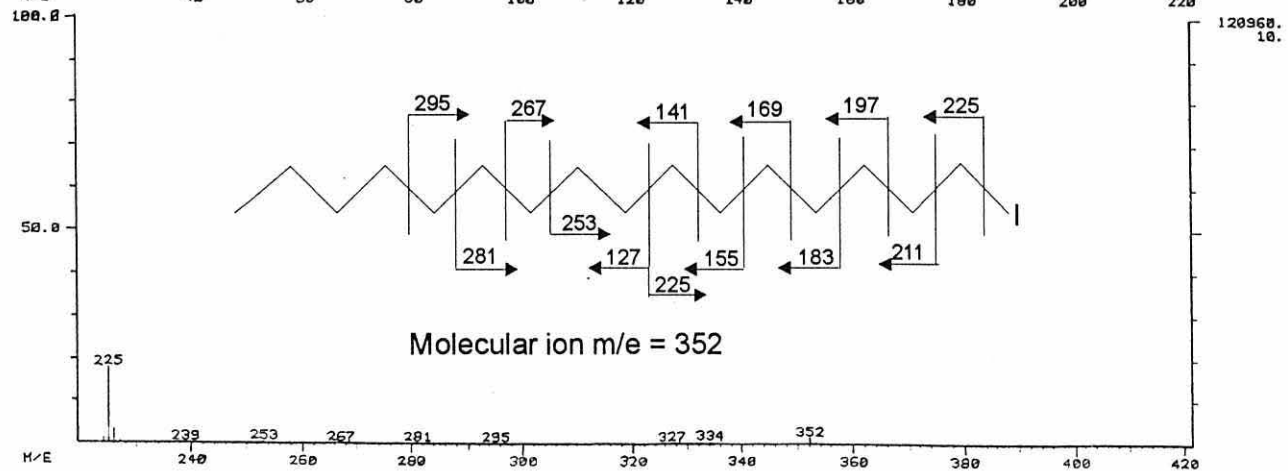
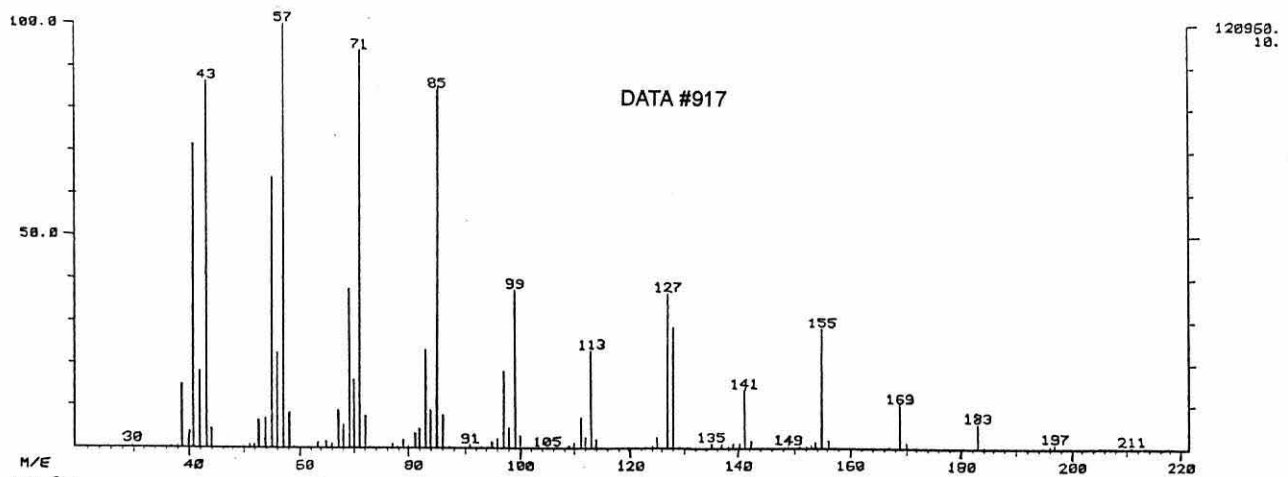
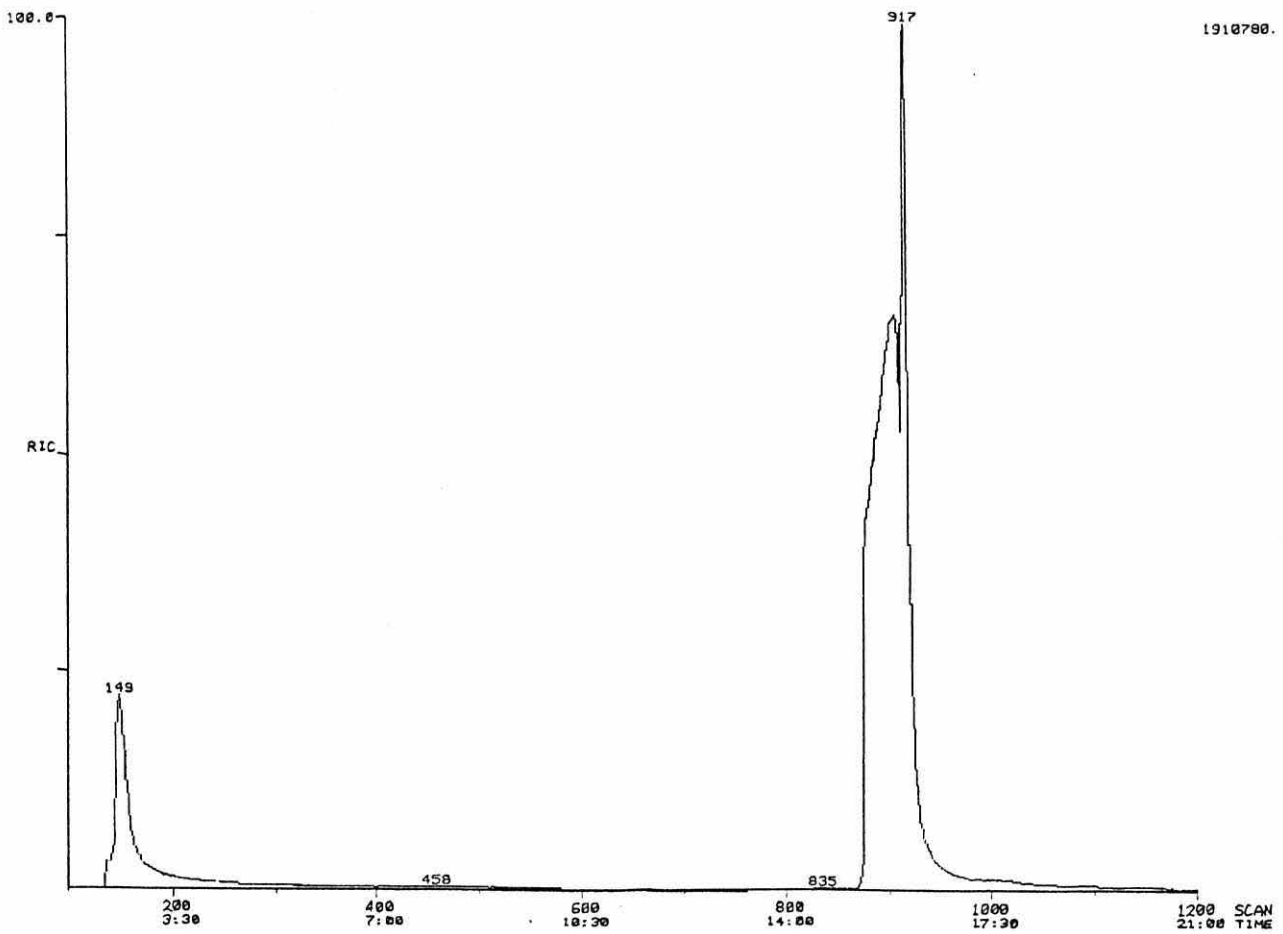


Figure 3.2. GC/MS (electron ionisation) spectrum of the ether cleavage product of the internal standard material using hydriodic acid. Fragmentation data indicates that both parts of the split RIC peak have a molecular ion of m/e 352, which corresponds to the 1-iodohexadecane derivative.

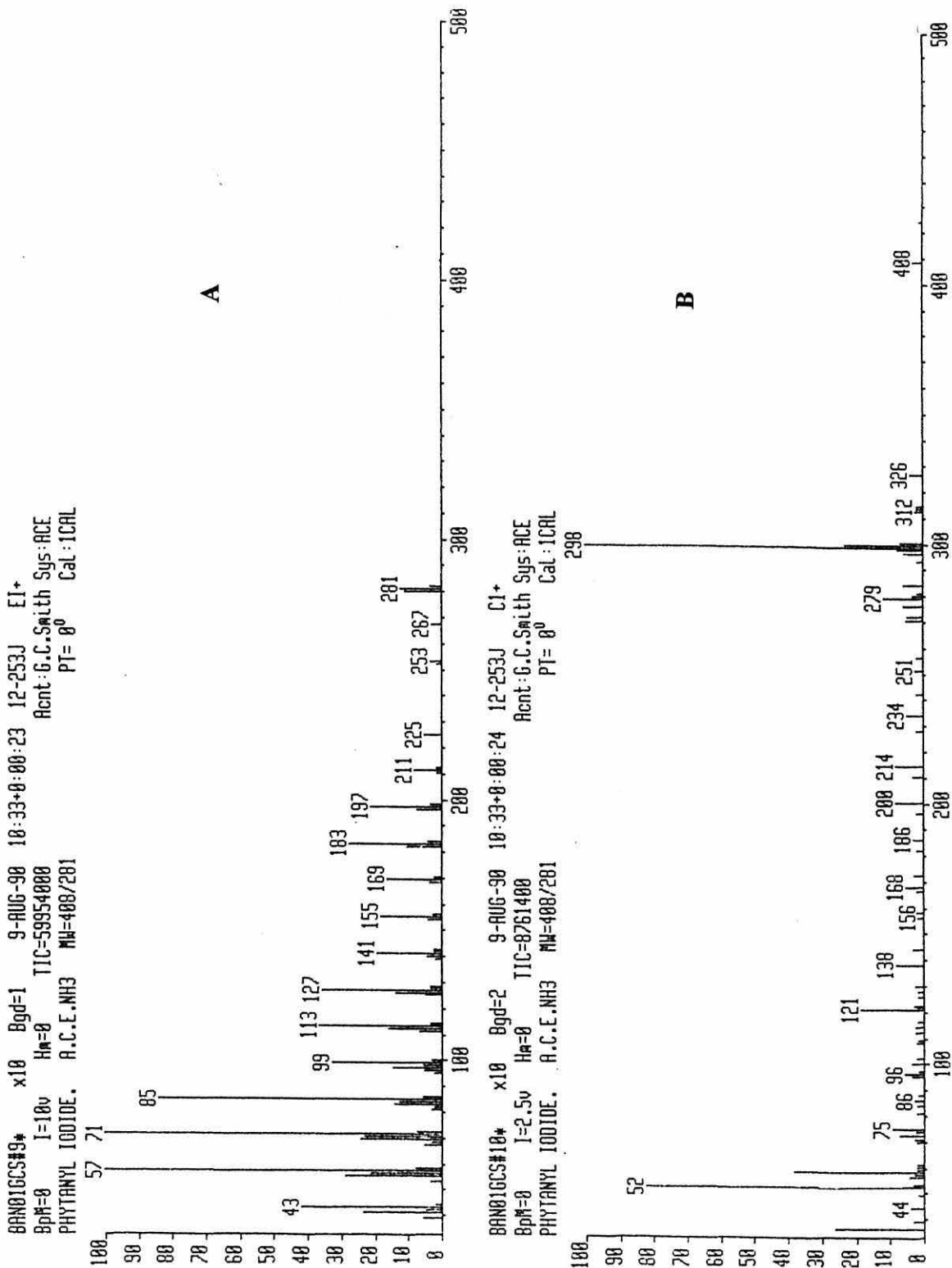


Figure 3.3. Mass spectra of 1-iodophytane. The electron ionisation spectrum (A) shows a molecular ion of m/e 281 corresponding to phytane whereas the low resolution chemical ionisation (NH_3) spectrum (B) indicates a molecular ion of m/e 408 corresponding to the 1-iodophytane derivative.

Nishihara (*pers. comm.*, 1991) suggested that such problems are common when trying to use the iodo-derivatives, probably due to the strong adsorption to the liquid phase of the capillary column. Analysis of the C40 di-iodide derivative by gas chromatography was expected to show even greater retention time and peak area variation due to the much higher temperatures required to elute the molecule from the column, and so analysis of this derivative was not attempted. Although Pauly and Van Vleet (1986a) used the iodo-derivatives for quantitative determination of both the phytane and biphytane derivatives, Tornabene and Langworthy (1978) used the iodo-derivatives only for diether products and changed to acetate or alkane derivatives when analysing the tetraethers by gas chromatography.

Other ether cleavage reagents were used in the attempt to make a derivative that would give better quantification on the gas chromatograph (section 2.13.6.). Boron trichloride in chloroform was used to form the 1-chloro-hexadecane derivative (m/e 260) of the internal standard (Gerrard & Lappert, 1952; Kates *et al.*, 1964). Such derivatives have been used when identifying isoprenoid ether lipids in thermoacidophiles (De Rosa *et al.*, 1983). The mass spectrum (EI) of the total ion count showed a split peak corresponding to a low yield of approximately 60 % chloro-hexadecane, as shown in figure 3.4. The boron trichloride cleavage procedure provided a low yield of chloro-alkane and the chloride atom was also a more difficult leaving group than the iodide for the subsequent derivatisation reactions, therefore for these reasons all future methods proceeded via the hydriodic acid ether cleavage method.

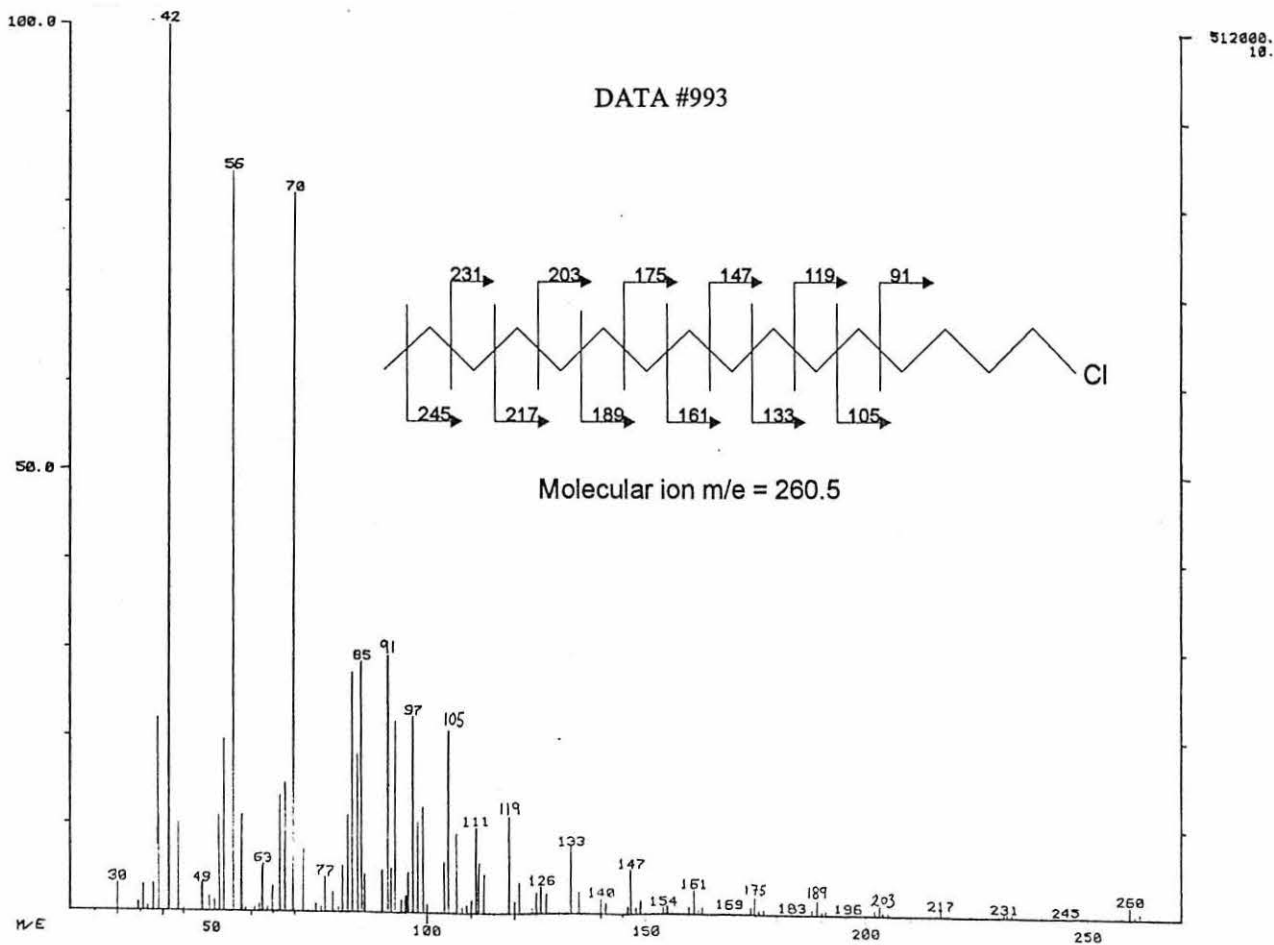
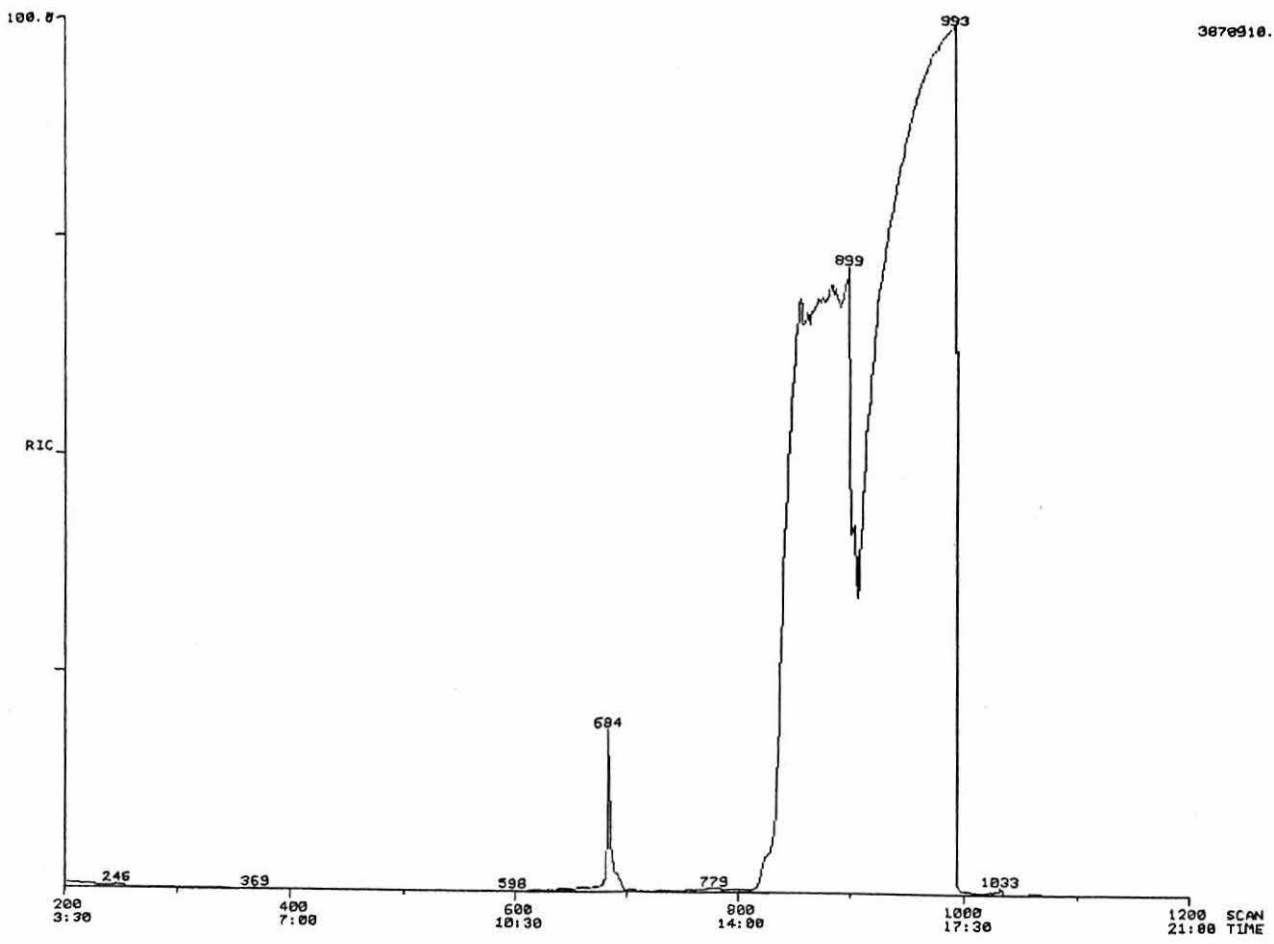


Figure 3.4. GC/MS (electron ionisation) spectrum of the ether cleavage product of the internal standard material using boron trichloride. Fragmentation data of the split RIC peak indicate that peak #993 is the 1-chloro-hexadecane derivative whereas peak #866 indicated a hexadecane product.

3.3.2.2. Analysis of Acetate Derivatives

The conversion of the iodo-alkane derivatives with silver acetate in acetic acid to the alkyl acetate (see section 2.13.8 of chapter 2) for analysis by gas chromatography has been reported (Kates *et al.*, 1964; Tornabene & Langworthy, 1978). Mass spectra (EI) of phytanyl acetate (figure 3.5A) and acyclic biphytanyl di-acetate (figure 3.5B) with one (figure 3.6A) and two (figure 3.6B) cyclopentyl ring equivalents are given with representative diagrammatic molecule fragmentations in the respective figures. Molecular ions of the phytanyl acetate (m/e 340) and the following di-acetates; acyclic biphytanyl (m/e 679), 1 cyclopentyl biphytanyl (m/e 677) and 2 cyclopentyl biphytanyl (m/e 675) are all shown by GC/MS (EI).

Analysis of the phytanyl acetate derivatives by gas chromatography gave good reproducible peak areas. However, when analysing the biphytanyl di-acetate derivatives, inconsistent peak areas were observed, often with the component not being detected at all. This was thought to be due to breakdown on the column at the high temperatures required for analysis and so a shorter 5m SE30 capillary column was recommended (Kates, *pers. comm.*, 1992). The shorter column helped to improve peak reproducibility but it was still noted that peaks sometimes consisted of smaller split peaks with two or more retention times even when using low sensitivity peak threshold values. Moreover peaks did not always elute from the column. An example of the retention times and peak areas encountered for one of the more optimum set of oven temperature programs (*i.e.* 30 to 220 °C at 10 °C min⁻¹, 220 to 320 °C at 6 °C min⁻¹) for both the phytanyl acetate and biphytanyl di-acetate standards is given in table 3.1.

Table 3.1. Peak area and retention time data for phytanyl acetate and biphytanyl di-acetate derivatives for six sequential runs on the gas chromatograph using a 30m SE30 column.

Run No.	Phytanyl acetate derivative		Biphytanyl diacetate derivative	
	Retention Time (mins)	Peak Area (units)	Retention Time (mins)	Peak Area (units)
1	25.33	105162	42.01	142803
2	25.38	106062	44.73*	84058*
			44.83*	17178*
			44.89*	33614*
3	25.37	108915	n.d.	n.d.
4	25.30	100054	42.00	133392
5	25.27	97397	42.04	132552
6	25.29	101162	n.d.	n.d.
Coefficient of Variation	0.2%	4.2%		77.6%

n.d. = not detected

* Component chromatographed as split peaks, therefore totaled values used for the calculation of coefficient of variation (%).

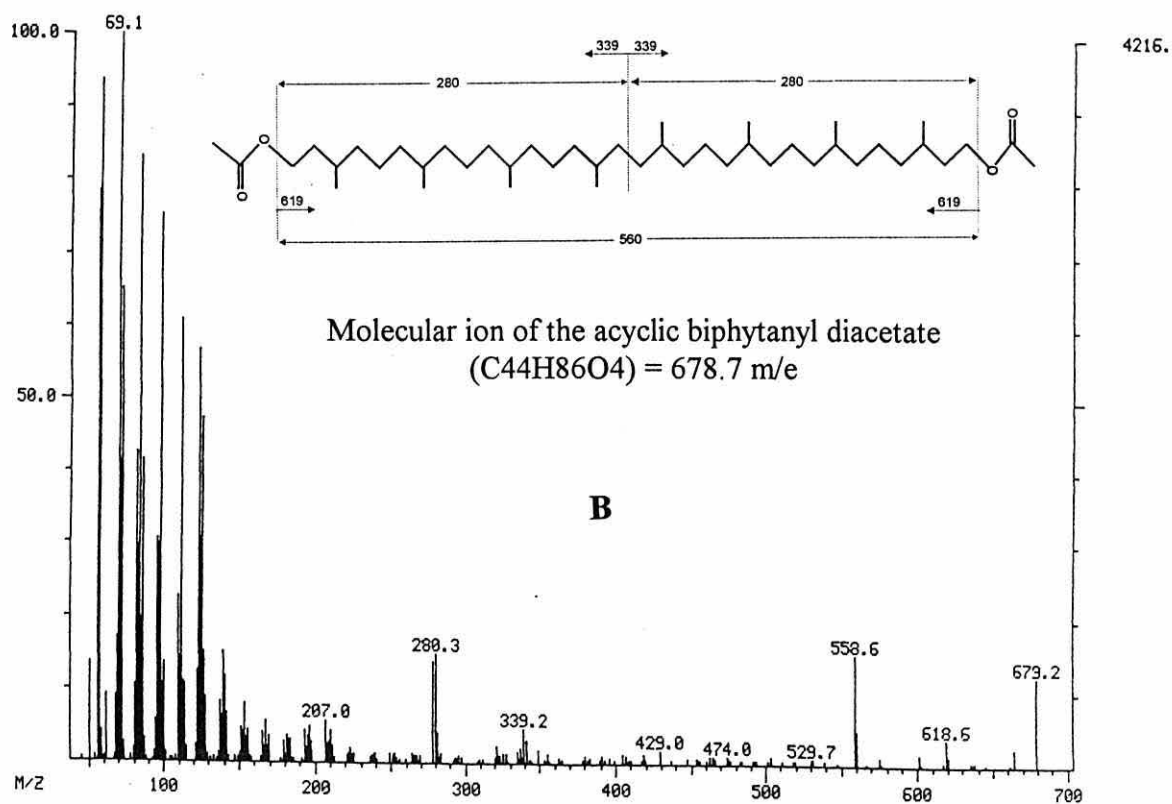
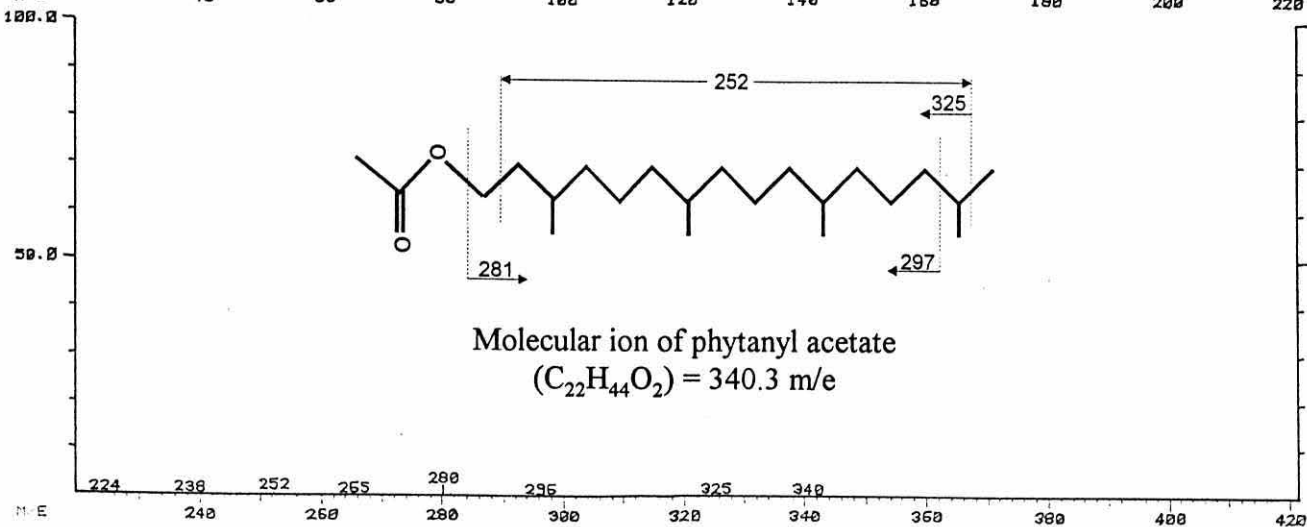
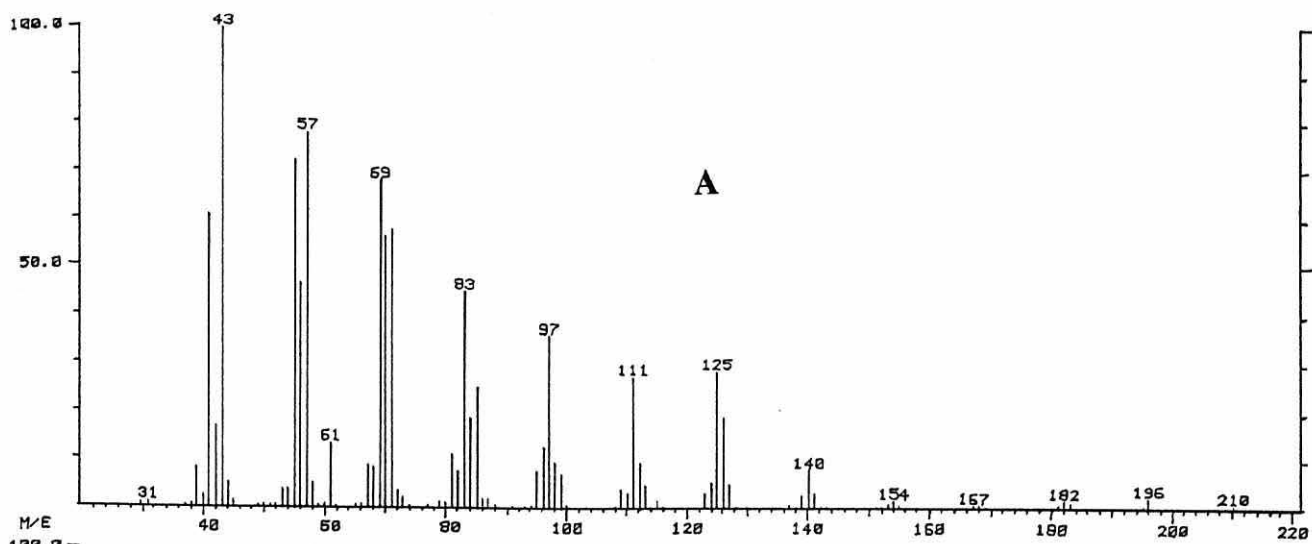


Figure 3.5. Mass spectra (EI) of the phytanyl acetate derivative of the diether lipid standard (A) and of the acyclic biphytanyl diacetate derivative of the acyclic tetraether lipid standard (B).

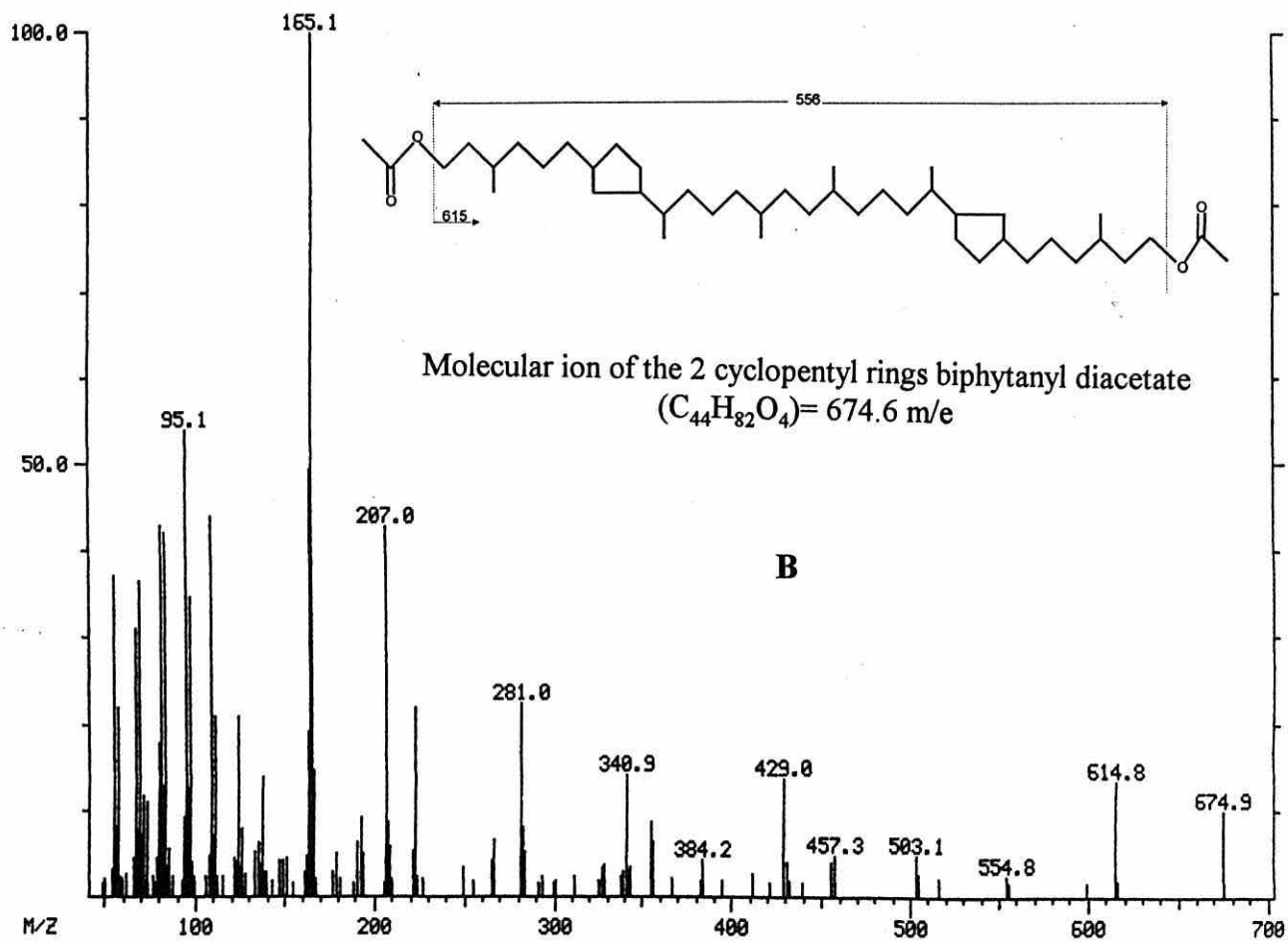
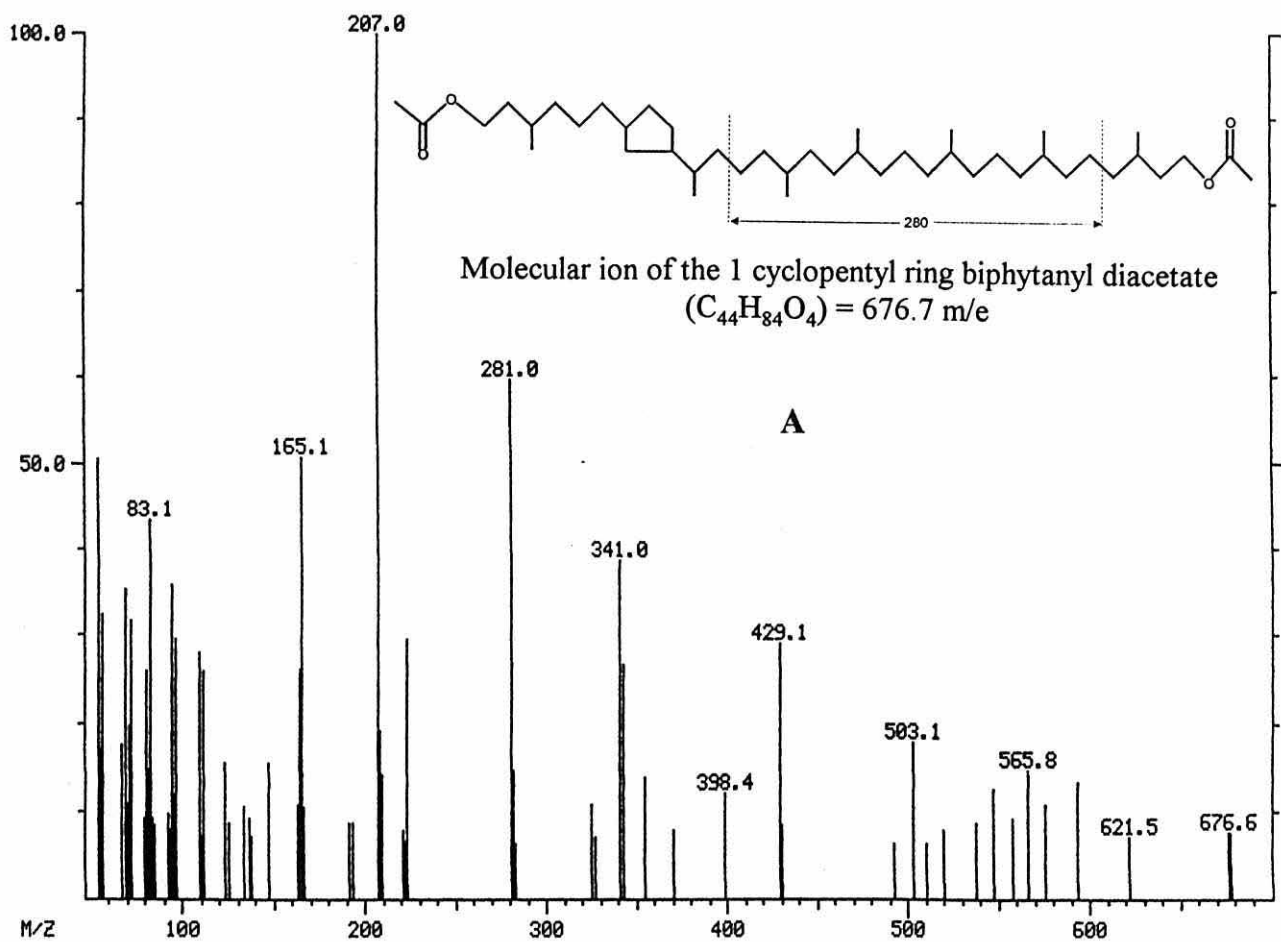


Figure 3.6. Mass spectra (EI) of the cyclised biphytanyl diacetate derivatives of the cyclised tetraether lipid standards. Figure 3.6A is the 1 cyclopentyl ring derivative and figure 3.6B is the 2 cyclopentyl ring derivative.

For the same gas chromatography runs less than a 4 % coefficient of variation (CV) in peak areas was reported for the repeat injection (n = 6) of phytanyl acetate, whereas the biphytanyl di-acetate demonstrated a 77 % CV in peak areas due to the peaks not always eluting from the column on some of the runs. The only difference in this method to that quoted by Pauly and Van Vleet (1986a) was in the lack of a rapidly heating injector system, which might be the reason for the elution problems described above. Nishihara (*pers. comm.*, 1991) also did not achieve quantitative results by gas chromatography for the di-acetate derivatives and decided that the high boiling point (low volatility) of the biphytane di-acetate derivative (C₄₄O₄H₈₆, Mw = 679) was the limiting factor. Nishihara (*Pers. comm.*, 1991) recommended using the more volatile alkane derivatives of the tetraether lipids.

3.3.2.3. Analysis of Alkane Derivatives.

The hydrocarbon derivatives gave the most reproducible peak areas and retention times for the tetraether lipids. This was the method adopted by Nishihara and Koga (1988) and involved reducing the iodo-alkane with lithium aluminium hydride to the alkane (section 2.13.7 of chapter 2). Repeat injection (n = 5) of diether and tetraether (0 to 4 pentacyclic rings) alkane derivatives gave approximately a 5 % coefficient of variation (CV) in peak areas and less than a 0.3% variation in retention times. By repeating (n = 3) the solvent extraction procedure on 3 sub-samples of the same homogenised sediment sample, it revealed a 5% coefficient of variation for the concentration of the diether lipid and approximately a 10% CV for the tetraether lipid. The reduced variation observed for the diether lipid might be due to the internal standard resembling the diether chemical structure more than tetraether lipid structure. The three extractions were performed on sub-samples of the 205-213 cm sediment depth of Holyhead core C, and are given in appendix VI.

Electron ionisation mass spectral analysis of the prepared alkane derivatives showed the following molecular ions; phytane (m/e 282, figure 3.7A), biphytane (m/e 562, figure 3.7B) and the 1 (m/e 560, figure 3.8A), 2 (m/e 558, figure 3.8B), 3 (m/e 556, figure 3.9A) and 4 (m/e 554, figure 3.9B) cyclopentyl ring biphytane derivatives. These figures also include molecular fractionation diagrams with the common ion fragment species identified. For the phytane and acyclic biphytane molecules given in figure 3.7 almost all of the ion fragments of the mass spectra can be identified from the fragmentation diagrams. For the cyclised biphytane derivatives most of the major ions identified by the mass spectrum can also be represented within the fragmentation diagrams of figures 3.8 and 3.9.

It can be noted from the mass spectra of the cyclic biphytane derivatives that the 194 m/e ion fragment is only produced from molecules that have a cyclopentyl ring with chains of 4 carbons one side and 5 carbons the other (figures 3.8 and 3.9). Therefore only molecules that have a single cyclopentyl ring in one half of the molecule form the 194 m/e ion when ionised.

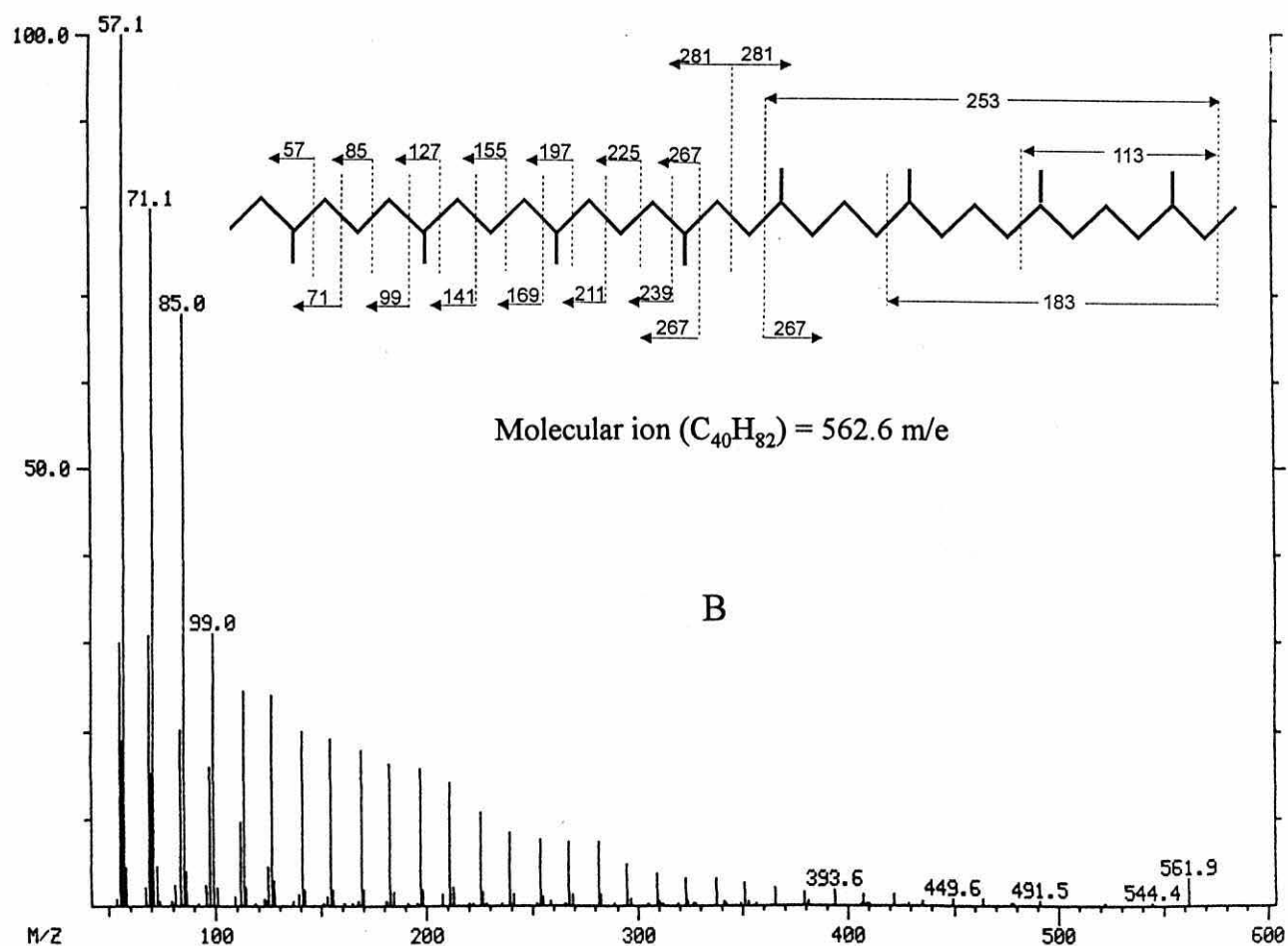
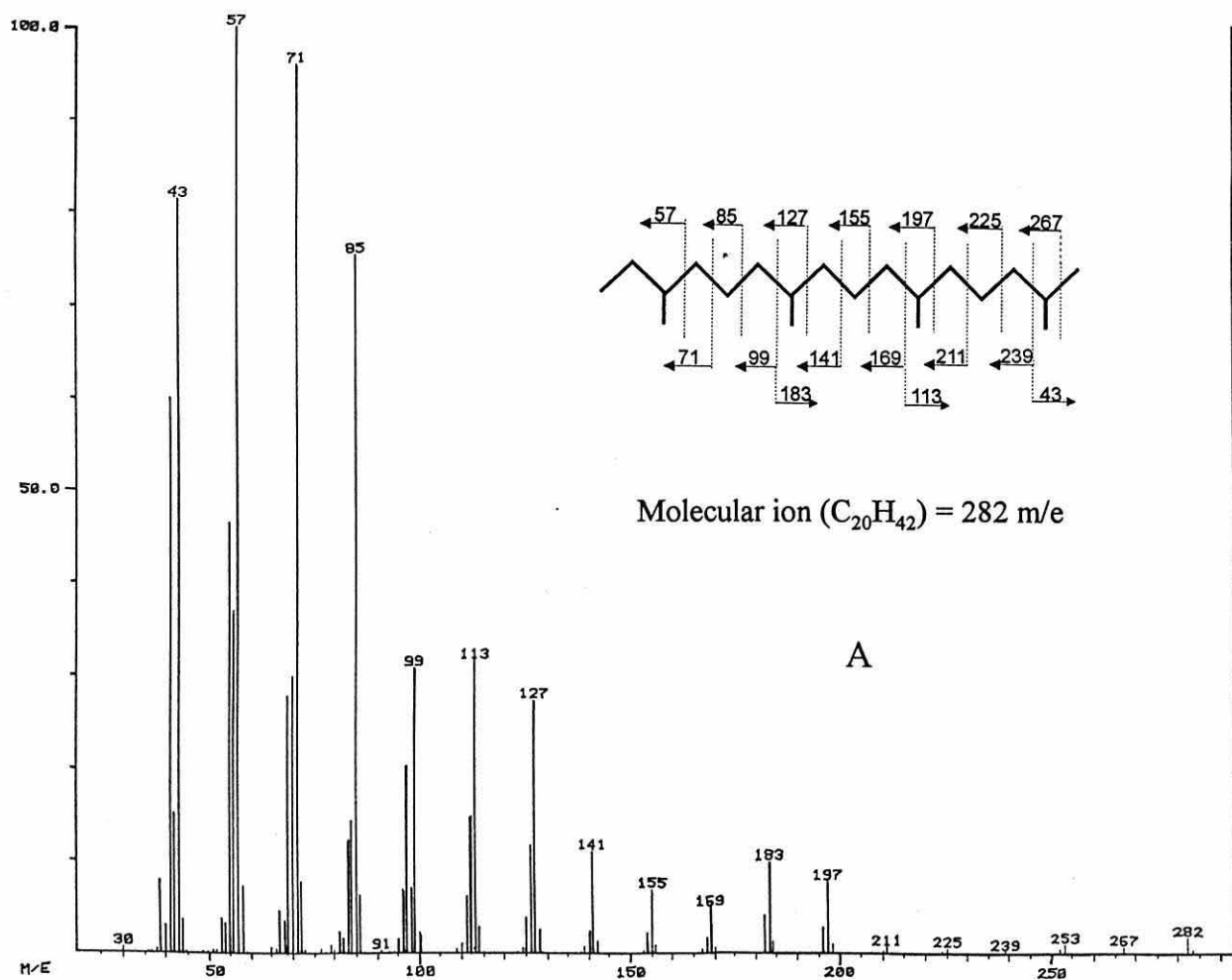


Figure 3.7. Mass spectra (Electron ionisation) with molecule fragmentation diagrams of the phytane (A) and biphytane (B) derivatives prepared from the diphytanyl glycerol diether and the acyclic bidiphytanyl glycerol tetraether respectively.

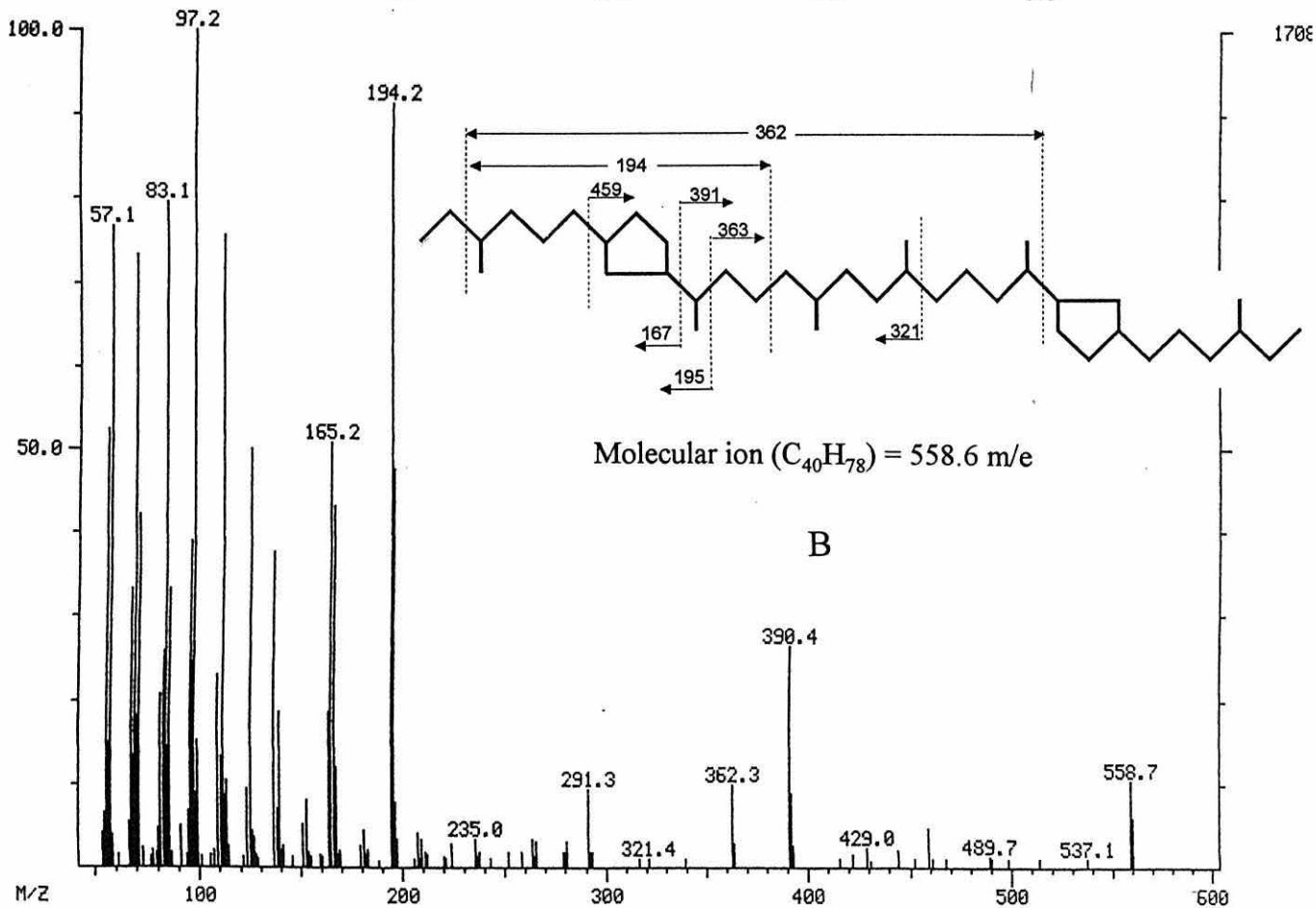
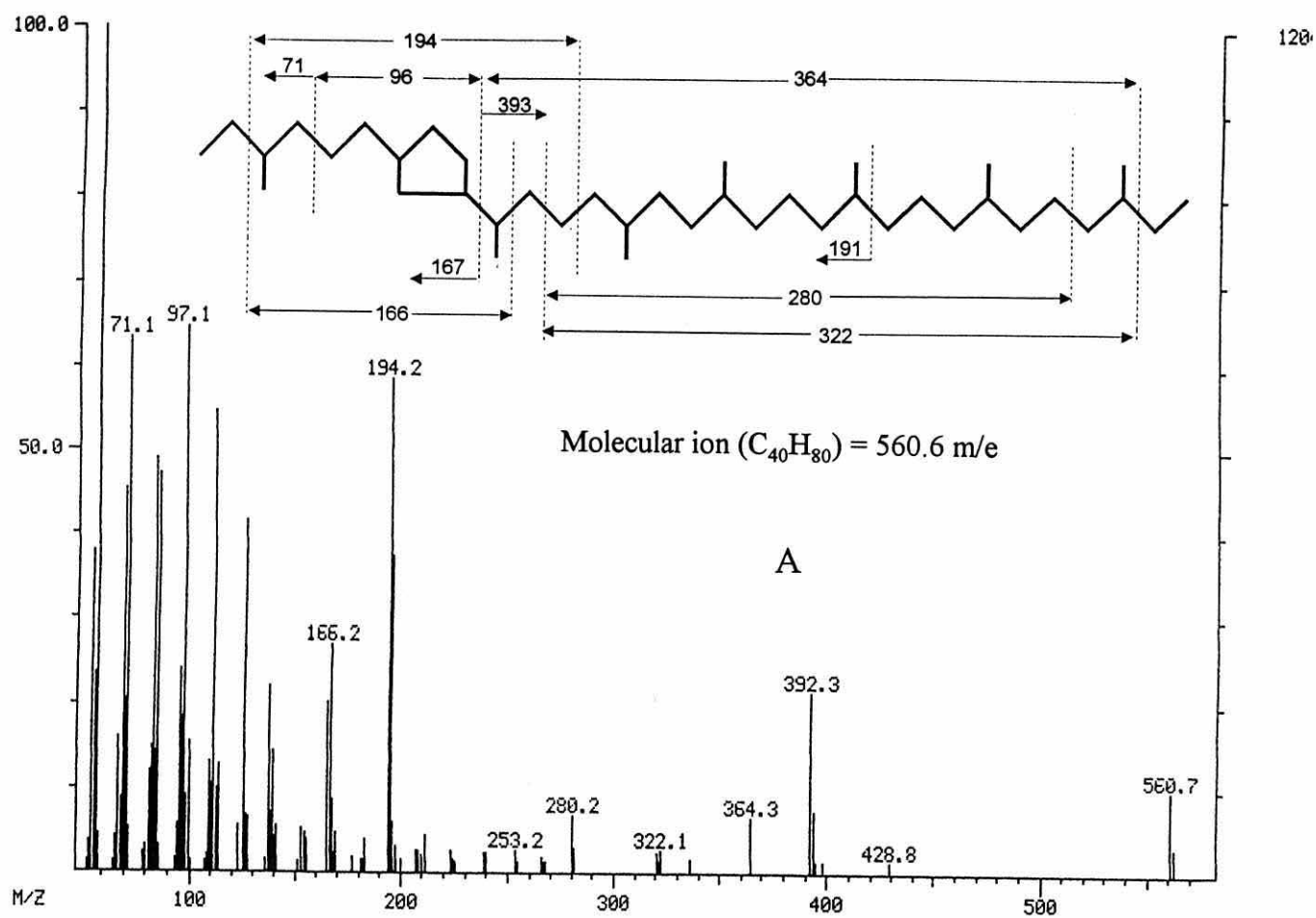


Figure 3.8. Mass spectra (Electron ionisation) with molecule fragmentation diagrams of the 1-pentacyclic (A) and 2-pentacyclic (B) biphytane derivatives prepared from the cyclised bidiphytanyl glycerol tetraether analogues.

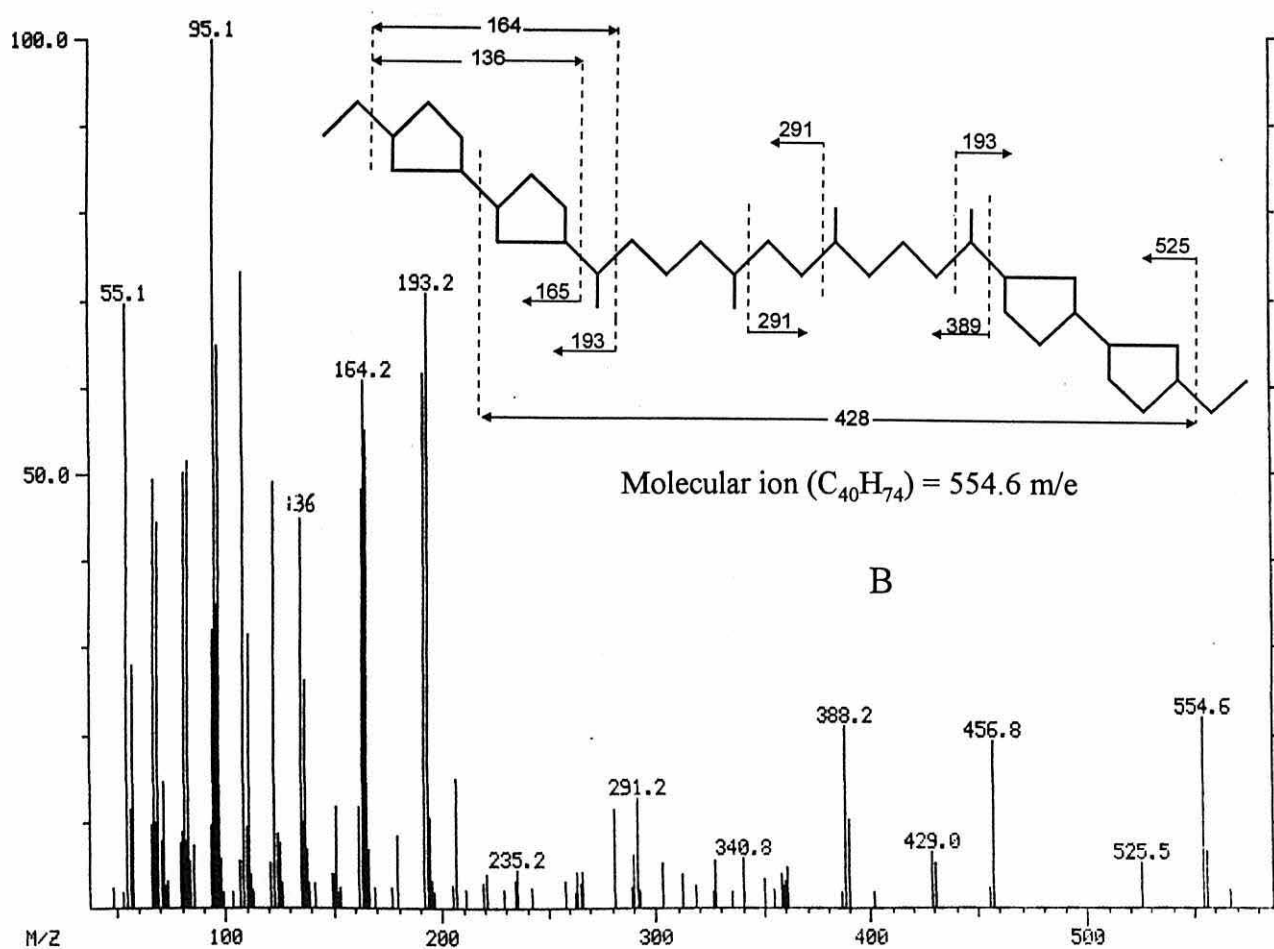
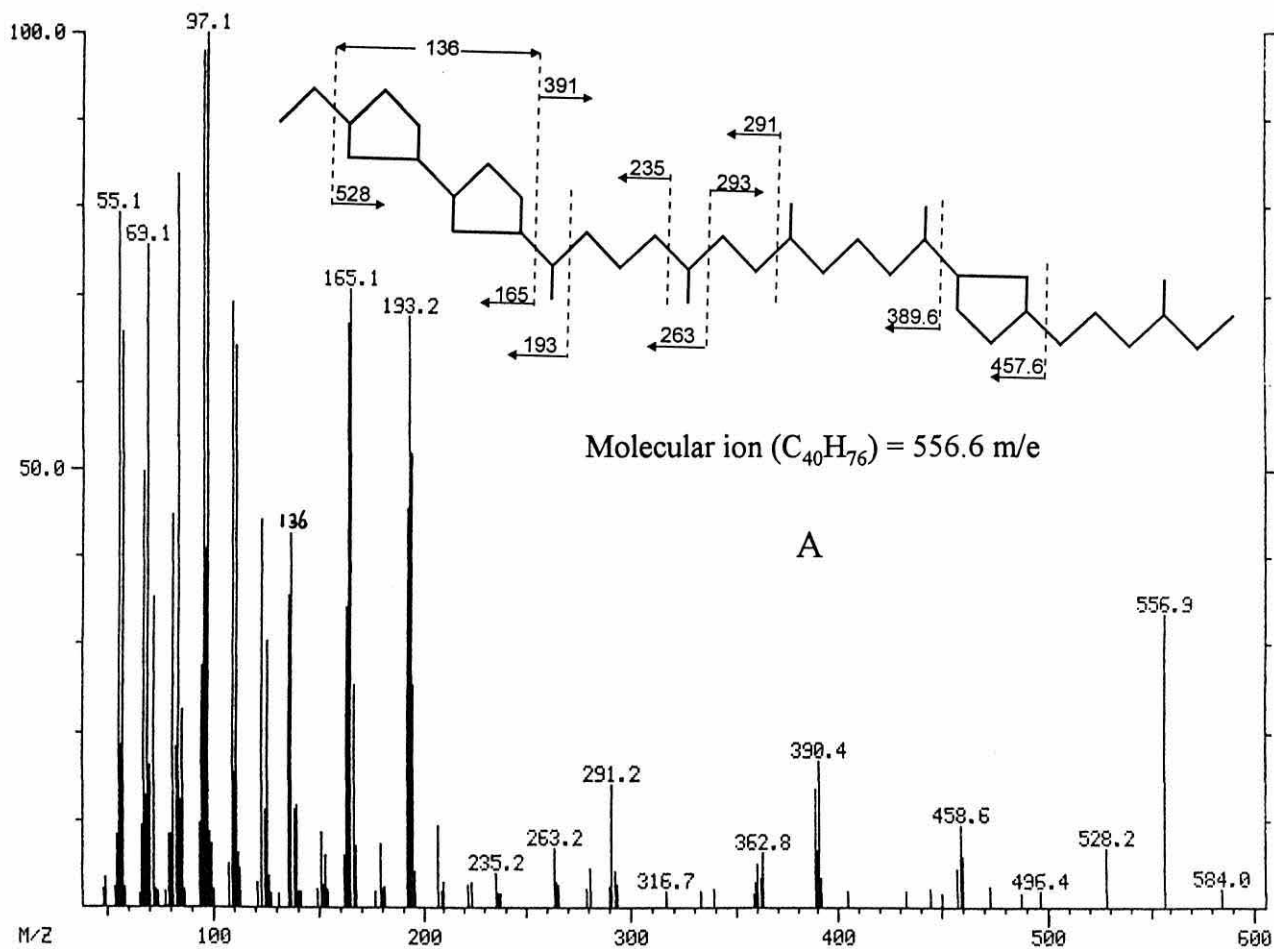


Figure 3.9. Mass spectra (Electron ionisation) with molecule fragmentation diagrams of the 3-pentacyclic (A) and 4-pentacyclic (B) biphytane derivatives prepared from the cyclised dibiphytanyl glycerol tetraether analogues.

Because the 194 m/e ion is formed from tetraether molecules which have a lone cyclopentyl ring in one half of the molecule the C_{40,1} (*i.e.* C₄₀H₈₀, figure 3.8A) and C_{40,3} (*i.e.* C₄₀H₇₆, figure 3.9A) molecules therefore form similar percentage abundances of the 194 m/e ion, the C_{40,2} (*i.e.* C₄₀H₇₈, figure 3.8B) forms the largest percentage abundance, and the C_{40,4} (*i.e.* C₄₀H₇₄, figure 3.9B) molecule, which has paired cyclopentyl rings in both halves of the molecule, does not form a 194 m/e ion. Conversely the 193 m/e fragment appears to be only present in the cyclic biphytane derivatives that have paired cyclopentyl rings in the same half of the overall molecule. Therefore only the C_{40,3} and C_{40,4} cyclic derivatives show the 193 m/e ionisation fragment (figures 3.9A and 3.9B, respectively).

Chemical ionisation (CH₄) of the alkane derivatives appeared to form molecular ions that had one less mass unit than the equivalent derivatives when analysed by electron ionisation MS. The chemical ionisation mass spectra of the acyclic biphytane (figure 3.10A), the 1-cyclopentyl ring biphytane (figure 3.10B), the 2-cyclopentyl ring biphytane (figure 3.11A), the 3-cyclopentyl ring biphytane (figure 3.11B), and the 4-cyclopentyl ring biphytane (figure 3.12) derivatives are given. Therefore it would appear that the methane molecules remove a proton from the alkane derivatives, rather than adding a proton as might normally be expected.

The reason for obtaining chemical ionisation spectra in addition to the electron ionisation spectra will become evident when comparing fragmentation patterns to the spectra of the uncharacterised alkane derivative isolated from the marine sediment samples (section 3.3.3).

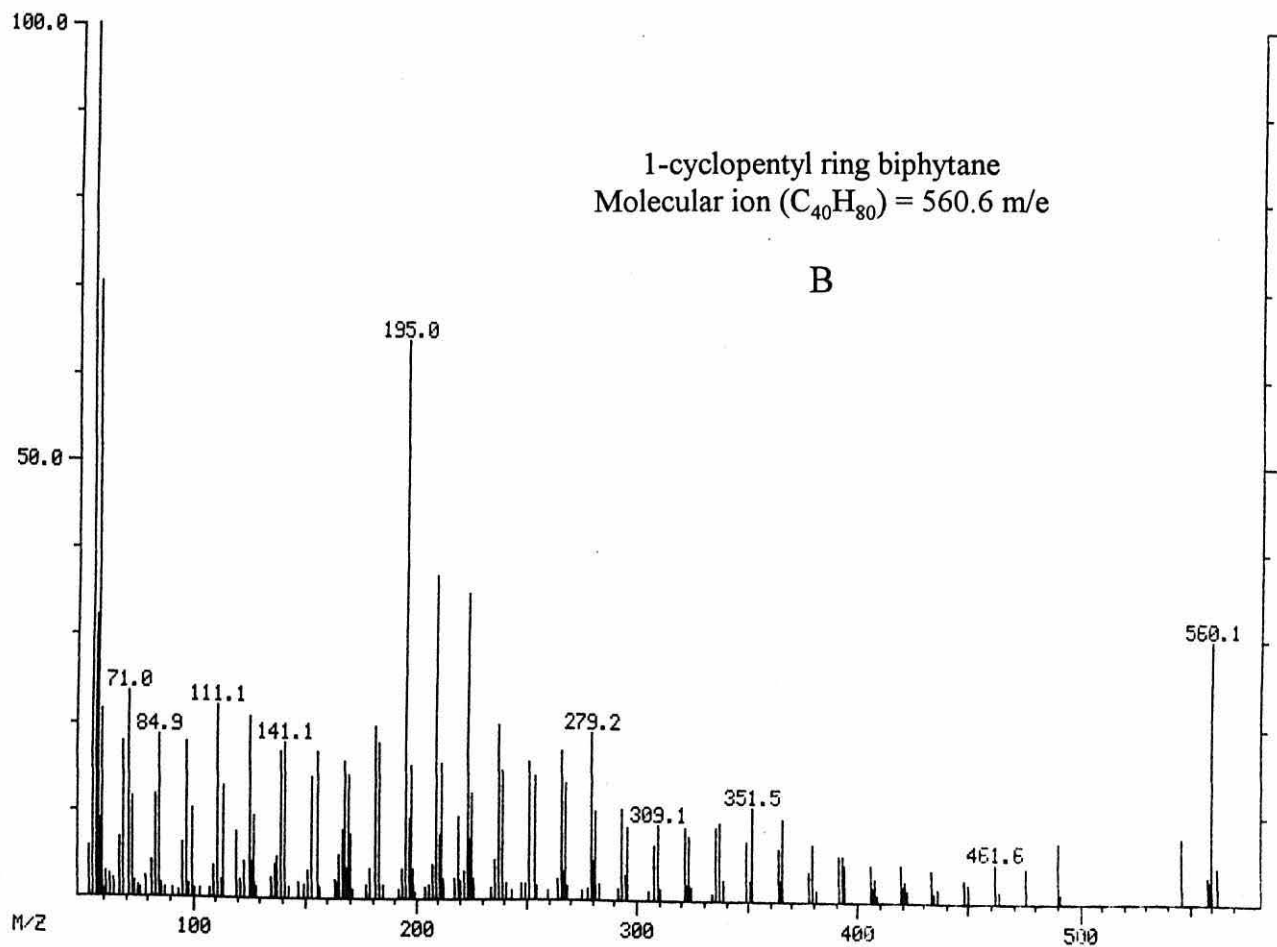
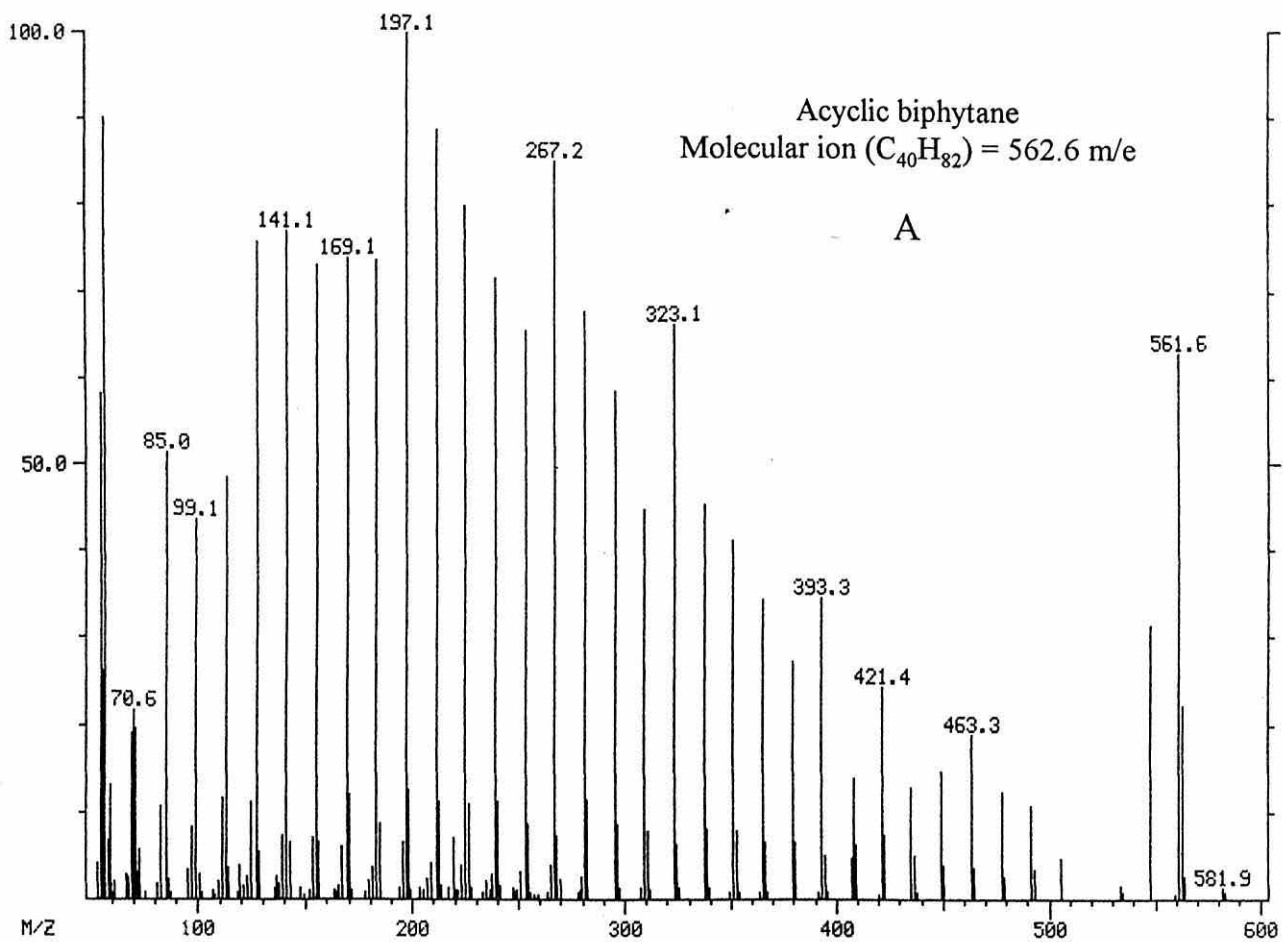


Figure 3.10. Mass spectra (chemical ionisation, CH_4) of the acyclic (A) and cyclic (1-cyclopentyl ring) (B) biphytanyl derivatives prepared from the bidiphytanyl glycerol tetraether lipids.

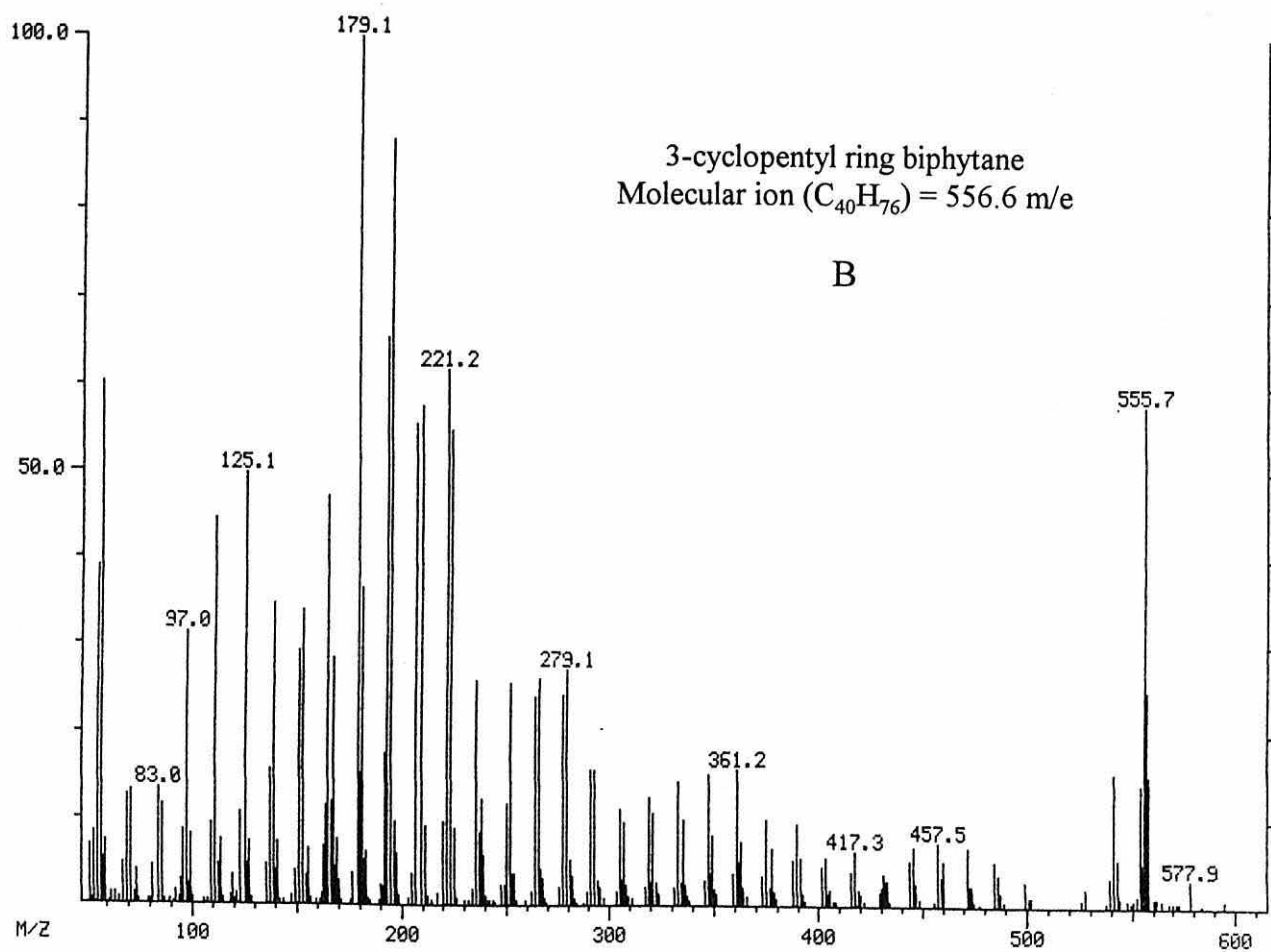
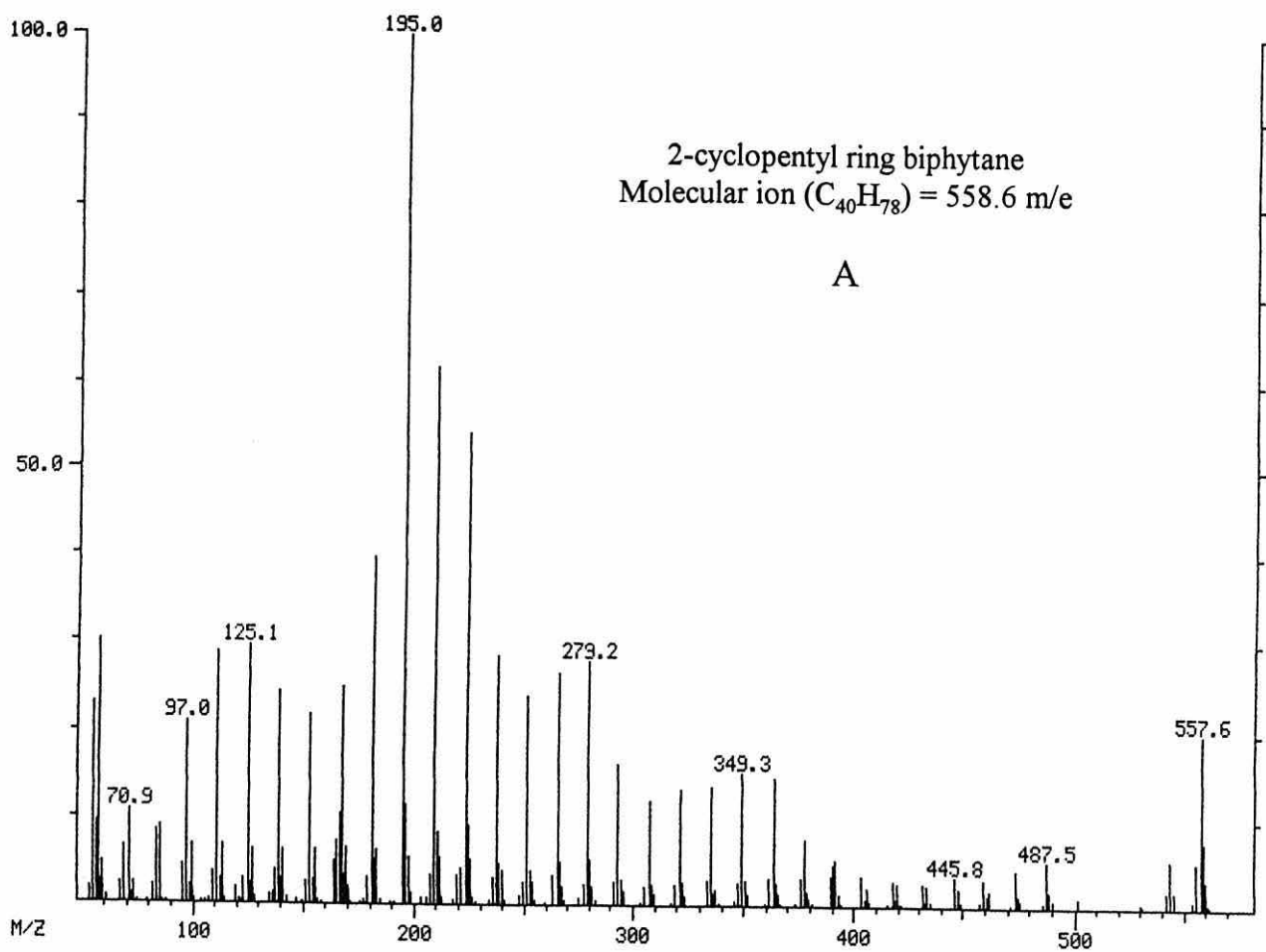


Figure 3.11. Mass spectra (chemical ionisation, CH_4) of the 2-cyclopentyl ring (A) and 3-cyclopentyl ring (B) biphytanyl derivatives prepared from the bidiphytanyl glycerol tetraether lipids.

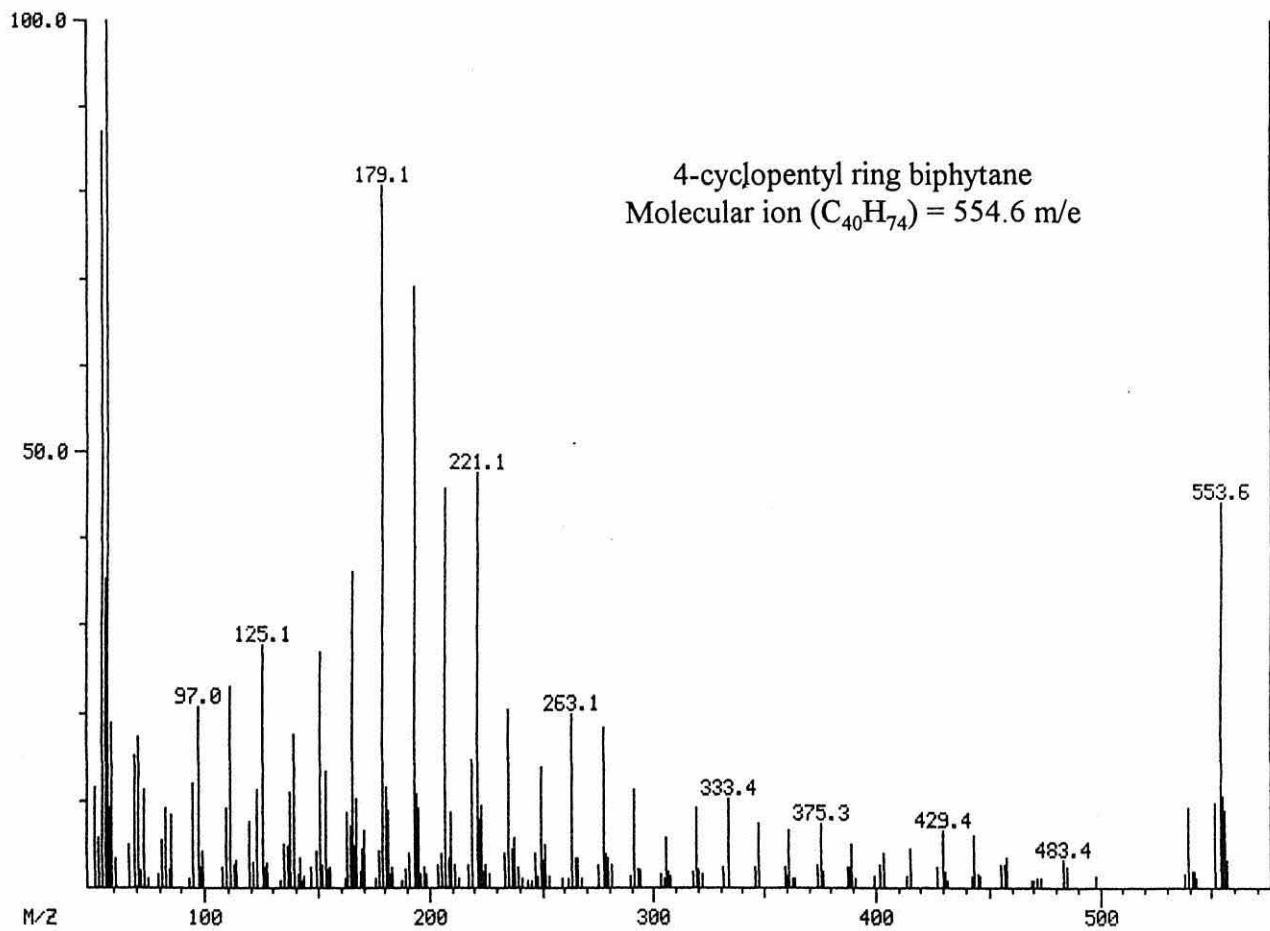


Figure 3.12. Mass spectra (chemical ionisation, CH_4) of the 4-cyclopentyl ring biphytanyl derivatives prepared from the bidiphytanyl glycerol tetraether lipids.

3.3.3. Alkane Derivatives Isolated from Marine Sediments

Core C, taken from the 80-85 cm horizon of Holyhead Harbour, was used for the mass spectral analysis due to it having a high concentration of the ether lipids. Typical runs taken from the gas chromatograph of both the Holyhead sediment sample and the prepared standards isolated from pure culture are presented in figure 3.13. It was possible to isolate the phytane, acyclic biphytane and the 1 and 2 cyclopentyl ring biphytanyl derivatives from most of the Holyhead and intertidal samples. The derivatives were identified in all of the samples by comparison with standard retention times. Some of the samples were also identified by coelution of the sample with authentic standard derivatives on the gas chromatograph.

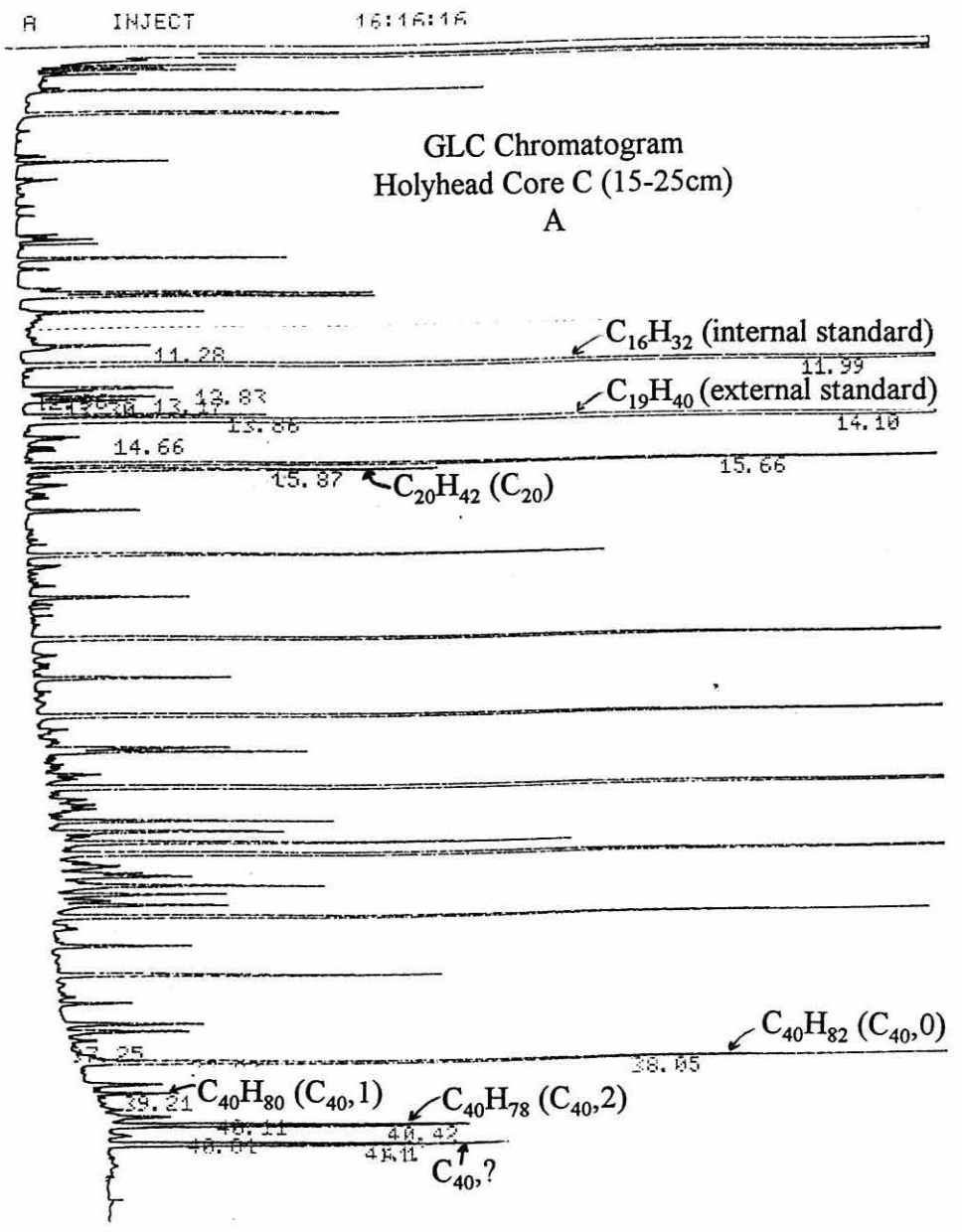
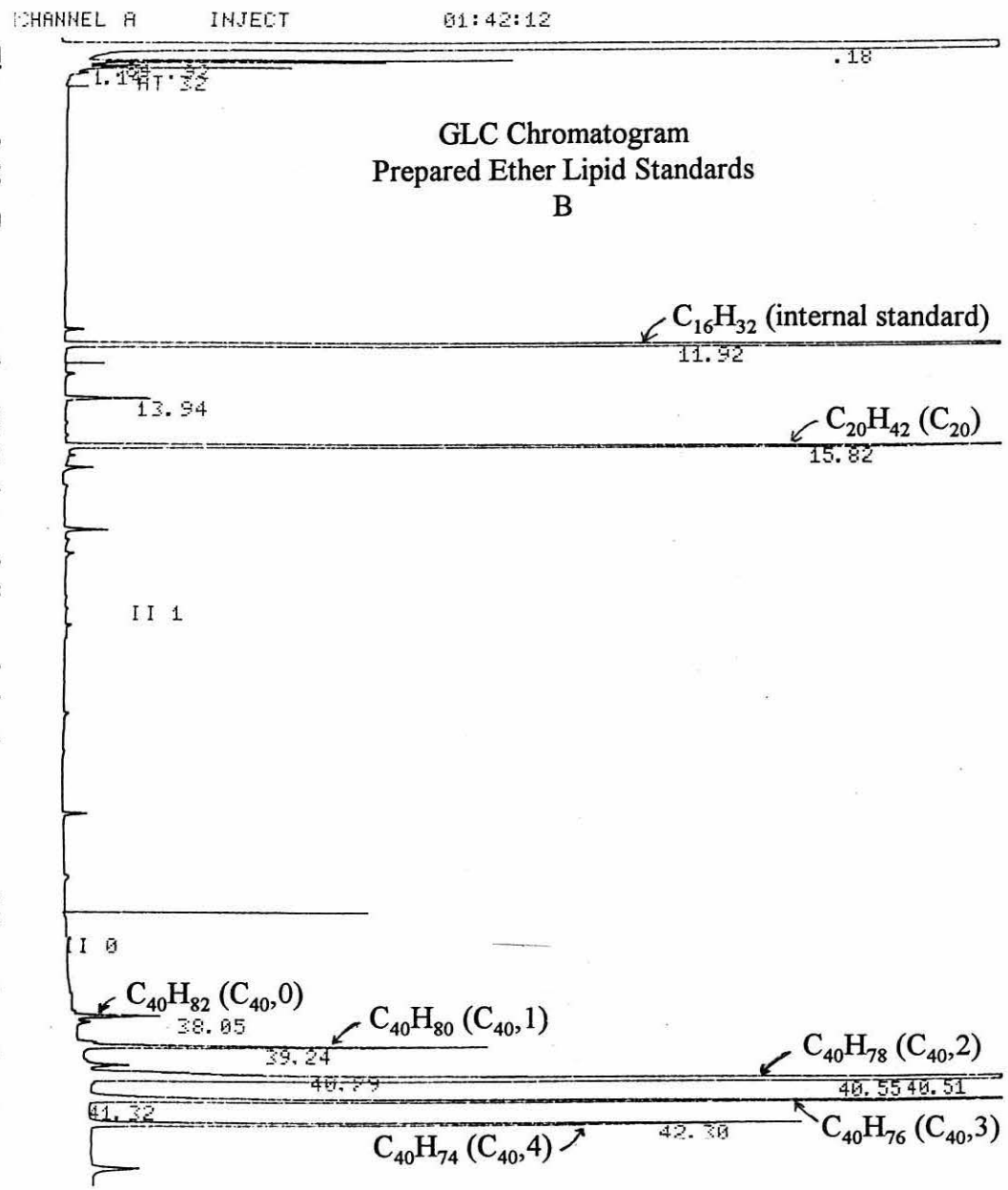
Mass spectral analysis, using both EI and CI, of these derivatives isolated from marine sediment revealed similar molecular ions and fragmentation patterns to the derivatives prepared from the ether lipid standard. From the gas chromatogram of the sediment extract, given in figure 3.13, it was noted that a large peak of similar concentration to that of the 2-cyclopentyl ring biphytane ($C_{40,2}$) eluted approximately 0.7 min after the $C_{40,2}$ peak. The uncharacterised derivative did not coelute with any of the biphytane standards, and was closest in retention time to the 3 cyclopentyl ring biphytane derivative ($C_{40,3}$) as shown in figure 3.13. From chapter 5 it is apparent that the uncharacterised derivative ($C_{40,?}$) is present in all sediment samples analysed, at approximately the same concentration to the $C_{40,2}$ derivative and is therefore possibly of ether lipid origin. An uncharacterised ether lipid derivative of comparative retention to the unknown of this study ($C_{40,?}$) has also been detected in marine sediments of varying ages (Pauly & Van Vleet, 1986b; Chappe *et al.*, 1982). Although the complete structure of this uncharacterised derivative has yet to be elucidated it is believed to be an isomer to the 2-cyclopentyl ring biphytane derivative (Chappe *et al.*, 1982).

3.3.3.1. Mass Spectral Analysis of Uncharacterised Ether Lipid Derivative

Electron ionisation and chemical ionisation mass spectra of the uncharacterised alkane derivative are given in figures 3.14A and 3.14B respectively.

Electron ionisation mass analysis did not reveal a molecular ion for the uncharacterised alkane derivative (figure 3.14A). Since the 1 and 2 cyclopentyl biphytane derivatives showed a molecular ion for the same ionisation conditions, it suggested that the uncharacterised derivative was less stable to ionisation than the other derivatives. Figure 3.14A also showed that the two largest fragmentation peaks of significant intensity (*i.e.* > 10% RIC) occurred at m/e 292 and 262. Therefore since these ion fragments are approximately half that of the expected molecular ion, it might suggest that the point of fragmentation is close to the centre of the molecule causing two fragments of similar molecular weight when ionised. The sum of the two fragments is $m/e = 554$, which if this was the molecular ion of the uncharacterised derivative would be a molecular weight similar to that of the 4-cyclopentyl ring biphytane

Figure 3.13. Representative GLC plots of alkane derivatives prepared from the solvent extracted sediment sample of Holyhead core C (15-25cm) (A), and also from ether lipid standards (B).



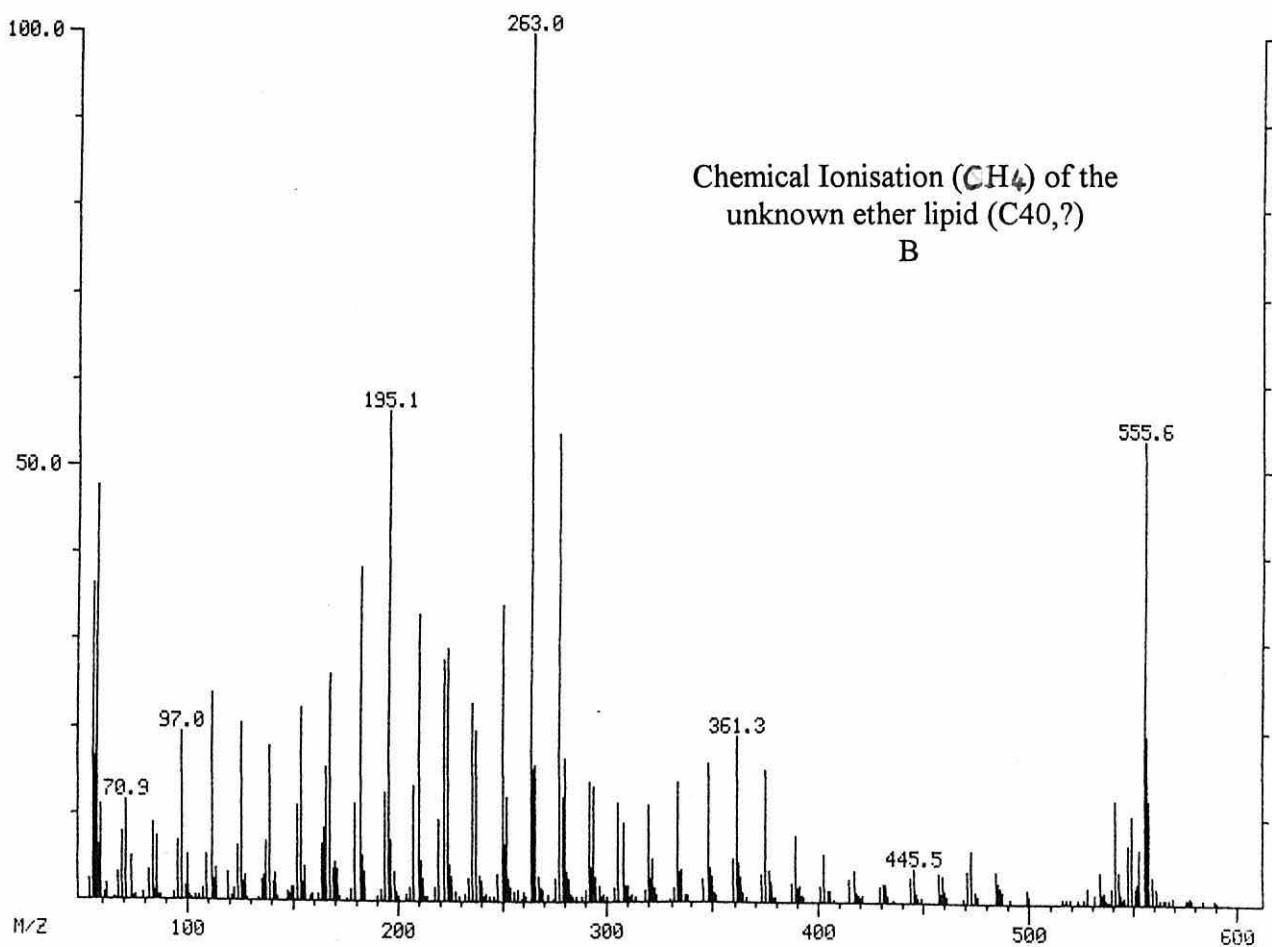
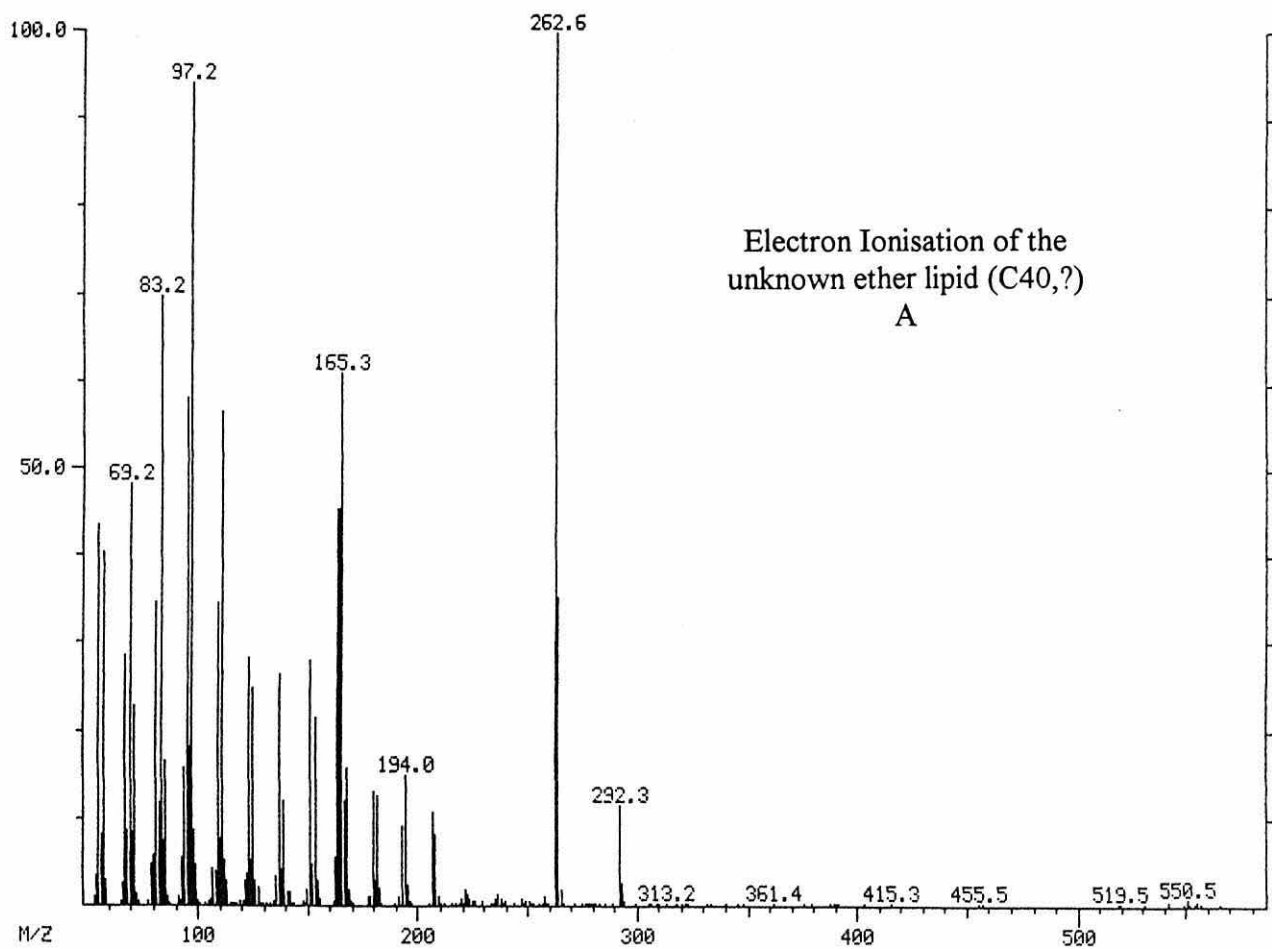


Figure 3.14. Mass spectra of the unknown lipid (C₄₀,?) isolated from sediment of Holyhead harbour and analysed using electron ionisation (A) and chemical (CH₄) ionisation (B) techniques.

derivative, and would therefore suggest the uncharacterised derivative could be an isomer of the C_{40,4} derivative. Other fragments of the electron ionisation mass spectra (figure 3.14A), such as the presence of the 194 m/e ion, suggest that the uncharacterised derivative contains an unpaired cyclopentyl ring in one half of the molecule. However, the fact that the percentage abundance of the 194 m/e peak is much smaller than for the C_{40,1} of C_{40,3} EI spectra (figures 3.8A and 3.9A) suggests this fragment is less likely to be formed on ionisation. Also the lack of a 193 m/e ion within the EI spectra suggests that an ion fragment with two paired cyclopentyl rings in one half of the molecule is unlikely.

Since the uncharacterised derivative is not stable to ionisation using EI mass spectrometry it was necessary to use a chemical ionisation technique (CH₄) to ensure that all of the molecular ion is not fragmented. Chemical ionisation of the uncharacterised derivative would suggest a molecular ion of m/e 556 (figure 3.14B), which is similar to the molecular ion using CI/MS of the C_{40,3} derivative as given in figure 3.11B. Since the molecular ion identified by chemical ionisation MS always underestimates the true mass of the tetraether derivative standards by one m/e unit, then if we apply this prediction to the spectrum (CI/MS; figure 3.14B) of the uncharacterised derivative it suggests a molecular ion of $555.6 + 1 = 557.6$ m/e, which would suggest that the derivative has a comparable molecular ion to the 3-cyclopentyl ring derivative. Chemical ionisation GC/MS of the uncharacterised derivative does not resemble the fragments of the C_{40,2} or C_{40,3} biphytane derivatives.

The total concentration of the uncharacterised ether lipid (C_{40,?}) was insufficient to be used on an MS/MS system, even when the total samples were pooled.

The concentrations of the ether lipid derivatives from the sediment samples are given in appendix VII and are discussed more fully in chapter 5. The uncharacterised derivative (C_{40,?}) was found to be almost equal in concentration to the C_{40,2} derivative (*i.e.* 1:1.09) in all sediment samples analysed with a very high correlation ($r = 0.98$, $n = 44$). The uncharacterised ether lipid (C_{40,?}) has not been detected in laboratory grown methanogens to date, and the 2 cyclopentyl ring derivative (C_{40,2}) has only been detected in very low concentrations in a limited number of methanogens. Therefore, it could be speculated that the uncharacterised ether lipid derivative (C_{40,?}) and the 2 cyclopentyl ring derivative (C_{40,2}) may be part of the larger tetraether lipid molecule. Further research is required to determine from which molecules and which species these derivatives originate.

Therefore from the limited information collected it is possible to speculate that the uncharacterised derivative, which is most likely to be of archaeobacterial origin (chapter 5), is an isomer of the 3- cyclopentyl ring biphytane derivative and is prone to ionisation close to the middle of the molecule.

3.4. Production of a Derivative for Electron Capture Detection (GC/ECD)

3.4.1. Introduction

The biomass of methanogens in marine sediments and the water column is small, and the ether lipids constitute a small fraction of that biomass. It is therefore advantageous to use the most sensitive analytical technique available to determine the ether lipids. The determination of ether lipids in sediments by gas chromatography with flame ionisation detection required a significant amount of sediment and a very large volume of solvent for each extraction (*i.e.* 350 ml) which proved to be expensive. Also, for certain types of samples it may not be possible to simply increase the amount of sample in order to compensate for inadequate detection limits. One such example is the determination of ether lipids in zooplankton samples whereby the collection of sufficient sample could be difficult.

Participation on a microbial ecology course at the Bermuda Biological Station in 1991 by the author, led to a small project studying methanogenesis in collected plankton samples. Although methanogenesis was demonstrated in certain samples which had anaerobic media added, the concentration of ether lipids in these samples was found to be below the detection limit for the GC/FID.

For these reasons stated above there was a need for greater sensitivity when determining the concentrations of methanogenic ether lipids. Gas chromatography using flame ionisation detection has a sensitivity of approximately 1 nano gram of lipid per injection. Electron capture detection (ECD) has the potential to achieve greater sensitivity of up to three orders of magnitude, depending on the electrophilic properties of the derivative analysed (Lovelock and Watson, 1978). The preparation of ether lipid derivatives that contained functional groups with electrophilic halogen elements was therefore attempted.

3.4.2. Production of ECD Sensitive Derivatives

Details relating to the specifications of the gas chromatograph, electron capture detector and the accessories built onto the instrument are given in section 2.14 of chapter 2.

The sensitivity of the electron capture detector to ether lipid derivatives is expected to increase as the number of electrophilic groups (*i.e.* halogens) attached to the derivative also increases. Therefore by substituting more halogen groups into the derivative, and preferentially from higher up in the periodic table where electrophilic activity is greater it is possible to increase the sensitivity of the ether lipid method. Response factors for polychloro-biphenyls have been shown to increase in sensitivity of up to 2 orders of magnitude when the number of chlorine atoms attached to the molecule was raised from 1 to 8 (Mullin *et al.*, 1984).

By partly following the method of acetate substitution using silver acetate in acetic acid as detailed in section 2.13.8 of chapter 2, attempts were made to prepare trichloroacetate derivatives of the iodide ether cleavage products. Different combinations of 1 iodo-hexadecane were reacted with many different combinations of silver acetate or silver trifluoroacetate, and trichloroacetic acid in acetic acid. Partial identification of the reaction products by thin layer chromatography with known standards, followed by mass spectrometry did not show any evidence of either trichloroacetate or trifluoroacetate hexadecanyl derivatives being produced. The reason why this reaction failed had been shown by Wood and Snyder (1966), who found that trifluoroacetate derivatives of glyceryl ethers hydrolyse completely within 20 minutes of being transferred from the solvent trifluoroacetic anhydride to n-hexane (Wood & Snyder, 1966). The use of non-electrophilic solvents when using ECD detectors is essential for the technique to be viable.

3.4.2.1 PentaFluoroPropionyl Derivatives

Pentafluoropropionyl derivatives are stable in solvents that are not electron capturing, such as n-hexane (Watson & Wilk, 1974), and have been used on compounds of comparable volatility to phytane (Blau & King, 1978). By reacting pentafluoropropionic anhydride in pentafluoropropanol with derivatives of alcohol or amine it was possible to prepare pentafluoropropionyl derivatives. The method is detailed in section 2.13.11 of chapter 2. However the iodide ether cleavage products do not react directly with this method and therefore need to be first converted to a functional group that will, that is an alcohol or amine.

Initially alcohol derivatives were prepared by refluxing the iodo-derivatives in a solution of sodium hydroxide (7 M) in methanol for 5 hours in a Reacti-vial. 1 iodo-hexadecane was used as the standard for preparation of the alcohol derivative which was compared to authentic alcohol and iodide standards by thin layer chromatography. Two products of approximately equal yield were apparent. One had a similar retention to the alcohol standard and the other appeared to be an alkene, possibly from the elimination reaction (Streitwieser & Heathcock, 1985).

In order to obtain higher yields of the alcohol derivative a different method of alcohol substitution of the alkyl halide was made using silver nitrate. Silver nitrate in methanol or industrial methylated spirit (IMS) was used under a variety of conditions with the iodo-derivatives. The conditions that were required to give a high yield used IMS with silver nitrate and the iodo-derivatives at 30°C for 24 h with intermittent stirring. Comparison of the products with standards by thin layer chromatography revealed that most of the product was the alcohol derivative. Reaction of the phytanyl alcohol derivative prepared in this manner with the pentafluoropropionyl anhydride in pentafluoropropanol (section 2.13.11) gave the molecular ion of m/e 444.5 (phytanyl pentafluoropropionate) when analysed by GC/MS (EI)

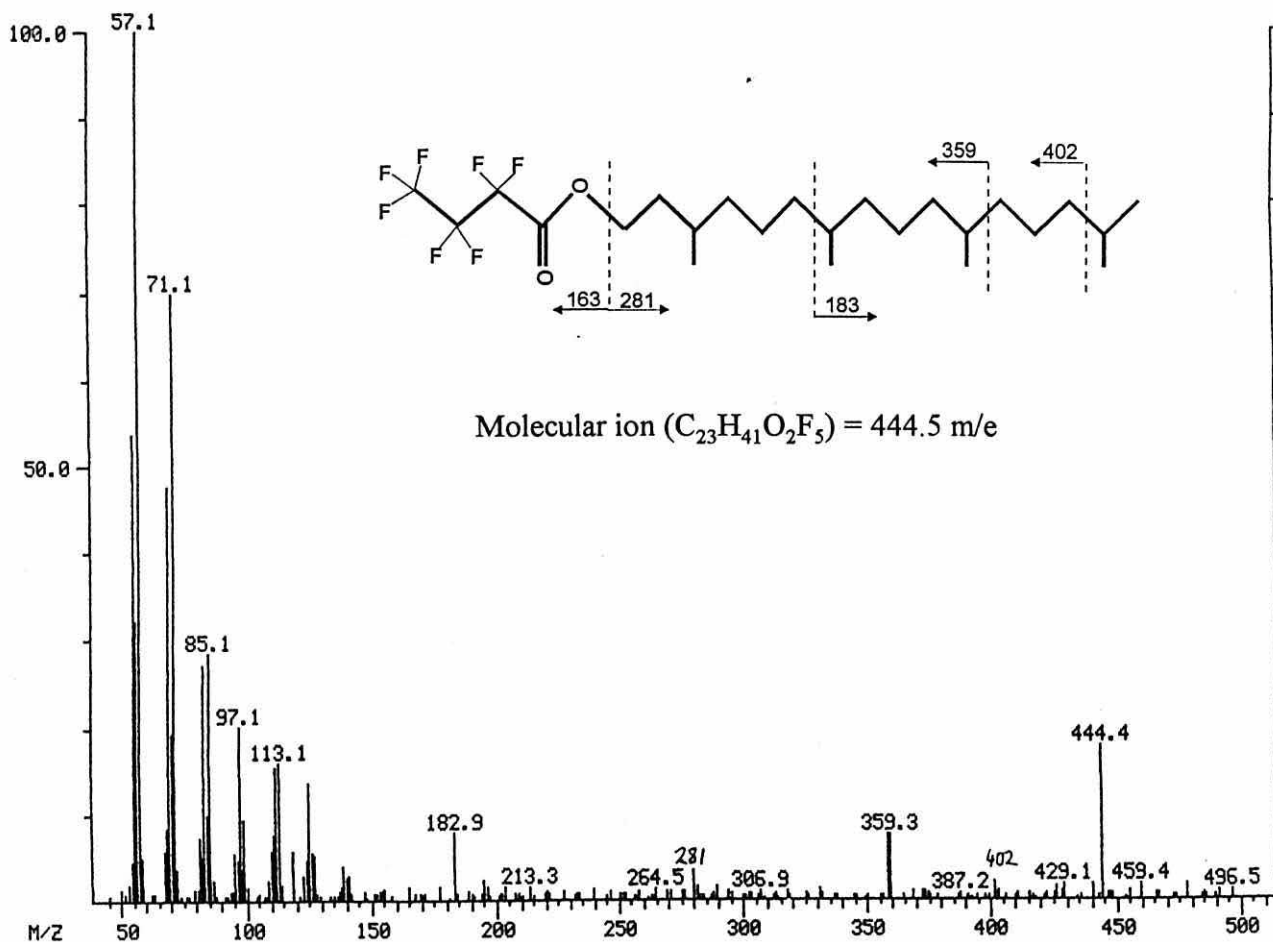


Figure 3.15. Mass spectrum (EI) of the phytanyl pentafluoropropionate derivative prepared indirectly from the methanogenic lipid diphytanyl glycerol diether.

(figure 3.15). Unfortunately analysis by electron capture detection was not possible due to an electrical malfunction of the instrument at the end of the experimental period and so response factors for this derivative were not determined.

3.5. Summary

It is not possible to analyse all of the intact methanogenic ether lipids directly by gas chromatography and the use of mass spectrometry alone requires purified samples which are difficult to prepare from sediment extracts. It was, however, possible to provide semi-qualitative information on the ether lipids purified from pure culture samples by Fourier transform infra-red spectroscopy.

The internal standard (1,2 di-*O*-hexadecyl rac glycerol) was added to the samples to allow for losses during sediment extraction, derivatisation and clean-up. Repeat analysis of subsamples of a single homogenised sediment sample gave a coefficient of variation of approximately 5 % for the diether lipids and 10 % for the tetraether lipids.

Analysis of the biphytanyl di-iodide, di-chloride and di-acetate derivatives by gas chromatography suggested that such derivatives could not be analysed quantitatively. The most reproducible and quantitative results were obtained from the reduced bi-phytane derivative, such that repeat injection gave a 5 % coefficient of variation in peak area and 0.3 % for retention time.

The limited mass spectral information collected on the uncharacterised ether lipid derivative (*i.e.* C₄₀,?) suggested that it was an isomer of the 3-cyclopentyl ring biphytane derivative and is very susceptible to ionisation close to the middle of the molecule. The concentrations of the uncharacterised derivative and the 2 cyclopentyl ring derivative were very similar in all of the environmental samples. The uncharacterised ether lipid (C₄₀,?) has not been detected in methanogens to date, and the 2 cyclopentyl ring derivative (C₄₀,2) has only been detected in very low concentrations in a limited number of methanogens. Therefore, it could be speculated that the uncharacterised ether lipid derivative (C₄₀,?) and the 2 cyclopentyl ring derivative (C₄₀,2) may be part of a larger tetraether lipid molecule. Further study is required to determine from what molecules and what species these derivatives originate.

The addition of electrophilic halogen groups to a derivative can give lower detection limits of the derivative when analysed by GC/ECD. The preparation of pentafluoropropionyl derivatives of the phytane lipid was demonstrated. The sensitivity of this derivative to electron capture detection has yet to be determined.

CHAPTER 4. COMPARISON OF ETHER LIPID CONCENTRATIONS WITH METHANOGENIC BIOMASS AND METHANE PRODUCTION IN AXENIC CULTURE EXPERIMENTS, AND ETHER LIPID DEGRADATION STUDIES.

4.1. Introduction

Before attempting to use the methanogenic ether lipids as bioindicators of methanogenic biomass in sediments it was first necessary to determine how well the concentration of the ether lipids reflected the biomass of the methanogenic bacteria. When grown under axenic laboratory conditions the biomass of the methanogens could be determined from a range of parameters that could be directly measured from pure cultures. The parameters which were related to the biomass of the methanogenic bacteria in the pure culture experiments are detailed below.

(1) The cell number and cell diameter from which the total cell surface area or cell volume could be determined. An indirect estimate of the concentration of methanogenic cells in the growth culture was also obtained from the amount of light omitted from passing through the turbid culture, *i.e.* turbidity or optical density. Optical density measurements have frequently been used as an indirect method to monitor bacterial growth in pure cultures and have also shown good correlation with methane production for pure cultures of methanogens (Taylor & Pirt, 1977).

(2) Phospholipids constitute approximately 50 % of eukaryotic lipids and 98 % of bacterial membrane lipids (White, 1983), and are not present within the cells as storage lipids (Kates, 1972). Phospholipid phosphate has proved to be an accurate measure of the microbial biomass due to it remaining constant in diverse bacterial monocultures over a variety of different conditions which are comparable to stresses found in nature (Wilkinson *et al.*, 1972, White *et al.*, 1979b). Phospholipid phosphate has been favourably compared with ATP content as a means of estimating sediment biomass (White *et al.*, 1979a,b). Greater concentrations of phospholipid phosphate can be extracted from sediment samples using solvents than the corresponding removal of the intact cells by aqueous methods. Total cell counts can underestimate the true cell number in the sediment due to sediment-cell interactions (Findlay *et al.*, 1989). Lipid phosphate has previously been used to estimate microbial biomass in marine sediments (Findlay *et al.*, 1989), estuarine sediments (Martz *et al.*, 1983; White *et al.*, 1979a,b) and sewage digesters

(Henson *et al.*, 1985; Nichols *et al.*, 1987). Therefore phospholipid phosphate is a good general biomass indicator, which has a calculated conversion factor of 50 μ moles lipid phosphate per dry gram of bacterial cells (White *et al.*, 1979a,b).

(3) The methane concentration can also be considered to reflect the biomass of the methanogens when in a closed system growth experiment since the methane produced cannot escape or be subsequently oxidised. Anaerobic methane oxidation has, however, been observed to occur in some methanogens but the rates were very low and were almost negligible when compared to the rate of methane production (Zehnder & Brock, 1979). Pauly and Van Vleet (1986a) postulated that there was a rough proportionality between methanogen carbon assimilation and methane formation. Fuchs and Stupperich (1984) found that typically about 90 % of a carbon substrate was reduced to methane and approximately 10 % was reduced to cell carbon. Methane is produced in all energy producing reactions in methanogens (Jones *et al.*, 1987; Oremland, 1988), and from table 1.1 of chapter 1 it is possible to compare how the free energy yield per mole of methane produced varies between the various substrates available to the methanogens. Kuivila *et al.* (1990) has shown that CO_2/H_2 was the major substrate (*i.e.* 52 to 58 %) below the SRZ, while acetate accounted for the remainder of the methanogenesis in two coastal sediments. King *et al.* (1983) showed that trimethylamine accounted for 35 to 61 % of the total methanogenesis by acetate, methanol and methylamines within the SRZ of sediments of an intertidal sediment. There has not been a study to date which has determined the rate of methanogenic metabolism using all of the radioactively labelled substrates that are potentially available to methanogens down a sediment core. Unfortunately, facilities were not available during this study to remedy this deficiency.

As well as determining how well the concentration of the methanogenic ether lipids compared to the biomass related parameters of the growth experiments it was also necessary to determine whether the amount of methane produced per mole of ether lipid produced was a function of the growth conditions.

By determining a ratio of the amount of methane produced per unit ether lipid it is possible to indirectly estimate from the total ether lipid data, the total amount of methane that is expected to have been generated in a sample. Within geologically dated sediment samples, this ratio is potentially available for setting maximum limits of methane production in paleoenvironmental reconstructions (Pauly & Van Vleet, 1986a). Similarly, within relatively recent sediments, the concentration of ether lipids could indirectly estimate the amount of methane that would be expected to be present, which together with direct methane measurements could give estimates of the amount of methane which had migrated or been oxidised. Methane is known to migrate from its point of production (Hovland & Judd, 1988) and is also oxidised in the presence of sulphate (Ward & Winfrey, 1985). In areas of rapid sedimentation, the total ether lipid is made

up of the lipid formed *in-situ* together with any relic lipid being deposited. Clearly this additional material must be considered in any calculation of the amount of methane that is removed from the system by migration or oxidation. Therefore in certain environments where the majority of the ether lipid is from *in-situ* methanogenesis it is possible that these estimates could indirectly suggest an amount of methane lost from the sedimentary system by migration or oxidation.

Therefore for these reasons there was a need to directly determine the ratio of the methane produced per mole of ether lipids synthesised. The published research to date has not directly calculated the amount of methane produced, per mole of ether lipid for pure methanogenic cultures. Pauly and Van Vleet (1986a) devised a series of equations to calculate methane/ether lipid ratios by combining values for; (1) methane per dry cell weight (0.16 to 0.63 mmol mg⁻¹), (2) total lipid weight per dry cell weight (mean = 40 µg mg⁻¹), and (3) total lipid weight per ether lipid weight (mean = 1.25 µg µg⁻¹), for a range of methanogenic species. However, the problems of indirectly calculating such ratios is apparent from the large errors in the final result. These authors calculated that between 3268 and 12867 moles of methane were expected to have been produced per mole of diether (*i.e.* mean = 8039) and between 6500 and 25490 moles of methane per mole of tetraether (*i.e.* mean = 16014). The mean values are equivalent to 12.3 moles CH₄ per gram of total diether and tetraether lipid present.

Therefore the aims of this chapter were to:

- (1) determine how the concentration of the ether lipids of methanogens grown axenically under controlled conditions compares with other criteria that have been used as biomass indicators.
- (2) determine whether the concentration of the ether lipids was proportional to the total amount of methane produced during the growth experiments, and to ascertain whether this proportionality changed with:
 - (a) changes in the growth phase (*i.e.* lag, exponential and stationary growth phases)
 - (b) different methanogenic species.
 - (c) different initial gas pressures.

Changes in the biochemical lipid constituents of methanogens have been observed as a result of significant changes in temperature (Sprott *et al.*, 1991). Mesophilic methanogens present in sediments below seawater are not expected to be exposed to large changes in temperature. The effect of change in pressure was considered to be a factor which might warrant study to determine whether an effect on the ether lipid and methane produced could be observed in mesophilic methanogens. Changes in metabolic processes have been observed to occur with changes in pressure (Rheinheimer, 1991).

It was not possible to determine whether the proportions of diether to tetraether lipids may have changed in certain species of methanogens by the conditions given in (2a) to (2c) above because the analytical methodology for the tetraether lipids was not established until the latter part of the experimental programme. The mass spectrometry facility at the Chemistry Dept., U.C. Wales; Bangor did not offer the sensitivity to determine the mass spectra of low concentrations of derivatives present in environmental samples of mixed components. All of the analysis of the diether derivatives that were made in the growth experiments and earlier studies relied upon comparing the retention with a standard that had been prepared from the compound phytol. Chemicals prepared from pure sources were used on the mass spectrometer in milli-gram quantities at the Chemistry Dept. to obtain mass spectra. The mass spectral analysis of the diether and tetraether derivatives from mixed component standards were obtained from the mass spectrometer at the School of Ocean Sciences, which only became available for these measurements towards the end of the experimental programme.

When attempting to relate the methanogenic biomass to the total amount of methane that would have been expected to be produced, it is important to determine the residence time of the ether lipids in the sediments once the cells have died. There is very little information available in the literature on the turnover of methanogenic cells in marine sediments. The rate with which methanogenic cells die and the degradation rate of the ether lipids in marine sediments will control whether the ether lipid concentration will reflect predominantly the viable biomass present or the dead, non-viable, necromass. Harvey *et al.* (1986) showed that unbound ester linked phospholipids were degraded at rates of over 20 times faster than unbound ether linked glycolipids in marine sediments. Organic carbon and the presence of oxygen were also shown by these workers to have a significant effect on the degradation rates. Again this report provided a good insight into the degradation rates of the ether lipids relative to ester linked lipids under a variety of conditions. They suggested that since the unbound, TLC pure lipids would partition into the organic phase of the sediment, it would isolate them from degradation enzymes found in the aqueous phase. It could be argued however, that fragments of the bound cell membrane would show more hydrophilic properties than the hydrophobic unbound glycolipids used in the study of Harvey *et al.* (1986). The bound membrane lipids could therefore be expected to be more exposed to the enzymes within the aqueous phase of the sediments than the unbound lipids used in the study of Harvey *et al.*, (1986).

(3) determine how the bound ether lipids that are still attached to the cell membrane would degrade under different conditions. The types of environments tested included; aerobic and anaerobic conditions, high and low temperature conditions, and axenic and mixed culture conditions.

RESULTS AND DISCUSSION

4.2. Results of the Growth Experiment using *Methanosarcina acetivorans*

As carbon dioxide/hydrogen (80:20) mixtures showed only limited growth, *Methanosarcina acetivorans* was cultured at atmospheric and 2.5 times atmospheric pressure with trimethylamine as carbon substrate for 140 hrs. Details of the media, measuring techniques and other conditions are given in section 2.2.1. of Chapter 2 and section A1.3 of appendix I. The following parameters were recorded;

1. Gas phase pressure.
2. Cell numbers.
3. Cell diameters.
4. Surface area of the cells.
5. Dry weight of the cells.
6. Turbidity - optical density.
7. Methane evolved.
8. Phospholipid phosphate concentration.
9. DPGE ether lipid concentration.
10. Moles of methane produced per mole of DPGE.

4.2.1. Comparison of the DPGE Ether Lipid Concentration with other Biomass Related Parameters for *Methanosarcina acetivorans*.

The values of the biomass related parameters measured during the growth experiment are given in table 4.1. The mean values of the replicated samples at each analysis time were plotted versus time. Figures 4.1 to 4.5 show how each of the biomass related parameters compare with the concentration of the DPGE membrane lipid over the growth culture experiment at initial pressures of atmospheric (atm) and 2.5 times atmospheric pressure.

Figure 4.1 illustrates how similar the methane concentrations and DPGE lipid concentrations were over the growth period. Correlation coefficients of the methane and DPGE concentrations were significant at $r = 0.985$ ($Df = 8$, $p < 0.001$) for the experiment starting at atmospheric pressure, and $r = 0.993$ ($Df = 8$, $p < 0.001$) for 2.5 times atmospheric pressure. Figure 4.2 also demonstrated similar growth curves between the total cell surface area and DPGE lipid concentration, which had significant correlation coefficients at $r = 0.982$ ($p < 0.001$) and $r = 0.960$ ($p < 0.001$) for the atmospheric and the 2.5 times atmospheric initial pressures, respectively. Figure 4.3 also demonstrated high correlation coefficients between phospholipid phosphate and the DPGE lipid concentrations at $r = 0.971$ ($p < 0.001$) and $r = 0.982$ ($p < 0.001$) for the atmospheric and 2.5 times atmospheric initial pressures, respectively. Similarly correlation coefficients between the DPGE lipid and the cell dry weight (see figure 4.4, $r = 0.876$ for atm, $r = 0.899$ for 2.5 atm), and the turbidity measurements (see figure 4.5, $r = 0.930$ for atm, $r = 0.962$ for 2.5 atm) were all significant, *i.e.* $p < 0.001$.

Table 4.1. Biomass related parameters measured from cultures of *Methanosarcina acetivorans* at initial growth pressures of atmospheric and 2.5 times atmospheric pressure.

Time (h)	Pressure (Atm)	Cell No. ($\times 10^6$ ml ⁻¹)	Mean Cell Diameter (μ m)	Total cell surface area (μ m ² ml ⁻¹)	Methane (μ mol ml ⁻¹)	Cell Dry Weight (mg ml ⁻¹)	Turbidity (560 nm)	Phospho-lipid Phosphate (nmol ml ⁻¹)	DPGE (nmol ml ⁻¹)	Moles of * methane per mole of diether
Atmospheric Pressure				($\times 10^9$)						
0	1	137	1.12	0.54	0	0.01	0.32	0.12	0.21	n.d.
43	1.2	41	1.82	0.42	5	n.d.	0.39	0.21	0.19	n.d.
43	1.25	37	1.80	0.38	16	0.07	0.41	0.18	0.18	n.d.
68	1.55	97	1.84	1.03	28	0.08	0.78	1.39	0.86	43077
68	1.5	62	1.85	0.66	26	0.08	0.76	1.11	0.77	46429
93	2.25	183	1.86	1.99	59	0.07	1.63	3.64	1.47	46825
93	2.25	212	1.98	2.61	73	0.08	1.76	5.34	1.98	41243
117	3.5	390	1.77	3.84	159	0.21	2.52	7.54	3.14	54266
117	3.9	473	1.88	5.25	174	0.14	2.68	11.04	3.23	57616
140	4.58	662	1.54	4.93	177	0.20	2.73	11.34	3.61	52059
140	4.58	788	1.57	6.10	176	0.20	2.20	9.79	3.82	48753
										Mean = 48784
2.5 times Atmospheric										
0	2.5	137	1.12	0.54	0	0.01	0.32	0.12	0.21	n.d.
43	2.6	42	1.90	0.47	10	0.04	0.40	1.14	0.46	40000
43	2.55	43	2.01	0.55	10	0.06	0.38	0.51	0.47	38462
68	2.85	82	1.89	0.92	27	n.d.	0.88	1.63	0.86	41538
68	2.75	98	1.87	1.07	35	0.08	0.84	1.49	0.84	55556
93	3.65	198	2.10	2.74	79	0.06	1.81	4.87	2.24	38916
93	3.45	206	1.95	2.46	74	0.10	1.77	5.24	2.31	35238
117	4.98	522	1.95	6.24	139	0.13	2.72	11.17	3.89	37772
117	4.95	525	1.85	5.64	136	0.19	2.82	11.70	3.65	39535
140	5.1	982	1.75	9.45	144	0.21	2.72	11.61	4.49	33645
140	5.8	786	1.85	8.45	155	0.26	2.72	12.78	4.59	35388
										Mean = 39605

* In order to allow for the initial concentration of the DPGE lipid added to the cultures at time zero the DPGE concentration at time zero was subtracted from all subsequent DPGE concentrations before the ratio of methane per DPGE lipid was determined.

n.d. = not determined, most of ether lipid represents the methanogens added during inoculation therefore the errors associated with the change in DPGE lipid are significant.

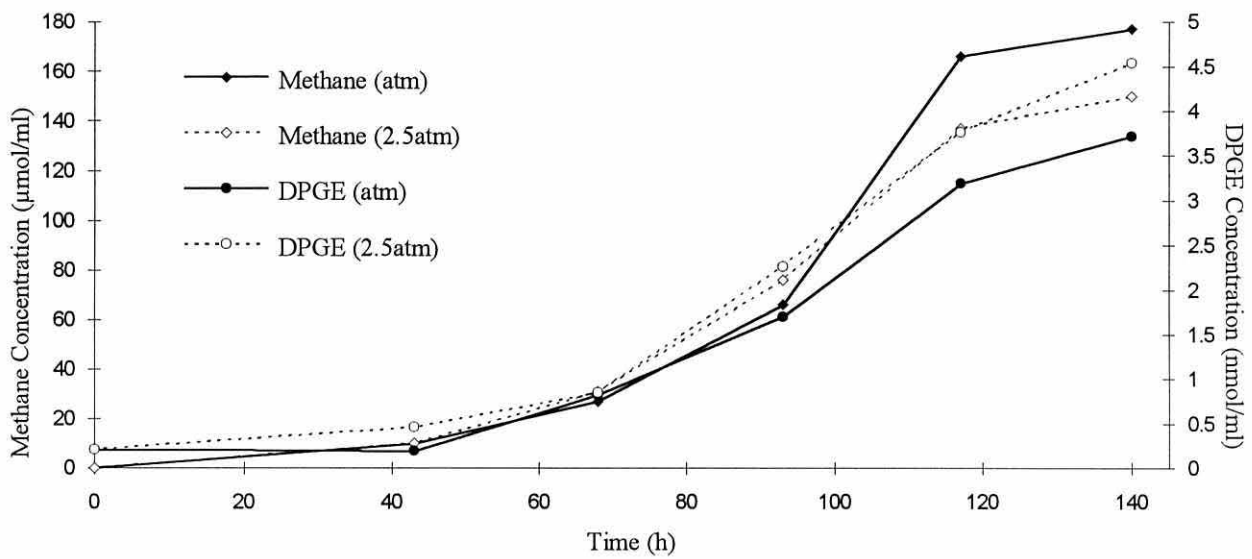


Figure 4.1. Growth curves for *Methanosarcina acetivorans* comparing mean concentrations of methane produced and mean concentrations of the DPGE diether membrane lipid at initial growth pressures of atmospheric and 2.5 times atmospheric pressure.

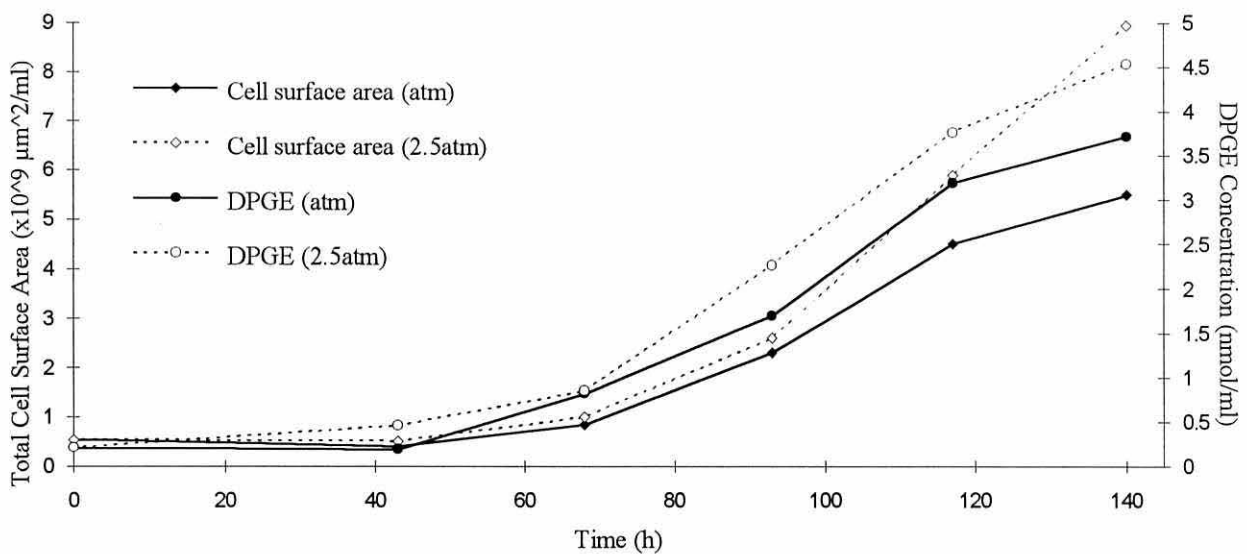


Figure 4.2. Growth curves for *Methanosarcina acetivorans* comparing mean total cell surface areas and mean concentrations of the DPGE diether membrane lipid at initial growth pressures of atmospheric and 2.5 times atmospheric pressure.

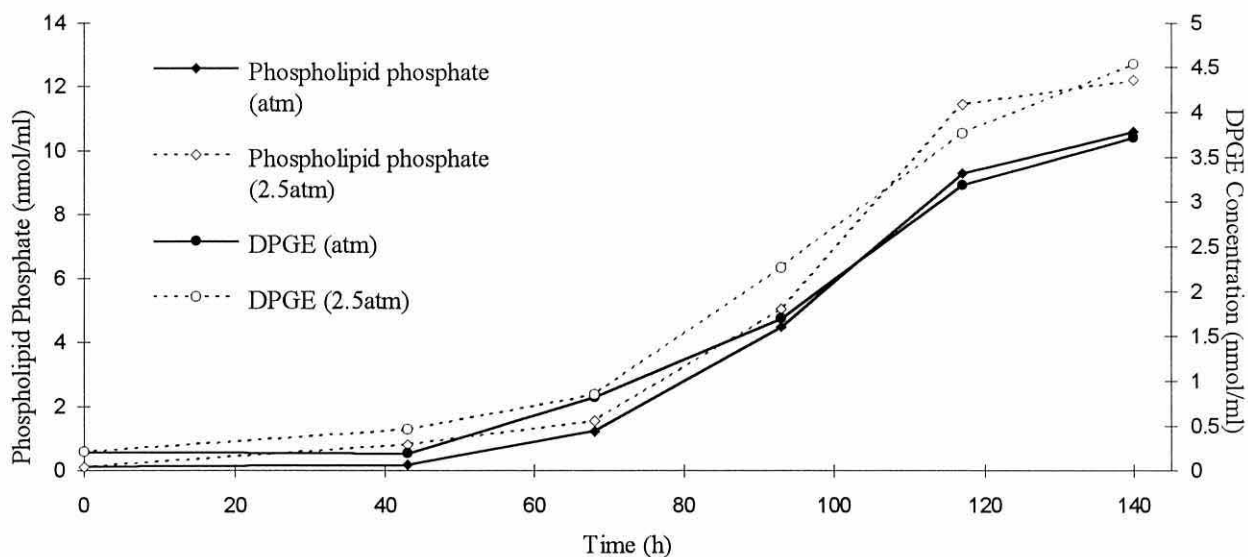


Figure 4.3. Growth curves for *Methanosarcina acetivorans* comparing mean concentrations of phospholipid phosphate and mean concentrations of the DPGE diether membrane lipid at initial growth pressures of atmospheric and 2.5 times atmospheric pressure.

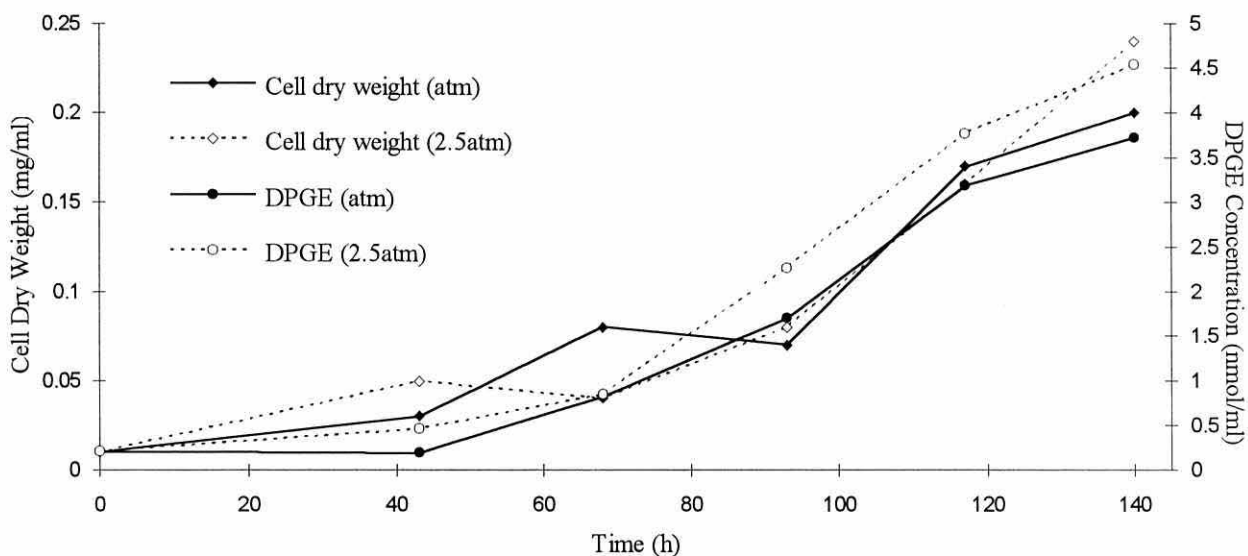


Figure 4.4. Growth curves for *Methanosarcina acetivorans* comparing mean total cell dry weight and mean concentrations of the DPGE diether membrane lipid at initial growth pressures of atmospheric and 2.5 times atmospheric pressure.

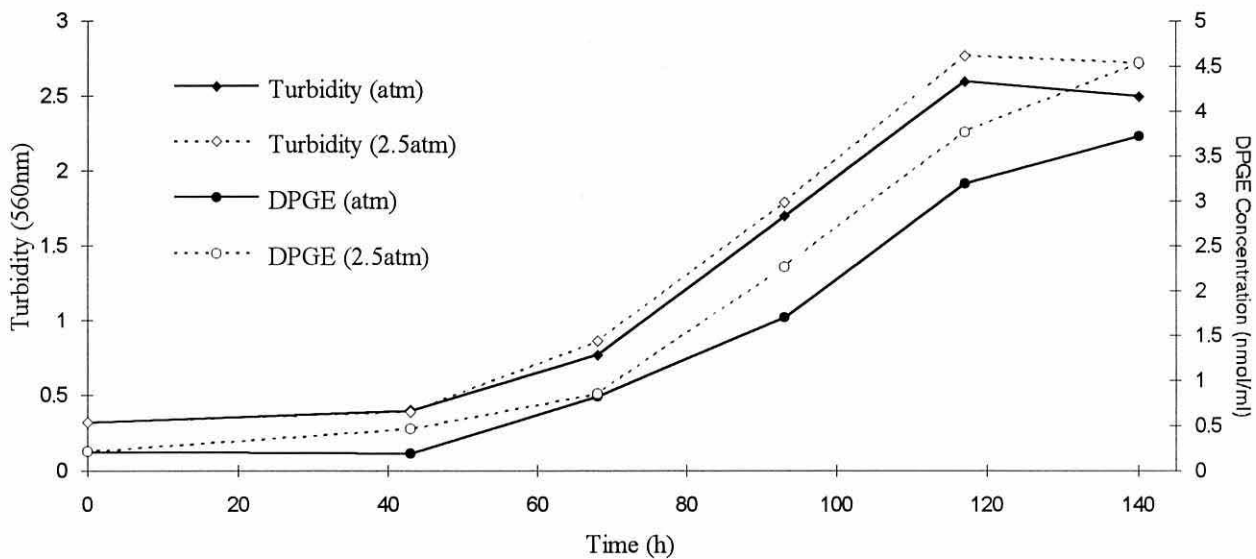


Figure 4.5. Growth curves for *Methanosarcina acetivorans* comparing mean culture turbidity at 560 nm and mean concentrations of the DPGE diether membrane lipid at growth pressures of atmospheric and 2.5 times atmospheric pressure.

Therefore it can be concluded that the concentration of the DPGE lipid correlated significantly and therefore changed proportionately with the cell dry weight of the methanogens and also with the other parameters measured during the growth experiment.

Analysis of covariance was used to compare the effect of pressure on the concentration of DPGE per unit measure of other biomass parameters. The analysis was performed by the general linear modeling (GLM) program on the Minitab statistical package. The analysis of covariance was therefore used to test whether the slopes of the regression lines of the biomass related parameters *versus* the DPGE lipid concentration were homogeneous for the two different growth pressure treatments (*i.e.* starting pressures of atmospheric and 2.5 times atmospheric).

GLM revealed that for the parameters of; cell surface area ($p = 0.648$), cell dry weight ($p = 0.824$), turbidity ($p = 0.501$) and phospholipid phosphate ($p = 0.712$), the regression lines with the DPGE lipid concentration did not show any difference between the slopes of the two growth pressure treatments, within the error. Also, there was no difference in the intercepts, *i.e.* adjusted means of Y, between the two treatments for a common mean of X and a common regression line.

However, GLM analysis of the methane *versus* DPGE lipid regression line showed that there was a difference in the slopes of the two growth pressure treatments (*i.e.* $p < 0.001$). The reason for this significant difference in the slopes of the regression lines for the two treatments might have

been due to one of the treatments having a longer lag phase period due to the pressure change imposed at time zero. In order to check this possibility the growth curve of one treatment was moved along the time axis to achieve the best overlap of the two growth curves. The new methane and DPGE concentrations were read directly from the graph at corresponding analysis times of the unadjusted treatment curve. However, GLM analysis showed that the slopes of the regression lines were still different between treatments, even after the growth curves were adjusted for the best overlap. Therefore it would appear that different periods of lag phase were not the reason for the difference in the slopes.

The slope of the methane/DPGE regression line for the atmospheric pressure treatment was greater than the slope of the treatment started at 2.5 times atmospheric pressure. Therefore less methane was present in the culture tubes incubated at the higher pressure relative to the lower pressure incubations, as seen in figure 4.1. Although the initial gas pressures began at atmospheric and 2.5 times atmospheric, the pressure increased during the growth experiment such that at the time of the final measurements (*i.e.* 140 hours) the average pressures were approximately 4.6 and 5.5 atmospheres, respectively. The pressures were determined from the volume of gas purged from the known volume of headspace and the values are given table 4.1. Figure 4.1 illustrated that the methane produced for the atmospheric and 2.5 times atmospheric pressure treatments were similar up to 93 hours with respective pressures of 2.25 and 3.5 atmospheres. After 93 hours (*i.e.* 117 and 140 hours) the concentration of methane in the treatment that was started at atmospheric pressure became greater than for the corresponding times of the 2.5 times atmospheric pressure treatment. Therefore although the pressure was gradually increasing for both treatments over the growth period it was only until 5.0 atmospheres of pressure (*i.e.* time 117 hours of the 2.5 atmospheric pressure treatment) was reached that the methane concentration reduced relative to the lower pressure treatment. The maximum pressure reached of the lower pressure treatment was 4.6 atmospheres.

The DPGE lipid concentrations were similar between the two treatments up until time 68 hours. However, after this time the DPGE concentration of the treatment started at 2.5 atmospheres pressure began to increase relative to the treatment at atmospheric pressure (see figure 4.1). This result was unusual in that after 117 hours less methane but more DPGE lipid was produced in the treatment started at 2.5 atmospheres relative to the treatment started at atmospheric pressure. The reasons for this observation are unclear from the data set. However, it could be due to a change in the biochemical reactions of the methanogens from methane production to a greater production of cell carbon. It is also possible but unlikely however, that methane escaped through the septa of the incubation tubes due to the higher pressure in the treatment. This would cause lower methane concentrations in the higher pressure treatment relative to the lower pressure treatment (*i.e.* atmospheric).

4.2.2. DPGE Lipid - Methane Ratios for *Methanosarcina acetivorans*.

In order to determine the ratio of methane to DPGE lipid it was first necessary to subtract the initial concentration of ether lipid added to the culture at time zero when negligible methane was present in the headspace. Therefore the subsequent ether lipid production would be more directly related to the concentration of methane produced from the subsequent energy yielding metabolism reactions. At the beginning of the experiment the majority of the DPGE lipid was from the methanogens that were inoculated into the tubes. Therefore the errors associated with the initial changes in DPGE lipid were expected to be high. The ratios of methane to DPGE ether lipid determined at each analysis time and at different initial growth pressures of the growth experiment using *M. acetivorans* are given in table 4.1.

The mean methane to DPGE ether lipid ratio for each growth pressure shows that more methane is produced per diether lipid for the cultures which began at atmospheric pressure (*i.e.* 48784 moles/mole, SD = 5575) than the cultures started at 2.5 times atmospheric pressure (*i.e.* 39605 moles/mole, SD = 6109). These mean ratios are equivalent to 74.8 and 60.7 moles CH₄ per gram ether lipid, respectively. Confidence limits for these ratios suggested that the deviations about the means of the two treatments did not overlap at the 95 % confidence level. For the atmospheric pressure treatment the 95 % confidence limits ranged from 44122 to 53446 moles/mole (*i.e.* 67.7 to 82.0 moles per gram), and for the 2.5 times atmospheric pressure treatment the 95 % confidence limits ranged from 35235 to 43975 moles/mole (*i.e.* 54.0 to 67.4 moles/gram). The 95 % confidence intervals were calculated using; $\bar{X}(\text{mean}) \pm t_{0.05[n-1]} s / \sqrt{n}$, where $t_{0.05[n-1]}$ is the t-value for n-1 degrees of freedom at the 0.05 probability, s is the standard deviation and n is the number of samples.

Regression analysis of the methane/DPGE lipid ratio versus time for the atmospheric growth pressure treatment gave a positive slope with 95 % confidence intervals that incorporated zero. Similarly, for the 2.5 times atmospheric pressure treatment the slope also incorporated zero, which suggested that there was no overall increasing or decreasing trend in the methane/ether lipid ratio over the lag, exponential and stationary growth phases for either pressure treatment. Similar results were also recorded when regressing methane/DPGE values *versus* the pressure measured in the headspace above the cultures.

Determination of the ratio of phospholipid phosphate per gram of dry methanogen cells from the data revealed values of 38.5 $\mu\text{moles g}^{-1}$ (SD = 26.0) for the experiment initiated at atmospheric pressure, and 45.3 $\mu\text{moles g}^{-1}$ (SD = 27.5) for the experiment initiated at 2.5 times atmospheric pressure. These values were close to the mean ratio for many eubacterial species at 50 $\mu\text{moles g}^{-1}$, as determined by White *et al.* (1979a). Ratios of the DPGE ether lipid per dry gram of the methanogen cells were 16.5 $\mu\text{moles g}^{-1}$ (SD = 7.0) and 19.9 $\mu\text{moles g}^{-1}$ (SD = 8.9) for the atmospheric and 2.5 times atmospheric growth pressures, respectively. The values of this

experiment were higher than the mean ratio reported by Nichols *et al.* (1987) at 2.5 $\mu\text{moles g}^{-1}$ of glycerol ether phospholipid per dry gram of methanogenic cells. However, one reason for the lower value determined in the study of Nichols *et al.* (1987) would be due to the methanogens containing significant amounts of tetraether relative to the diether membrane lipid, *i.e.* 1 mole tetraether = 2 moles of diether. Also it is not clear from Nichols *et al.* (1987) whether the 2.5 $\mu\text{moles g}^{-1}$ refers to the hydrolysed ether lipid or the ether lipid with the phospholipid headgroup attached. The latter would also reduce the $\mu\text{mole per gram}$ value given.

4.3. Results of the Growth Experiment using

Methanococcoides methylutens

The material and methods specific to this experiment are given in section 2.2.1. of Chapter 2 and section A1.2 of appendix I. Trimethylamine was the carbon source used during this growth experiment. The data collected for the biomass related parameters during the growth experiment with *Methanococcoides methylutens* are given in table 4.2. Problems encountered during the enumeration of the methanogens (see section 2.2.1) meant that the data concerning the cell number and total cell surface area were not determined.

4.3.1. Comparison of the DPGE Ether Lipid Concentration with other Biomass Related Parameters for *Methanococcoides methylutens*.

Correlation analysis revealed that none of the parameters measured during this growth experiment correlated as highly as in the growth experiment of section 4.2. Therefore comparison of the biomass related parameters with the concentration of ether lipids also gave correspondingly lower correlation coefficients. The correlation coefficient of the mean values of methane *versus* DPGE lipid concentration was recorded at $r = 0.794$, which was significant at $p < 0.02$. Mean concentrations of phospholipid phosphate and the DPGE lipid compared more favourably and had a correlation coefficient of $r = 0.806$ (*i.e.* $p < 0.01$). The turbidity analyses made at 560 nm were the most variable of all the parameters measured during the growth experiment (see table 4.2). Therefore comparison of the mean turbidity and DPGE lipid measurements gave a low correlation coefficient which was not significant at the 90 % confidence level (*i.e.* $p > 0.1$).

4.3.2. Methane - DPGE Lipid Ratios for *Methanococcoides methylutens*.

The ratios of methane per DPGE lipid produced during the growth experiment are given in table 4.2. The mean value of 72638 moles of methane per mole of DPGE lipid had 95 % confidence intervals that ranged from 53479 to 91797 moles per mole. Such ratios for the DPGE lipid were equivalent to 111.4 moles CH_4 per gram of ether lipid with limits of 82.0 and 140.8 moles g^{-1} for the total ether lipids. These results were significantly higher than the ratios calculated for other species from the publication of Pauly and Van Vleet (1986a).

Table 4.2. Biomass related parameters measured from cultures of *Methanococcoides methylutens* during a growth culture experiment.

Time (h)	Methane ($\mu\text{mol ml}^{-1}$)	Turbidity (560 nm)	Phospholipid Phosphate (nmol ml^{-1})	DPGE (nmol ml^{-1})	Methane per DPGE * (mole/mole)
0	0.3	0.05	0.81	0.24	n.d.
12	17.0	0.05	0.50	0.56	53125
12	n.d.	n.d.	n.d.	0.52	n.d.
24	41.8	0.05	0.72	0.77	78868
24	60.8	0.05	1.01	0.87	96508
36	81.9	0.24	5.15	1.03	103671
36	91.4	0.47	n.d.	n.d.	n.d.
48	46.8	0.09	2.20	1.33	42936
48	29.7	0.28	1.04	1.62	21522
60	167.4	0.33	2.81	2.07	91475
60	131.1	0.47	5.70	1.25	129802
72	150.5	0.20	6.06	2.33	72009
72	108.2	0.37	5.11	5.09	22309
84	203.9	0.22	5.88	2.02	114551
84	87.8	0.46	2.05	2.32	42212
96	198.5	0.21	6.05	2.79	77843
96	165.5	0.22	6.77	n.d.	n.d.
196	203.3	n.d.	8.34	3.14	70103
				Mean =	72638

* In order to allow for the initial concentration of the DPGE lipid added to the cultures at time zero the DPGE concentration at time zero was subtracted from all subsequent DPGE concentrations before the ratio of methane per DPGE lipid was determined.

n.d. = sample lost or not determined, most of ether lipid represents the methanogens added during inoculation therefore the errors associated with the change in DPGE lipid are significant.

4.4. Results of Growth Experiment Using *Methanlobus tindarius*

The results of the growth experiment using *Methanlobus tindarius* were presented at the conference "Shallow Gas in Marine Sediments" held at the Heriot-Watt University, Edinburgh in 1990. Much of the data and results for this experiment were published (Smith & Floodgate, 1992), a copy of which is given in appendix IX. *Methanlobus tindarius* was grown on methanol and trimethylamine in the growth experiment. The various growth parameters analysed, which was not included in the publication, is however, given in table 4.3.

Table 4.3. Biomass related parameters measured during the growth experiment of *Methanolobus tindarius*.

Time (h)	Cell Number ($\times 10^9 \text{ ml}^{-1}$)	Methane ($\mu\text{moles ml}^{-1}$)	Turbidity (560 nm)	DPGE (nmol ml^{-1})	Methane * per DPGE (mole/mole)
0	0.4	0.0	0.05	0.17	n.d.
8	0.3	0.0	0.00	0.14	n.d.
16	0.4	0.3	0.00	0.26	3398
24	0.7	1.2	0.12	0.30	8918
32	2.0	3.0	0.19	0.46	10363
40	3.7	4.4	0.30	0.57	10986
48	14.5	16.8	0.40	0.88	23568
56	360.0	28.8	0.66	1.71	18653
64	460.0	40.8	0.98	4.54	9329
72	573.0	61.5	1.28	4.43	14425
80	250.0	92.6	1.57	6.09	15626
88	530.0	146.3	1.86	10.50	14157
96	612.0	142.6	1.91	12.40	11656
				Mean =	12825

* In order to allow for the initial concentration of the DPGE lipid added to the cultures at time zero the DPGE concentration at time zero was subtracted from all subsequent DPGE concentrations before the ratio of methane per DPGE lipid was determined.

n.d. = not determined, most of ether lipid represents the methanogens added during inoculation therefore the errors associated with the change in DPGE lipid are significant.

The graphical comparison of the DPGE lipid concentration with the other biomass related parameters is given in the publication in appendix IX. Correlation analysis of the cell number, methane and turbidity measurements versus the DPGE lipid concentration gave significantly high correlation coefficients at $r = 0.846$, $r = 0.985$ and $r = 0.953$, respectively (*i.e.* $p < 0.001$).

The ratios of methane per DPGE lipid produced for the *Methanolobus tindarius* growth experiment are given in table 4.3. The mean ratio of 12825 moles/mole had 95 % confidence limits which ranged from 9217 to 16435 moles per mole, which is slightly higher than the ratios calculated by Pauly and Van Vleet (1986a). Equivalent ratios of $19.7 \text{ moles g}^{-1}$ with 95 % confidence intervals of 14.1 to $25.2 \text{ moles g}^{-1}$ were calculated. Regression analysis of the methane per DPGE lipid *versus* time gave a positive slope with 95 % confidence intervals that incorporated zero. Therefore there did not appear to be any significant increasing or decreasing trends noticed in the ratios over the lag, exponential and stationary phases of the growth experiment.

4.5. Mean Ratios of Methane Produced per Ether Lipid Synthesised

The ratios of methane per DPGE lipid varied measurably between the three different species of methanogens analysed. Mean values were 12825 moles per mole for *Methanolobus tindarius*, 72638 moles per mole for *Methanococcoides methylutens*, and 48784 moles per mole for *Methanosarcina acetivorans* when incubated at initial growth pressures of one atmosphere. It could not be explained whether the increased pressure of the *M. acetivorans* experiment caused less methane to be produced relative to cell carbon production or perhaps more methane to escape at the high pressures created, therefore the ratio of the 2.5 atmospheric pressure treatment (*i.e.* 39605 moles methane per mole DPGE lipid) was not included when determining the mean ratio. From this study methane/DPGE ratios were calculated for three species of methanogens from the same methanogenic family and with substrates of trimethylamine and methanol. It is suggested that further work should also select more carbon substrates and more methanogen species including ones that can metabolise carbon dioxide and hydrogen from other families of methanogens. The methane/DPGE ratios may therefore show greater variation than the values calculated in this study.

For the diether lipid (*i.e.* DPGE) the mean ratio of methane to DPGE lipid for the three methanogenic species analysed was 44749 moles per mole (*i.e.* 68.6 moles g⁻¹). The limits used when applying this ratio to the diether lipid data of the marine sediment cores, given in chapter 5, were taken as 12825 and 72638 moles per mole for the diether lipids. The tetraether lipids, however, form a monolayer configuration in the cell membranes of the methanogenic bacteria as opposed to the bilayer configuration of the diether lipids. Therefore a single tetraether lipid molecule can bridge the outer cell membrane to the inner cell membrane, whereas two diether lipids are required to provide a similar membrane structure. Therefore 1 mole of tetraether, with a typical molecular weight of 1302 per molecule, is equivalent to 2 moles of the diether lipid which has a molecular weight of 652 (*i.e.* approximately half). Alternatively the mean ratios of methane per DPGE lipid concentration could be given in the units of moles per gram (μ moles per μ gram) of total ether lipid present. Therefore the mean ratios of 68.6 moles of methane produced per gram of total ether lipid present could be applied to the total concentration of all diether (*i.e.* Mw 652 x 68.6 = 44749 moles CH₄ per mole diether) and tetraether (*i.e.* Mw 1302 x 68.6 = 89361 moles CH₄ per mole tetraether) methanogenic lipids.

4.6. Ether Lipid Degradation Experiment

The materials and methods pertaining to the ether lipid degradation experiment are given in section 2.2.4 of Chapter 2. The data collected during the ether lipid degradation experiment are given in table 4.4.

Table 4.4 shows the diether lipid concentrations determined over time for culture flasks exposed to various conditions. The conditions were imposed on three month old methanogenic cultures of *Methanolobus tindarius* that were expected to be already well into their stationary phase. It is evident from table 4.4 that the diether lipid was present in all conditions studied over the entire period of the experiment. Although three subsamples were taken from each flask at each sampling time the three samples were only analysed from flask number 1 at the 2 month sampling time. This result showed that the ether lipid concentration was variable for this sampling point (*i.e.* mean = 8.9 $\mu\text{g ml}^{-1}$, SD = 3.8, CV = 42%). For this reason and especially in light of the long sample work-up period for each determination it was decided to only analyse one subsample from the remaining flasks of the time course experiment.

Table 4.4. Ether lipid degradation experiment showing the change in diether lipid concentration of a culture of *Methanolobus tindarius* over time for various conditions.

Conditions	Diether Lipid Concentration ($\mu\text{g ml}^{-1}$)				
	0	1 Month	2 Months	3 Months	4 Months
1 Anaerobic Axenic, 4°C	13.3	6.2	9.6 12.2 4.8	6.9	9.8
2 Anaerobic Axenic, 25°C	3.1	0.7	6.4	9.6	7.2
3 Anaerobic Sediment, 4°C	13.8	6.2	20.5	18.7	15.0
4 Anaerobic Sediment, 25°C	7.6	17.9	26.5	26.8	14.7
5 Aerobic Axenic, 25°C	12.0	9.5	6.8	5.5	7.2
6 Aerobic Sediment, 25°C	20.9	7.0	12.7	16.2	13.3
7 Aerobic Sediment, 25°C Killed control	14.1	16.2	8.9	10.3	12.1

Also there did not appear to be any consistent trends with increasing time in the experiment for any of the conditions analysed, including the killed control (see table 4.4). Harvey *et al.* (1986) demonstrated the greatest rates of ether lipid degradation occurred under aerobic conditions, therefore it may have been expected for the aerobic flasks (*i.e.* flask Nos. 5 and 6) to show the fastest removal of ether lipids.

Microscopy showed the presence of motile cells that were expected to be the methanogen *Methanolobus tindarius* in all of the axenic, anaerobic flasks (*i.e.* flask Nos. 1 and 2) over the 4 month period following set-up of the conditions. This was not observed for the axenic, aerobic flask (*i.e.* flask No. 5) which may have been due to the excessive clumping of the cells that occurred in this flask. The presence of active methanogens in these anaerobic, axenic flasks suggests that methanogenesis had not had sufficient time for all cells to reach a senescent growth stage and it may also be expected that some re-cycling of the dead cell constituents provided growth substrates for subsequent methanogenic growth. It may have been more beneficial for this experiment to break up the cells by sonication just before the degradation conditions were initiated.

Within two months of establishing the cultures in the seven flasks it was noticed that the cells began to clump in all flasks. It was apparent that before every sampling period these clumps did not break up after rigorous shaking and also became attached to the sides of the glass surfaces. Pre-combusted sand (~ 10 g) was added to each flask to help with the mixing process and was observed to help break up some of the clumps. *Methanolobus tindarius* has been shown to be a non-clumping, motile species in the growth experiments. The formation of incompact slimy aggregates has however, been observed in this species (König & Stetter, 1982) and the formation of protective coatings encompassing clusters of cells when dormant has also been observed in methanogens from the same family as *Methanolobus tindarius* (Robinson, 1986). Observations of the clumps taken from the aerobic, axenic flask under the microscope could not identify motile cells even after the clumps were broken up when in view.

Although, the effect of the sand appeared to break up the clumped methanogenic material sufficiently during the sampling the results from the analysis, that were made up to 3 months after the last sample had been collected, suggested that sample homogeneity had not been achieved by this sampling technique. The use of such high concentrations of methanogens in this study was probably a contributing factor to the significant clumping observed. It is apparent, however, that under the aerobic conditions given in flask No. 5 where motile methanogens were not observed that the diether membrane lipid appeared to be resistant to degradation for periods in excess of 4 months. From the observations made with the microscope it would appear that due to the cells not being killed when the conditions for degradation were initiated in the anaerobic flasks the potential of chemicals becoming re-cycled for subsequent methanogenic growth would be

possible. The potential for new methanogenic growth from the re-cycling of cell constituents in the aerobic flasks would, however, be expected to be minimal and therefore the presence of diether lipids in these flasks possibly emphasises further the resistance of these lipids to degradation even when in aerobic conditions.

4.7. Summary

Good correlation was observed between the DPGE lipid and the other biomass related parameters measured during the growth experiment of the methanogen *Methanosarcina acetivorans* (*i.e.* $p < 0.001$). The *Methanobrevibacter smithii* growth experiment also demonstrated highly significant correlation coefficients between the DPGE lipid and the other parameters which reflected the biomass of the methanogen (*i.e.* $p < 0.001$). For the growth experiment using *Methanococcoides methylutens* it was noted that all growth parameters did not correlate as highly as in the *M. acetivorans* and *M. smithii* growth experiments. This was also reflected in the correlation with the DPGE lipid, though correlations with the ether lipid were as high as with any of the other parameters measured. Therefore it would appear that the concentration of the DPGE lipid reflected the biomass of the methanogenic bacteria as well as the other parameters measured in the axenic growth cultures. The benefits of interpreting the DPGE lipid concentration become evident when estimating methanogenic biomass in mixed cultures or environmental samples, when parameters such as phospholipid phosphate, turbidity and cell volume are not specific indicators of methanogenic biomass.

The effect of the different incubation pressures on the growth experiment using *M. acetivorans* gave similar growth curves between most of the biomass related parameters and the DPGE lipid. However significantly less methane was observed in the higher pressure treatment than would have been expected on the basis of the biomass related parameters, such as DPGE lipid concentration. This might have been explained by gas escaping during the high incubation pressures (*i.e.* ≥ 5 atmospheres). However, since every care was taken to avoid this it could suggest that a change occurred in the biochemical reactions of the methanogens from methane production to a greater production of cell carbon.

Ratios of methane produced per DPGE lipid showed neither increasing nor decreasing trends with time over the lag, exponential and stationary growth phases of the growth experiments using the three species of methanogens. Mean values of the methane per DPGE lipid ratio were; 12825 moles of methane per mole of DPGE (19.7 moles $\text{CH}_4 \text{ g}^{-1}$ ether lipid) for *Methanobrevibacter smithii*, 72638 moles CH_4 per mole DPGE (*i.e.* 111.4 moles $\text{CH}_4 \text{ g}^{-1}$ ether lipid) for *Methanococcoides methylutens*, and 47784 moles CH_4 per mole DPGE (*i.e.* 73.3 moles $\text{CH}_4 \text{ g}^{-1}$ ether lipid) for *Methanosarcina acetivorans* when grown at an initial pressure of one atmosphere.

The methane/DPGE ratios for the *M. acetivorans* experiment started at 2.5 times atmospheric pressure were significantly lower (*i.e.* mean = 39605, 95 % confidence intervals = 35235 to 43975 moles per mole) than the atmospheric pressure treatment (*i.e.* mean = 47784, 95 % confidence intervals = 44122 to 53446 moles per mole). The reasons for this result could not be explained from the data set but due to the possibility that methane might have escaped from the culture tubes at the higher pressures generated (*i.e.* ≥ 5 atmospheres) this data was not included in the methane/DPGE ratios.

Mean values for the methane/DPGE lipid ratios from the three growth experiments were 44749 moles CH₄ per mole DPGE (Mw = 652) which was equivalent to (44749/652) 68.6 moles CH₄ per gram of ether lipid. By assuming that this ratio can be applied to tetraether lipids such as C40,0 (Mw = 1302) 68.6 moles CH₄ would be expected to be produced per gram of tetraether, which equates to approximately (68.6 x 1302) 89361 moles CH₄ per mole of C40,0. It is suggested that further work on methane/ether lipid ratios should also select more carbon substrates from more methanogen species including ones that can metabolise carbon dioxide and hydrogen from other families of methanogens.

The ether lipid degradation experiment showed that the intact ether lipids in the aerobic cultures were present for up to periods of 4 months. However, problems were attributed to not being able to obtain homogenous samples and also to the continued methanogenic growth after the conditions were initiated in certain anaerobic flasks. Suggestions for where improvements in this method could be made are considered. Firstly, for subsequent experiments it is recommended that the cultures could be split into their respective subsampling containers before the material clumps, therefore the entire contents of the container could be extracted at the time of sampling. Secondly, smaller methanogenic concentrations could be used. Thirdly, the cells should be killed at the onset of the degradation conditions by a technique that would not affect other bacteria present in the samples which had the sediment additions. The use of sonication could be used to break up the cells before the various conditions were initiated.

Hence it can be concluded that the concentration of ether lipids, estimated by the technique in this thesis, is a good criterion for the determination of methanogenic biomass in pure culture, since it correlates well with other biomass determinants, including the dry weight of organism. However, because of the recalcitrant nature of the lipid, especially under anaerobic conditions, the problem of estimating the fraction of the material measured that is from moribund organisms, is a major drawback especially in old cultures.

CHAPTER 5. ANALYSIS OF THE FACTORS ASSOCIATED WITH THE BIOLOGICAL PRODUCTION, DISTRIBUTION AND FATE OF METHANE IN ACOUSTICALLY TURBID AND GAS FREE MARINE SEDIMENTS.

5.1. Introduction

It has been shown that the membrane ether lipids of methanogenic bacteria are indicators of methanogenic biomass when in pure culture experiments (see chapter 4) and also when in samples where methanogenic bacteria are abundant (Nichols *et al.*, 1987; Hedrick *et al.*, 1992; Hedrick *et al.*, 1991b, c; Ohtsubo *et al.*, 1993). There have been very few studies of methanogenic ether lipids in sediments and those which have been performed have included freshwater sites (Pauly & Van Vleet, 1986a; Martz *et al.*, 1983), two samples at an estuarine site (Martz *et al.*, 1983) and geologically dated (*i.e.* millions of years, Ma) marine and freshwater sediments (Pauly & Van Vleet, 1986b; Chappe *et al.*, 1982). This was the first study to concentrate on the abundance of ether lipids in recently deposited (*i.e.* < 50 years), near-shore, marine sediments.

In Holyhead Harbour the significant concentrations of methane are understood to have formed from methanogenic bacteria (Floodgate *et al.*, 1984; Jones *et al.*, 1986). From data given in Martz *et al.* (1983) it could be suggested that a relationship between ether lipid content and methane concentration might exist. However, the limited number of samples taken from the freshwater and estuarine sediments in Martz *et al.* (1983) was insufficient to draw any conclusions and there has not been another study which simultaneously measured ether lipid and methane concentration in sediments. One of the aims of this work was therefore to determine whether a relationship does exist between ether lipid and methane concentration in recently deposited sediments that are understood to contain significant methanogenic activity. For comparison a gas free sediment core was also analysed.

Incubated samples analysed from Holyhead Harbour on a previous study showed the maximum net methane production to occur at a depth just below the point where the sulphate concentrations had diminished (Jones *et al.*, 1986). Studies using radioactive labelled substrates have shown that methanogenic activity is often maximum below the sulphate reduction zone

(Ward & Winfrey, 1985; Kosiur & Warford, 1979; Winfrey *et al.*, 1981). Pauly & Van Vleet (1986b) have tentatively shown that the total concentration of ether lipids at the base of the sulphate reduction zone of a deep sea sediment increased by a factor of five above more surface sediments. The viable methanogenic bacteria and the total ether lipid concentration were therefore analysed to determine whether the significant methanogenic activity was reflected in a noticeable change in biomass with increasing depth in these sediments.

5.2. Description of Study Areas

5.2.1. Holyhead Harbour

Holyhead Harbour is located on the north western corner of Anglesey and the sediment cores were taken from approximately Lat: 53° 19.62' N and Long: 4° 37.10' W. Holyhead Harbour receives a significant amount sewage from the 11 K populace in the catchment area (Jones, 1977; Gant *pers. comm.*, 1996) which when combined with high sedimentation rates can form anoxic sediments with significant methanogenic activity. The new harbour contains extensive areas of acoustically turbid anoxic sediment to a maximum depth of approximately 10m (Jones *et al.*, 1986; Floodgate *et al.*, 1984). Some of the gravity cores taken from Holyhead Harbour on previous studies were unsuccessful in penetrating the band of high methane concentrations whereas other cores only penetrated to a limited depth (Jones *et al.*, 1986; Peters, 1988). Therefore due to these limitations with the gravity coring technique it was considered appropriate to core in an area where the acoustic turbidity appeared closest to the sediment surface (see positions A, B, C and D in figure 5.1). The presence of acoustic turbidity in "gassy" sediments is usually detected from the ocean surface using a high resolution sub-bottom profiling system called a "pinger". This system was not available at the time when sediments for this study were cored. However, since the cores were being taken from the same area that Jones *et al.* (1986) sampled and obtained simultaneous "pinger" data (see figure 5.2), it is reasonable to assume that the gas distribution within the cores would not be dissimilar between the two sampling periods. On the 29th August 1991 four sediment cores were taken from an area shown in figure 5.1. This area was close to core position 7 of Floodgate *et al.* (1984) (see figure 5.1) which was where the acoustic turbidity was observed closest to the sediment surface (*i.e.* < 1 m) (see figure 5.2)

5.2.2. Intertidal Core

The intertidal core was collected on the 23rd May 1991 from Cadnant Creek in the Menai Strait at approximately Lat: 53° 13.91' N and Long: 4° 9.18' W. The area was chosen due to the deep mud banks that allowed a core of 1 m to be retrieved by hand. Although grain size measurements were not made, it was noticed that the fine mud sediments also contained sand grains.

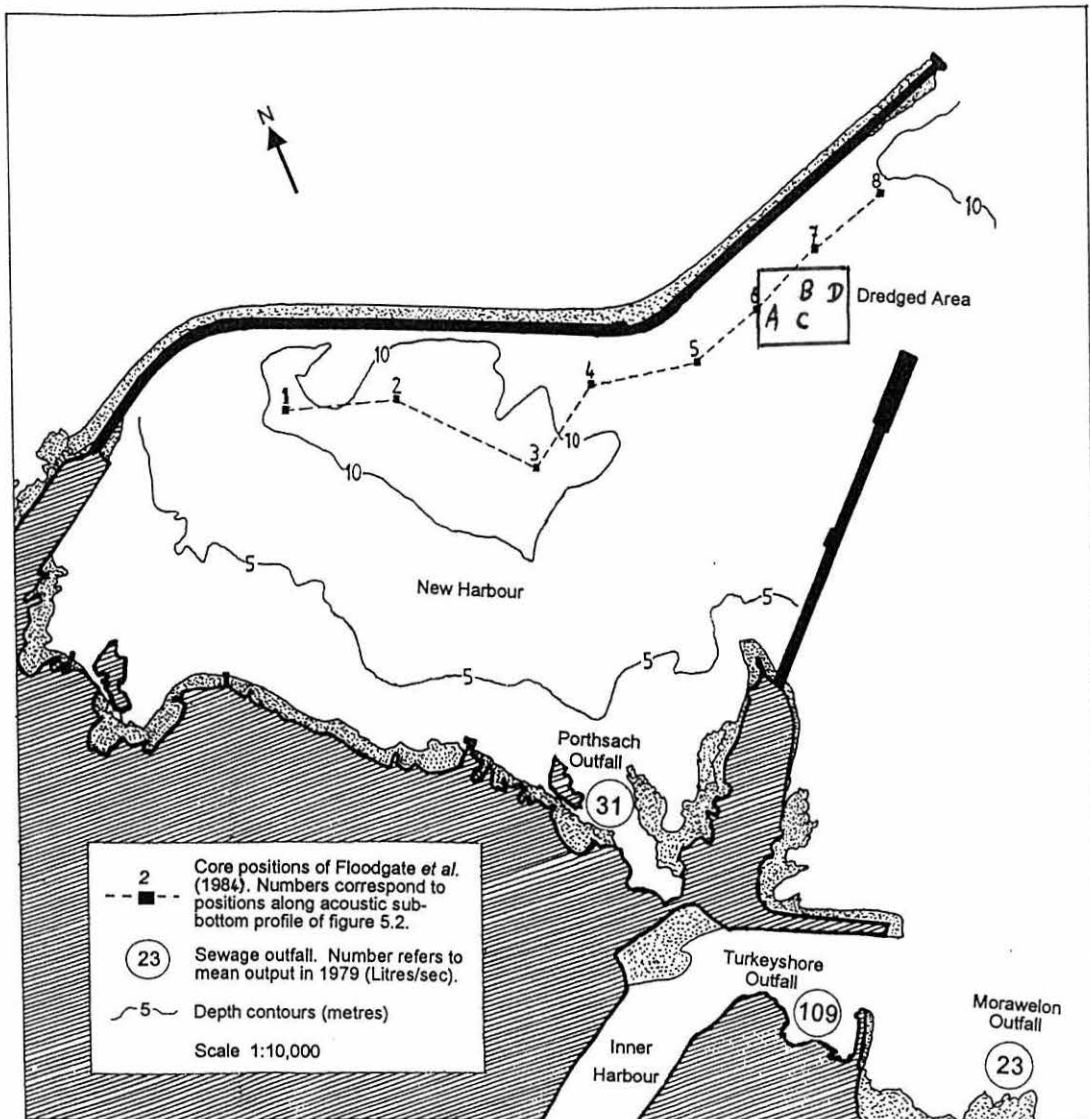


Figure 5.1. Map of Holyhead harbour illustrating the approximate positions of the sediment cores (A to D) and the areas of sewage outfall.

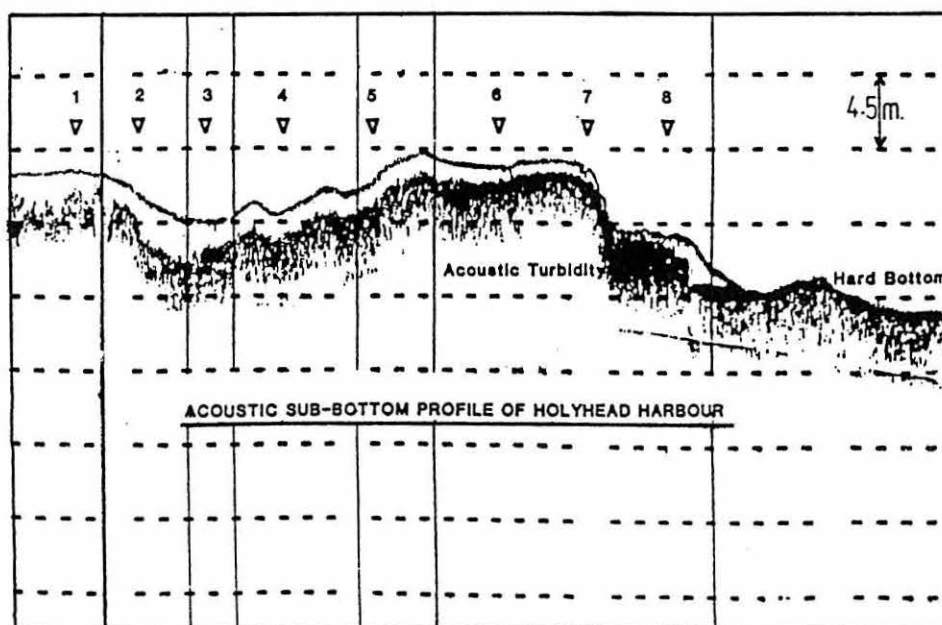


Figure 5.2. Acoustic sub-bottom profile showing positions that correspond to figure 5.1, taken from Floodgate *et al.* (1984).

5.3. Bathymetry of Holyhead Harbour and Sedimentation Rate

Two bathymetric surveys of the same area over two sampling periods were compared to estimate the approximate sedimentation rate. By calculating the sedimentation rate together with other sediment parameters it was anticipated that an estimate could be made of what factors govern the methane profiles in the sulphate reduction zone (SRZ).

The bathymetric data comprised of two surveys taken by two independent hydrographic companies from 1985 and 1993, as detailed in section 2.3.3 of the materials and methods. Two maps of the Holyhead area showing the points where depth soundings were made were received from Mr D. Roberts (Anglesey Aluminium Ltd). The depth soundings had been normalised to a mean seawater depth (*i.e.* Newlyn) in order to allow for changes in tidal height between the two survey periods. These surveys were performed to determine whether certain areas required dredging. However, for this work it was necessary to determine the change in the overlying water depths for the area between these two surveys in order to calculate the sedimentation rate. For this study the information on the maps had to be converted to a tabular form so that the data could be directly compared at similar grid points over the two sampling periods. It was necessary to construct contour diagrams to determine the intermediate values between the depth soundings because very few of the depth soundings corresponded to the same position between the two surveys. This area had not been dredged during the intervening period (Mr D. Roberts, *pers. comm.* 1994).

The depth soundings, in metres below chart datum, for the 1985 and 1993 survey periods are given in tables A10.1 and A10.2 of appendix X, respectively. The depths given in the shaded boxes of tables A10.1 and A10.2 (appendix X) are the normalised depth soundings reported by the hydrographic companies, whereas the values in the remaining intermediate boxes were determined from contour diagrams which were constructed through the reported depth soundings. The intermediate distances ranged from 10 to 30 m, approximately. The 1993 survey showed that the area consisted of two plateaux; an upper plateau to the western side at approximately 6-7 m water depth where the sediments were cored, and a lower plateau to the eastern side at 10-11 m water depth. Unfortunately the bathymetric survey of 1985 concentrated on the eastern area closest to the Anglesey Aluminium Jetty and therefore did not quite include the western upper plateau area where the sediments were cored. The topographies constructed from each of the bathymetric surveys of the 1985 and 1993 periods are given in figures 5.3 and 5.4, respectively. The positions of the four sediment cores are also highlighted on 1993 survey of figure 5.4. It should be noted that at the time of coring the water depth at the site where core D was collected was approximately 2 m greater than the depths of the other cores. This was consistent with the topography diagram of figure 5.4 where core D is located at the drop-off between the two plateau areas.

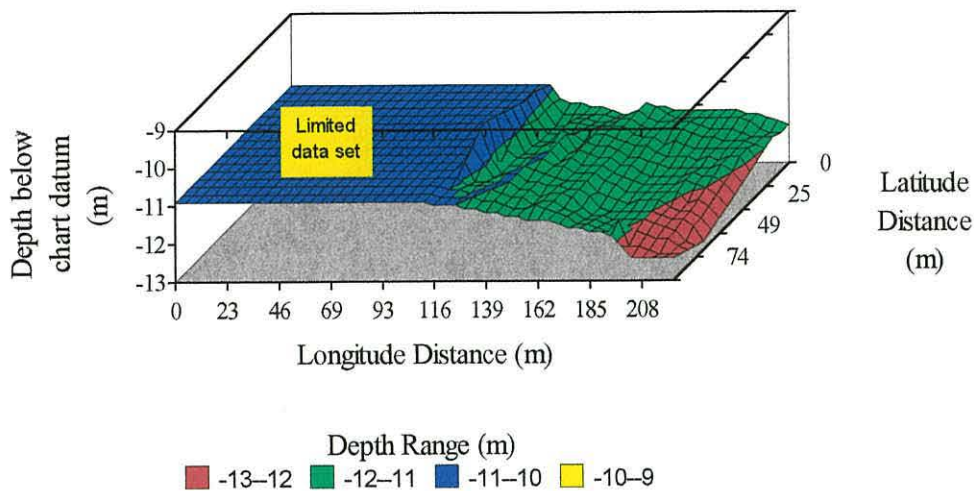


Figure 5.3. Bathymetric survey of Holyhead Harbour in 1985 from Lat: 53° 19'36.0", Long: 4° 37'7.8" to Lat: 53° 19'39.0", Long: 4° 37' 2.0".

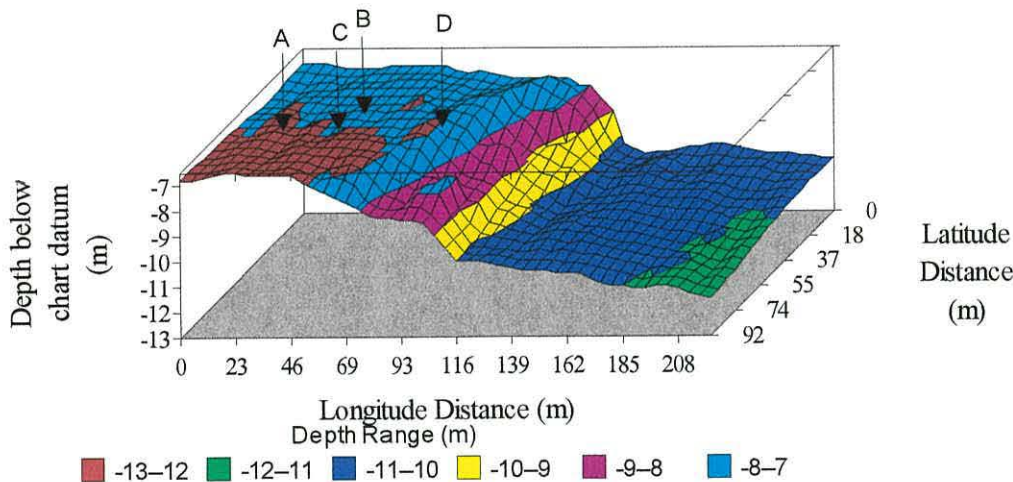


Figure 5.4. Bathymetric survey of part of Holyhead Harbour in 1993 from Lat: 53° 19'36.0", Long: 4° 37'14.0" to Lat: 53° 19'39.0", Long: 4° 37' 2.0". The sediment cores were taken from the points marked A, B, C and D.

Comparison of the change in sedimentation for the two survey periods could therefore only be made for the deeper eastern plateau and not for the shallower western area where the sediment cores were taken. The change in the sediment height for the adjacent eastern plateau was calculated by subtracting the overlapping data points of the 1985 survey (given in table A1) from the data of the 1993 survey (see table A2, appendix X). The change in sediment height over the two periods represented an increase of between 0.5 to 3.3 m from 1985 to 1993 and had a mean of 1.03 m, median of 1 m and a mode of 1 m. The change in sediment height is

given in table A3 of appendix X and is shown in figures 5.5. It can be seen from figure 5.5 that there was an increase in the sediment height over most of the area of approximately + 1 m. However, at the point where the gradient increased from the lower to upper plateau increases in the sedimentation of up to 3.3 m were reported (see table A3, appendix X).

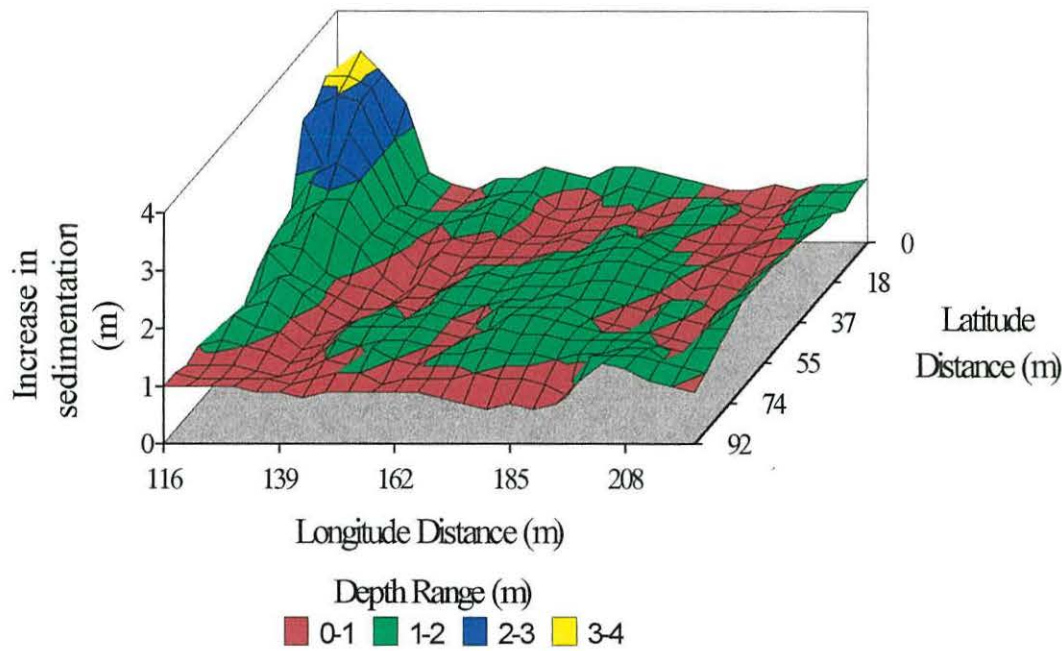


Figure 5.5. Bathymetry showing the change in the sedimentation from 1985 to 1993 for the lower eastern plateau.

The reasons for the observed greater sedimentation at the gradient between the two plateaux could be either real or an artifact of the method used to calculate the sedimentation rate. Real explanations could include the drop-off providing a lower energy environment which would promote greater sediment accumulation than more exposed areas that are of higher energy. This phenomenon would cause the upper plateau of the western area to appear to extend eastwards into the eastern area over time. This might therefore be expected to be limited to the steep gradient area and not the upper plateau area where the cores were taken.

The distances between the reported depth soundings of the surveys were large (*i.e.* 10 to 30 m), therefore the errors associated with the estimated intermediate values could be significant. Within the plateau areas these values changed little over the intermediate distances (*i.e.* <0.5m), however, at the gradient between the two plateaux large changes were observed across the intermediate distances (*i.e.* 3 m). Therefore the error in estimating the intermediate values from approximated contour diagrams would have been much greater at the steeper gradient area than at the plateau region. This latter explanation was reason enough to omit the data of the steep

gradient area from the sedimentation calculations. Also the proportion of the data attributable to the steep gradient area was small (< 5 %) compared to the data of the rest of the plateau.

The error associated with the depth soundings was ± 0.1 m and the period between the two surveys of January 1985 and June 1993 was 7.6 years. Therefore the calculated sedimentation rates for the area were determined to the nearest 1.3 cm y^{-1} increment. Figure 5.6 shows the sedimentation rate in increments of 1.3 cm y^{-1} (*i.e.* X axis) and the number of counts that were attributed to each sedimentation increment from the total 384 data points (*i.e.* Y axis) for the lower eastern plateau.

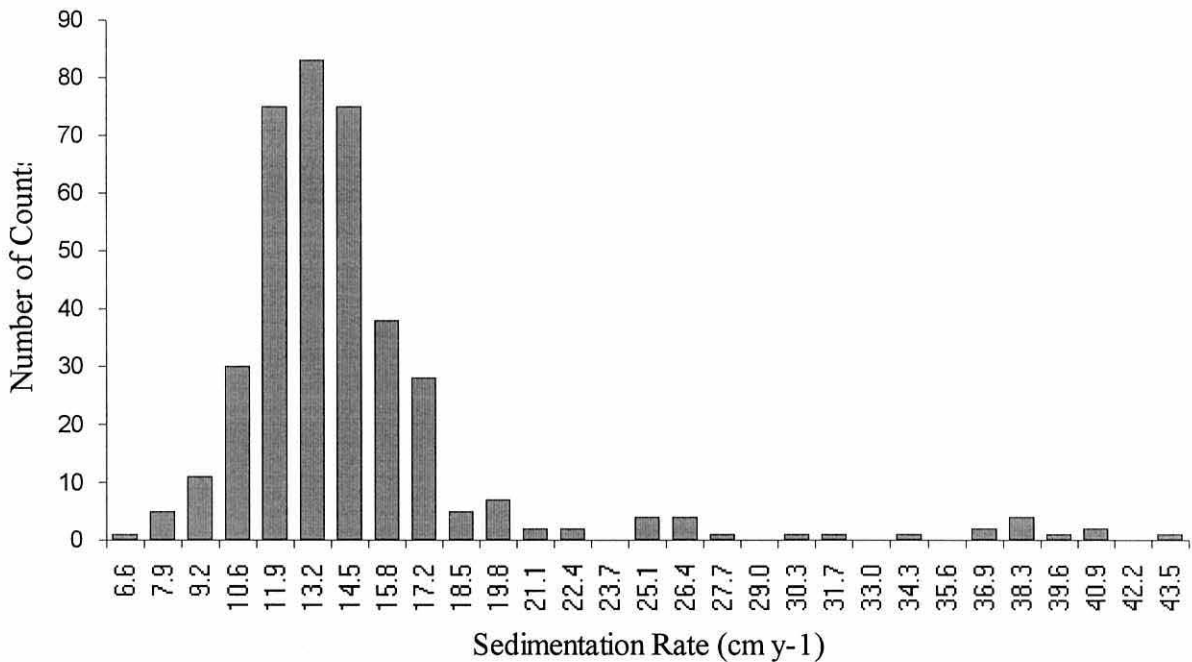


Figure 5.6. Histogram showing the number of counts of the total reported and estimated values (*i.e.* 384 data points) *versus* the sedimentation rate in increments of 1.3 cm y^{-1} from 1985 to 1993 for the lower eastern plateau area of Holyhead Harbour.

The mean sedimentation rate was approximately 13 cm y^{-1} for the lower plateau area with a 95 % confidence range of 9 to 17 cm y^{-1} . The distribution of counts about the 13 cm y^{-1} mean was almost a normal distribution with a skewness of 0.47, suggesting a slight asymmetrical tail towards sedimentation values greater than 13 cm y^{-1} , and a kurtosis of 0.89 suggesting slightly less peakedness with respect to a normal distribution. The calculated sedimentation rate used the total reported and estimated intermediate values generated in tables A10.1 and A10.2 of appendix X. A total of 68 reported depth soundings were made to generate the total bathymetric data of the area in 1985 and 55 were used for the 1993 survey. Ten of these data points were found to overlap within the ± 2 m error of the GPS system from the two sampling periods, as shown in the shaded boxes of table A10.3 of appendix X. The mean sedimentation rate calculated from the reported depth soundings which overlapped over the two sampling dates (*i.e.* 14 cm y^{-1}) showed good agreement with the total reported and estimated values for the area (*i.e.* 13 cm y^{-1}).

At the Skagerrak and Kattegat offshore sites of Denmark where acoustic turbidity has also been acknowledged (Hovland & Judd, 1988; Hovland, 1992; Laier *et al.*, 1992; Jørgensen *et al.*, 1990) sedimentation rates were found to be typically two orders of magnitude lower than Holyhead Harbour at 0.05 to 0.29 cm y⁻¹ (Iversen & Jørgensen, 1985). Sedimentation rates at other sites where significant methane concentrations have been reported have included 0.3 cm y⁻¹ at Long Island Sound, Connecticut (Martens & Berner, 1977), 1 cm y⁻¹ for Saanich Inlet, British Columbia (Murray *et al.*, 1978), 3 cm y⁻¹ from model data (Martens & Val Klump, 1980) and 8-10 cm y⁻¹ from radioactive dating (Martens & Val Klump, 1980) for sediments at Cape Lookout Bight, North Carolina.

Newhaven Harbour on the south east coast of England receives fine silt and alluvial sediments from the River Ooze and coarse sediments from south westerly gales. Comparison of two bathymetric surveys from November 1993 and October 1996 (see section 2.3.3) showed that the sedimentation rate ranged from areas of erosion over this period to 27 cm y⁻¹ with a mean of 16 cm y⁻¹ for the area. Sediment rates for Sovereign Harbour, Eastbourne were estimated to range up to 20 - 30 cm y⁻¹ (Mr C Carvel, *pers. comm.*, 1996). Therefore the sedimentation rate determined for Holyhead Harbour was comparable to other harbours located around Britain.

5.4. Distribution of Sulphate and Methane with Depth in the Sediment Cores

In the SRZ of marine sediments sulphate reduction clearly dominates methanogenesis and in many marine sediments a vertical stratification of sulphate reduction above methane production has been reported (Ward & Winfrey, 1985). The rates of methane production within the methane dominated zone have been reported to be greater than in the SRZ via substrates such as acetate and bicarbonate by up to factors of; 80 (Sansome & Martens, 1981), 140 (Winfrey *et al.*, 1981) and 2-8 (Kosior & Warford, 1979). This vertical stratification of the major sulphate reduction and methanogenic activities can, in some sediments, also be reflected in the sulphate and methane profiles whereby decreasing concentrations of sulphate reflect sulphate reduction and increasing concentrations of methane reflect methanogenesis (Ward & Winfrey, 1985). However, methanogenesis can also exist in the presence of sulphate via substrates such as methyl amines and methanol which are not competed for by the sulphate reducers, as detailed in section 1.5 (Oremland *et al.*, 1982). Within the SRZ of an intertidal core trimethylamine was shown to account for 35 to 61 % of the total methanogenesis (King *et al.*, 1983). There is presently very little information on the rates of methanogenesis measured simultaneously from all of the substrates that are potentially available to methanogens over a single marine profile which encompasses sulphate and methane containing depths. However, if methanogenesis can increase down a sediment core, especially across the sulphate - methane transition by a factor of 2-140 via acetate and bicarbonate metabolism when 35 to 61 % of the methanogenesis in the SRZ is

from trimethylamine, it would suggest that in many marine sediments the total methanogenic activity from all potentially available substrates would still be expected to show a significant increase across the sulphate - methane transition.

However, there may be exceptions to this pattern for marine sediments and it is largely controlled by the type of organic input to the sediment. Sediments receiving raw sewage were shown to have a greater methane production rate from acetate by a factor of 30 in the SRZ compared to sediments receiving aerobically treated sewage (Warford & Kosiur, 1979). However, rate measurements were not made below the SRZ where increased methane production could also occur as a result of increased organic loading thereby causing a proportionately greater rate of methanogenesis below the SRZ.

Studies of Holyhead Harbour have not determined the rates of methanogenesis down a core profile via radioactive labelled substrates but have shown that the net methane production in incubated sediments is greatest when sulphate concentrations have become limited (Jones *et al.*, 1986). At other sites where acoustic turbidity has also been reported (*i.e.* Saanich Inlet, British Columbia, Devol, 1983; Skagerrak and Kattegat, Denmark, Iversen & Jørgensen, 1985) maximum rates of anaerobic methane oxidation and increases in sulphate reduction have been shown to coincide at the sulphate - methane transition. The organisms responsible for anaerobic methane oxidation are largely unknown as discussed in section 1.5. Anaerobic methane oxidation has not been investigated at Holyhead Harbour therefore its presence can not be confirmed.

5.4.1. Holyhead Harbour

Concentrations of methane, sulphate and sulphide in the pore waters of the Holyhead cores are given in table 5.1 and are illustrated in figure 5.7. Methane concentrations were originally determined per dry gram of sediment, but it was considered more useful to represent the methane concentrations as milli-moles per litre (*i.e.* mM) when comparing to other chemicals dissolved in the pore waters.

Methane concentration per gram of sediment was converted to concentration per volume of pore water using the percentage water content (by weight) for each sample. It was assumed that the volume of the sediment attributable to undissolved gas was negligible in the surface sediments, and for the deeper sediments that the undissolved gas displaced both sediment and pore water to similar extents. For example, 15.0 $\mu\text{moles g}^{-1}$ methane in core B at 110 cm with a water content of 47.1 % equated to $[(100-47.1)/47.1] \times 15.0 = 16.8$ mM methane in the pore water. The raw data for the sediments collected for methane analysis and water content are given in table A11.1 of appendix XI.

The methane profiles of the Holyhead sediment cores were similar in that they were generally low over the upper 0-30/70 cm of sediment (*i.e.* $\cong 0.1$ mM) and increased significantly by up to two orders of magnitude over the 50 to 90 cm depth range. Peak area gave greater precision than peak height which was probably due to the lack of a split option on the injection port of the gas chromatograph. Peak areas for both gas free and gas charged sediments were within the limits of the peak areas of the methane calibration (Appendix II). Therefore the large errors associated with the methane analysis were attributed to the extremely temperamental Dani gas chromatograph producing a variable response. The peak areas for five successive injections typically gave a coefficient of variation of 50 %.

However, by considering these errors then the increase in methane with increasing sediment depth ranged from between one to three orders of magnitude across the sulphate - methane transition. Similar increases in the methane concentration with sediment depth by up to two orders of magnitude have also been reported in other marine sediments of known acoustic turbidity (Kosiur & Warford, 1979; Kuivila *et al.* 1990).

Below the surface 0-30/70 cm of sediment methane concentrations appeared to increase with depth either linearly as in Holyhead cores A, B and D or exponentially as in Holyhead core C to a maximum concentration of approximately 15-25 mM. Kosiur and Warford (1979) found that methane concentrations did not exhibit a gradient in the surface marine sediments, which was followed by an exponential increase near the bottom of the sulphate reducing zone, then increased linearly with depth.

Methane concentrations were typically one order of magnitude greater than those reported in a similar area of a previous study (Floodgate *et al.* 1984; Jones *et al.*, 1986). An explanation for the increased methane concentrations detected in this present study of August 1992 when compared to the study of Floodgate *et al.* (1984) in March 1982 could be due to seasonal changes. Senior *et al.* (1982) have reported increases in both sediment methanogenesis and *in-situ* methane concentrations by up to two orders of magnitude from winter to summer months of a saltmarsh site in the south east of England. Expected seawater temperatures for the north coast of Anglesey for August and March are 15 and 7 °C, respectively (Jones & Jeffs, 1991). Temperature measurements that were taken on a subsequent trip to Holyhead Harbour (29th August 1994, Marine Chemical and Biological Consultants) indicated that the temperature of the surface water was similar to the bottom water and surface sediments of Holyhead Harbour (*i.e.* 15 °C, SD = <0.1 °C).

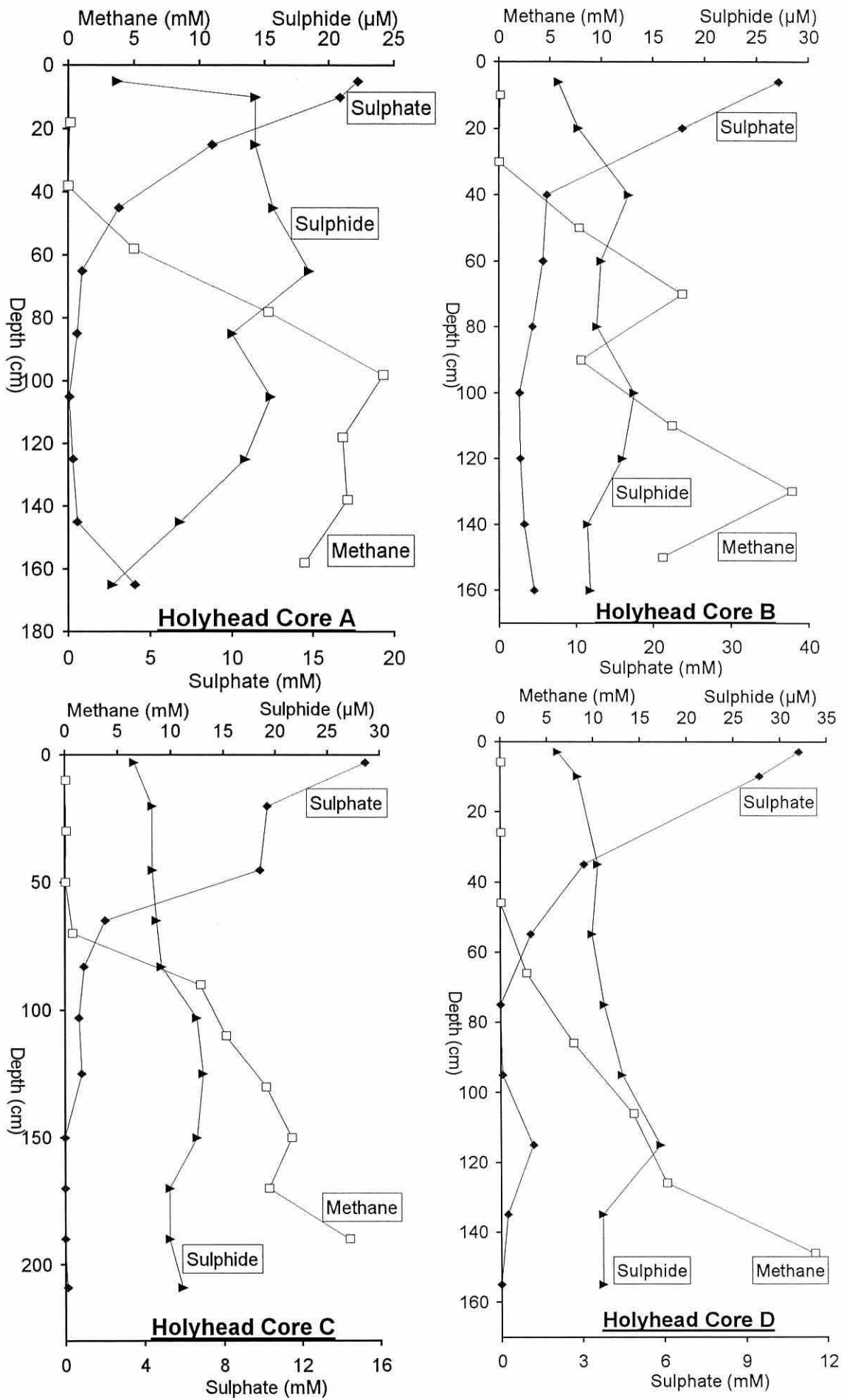


Figure 5.7. Pore water methane, sulphate and sulphide concentrations for the Holyhead cores.

cm?

Table 5.1. Pore water methane, sulphate and sulphide contents of the Holyhead cores

Depth (m)	Methane ($\mu\text{moles g}^{-1}$) (95% confidence)	Methane (mM) <i>a</i>	Water Content (%) <i>b</i>	Depth (m) <i>c</i>	Sulphide (μM)	Sulphate (mM)
Holyhead Core A						
18	0.1 (<0.1-0.2)	0.2	45.0	5	3.8	17.8
38	<0.1 (<0.1-<0.1)	<0.1	46.5	10	14.3	16.7
58	3.4 (2.0-5.9)	5.0	40.3	25	14.3	8.8
78	10.9 (6.3-19.7)	15.3	41.5	45	15.7	3.1
98	14.9 (8.5-27.5)	24.2	38.1	65	18.5	0.9
118	11.7 (6.7-21.2)	21.1	35.6	85	12.5	0.6
138	16.3 (9.3-30.3)	21.4	43.2	105	15.5	0.1
158	12.7 (7.3-23.2)	18.1	41.2	125	13.5	0.3
				145	8.6	0.6
				165	3.4	4.1
Holyhead Core B						
10	0.1 (0.1-0.2)	0.1	47.3	6	5.8	36.2
30	<0.1 (<0.1-<0.1)	<0.1	43.8	20	7.8	23.8
50	6.1 (3.6-10.8)	7.8	43.9	40	12.7	6.3
70	12.3 (7.1-22.5)	17.8	40.9	60	10.0	5.8
90	6.6 (3.8-11.6)	8.0	45.1	80	9.5	4.4
110	15.0 (8.6-27.7)	16.8	47.1	100	13.2	2.7
130	21.6 (12.2-41.0)	28.4	43.2	120	12.0	2.8
150	13.0 (7.5-23.9)	15.9	45.1	140	8.6	3.3
				160	8.9	4.6
Holyhead Core C						
10	<0.1 (<0.1-<0.1)	0.1	48.7	3	6.6	15.3
30	0.1 (0.1-0.2)	0.1	49.5	20	8.3	10.3
50	0.1 (<0.1-0.1)	0.1	48.3	45	8.3	9.9
70	0.7 (0.4-1.3)	0.8	49.3	65	8.7	2.0
90	13.8 (7.9-25.3)	12.9	51.7	83	9.2	1.0
110	14.8 (8.5-27.4)	15.2	49.3	103	12.5	0.7
130	12.9 (7.4-23.6)	19.1	40.3	125	13.1	0.9
150	16.7 (9.6-31.2)	21.5	43.7	150	12.5	0.0
170	15.4 (8.8-28.6)	19.4	44.3	170	9.9	0.0
190	18.8 (10.7-35.3)	27.1	41.0	190	9.9	0.0
				209	11.1	0.1
Holyhead Core D						
6	<0.1 (<0.1-<0.1)	<0.1	48.0	3	6.2	11.0
26	<0.1 (<0.1-<0.1)	<0.1	48.4	10	8.4	9.5
46	<0.1 (<0.1-<0.1)	<0.1	47.7	35	10.5	3.1
66	3.2 (1.9-5.5)	2.8	53.4	55	9.9	1.1
86	7.2 (4.2-12.7)	7.9	47.6	75	11.2	0.0
106	8.8 (5.1-15.7)	14.2	38.1	95	13.1	0.1
126	11.3 (6.5-20.5)	17.8	38.8	115	17.1	1.2
146	19.7 (11.2-37.2)	33.6	37.0	135	11.0	0.3
				155	11.0	0.0

Footnote to table 5.1:

- a. Concentration of methane per litre of pore water was determined using the water content data.
- b. Percentage of pore water in the total sediment by weight.
- c. Mean depth of a depth range with approximately ± 5 cm.

Pore water sulphate profiles showed similar trends between cores with maximum values in the more surface sediments which decreased almost exponentially with depth (see figure 5.7). The sulphate concentrations in the near surface sediments (*i.e.* 3 to 6 cm mean depths) varied significantly between cores (*i.e.* 11 to 36 mM, respectively) and suggested that there existed contrasting depositional environments between these cores (see table 5.1). At a depth where methane concentrations were observed to rise sharply the sulphate concentrations were less than 1.2 mM in cores A, C and D and approximately 6 mM in core B. Below this depth sulphate concentrations decreased to <1 mM in cores A, C and D, but the reasons for the higher sulphate concentration throughout core B (*i.e.* $\cong 3$ mM) are not known. The observed rise in sulphate concentrations at the base of Holyhead cores A, B and C could be due to seawater entering the bottom of the sediment cores via the core cutter during retrieval through the water column.

From the current literature it would appear that much of the sulphate reduction occurs at depths where sulphate is present but decreasing with increasing depth (*i.e.* $\cong 20$ mM down to 1 mM) (Jørgensen, 1978; Iversen & Jørgensen, 1985; Kuivila *et al.*, 1990). The succession from sulphate reduction, when sulphate becomes limiting, to methanogenesis with increasing depth has been previously observed within shallow water sediments (Kristjansen *et al.*, 1982; Schonheit *et al.*, 1982). Indirect evidence has also led to a hypothesis that a lag period exists between the end of sulphate reduction, once sulphate concentrations have become limiting, and the start of methanogenesis in one organic rich marine sediment (Alperin *et al.*, 1994). Limiting sulphate concentrations for sulphate reducing bacteria in freshwater sediments have been determined at 0.3 to 1.5 mM (Devol *et al.*, 1984) and 1.2 mM in marine sediments (Berner, 1974). Therefore by using the decreasing concentrations of pore water sulphate as an indirect indicator of sulphate reduction it would appear that much of the SRZ generally extended from the surface sediments to a depth of approximately 30/70 cm in the Holyhead cores. The high methane concentrations began at a depth of approximately 50/90 cm and extended beyond the base of all cores. Previous incubation experiments on sediments of Holyhead Harbour revealed that the net methane production was largely confined to sub-surface depths (*i.e.* 80 to 180 cm) which coincided with the high methane concentrations of the acoustically turbid depths (Jones *et al.*, 1986). The net methane production in the shallower sulphate containing sediments of Holyhead Harbour was negligible (Jones *et al.*, 1986).

Concentrations of water soluble sulphide for the Holyhead cores are shown in figure 5.7 and are generally two orders of magnitude lower than reported values for sediments of Saanich Inlet

(Kuivila *et al.*, 1990). Jørgensen (1978) reported similar trends in the sulphide profiles to the Holyhead cores but with greater concentrations of up to a factor of five.

The chemical oxidation of sulphide to sulphate between core retrieval and analysis is not likely to account for the comparatively low sulphide concentrations since higher sulphate concentrations would have been expected over some of the low sulphate depths below the SRZ (see figure 5.7). The reason for the comparatively low concentrations of water soluble sulphide in Holyhead Harbour is not known, but might be from increased scavenging by metal ions, such as iron, forming less soluble sulphide products that would not be extracted in the pore water (Jørgensen, 1978). Sulphide is a product of sulphate reduction and elemental sulphur and pyrite may also be important end products of sulphate reduction (Jørgensen, 1977). Observations made from seismic profiles have identified coal ash discarded from steam ships approximately 1 century ago, overlying the bedrock and underlying the anaerobic muds of the outer harbour area of Holyhead (J. Bennell, *pers. comm.*, 1994). Coal ash is understood to be rich in iron (III) oxide (*i.e.* 4 to 19 % by weight) (Perry, 1963), which may diffuse through the pore spaces of the overlying fine-grained sediments as the sediment accumulates. Therefore the formation of less soluble iron sulphide products might be the cause for the comparatively low concentrations of soluble sulphide detected in the pore waters of Holyhead Harbour. In coastal marine sediments, that are not in the proximity of potentially high concentrations of iron, only about 10 % of the formed hydrogen sulphide is converted into the less soluble, iron sulphide pool (Jørgensen, 1977).

The sulphide profiles showed an increase in concentration with depth at the top of the cores where sulphate concentrations were shown to decrease (see figure 5.7). Similar trends have also been reported in marine sediments (Jørgensen, 1978; Devol *et al.*, 1984). Trends observed in the sulphide profiles included small increases in sulphide at the methane-sulphate transition (*i.e.* Holyhead cores A and B, figure 5.7). However it is apparent that methane is reported in millimoles per litre whereas sulphide is reported in micro-moles per litre. As anaerobic methane oxidation has not been studied in Holyhead Harbour and therefore not proven this discussion is speculation and perhaps these trends are purely incidental.

5.4.2. Intertidal Core

The concentration of methane per gram of sediment was converted to methane per litre of pore water using the percentage water content as for the Holyhead cores. The methane, sulphate and sulphide concentrations for the sediment pore water of the intertidal core are presented in table 5.2 and illustrated in figure 5.8.

Pore water analysis of the intertidal sediment showed high concentrations of sulphate throughout the entire 84 cm core (see figure 5.8). It has been suggested that the penetration of sulphate deep into the sediment such as this is indicative of a low organic loading resulting in limited

energy resources rather than limited electron acceptors such as sulphate for the sulphate reducing bacteria (Ward & Winfrey, 1985).

Table 5.2. Pore water methane, sulphate and sulphide data for the intertidal core.

Depth (m)	Methane ($\mu\text{moles g}^{-1}$)	Methane (mM) <i>a</i>	Water Content (%) <i>b</i>	Depth (m)	Sulphide (μM)	Sulphate (mM)
Intertidal Core						
7	0.006 (0.002-0.013)	0.013	29.8	6	3.2	21.5
17	0.004 (0.001-0.010)	0.011	27.4	18	11.9	26.9
27	0.002 (0.001-0.006)	0.006	29.5	30	3.6	26.3
37	0.004 (0.001-0.009)	0.007	33.4	42	0.8	24.9
47	0.003 (0.001-0.008)	0.009	27.5	56	0.4	24.3
57	0.004 (0.001-0.009)	0.009	28.1	66	0.1	24.1
67	0.004 (0.002-0.010)	0.010	30.1	78	0.0	23.8
77	0.069 (0.033-0.131)	0.170	28.9			

a. Concentration of methane per litre of pore water was determined using the water content data (by weight).

b. Percentage of pore water in the total sediment by weight.

c. Mean depth of a depth range with approximately ± 5 cm.

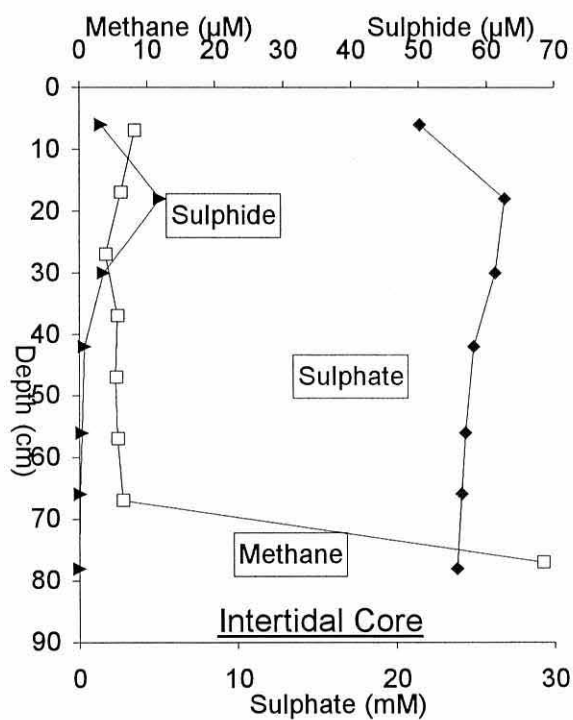


Figure 5.8. Pore water concentrations of methane, sulphate and sulphide for the intertidal core.

The organic carbon content of these sediments was not, however, determined on the core. The low sulphate concentration reported in the surface sediment of the intertidal core (*i.e.* 21.5 ± 1.5 mM, 0-12 cm) was determined on repeat analysis (*i.e.* $n = 5$) of the sample and might be explained by the freshwater stream that passed close to the cored area. The reasons why the sulphide concentration profile appeared to mimic the sulphate profile cannot be explained from the data set.

Methane concentrations were generally low over much of the core (*i.e.* 0.006-0.013 mM). The increase at the base of the core (*i.e.* 0.170 mM) was partly unexpected on the basis of the high sulphate concentrations but was only comparable to the low methane values reported in the SRZ of the Holyhead cores (*i.e.* 0.1 mM), and was significantly lower than the methane concentrations in the acoustically turbid depths of the Holyhead cores (*i.e.* $\cong 15$ mM). Attempts to find intertidal muddy areas where either sufficient core lengths could be taken or where the SRZ was confined to shallower depths proved unsuccessful.

5.5. Evidence and Extent of Acoustic Turbidity in the Holyhead Cores

The exact depth from the sediment surface to where the gas front begins, can be located remotely by interpreting the turbid acoustic returns (*i.e.* acoustic turbidity) from the high resolution sub-bottom profile. This is a common geophysical technique for determining the presence of undissolved gas in sediments, however it was not available for this research. Nevertheless, in order to compare parameters such as ether lipid concentration between the sediment depths showing acoustic turbidity and the gas free sediment depths, it was important to establish the depths where the acoustic turbidity began. Other techniques were therefore performed on the retrieved sediment cores to determine the depths of the acoustic turbidity.

Although the high resolution sub-bottom profiling would have provided a useful complimentary analysis of the in-situ acoustic turbidity there are distinct advantages that direct analysis of the retrieved sediment cores can have over the remote method. For example, the impact of a gravity corer and removal of the sediment is expected to cause some changes in the sediment characteristics and shape. Therefore direct analysis of acoustic turbidity on the retrieved sediment cores is expected to be more comparable to other parameters that are also determined on the retrieved sediment cores. Also the advantages of testing for acoustic turbidity on retrieved sediment cores is that the extent of the undissolved gas below the initial gas front can be determined. Seismic profiling is limited, in most instances, to only identifying the top of the gas front which can consist of as little as 1 % undissolved gas (Judd & Hovland, 1992). It is therefore not possible to differentiate small volumes of undissolved gas in thin acoustically turbid bands from much thicker bands which can contain significant quantities of undissolved gas. The

latter can prove hazardous during drilling operations due to blow-outs which have recently been attributed to large quantities of shallow gas (Judd, 1991).

Three types of analysis were performed on the retrieved sediment cores, each of which had its own advantage and included;

1. Measuring the sound velocity laterally across the sediment.
2. Measuring the methane concentration which together with solubility and compressibility data for methane was used to estimate the volume of undissolved gas voids that would be expected within the sediments.
3. Observing the internal structure of the sediment using X-ray analysis to locate the presence of gas voids.

5.5.1. Acoustic Turbidity - Sound Velocity

The measurement of the sound velocity across the sediment was used as a technique for determining the presence of acoustic turbidity due to the significant reduction of the sound velocity by undissolved gas (Yuan *et al.*, 1992). This was the simplest technique and was designed so that it could be quickly performed while on the research vessel and did not require removal of the sediment from the core barrel. Previous tests of the sound velocity across core barrels containing artificially prepared gas charged and gas free sediments (see section 2.9) suggested that this technique could be implemented to identify acoustic turbidity on retrieved sediment cores. The method is detailed in section 2.7 and specimen oscilloscope print-outs for both acoustically turbid and gas-free sediments are shown in figure A4.1 of appendix IV. The mean times of five replicate sound analyses to pass across the Holyhead core barrels with conversions to mean sound velocity and standard deviations (SD) are given in table A4.1 of appendix IV.

Faster sound velocities were recorded in the upper sediment depths (0-45/65 cm) of all cores with a mean of 1641 m s⁻¹ (SD = 10 m s⁻¹), and in deeper sediment horizons, generally below 45/65 cm, slower velocities of 1510 m s⁻¹ (SD = 45 m s⁻¹) were recorded. The change from surface to deep sediments represents approximately an 8 % reduction in sound velocity. Reductions of 15 % have previously been reported by Anderson and Bryant (1990). Sound velocities which ranged from 1500 m s⁻¹ above the acoustic turbidity to 1250 m s⁻¹ within the gas charged sediments were reported by Yuan *et al.* (1992) in sediments of the western Irish Sea.

5.5.2. Acoustic Turbidity - Calculated Volume of Undissolved Methane in the Sediment

The gas in Holyhead Harbour is found to be predominantly methane (Jones *et al.*, 1986). Larger gaseous hydrocarbons, such as ethane, propane or butane, were not detected in the head space analysis of this study. Therefore by determining the approximate methane solubilities for the

pore waters an estimate of the volume of undissolved methane within the sediments could be made from the measured methane concentrations.

Seawater temperature and salinity data for Holyhead Harbour for the month of August were determined to be 15 °C and 36 ‰ (with M.B.C.C., Bangor, August 29th 1994) which was also consistent with the temperature data of Jones and Jeffs (1991). The solubility of methane in seawater at 15 °C and 36 ‰ was calculated using the Bunsen solubility coefficients of Wiesenburg and Guinasso (1979), *i.e.* 0.0305ml methane per ml seawater \cong 1.36 mM.

For gases, such as methane, that are sparingly soluble in a given liquid, the concentration of the dissolved gas is usually low enough for the solution to be approximately ideally dilute, and Henry's law holds well. Weisenburg and Guinasso (1979) estimated that at low pressures methane only deviates from ideality by -0.26 %.

Typical pressures experienced by the sediment cores (*i.e.* 1.6 to 2.1 m) under approximately 8 m of water were calculated at 2 atmospheres. It was not necessary to determine the exact pressures because significant pressure changes were expected to occur from tidal height oscillations (*i.e.* 3 m). Therefore the expected methane solubility at 15 °C, 36 ‰ and 2 atmospheres pressure was approximated at:

$$2 \times 1.36 \times (1 - 0.0026) = 2.7 \text{ mM}$$

A value of 2.6 mM was approximated for much of the sediments below 2 - 7 m water depth at the site of Long Island Sound, Connecticut (Martens & Berner, 1977). Therefore for methane concentrations in excess of 2.7 mM the presence of undissolved gas voids in Holyhead Harbour would be expected. In order to determine the volume that the gas voids would occupy it is necessary to determine the compressibility of the gas. Real and ideal gases can be compared at various pressures and various temperatures by noting the extent to which the value of PV/(RT) deviates from 1 (Barrow, 1988). The quantity PV/(RT) is known as the compressibility factor (Z), and for methane at 15°C can be approximated at 0.998 and 0.996 for 1 and 2 atmospheres pressure, respectively (Barrow, 1988).

For example, in order to calculate the expected volume of gas that would be occupied by 16.8 mM methane at 2 atmospheres pressure (*i.e.* Holyhead core B, 110 cm):

$$16.8 \text{ mM} - 2.7 \text{ mM} = 14.1 \text{ mM undissolved methane}$$

$$14.1 \text{ mM} = (14.1 \times 10^{-3} \times 22400) = 315.8 \text{ cm}^3 \text{ methane per 1l pore water}$$

$$\text{Therefore using: } Z_1 P_1 V_1 = Z_2 P_2 V_2$$

where Z is the compressibility factor, P = pressure, V = volume of undissolved gas and the subscripts denote the values pertaining to each pressure. Then by assuming constant temperature.

$$0.998 \times 1 \times 315.8 = 0.996 \times 2 \times V_2$$

Therefore $V_2 = 158.2 \text{ cm}^3$ undissolved methane per litre of pore water at 2 atmospheres pressure. The volumes of undissolved methane at the expected *in-situ* conditions together with the sound velocities for the Holyhead cores are given in table 5.3 and are shown in figure 5.9.

Generally within the upper 0-45/65 cm of each core the methane concentration falls below the solubility limit for methane and therefore the methane is expected to be dissolved in the pore waters (*i.e.* $0 \text{ cm}^3 \text{ l}^{-1}$). Within the deeper sediments the volumes of undissolved methane were significant and ranged from 1 to $347 \text{ cm}^3 \text{ l}^{-1}$ of pore water. This was equivalent to between 0.1 and 22 % of the total sediment by volume (see table 5.3).

5.5.2.1. Correlation of Undissolved Methane and Sound Velocity Measurements

The advantages of being able to directly relate the sound velocity across the sediment core barrel with the concentration (or presence) of undissolved methane gas is that the depth range of the acoustically turbid band can be quickly determined on the retrieved sediment core without the necessity to perform chemical analyses. There was therefore a need to determine whether the sound velocity data could differentiate between acoustically turbid and gas-free sediments.

It is apparent from figure 5.9 that the sound velocities which denote acoustic turbidity appears to be inversely proportional to the expected volume of methane gas. Correlation analysis between the sound velocity measurements and the volumes of undissolved methane gas were significantly high for cores A ($r = -0.93$, $p < 0.001$), B ($r = -0.69$, $p = 0.05$) and C ($r = -0.96$, $p < 0.001$) and slightly lower for core D ($r = -0.67$, $p = 0.06$).

The varying volumes of undissolved methane within the band of acoustic turbidity was not consistently correlated with the sound velocities. This difference in correlation coefficients may be attributed to the depths of each methane analysis and sound velocity not corresponding exactly (see table 5.3). Also due to the sound wave from the transducer passing through the core barrel material, it meant that the sound velocities reported for very acoustically turbid sediments were sometimes comparable to the velocities recorded for just an empty core barrel set-up, *i.e.* the sound wave passed through the barrel material. Also Yuan *et al.* (1992) highlighted that the relationship between the percentage gas volume and the sound velocity is expected to be controlled, to some degree, by the bubble size, bubble stiffness and the acoustic frequency used, therefore a simple relationship is not expected to exist.

Therefore it would appear that sound velocity analysis of the sediment cores while still in the core barrel could be effectively used as a means of differentiating gas charged from gas-free sediments and could also determine the thickness of the acoustically turbid band. However, this technique may be limited when trying to relate the sound velocity to the expected volume of methane within the acoustically turbid sediment depths.

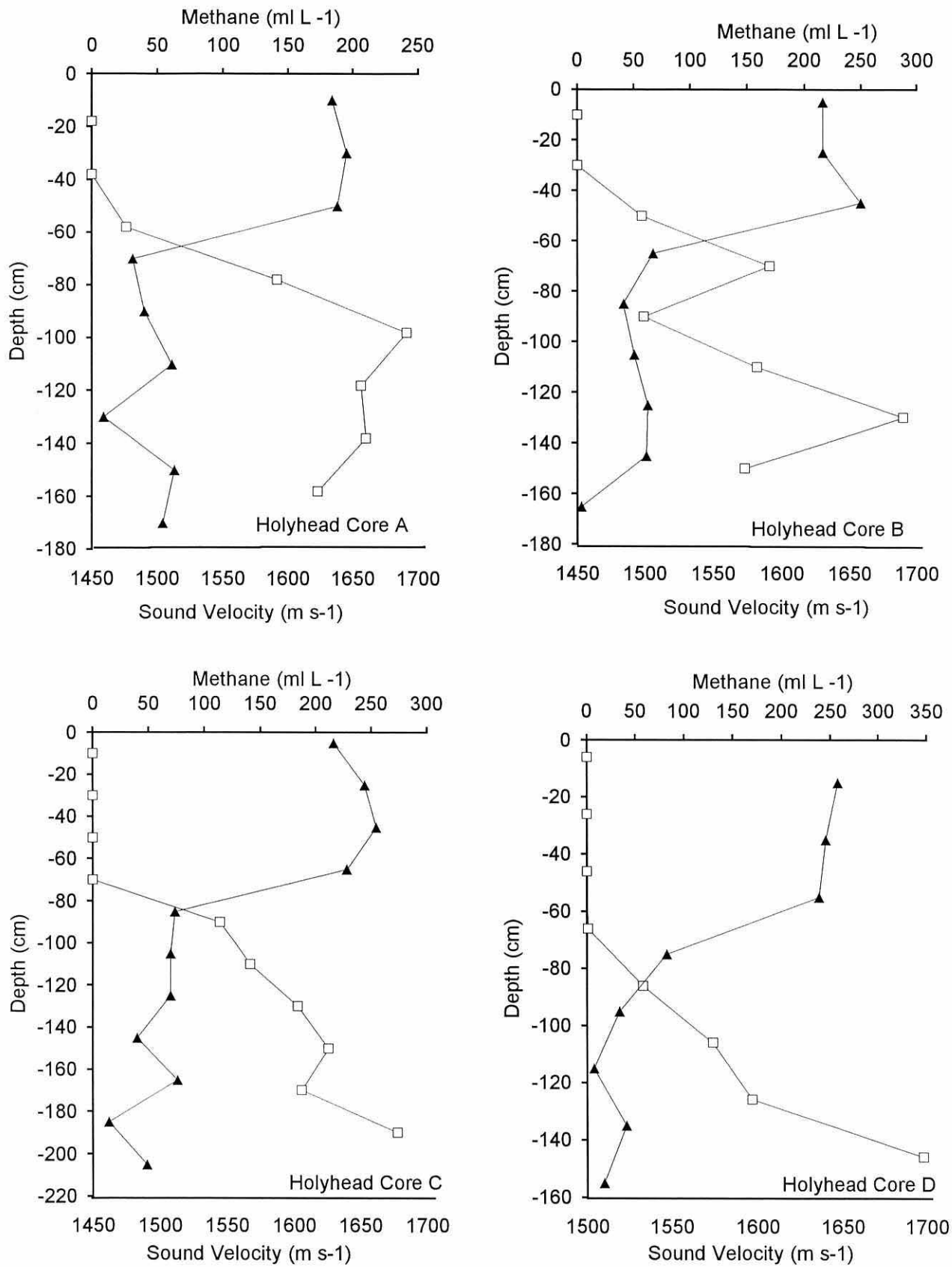


Figure 5.9. In-Situ volumes of undissolved methane gas per litre of pore water (—□—) and sound velocities measured across the core barrels of the Holyhead cores (—▲—).

Table 5.3. In-situ volume of undissolved gas voids and sound velocities for the Holyhead sediment cores.

Depth (cm)	Methane (mM)	In-situ volume of methane gas voids per volume of pore water (ml l ⁻¹) a	Percentage of undissolved methane of the total sediment by volume	Depth (cm)	Sound Velocity (m s ⁻¹) b
Holyhead Core A					
18	0.2	0	0	10	1634
38	<0.1	0	0	30	1645
58	5.0	26	1.7	50	1638
78	15.3	141	10.3	70	1481
98	24.2	241	16.6	90	1490
118	21.1	206	13.6	110	1511
138	21.4	210	14.0	130	1459
158	18.1	173	10.5	150	1513
				170	1504
Holyhead Core B					
10	0.1	0	0	5	1630
30	<0.1	0	0	25	1630
50	7.8	57	4.4	45	1658
70	17.8	170	12.1	65	1506
90	8.0	59	4.7	85	1484
110	16.8	158	12.0	105	1492
130	28.4	288	21.4	125	1502
150	15.9	148	10.8	145	1501
				165	1453
Holyhead Core C					
10	0.1	0	0	5	1630
30	0.1	0	0	25	1653
50	0.1	0	0	45	1662
70	0.8	0	0	65	1640
90	12.9	114	9.6	85	1511
110	15.2	141	12.0	105	1508
130	19.1	184	13.2	125	1508
150	21.5	211	15.3	145	1483
170	19.4	187	13.7	165	1513
190	27.1	273	19.6	185	1462
				205	1490
Holyhead Core D					
6	<0.1	0	0	15	1647
26	<0.1	0	0	35	1640
46	<0.1	0	0	55	1636
66	2.8	1	0.1	75	1547
86	7.9	58	4.8	95	1519
106	14.2	129	9.9	115	1504
126	17.8	169	12.3	135	1523
146	33.6	347	21.6	155	1510

Footnote to table 5.3:

- a. Estimated volume of the gas voids per litre of pore water at 2 atmospheres pressure, 15°C and 36‰ calculated using the equations given in the text.
- b. Standard deviations for five sound velocity measurements are given in parentheses and are detailed in appendix IV (section A4.2).

5.5.3. Acoustic Turbidity - X-ray Analysis

X-ray analysis of the Holyhead sediment was performed to observe the shapes of the gas voids within the sediment. The absence or presence of gas voids was also another indicator of the presence of acoustic turbidity. X-ray photographs of sub-samples taken from cores A to D of Holyhead Harbour are illustrated in figures 5.10 to 5.13. The method of sample preparation and details relating to the instrumentation used are given in section 2.8. of chapter 2.

Each 'dislike' sediment sub-sample was prepared in a similar manner, which made the direct comparison between gassy and gas-free sediments more consistent per unit depth of sediment penetrated. The fragile edges of the sediment sub-samples were sometimes broken during sectioning, and larger cracks and holes (white colour) seen, for example, at depths 120 and 165 cm of Holyhead core B (fig. 5.11) can also be attributed to sample preparation. The elongated (*i.e.* white areas of 3 to 5 mm long, 1 mm wide) gas voids formed due to undissolved gas can be differentiated from the voids created from the sample preparation (*i.e.* larger, rounded white areas) simply by their shape.

The voids were oriented with the long axis in the vertical plane which may suggest a mechanism of gas migration. The elongated gas voids did not show any overall direction of penetration in the horizontal plane (see figs. 5.10 to 5.13). The X-ray photographs did not provide any indication that spherical gas voids were present in the acoustically turbid sediments. Non-spherical gas void morphology such as this was also similar to the observations made from the X-ray analysis of gassy sediments from the Chesapeake Bay area (Schubel, 1974; Hill *et al.*, 1992).

The X-ray photographs illustrated the depth where acoustic turbidity began in the Holyhead sediment profiles and these results were in agreement with the methane and acoustic turbidity profiles within the sampling resolution for each technique. The elongated gas voids of Holyhead core A (see figure 5.10) began at approximately 55 cm and were subsequently found in all core sub-samples of greater depth. Holyhead core B samples were gas-free to a depth of 45 cm and gas voids were extensively permeated through the sediment by 65 cm, and continued throughout all of the deeper sediment samples (see figure 5.11).

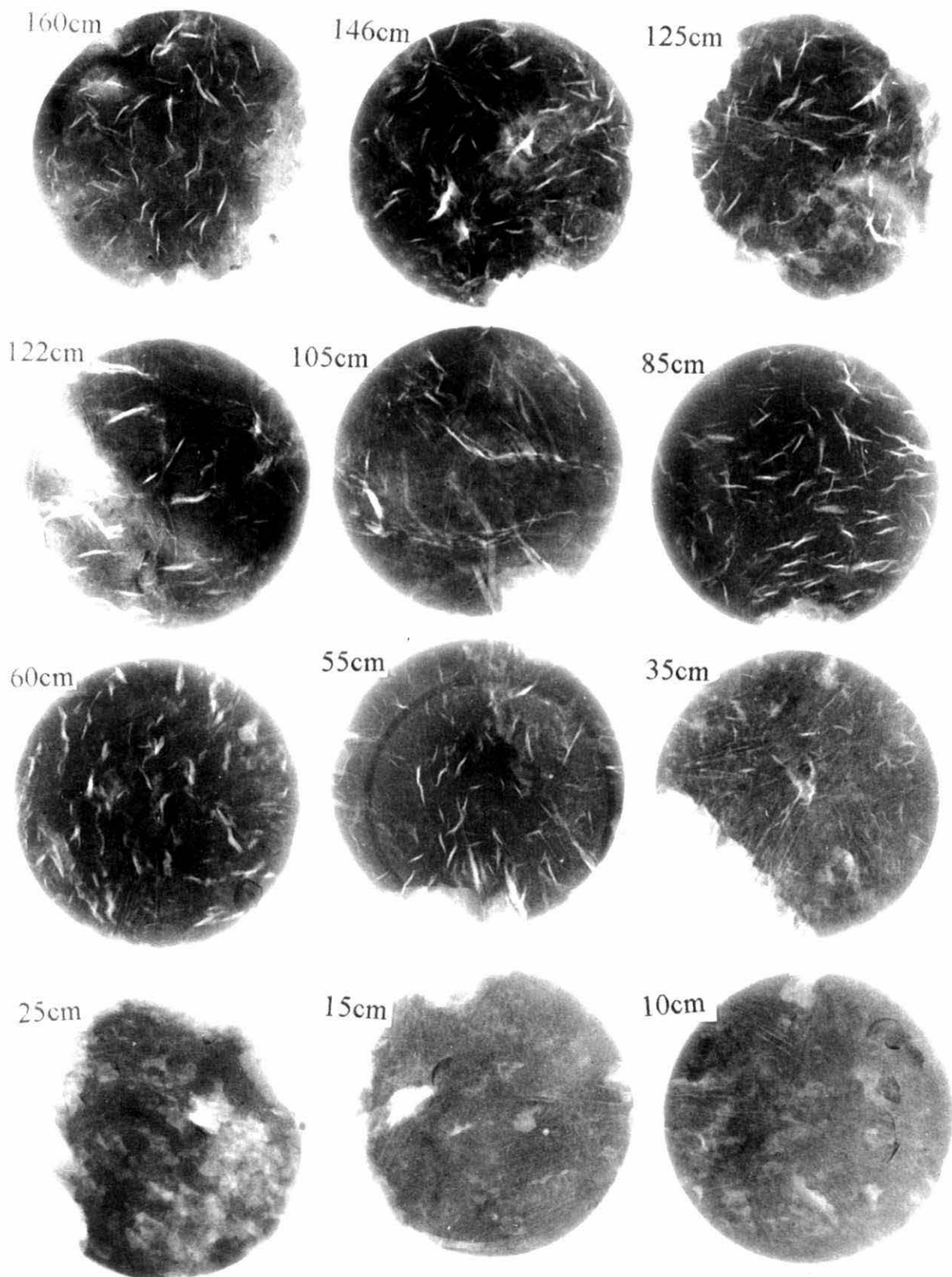


Figure 5.10. X-ray analysis of sediment sections taken from Holyhead Core A. The elongated gas voids are shown to begin mainly at the 55 cm sediment section and continue through sections of greater depth.

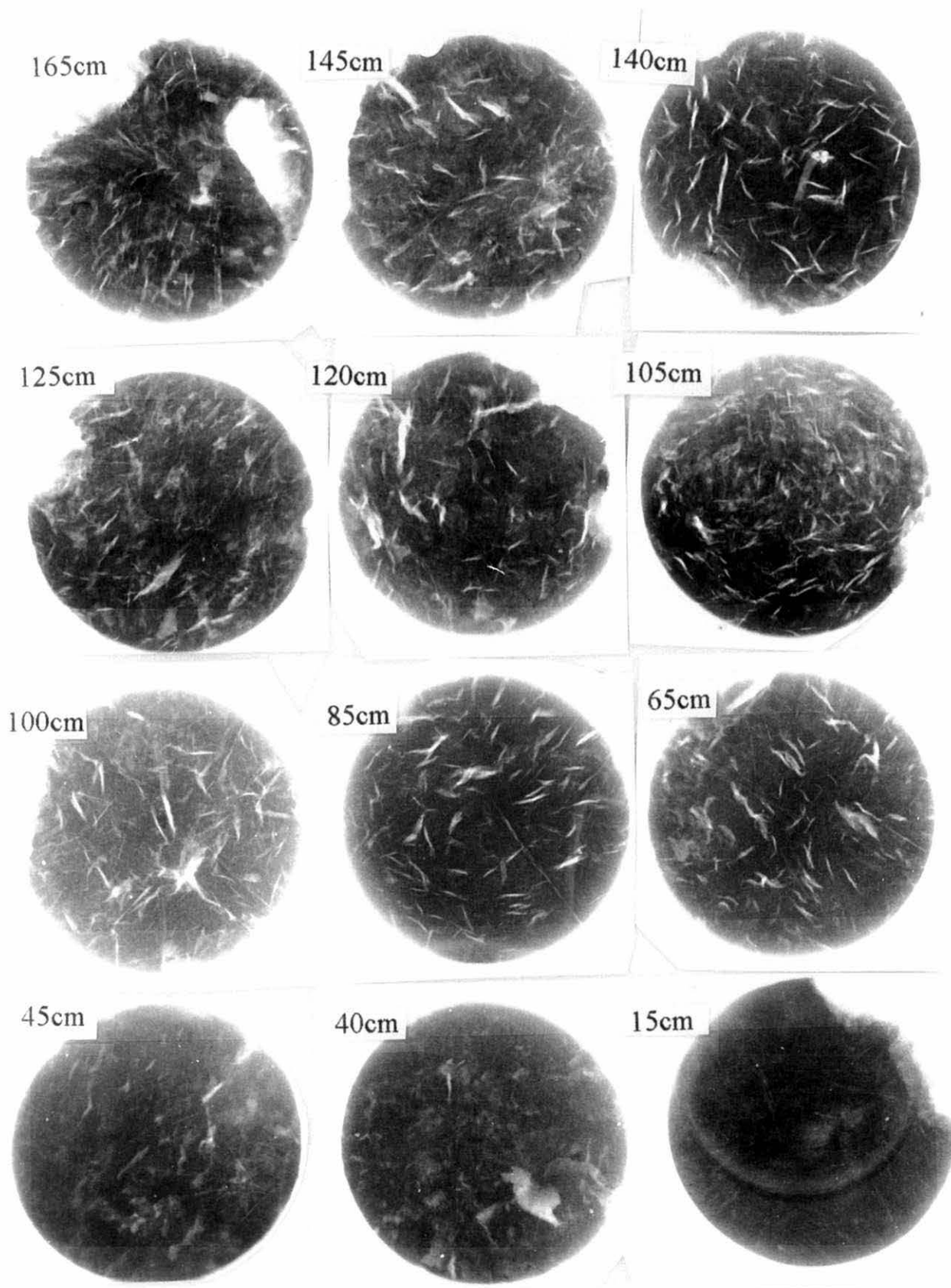


Figure 5.11. X-ray analysis of sediment sections taken from Holyhead Core B. The elongated gas voids are shown to begin mainly at the 65 cm sediment section and continue through sections of greater depth.

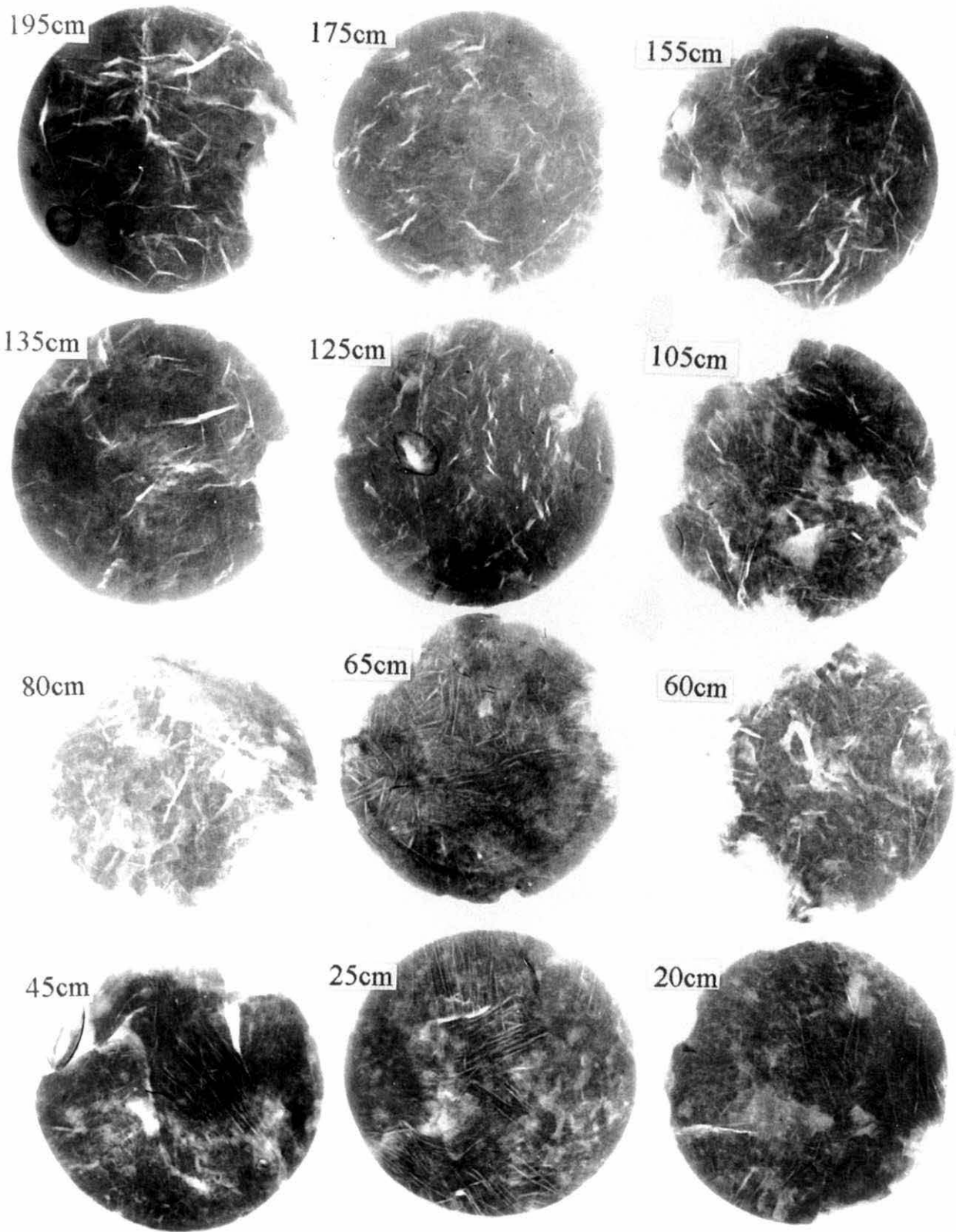


Figure 5.12. X-ray analysis of sediment sections taken from Holyhead Core C. The elongated gas voids are not clearly shown and begin at approximately 80 or 105 cm and continue through sections of greater depth.

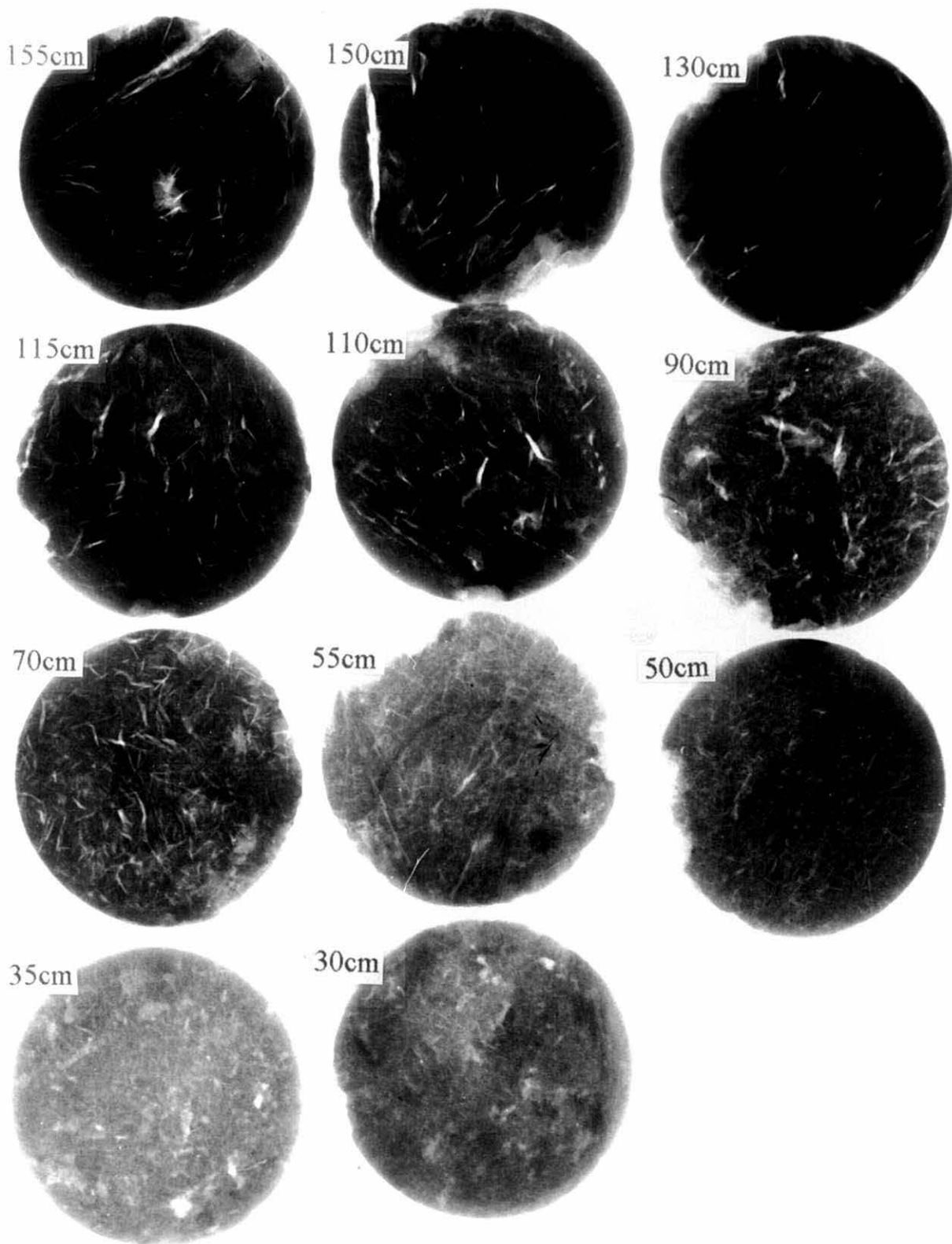


Figure 5.13. X-ray analysis of sediment sections taken from Holyhead Core D. The elongated gas voids are shown to begin at 70 cm and continue through sections of greater depth.

It was difficult to depict whether the gas voids began at 80 cm or 105 cm in Holyhead core C (see fig. 5.12). Holyhead core D was gas-free with negligible gas voids to a depth of at least 55 cm (see fig. 5.13). The gas voids were apparent at approximately 70 cm and continued throughout the rest of the core, but not to as great an extent as with the other cores. This was perhaps reflected by the lower methane concentrations in much of the acoustically turbid depths of core D (see table 5.1). By using the combined results of methane, acoustic turbidity and X-ray analyses it was possible to be more accurate with regards to the point where the actual gassy zone began; core A between 50 and 58 cm, core B between 45 and 50 cm, core C between 70 and 85 cm, and core D between 55 and 66 cm.

The difference in pressure experienced by the sediment upon retrieval would be approximately -1 atmosphere (8 m water and 0-2 m sediment) which would lower the solubility of methane and cause the existing methane pockets to expand in size, though it may be expected for the sediment to show some plasticity. The seismic profile taken using the pinger method of Floodgate *et al.* (1984) (*i.e.* figure 5.2) demonstrated that the *in-situ* acoustic turbidity began at a depth similar to that of the acoustic measurements performed on the retrieved sediment cores. This may suggest that the decrease in pressure had a limited effect on the acoustic properties. This has also been described by Sills and Wheeler (1992) when decreasing the pressure from artificially prepared, fine grained gassy sediment cores.

Acoustic turbidity in fine-grained sediments results from occluded gas bubbles (Premchitt *et al.*, 1992). Gas bubbles that are spherical in shape have been observed by electron microscopy (Sills & Wheeler, 1992; Yuan *et al.*, 1992). The movement of gas bubbles in clay sediments is unlikely to displace the soil while maintaining a spherical bubble structure (Wheeler, 1990). However it might be possible for gas migration to occur if local weaknesses exist which allow particles to be pushed apart (Sills & Wheeler, 1992). Such fissures are not uncommon in stiff clays (Sills & Wheeler, 1992), and might account for the elongated gas voids detected by X-ray analysis. This must therefore be considered a possible mechanism for gas migration in the sediments of Holyhead Harbour. The lack of gas voids in the upper sediment suggest that such gas migration via fissures is slower than the rate of methane removal in the SRZ.

5.6. Physical Factors Influencing Methane Distributions in the SRZ of the Holyhead Cores

In addition to the microbiological and chemical factors, physical factors notably sediment porosity and the diffusion coefficient of the gas which is affected by temperature also determine the distribution of gas within a core.

5.6.1. Determination of the Sediment Porosity and Diffusion Coefficients

The porosity was determined using the raw data used to calculate the water content of the sediments. The dry weight, wet weight and water content of the sediments collected using cut-off syringes (5 cm^3 mean volume collected for each sample) are given in table A11.1 of appendix XI. A mean sediment density of 1.7 g cm^{-3} was determined from this data. The porosity was calculated as the proportion of pore water of the total sediment by volume and values for cores A to D are presented in figure 5.14.

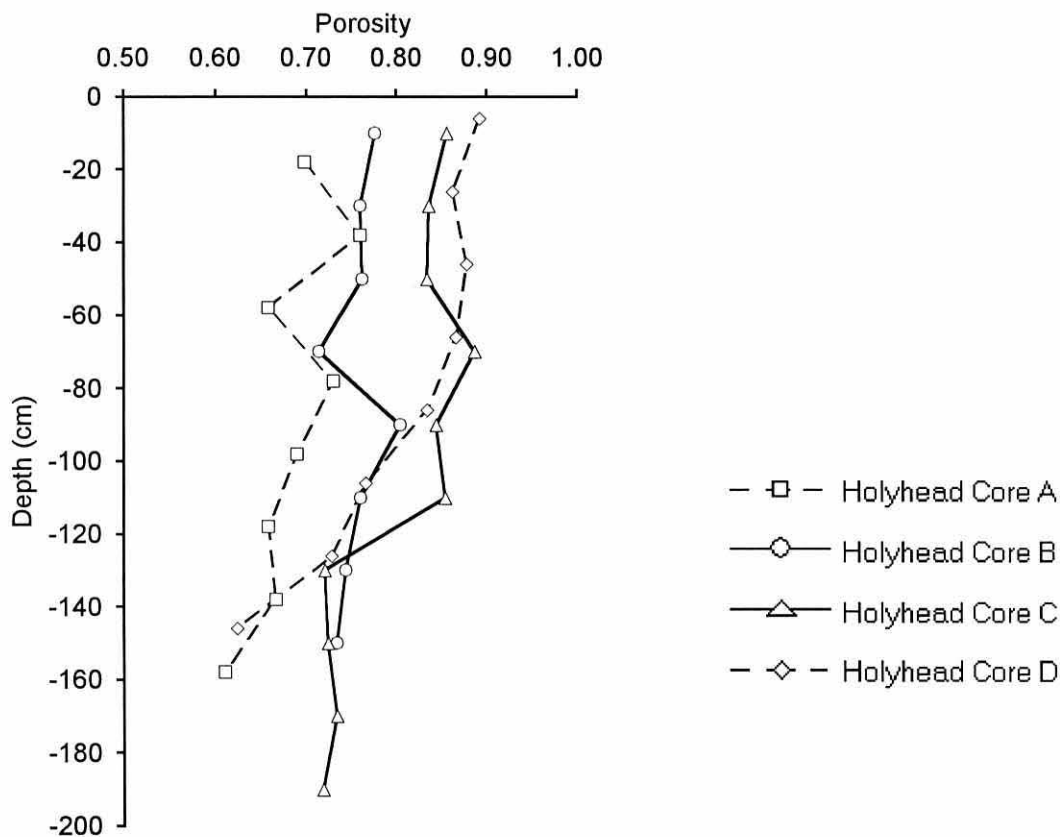


Figure 5.14 Sediment porosity versus depth for the sediment cores of Holyhead Harbour.

Figure 5.14 showed sediment porosity typically decreased with increasing sediment depth for cores A (*i.e.* 0.70 to 0.61), B (*i.e.* 0.78 to 0.73), C (*i.e.* 0.86 to 0.72) and D (*i.e.* 0.89 to 0.62) with a mean of 0.76 (SD = 0.08).

Similar decreases in porosity with increasing sediment depth have also been reported in acoustically turbid sediments of the Kattegat area of Denmark with values for surface sediments ranging from 0.80 to 0.90 and for greater depths at 0.60 to 0.75 (Iversen & Jørgensen, 1985). Acoustically turbid sediments of Saanich Inlet showed higher porosities ranging from 0.97 at the surface to 0.92 at depths of 40 cm (Devol *et al.*, 1984).

There has been very few direct determinations of the molecular diffusion coefficient for methane in marine sediments in the literature. Much of the literature has used indirect models to relate the diffusion coefficient for methane in water (D_o) to the diffusion coefficient for the bulk sediment (D_s) using the theoretical relationship: $D_s = D_o / \theta^2$, where θ is the tortuosity (Iversen & Jørgensen, 1993). Tortuosity is defined as the mean path length through the pore space between two points relative to a straight line between the same two points (Iversen and Jørgensen, 1993). The tortuosity has been shown to be related to the product of sediment porosity and the formation factor of the sediment (F) (Ullman & Aller, 1982), $\theta^2 = F \phi$. An empirical relationship between the formation factor and porosity has been given in Iversen & Jørgensen, (1993), where $F = 1/\phi^m$. Therefore the molecular diffusion coefficient for water is related to that for the sediment by equation (1):

$$D_s = \frac{D_o}{\phi (1/\phi^m)} \quad (1)$$

For clay and silt sediments the value of 'm' has been determined experimentally to range from 2.5 to 5.4 (Manheim & Waterman, 1974; Ullman & Aller, 1982; Iversen & Jørgensen, 1993). For a mean porosity of 0.76 and a seawater diffusion coefficient of $1.50 \times 10^{-5} \text{ cm}^2 \text{ s}^{-1}$ at 15°C (Iversen & Blackburn, 1981) the sediment diffusion coefficient for methane was found to range from $0.45 \times 10^{-5} \text{ cm}^2 \text{ s}^{-1}$ (*i.e.* $m=5.4$) to $0.99 \times 10^{-5} \text{ cm}^2 \text{ s}^{-1}$ (*i.e.* $m=2.5$).

Recently, an empirical equation has been established from experimental data taken from an area of known acoustic turbidity to directly relate the molecular diffusion coefficient of methane in seawater to that of the bulk of the sediment as given in equation (2):

$$D_s = \frac{D_o}{1 + n(1 - \phi)} \quad (2)$$

where: $n = 3$ for clay-silt sediments (Iversen and Jørgensen, 1993)

$D_o =$ molecular diffusion coefficient for methane in seawater for a given temperature

$\phi =$ sediment porosity

$D_s =$ molecular diffusion coefficient for methane in the sediment

Using equation (2) the sediment diffusion coefficients for methane were determined for all the sediment samples and are presented in table A11.1 of appendix XI. A mean sediment diffusion coefficient of $0.90 \times 10^{-5} \text{ cm}^2 \text{ s}^{-1}$ ($SD = 0.13 \times 10^{-5}$) was determined from the data with a coefficient of variation of 14 % for all Holyhead samples (see table A11.1, appendix XI).

Experimentally determined molecular diffusion coefficients for methane in acoustically turbid sediments of the Kattegat area of Denmark have been shown to range from 0.42 to 0.67 $\times 10^{-5}$ $\text{cm}^2 \text{s}^{-1}$. Many of the other values quoted in the literature have been determined via the empirical equation (1) and have given values of 0.50 $\times 10^{-5}$ $\text{cm}^2 \text{s}^{-1}$ (Bernard, 1979), 0.80 and 0.96 $\times 10^{-5}$ $\text{cm}^2 \text{s}^{-1}$ (Kuivila *et al.*, 1990) and 1.0 $\times 10^{-5}$ $\text{cm}^2 \text{s}^{-1}$ (Devol *et al.*, 1984). The values determined for the Holyhead sediments therefore compare well with these values quoted from the literature.

5.6.2. Which Model Best Describes the Methane

Profiles of Holyhead Harbour?

There has been little direct evidence to link methane oxidation to sulphate reduction (Iversen & Jørgensen, 1985; Alperin & Reeburgh, 1985). Anaerobic methane oxidation has not been investigated at Holyhead Harbour therefore its presence and extent is unknown. Some of the strongest evidence for anaerobic methane oxidation in the sediments comes from geochemical models of methane distributions in anoxic marine sediments (Devol *et al.*, 1984; Martens & Berner, 1977; Bernard, 1979). A methane consumption term has often been required to model the concave-up-wards methane profiles found in numerous marine sediments. These profiles could not be adequately described by simple diffusion and depositional advection because sedimentation rates were relatively slow compared to the diffusive processes.

It has been shown, however, that in the Holyhead area the sedimentation rates are significant at 13 cm y^{-1} and could therefore potentially give concave-up-wards methane profiles due to diffusion and depositional advection alone. The aim of this section is to determine which model best describes the methane distribution profile using the known parameters available for Holyhead Harbour.

Initially considered is the model to describe the methane profile that would exist in the surface sediment depths above the point of methane saturation if diffusion and depositional advection were the only processes acting on the methane in the sediment. This model is given in equation 3 (Martens & Berner, 1977):

$$D_s \frac{\delta^2 C}{\delta x^2} - \omega \frac{\delta C}{\delta x} = 0 \quad (3)$$

where: x = depth below the sediment-water interface measured positively downward

C = concentration of dissolved methane in the pore water

ω = rate of sedimentation (cm s^{-1})

D_s = Diffusion coefficient for methane in the sediment

The assumptions that this model is based on include:

1. The system is in steady state. Methane profiles taken from this site on a previous occasion (*i.e.* station 7 in April, 1982, Jones *et al.*, 1986; Floodgate *et al.*, 1986) showed similar types of profiles to the data given here with methane concentrations increasing between depths of 20 and 80 cm. However, the concentrations were typically lower by less than an order of magnitude which possibly reflected the time of year.
2. Bioturbation is neglected. There was little evidence of bioturbation in the Holyhead cores, and the presence of soluble sulphide in surface depths also reinforced this observation.
3. The significant reactions involving sulphate and methane are biologically catalysed.
4. The effects of compaction are small. Murray *et al.* (1978) found this to be true in anaerobic sediments of Saanich Inlet where sedimentation rates have been determined at 1 cm y⁻¹. The sedimentation rate for Holyhead Harbour was estimated to be much greater at 13 cm y⁻¹ but porosity calculations showed only a small variation over depth in the cores (*i.e.* CV = 8 %). Comparable variations in porosity with increasing depth were also found in sediments with lower sedimentation rates (*i.e.* 0.05 to 0.25 cm y⁻¹) (Iversen & Jørgensen, 1985).

Upon the solution for the two point boundary condition; when $x = 0$ then $C = 0$ due to the oxidation of methane by ^{oxygen} ~~oxygen~~ ^{from bacteria utilizing} from over lying seawater, and when $x = X$ then $C = C_x$ which is methane saturation, it follows that:

$$C = \frac{\text{EXP}[(\omega / D_s) x] - 1}{\text{EXP}[(\omega / D_s) X] - 1} C_x \quad (4)$$

It should be noted that the solution given in Martens and Berner, (1977) shows the brackets to equation (4) to be in the wrong place. Using this equation the expected methane concentrations at depths above the point of methane saturation were calculated for a system whereby only diffusion and depositional advection were accounted for. The concentration of methane required to exceed the solubility in the pore water has been determined in section 5.6.2 at approximately 2.7 mM. The initial depth sampled at which the methane solubility of 2.7 mM was exceeded was 58 cm, 50 cm, 90 cm and 66 cm for cores A, B, C and D, respectively. The depth where the methane concentration of 2.7 mM was expected was inferred from the data as 48.7 cm, 36.9 cm, 73.2 cm and 65.4 cm for cores A, B, C and D, respectively. The average sedimentation rate determined from a nearby locality (*i.e.* 13 cm y⁻¹, section 5.3) was used in equation (4) as well as the 95 % confidence values (*i.e.* 9 and 17 cm y⁻¹) to give some comparative profiles. Also, to give some scale to the profiles an anomalous high sedimentation rate of 30 cm y⁻¹ was used for comparison. These modelled methane profiles for a system whereby only diffusion and depositional advection was considered are presented in table A11.2 of appendix XI with the actual methane concentrations for comparison, and are also shown in figure 5.15.

It is evident from figure 5.15 that for all sedimentation rates used (*i.e.* 9 to 30 cm y^{-1}) there was significant curvature on the modelled methane profiles for all Holyhead cores. This was not observed in other marine sediments of notable methane production from the literature because sedimentation rates were typically much lower at 0.3 and 1.0 cm y^{-1} (Martens & Berner, 1977; Devol *et al.*, 1984, respectively). The curvature of the modelled profiles was however not great enough to account for the measured methane value at the next shallowest depth above the depth of methane saturation. This result was also consistent even when the errors associated with the methane analysis were taken into account (see table 5.1 and table A11.2, appendix XI). The 20 cm depth interval of the methane sampling suggested that there was almost a 20 cm depth range from which the estimated point of methane saturation (*i.e.* 2.7 mM) could be located. Core D however, showed that the point of methane saturation was slightly shallower than the 66 cm sampling depth of 2.8 mM. For cores A, B and C it was feasible, though unlikely, that the point of methane saturation could also begin at potentially greater depths just above the methane saturation sampling depth, *i.e.* 57 cm for core A, 49 cm for core B and 89 cm for core C.

Figure 5.16 shows the actual and modelled methane profiles for the Holyhead cores using the greatest potential depths for methane saturation within the 20 cm sampling interval. The arrows in figure 5.16 show the potential change in depth for the methane saturation point. It was evident that core C showed a methane profile that could almost be represented by the modelled data with a sedimentation rate of 17 cm y^{-1} . The 95 % confidence limits of the methane analysis (see table 5.1) for the 70 cm sampling depth just overlapped with the data generated from the 95 % confidence limits for the sedimentation rate (see table A11.2 of appendix XI). At the 50 cm sampling point however, the curvature of the modelled data was insufficient to incorporate the actual methane concentration even when allowing for the large errors associated with the methane analysis. The remaining cores also showed that the actual methane values could not be represented by the modelled data.

The lowest sediment diffusion coefficient obtained from equation (1) using a value of $m=5.4$ was 0.45 cm² sec⁻¹. By using this value it was also evident that the measured methane concentrations could not be modelled simply in terms of diffusion and depositional advection (data not shown).

There was little evidence of bioturbation in the Holyhead cores. Bubble ebullition into the overlying water column was not observed at this site on previous trials (M. Yarrington, *pers. comm.*, 1990) and the X-ray analysis did not reveal any bioturbation marks or bubbles within the 0-40 cm depth range of any cores (see section 5.6.3). If bubble ebullition was present then this would be expected to produce a profile that more resembled the simple diffusion and depositional advection profile described by the model (equation 3).

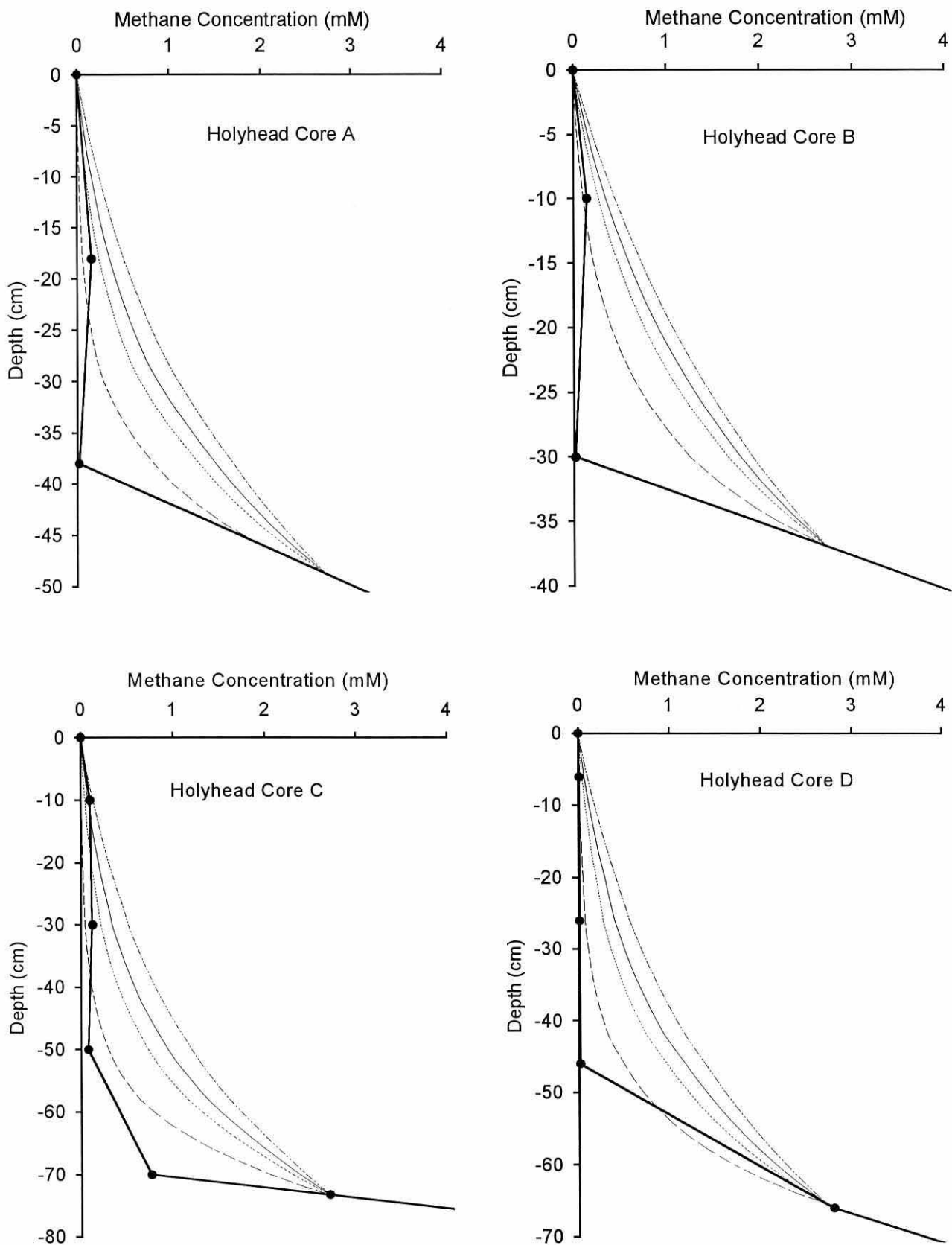


Figure 5.15. Methane concentrations of the Holyhead Harbour sediment cores showing the actual measured values (—●—) and model fits of the data from the point of saturation (i.e. 2.71 mM) for diffusion and depositional advection only for different sedimentation rates; 9.2 cm y⁻¹ (- · - · -), 13.2 cm y⁻¹ (—), 17.2 cm y⁻¹ (·····) and 30 cm y⁻¹ (- - -).

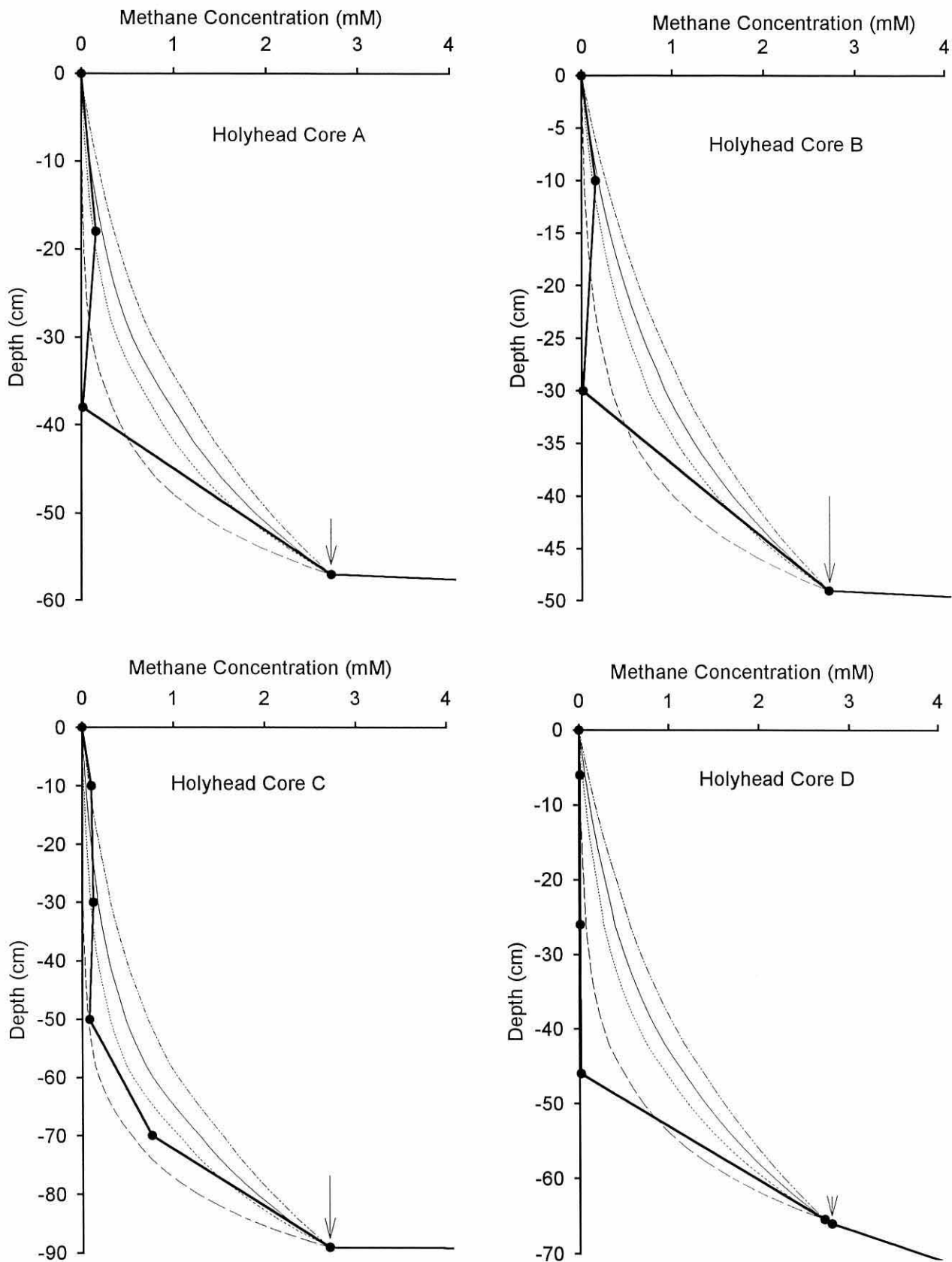


Figure 5.16. Methane concentrations of the Holyhead Harbour sediment cores showing the actual measured values (—●—) to the maximum depth possible for methane saturation (2.71 mM) and model fits of the data from the point of saturation (i.e. 2.71 mM) for diffusion and depositional advection only for different sedimentation rates; 9.2 cm y⁻¹ (-----), 13.2 cm y⁻¹ (———), 17.2 cm y⁻¹ (.....) and 30 cm y⁻¹ (- · - · -).

Therefore this information suggested that the actual methane distribution, if in steady state, could not be explained simply in terms of diffusion and depositional advection even when the large sedimentation rates were taken into account. Therefore it could be suggested that methane was being removed from the more surface sediments by another process besides diffusion, depositional advection and ebullition.

The simple diffusion and depositional advection model given in equation (3) was therefore modified to incorporate anaerobic methane consumption. Results from other studies have shown that the rates of anaerobic methane oxidation is not constant with depth suggesting that methane consumption is not a zero order reaction, *i.e.* rate is not expected to be constant over the depths where sulphate concentrations decline with increasing depth (Reeburgh, 1980; Alperin & Reeburgh, 1985; Iversen & Jørgensen, 1985; Lidstrom, 1983).

Methane consumption is dependent on two factors: methane and sulphate concentration. Just below the methane-sulphate transition the net methane production is expected to be at a maximum, as determined on a previous trial of this area (Jones *et al.*, 1986). At a slightly shallower depth methane oxidation is also expected to be maximum from the increased diffusion of methane from deeper sediments into a zone where there is sufficient concentration of sulphate to act as the oxidising agent. Devol *et al.* (1984) produced a model from a detailed study to describe methane oxidation as second order. First order with respect to sulphate in an upper zone and also first order with respect to methane in a lower zone. This study required manipulating the modelled data to best fit the real data in order to estimate the three unknowns in the four coupled equations to determine the methane oxidation rate profiles. A sediment sampling interval of 3 cm was used in the study of Devol *et al.* (1984) compared to 20 cm for the Holyhead sediments. Therefore it would be unwise to attempt similar second order model manipulations for the Holyhead study which had a limited data set around the sulphate-methane transition.

The methane consumption inferred in the Holyhead cores was therefore taken to be first order with respect to the methane concentration with the following assumptions;

1. At the depth of high methane concentrations (*i.e.* at the point of saturation) methane consumption did not occur.
2. Sediment depths shallower than the depth of methane saturation the methane oxidation is proportional to the methane concentration and has sufficient concentration of sulphate to act as the oxidising agent.

The concentration of sulphate at the point of methane saturation was expected to be between 8.8 and 0.9 mM for core A, 23.8 and 5.8 mM for core B, 2.0 and 0.7 mM for core C and 3.1 and 0.01 mM for core D.

then:
$$D_s \frac{\delta^2 C}{\delta x^2} - \omega \frac{\delta C}{\delta x} - K_1 C = 0 \quad (5)$$

where: K_1 = first order rate constant

Upon solving the boundary conditions; when $x = 0$ then $C = 0$ and when $x = X$ then $C = C_x$
then

$$C = \frac{\text{EXP}(\alpha x) - \text{EXP}(\gamma x)}{\text{EXP}(\alpha X) - \text{EXP}(\gamma X)} C_x \quad (6)$$

where:
$$\alpha = \frac{\omega + (\omega^2 + 4 K_1 D_s)^{1/2}}{2 D_s}$$

$$\gamma = \frac{\omega - (\omega^2 + 4 K_1 D_s)^{1/2}}{2 D_s}$$

Figure 5.17 shows the methane profile for Holyhead Harbour with the expected profiles for two rate terms describing the first order methane oxidation reaction. The depths of methane saturation were estimated at 48.7 cm, 36.9 cm, 73.2 cm and 65.4 cm for cores A, B, C and D, respectively. It is evident from figure 5.17 that the slower rate constant (*i.e.* $8.0 \times 10^{-9} \text{ s}^{-1}$ from Martens & Berner, 1977) is not sufficient to account for the decrease in methane. Also the faster rate constant of $2.5 \times 10^{-7} \text{ s}^{-1}$ was insufficient to account for the much lower methane concentration at the next depth even when errors in the methane analysis and sedimentation rates were taken into account. However, when the potential depth for methane saturation was moved to the maximum potential depth within the 20 cm sampling range it can be seen in figure 5.18 that the first order rate constant was sufficient to account for the methane profiles. This would suggest that the rate constant describing the removal of methane at depths above the point of methane saturation is of the order of $2.5 \times 10^{-7} \text{ s}^{-1}$. However, due to the limited sampling intervals across the sulphate-methane transition it would not be acceptable to try further to determine the exact rate of the anticipated anaerobic methane oxidation from this data.

By attempting to model the measured methane profiles in the SRZ of the Holyhead cores these results suggest that a methane consumption term is necessary which perhaps reflects the presence of anaerobic methane oxidation. Direct determination of the presence and rate of anaerobic methane oxidation in these cores via stable isotope tracer experiments would provide confirmation to the results of the modelled data of this study.

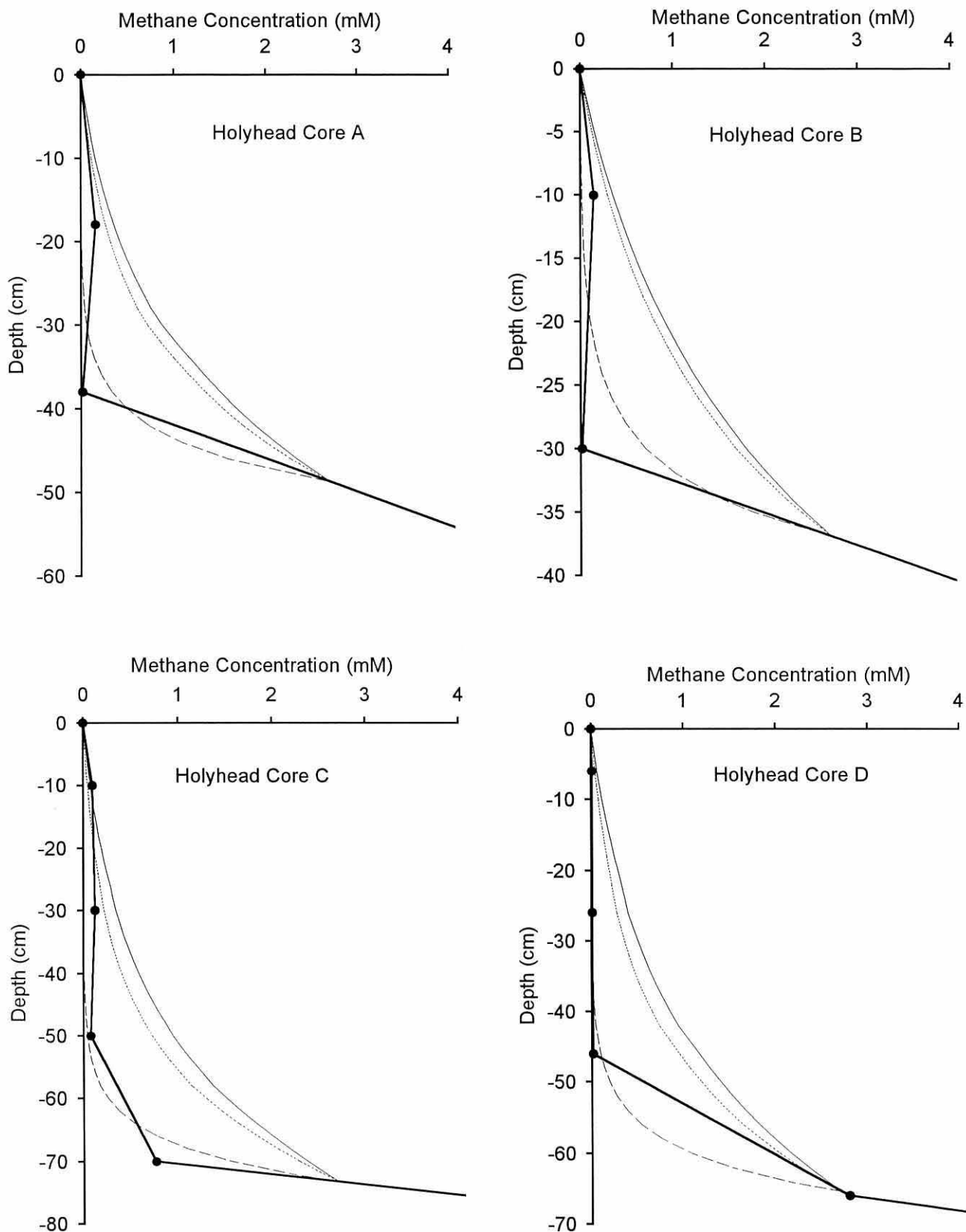


Figure 5.17. Methane concentrations of the Holyhead Harbour sediment cores showing the actual measured values (—●—) and model fits of the data from the point of saturation (i.e. 2.71 mM) for a sedimentation rates of 13.2 cm y^{-1} for diffusion and depositional advection (—) and methane consumption described by the first order rate constants $2.5 \times 10^{-7} \text{ s}^{-1}$ (---), $8.0 \times 10^{-9} \text{ s}^{-1}$ (.....).

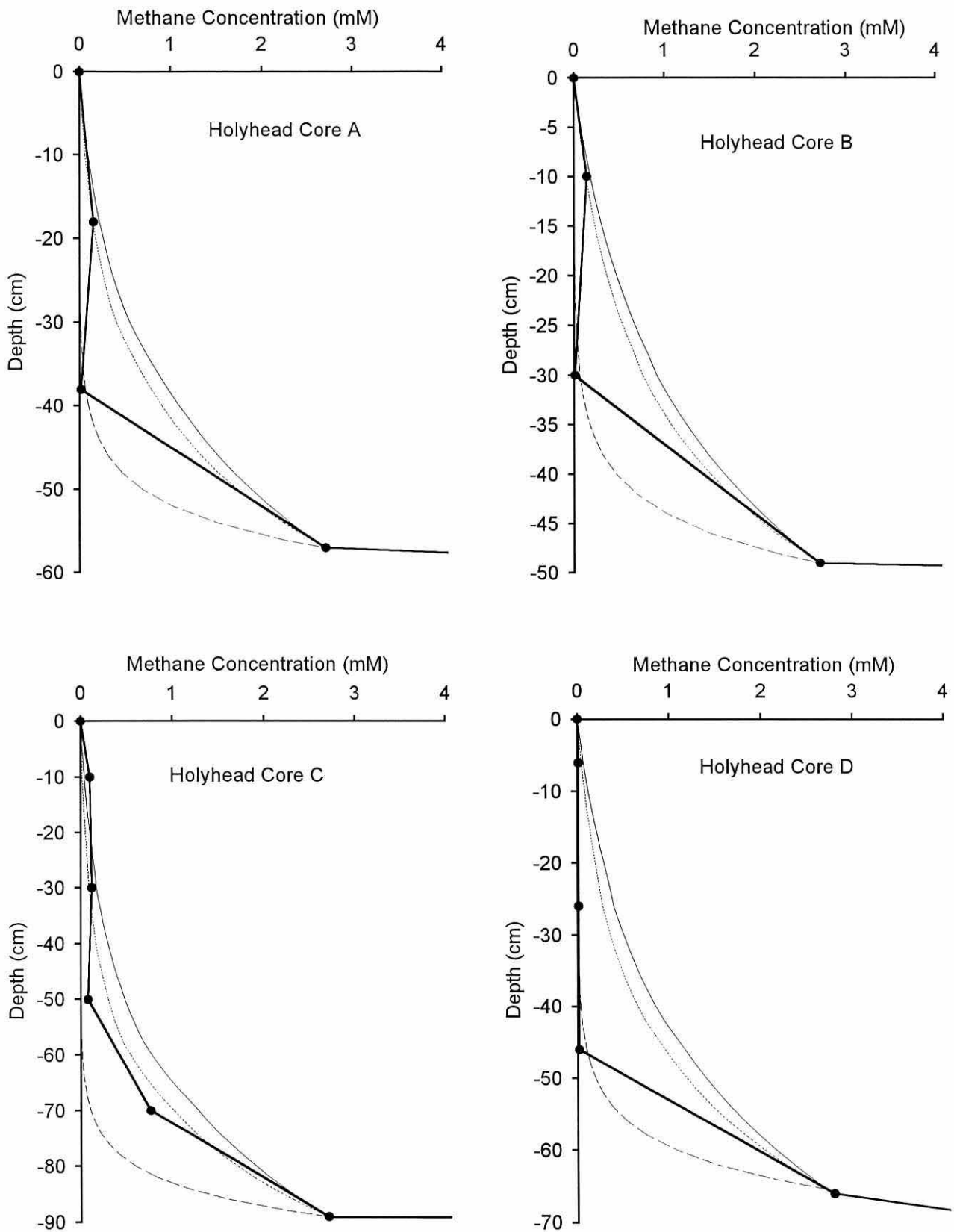


Figure 5.18. Methane concentrations of the Holyhead Harbour sediment cores showing the actual measured values (—●—) and model fits of the data from the maximum depth of methane saturation (i.e. 2.71 mM) for a sedimentation rates of 13.2 cm y⁻¹ for diffusion and depositional advection (—) and methane consumption described by the first order rate constants 2.5 × 10⁻⁷ s⁻¹ (---), 8.0 × 10⁻⁹ s⁻¹ (.....).

5.7. Ether Lipid - Methane Comparisons

A relationship between ether lipid and methane concentration could be tentatively suggested from the limited study of Martz *et al.* (1983). This was therefore investigated in the sediments of this study.

The methodology for the ether lipid determination is given in section 2.13 of Chapter 2 and the raw data generated is presented in appendix VI and VIII. The procedure used internal and external standards. It could be shown from the standards that the approximate yield of ether lipids from the extraction, preparation and analysis procedures was 27 % (SD = 12 %). A second more rigorous extraction of the sediment remaining after the initial routine extraction was performed on three sediments of core C (*i.e.* 60-70 cm, 80-85 cm and 100-105 cm, see appendix VI). These further extractions yielded approximately 2.7 % more internal standard which was < 9 % of that recovered with the initial extraction procedure. The concentrations of C20 and C40,0 lipids as determined relative to the internal standard gave a minimal variation on the values determined from the initial extraction procedure (*i.e.* < 4.4 % difference in C20 and < 2.9 % variation in C40,0). The cyclic ether lipids were not detected on the second extraction procedure (*i.e.* below detection limit), suggesting that they were either removed from the initial extraction or were chemically affected by the strong acid extraction. These results suggested that a small proportion of additional C20 and C40 lipids was liberated from the sediment after a second, more rigorous extraction which when the internal standard was taken into account gave similar results to the initial extraction.

5.7.1. Ether Lipid/Methane Comparisons - Holyhead Harbour.

Figure 5.19. illustrates the total ether lipid and methane concentration for Holyhead cores A, B, C and D. The ether lipid methodology showed less than a 10 % variation for three replicate analyses of the 209 cm depth of Holyhead Core C, as shown in figure 5.19. From figure 5.19, it was evident that the total ether lipid profile did not show low concentrations in the more surface sediments as was observed with the methane profile. Total ether lipid concentrations were found to show small variations in concentration with depth in contrast to the large variations observed with the methane profile.

The depth where the acoustic turbidity began coincided with the ether lipid maximum for core C (*i.e.* 70-85 cm) and with localised maxima in core A (*i.e.* 50-58 cm). Core B showed the methane and ether lipid profiles were very similar though the maxima were slightly displaced and core D showed the maximum ether lipid concentration at the top whereas the methane maximum was located at the bottom of the core.

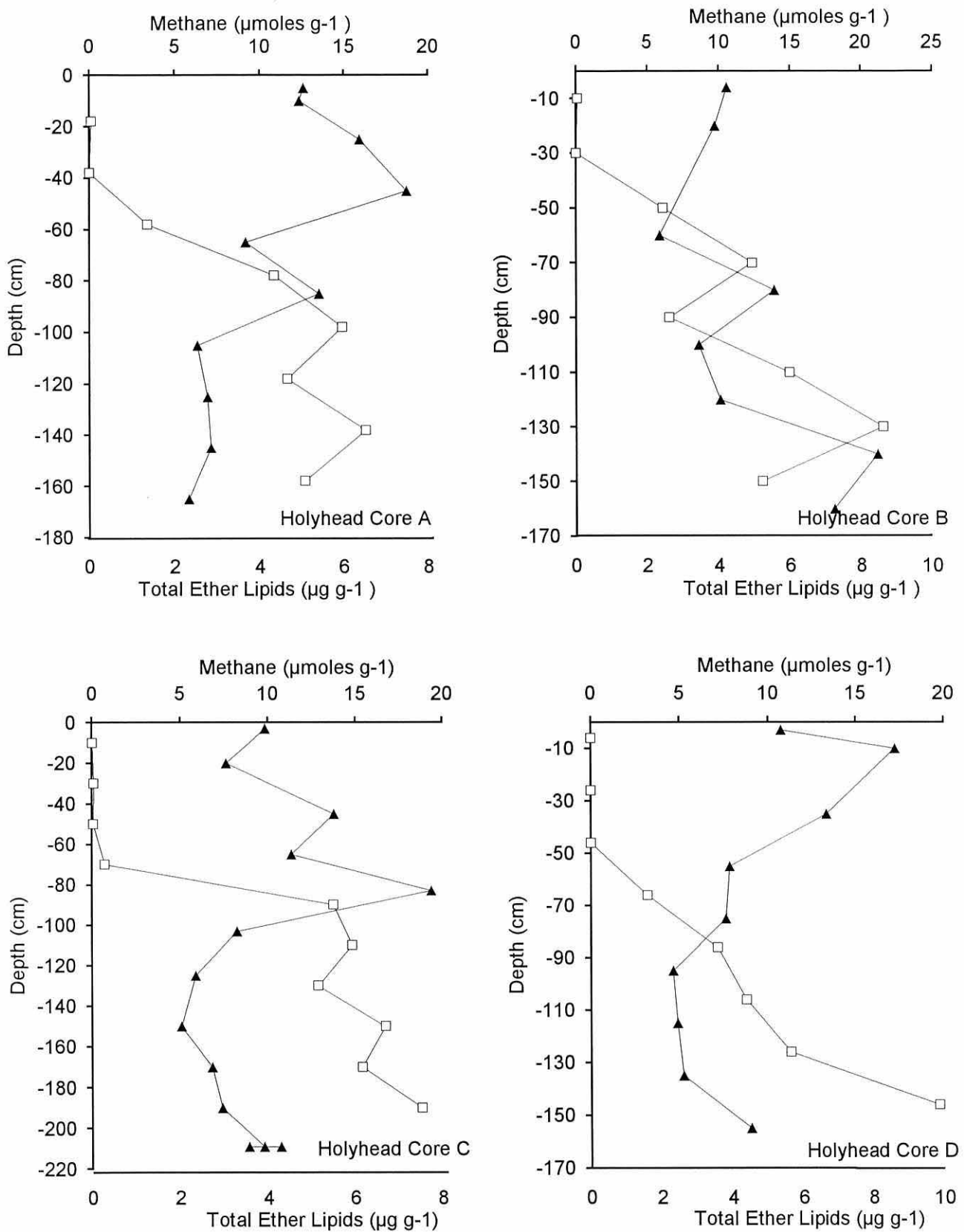


Figure 5.19. Sediment profiles of methane (—□—) and total ether lipid concentrations (—▲—) for sediment cores of Holyhead Harbour with replicate analyses of the 209 cm depth of Holyhead Core C.

Therefore from these observations there appeared to be no consistent relationship between the total ether lipid and methane concentration over the entire core length of these acoustically turbid sediments of Holyhead Harbour. Also there did not appear to be a consistent relationship between methane concentration and concentrations of some of the individual ether lipid species detected in the sediment (see tables 5.1 and A8.1 of appendix VIII).

Possible reasons why the ether lipid profile showed a small change in concentration relative to the methane profile which demonstrated a two order of magnitude change across the sulphate - methane transition are discussed in section 5.12.

5.7.2. Ether Lipid/Methane Comparison - Intertidal

After comparing the relationship between total ether lipid and methane concentration in marine sediments which demonstrated significant methanogenic activity it was necessary to compare with a relatively gas free sediment. Total ether lipid and methane concentrations for a comparatively gas free intertidal sediment at Cadnant Creek are shown in figure 5.20.

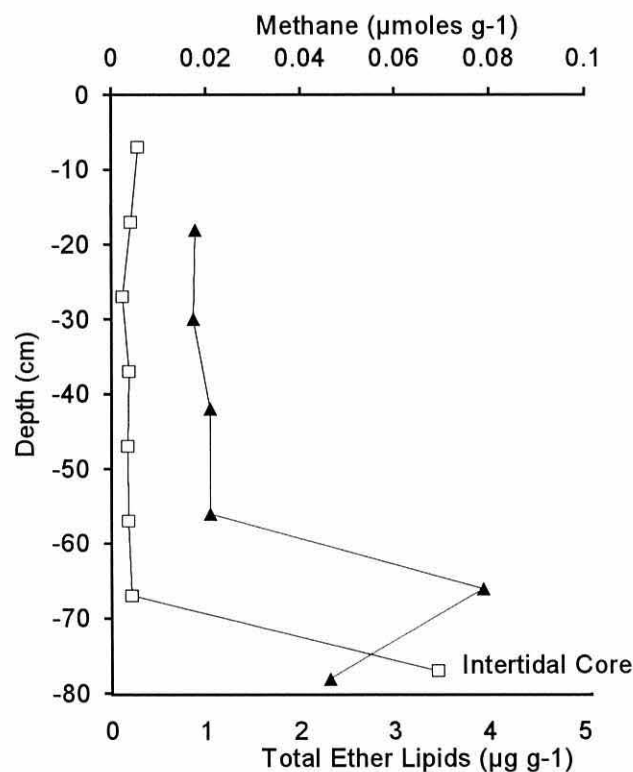


Figure 5.20. Sediment profile of methane (—□—) and total ether lipid concentrations (—▲—) for the intertidal core at Cadnant Creek.

Total ether lipid and methane concentrations remained unchanged down most of the intertidal core (see figure 5.20). Significant increases of the two parameters occurred at similar depths towards the bottom of the core, which may suggest a relationship between the two parameters though the single core is insufficient to base any firm conclusions on. From the sulphate profile

of the intertidal core (see figure 5.8) it is evident that the SRZ extended below the bottom of the intertidal sediment core. The methane values of the intertidal core were comparable to the low methane values reported in the SRZ of the Holyhead cores. Also the ether lipid concentrations were slightly lower than that observed for Holyhead Harbour but of a comparable order of magnitude.

5.8. MPN - Methane Comparisons

Incubation of Holyhead sediment samples in the study by Jones *et al.* (1986) suggested that there was a net production of methane at a depth of approximately 80 cm which also coincided with the measured increase in methane concentration. Whether maximum numbers of methanogens also occurred at this depth was, however, not determined in the study of Jones *et al.* (1986). Following the comparison between ether lipid and methane concentration, where ether lipids represented both viable biomass and necromass, it was necessary to compare whether a relationship existed between the numbers of viable methanogens (MPN technique) and methane concentration in sediments of significant methanogenic activity.

The number of viable methanogenic bacteria can be estimated using the most probable number technique (MPN), which relies on the production of methane to signify the presence of methanogenic bacteria. Approximate numbers of viable methanogens in a sediment sample can be estimated by determining the greatest dilution of the sample that produces methane after incubation. Media preparation (section 2.1.2) and inoculation with sediment samples for the most probable number determination (section 2.1.5) are given in chapter 2.

5.8.1 MPN/ Methane Comparisons - Holyhead Harbour

Problems were encountered with the most probable number technique for the Holyhead samples (as detailed in section 2.5) which led to the procedure being repeated on the remaining sediment that had been stored at 3 °C. It was evident that some of the samples had oxidised since they were collected therefore the MPN results were limited to the samples that appeared anaerobic from the sulphides that were visibly present. This second determination was made approximately one month after the samples were collected. Jones and Paynter (1978) have demonstrated that storage of sediment samples at 2°C for periods up to 9 days had a negligible effect on the MPN counts. The MPN results of Holyhead Harbour were of a comparable order of magnitude to those determined on a previous study of this area and at a similar time of year (Peters, 1988). Therefore this information may suggest that although the number of MPN data points were limited the actual values reported were of an order of magnitude to be expected in Holyhead Harbour. However, considering these shortcomings attempts were made to determine whether any relationships existed in the data.

What about cores B & C?

Figure 5.21. shows sediment profiles of the methanogen numbers (MPN) and the methane concentrations for Holyhead cores A and D. It was generally noted that in the surface sediments both methane and MPN values were low (*i.e.* $0.1 \mu\text{moles g}^{-1}$ and <1300 per g, respectively). With increasing sediment depth both the methane concentrations and MPN data showed maxima at similar sediment depths. Basic correlation analysis of the methane and MPN data points at the consistent sediment depths analysed suggested correlation coefficients of: $r = 0.64$ ($p = 0.22$) for Holyhead core A, and $r = 0.83$ ($p = 0.13$) for Holyhead core D. The relatively high probability of points falling outside this correlation could be attributed to the very low number of data points (*i.e.* core A $n = 5$, core D $n = 4$).

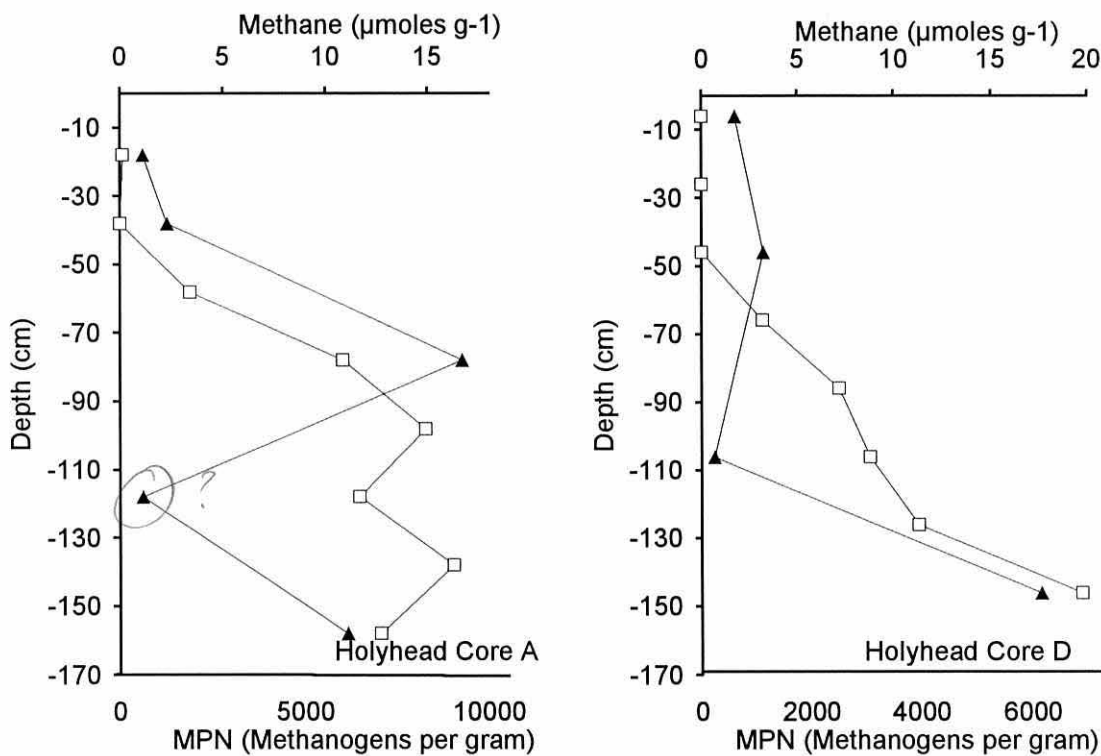


Figure 5.21. Methane (—□—) and methanogenic numbers (Most Probable Number determination) (—▲—) for Holyhead cores A and D.

The methanogen numbers and methane concentrations were initially compared to determine if there was a relationship between the two variables in acoustically turbid sediments. It was therefore considered appropriate to combine the methane and methanogen number data for the Holyhead cores A and D. This overcame the problem of limited data points, and statistical analysis revealed that the MPN and methane values were significantly correlated at the 95 % confidence interval (*i.e.* $r = 0.68$, $p = 0.04$, $n = 9$) for the combined data points of Holyhead cores A and D. Therefore from this limited data set it might appear that a relationship does exist between the viable methanogenic bacteria, as determined by MPN, and the methane concentration, though due to the limitations in the MPN data this relationship cannot be considered conclusive for the acoustically turbid sediments.

5.8.2. MPN / Methane Comparison - Intertidal Core

The problems encountered for the MPN determinations of the Holyhead cores did not apply to the intertidal core. Figure 5.22 illustrates the MPN and methane values for the sediment profile of the intertidal core. Methane concentrations in the intertidal core remained low over most of the core length and were observed to increase at the maximum sediment depth to values comparable to the SRZ of Holyhead Harbour. The maximum in methanogen numbers occurred at a shallower depth than the methane maxima, such that no correlation was observed between the methane and MPN values of this intertidal core (*i.e.* $r = 0.17$, $p = 0.68$).

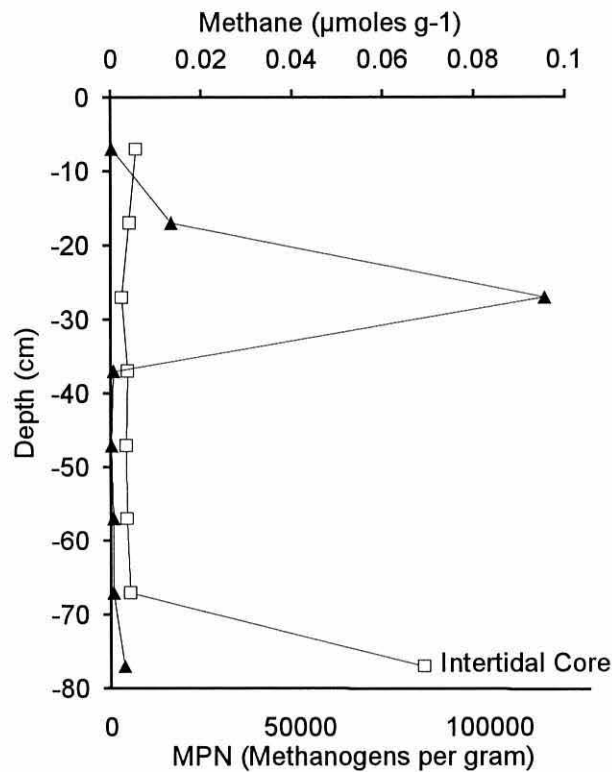


Figure 5.22. Methane (—□—) and methanogenic numbers (Most Probable Number determination) (—▲—) for the intertidal core.

It can be noted by comparing figure 5.8 with figure 5.22 that a sulphide maximum existed just above the maximum in methanogen numbers which might be due to methane oxidation in the presence of sulphate. One possible explanation for the high numbers of methanogens recorded at 27 cm might be due to increased methanogenic activity producing methane which in the high sulphate conditions (*i.e.* 26.3 mM) could be oxidised to form sulphide. This therefore might explain the sulphide maxima determined in the 12-24 cm depth range (see table 5.2). The reason as to why the maximum in viable methanogen numbers occurred at 27 cm is unknown from the data available. High MPN counts within the SRZ could be due to either methanogens metabolising substrates not competed for by the sulphate reducing bacteria or due micro-niches where sulphate concentrations had diminished sufficiently to allow methanogenesis to increase.

5.9. Ether Lipid - MPN Comparison

Following the previous sections it was not necessary to graphically compare the available MPN counts with the ether lipid data in a figure. The total ether lipid concentration did not show a positive relationship to the MPN counts in either Holyhead cores A or D or the intertidal core (compare fig 5.19 with 5.20 for Holyhead and figs 5.20 with 5.22 for the intertidal sediment).

5.9.1. Estimated Proportion of Ether Lipids in the Sediment that can be Accounted for by the Viable Methanogens Determined by the MPN Technique

Evidence gathered from the current literature (Chappe *et al.*, 1982; Harvey *et al.*, 1986) and the ether lipid degradation experiment (section 4.6.) would suggest that the ether lipids of the dead methanogenic cells and cell material would be expected to have a significant residence time in anaerobic marine sediments. Therefore, the ether lipid content of the sediments is expected to represent both the active, viable methanogenic cells (*i.e.* biomass) as well as the dead methanogenic cells and cell material (*i.e.* necromass).

The most probable number technique stimulates a proportion of the total viable population to grow in the sediment samples. From the current literature (Hedrick *et al.*, 1991a; Pauly & Van Vleet, 1986a) and data within chapter 4 it is possible to approximate a mean ether lipid content (with limits) per average methanogenic cell. Therefore by using this information an estimate could be made of the proportion of the total ether lipid content of the sediment accounted for by the viable methanogens determined by the MPN technique. The term viable in this context will include the methanogens which will divide and produce methane in the incubated MPN tubes. This approximation might therefore give an indirect estimate of the proportion of non-viable methanogenic material which will include inactive as well as dead methanogenic material (*i.e.* necromass) present in the sediment.

The use of conversion factors to potentially increase the information interpreted from the data requires careful consideration of the possible sources of error. Ideally conversion factors should be calculated from the samples that the data is being based on. However, this approach was not possible for the sediment samples of this study. By using a range of values collected from the literature then limits for each conversion factor used can be applied to the data to give a range of possible results about as a mean value.

In order to estimate the proportion of ether lipids that would be accounted for by the most probable numbers of viable methanogens present it was necessary to estimate an average ether lipid concentration per dry weight of methanogenic cells. Significant variation in ether lipid per dry weight was determined within the growth experiment of *Methanosarcina acetivorans* (see chapter 4) *i.e.* mean =13.9 mg (SD = 10.6 mg) ether lipid per gram (dry weight).

Determinations of ether lipid per dry weight for various methanogenic cells have also been calculated both directly and indirectly by other research groups. Reported concentrations range from 1.5 mg ether lipid g⁻¹ (dry weight) (De Rosa *et al.*, 1986a) to 53.7 mg g⁻¹ (Ferrante *et al.*, 1988).

Significant variation in ether lipid per dry weight of methanogenic cells of the same species has also been detected between different research groups. For example, concentrations of ether lipid per dry weight of *Methanosarcina barkeri* cells have been reported at 1.5 mg g⁻¹ (De Rosa *et al.*, 1986b), 3.0 mg g⁻¹ (Nichols *et al.*, 1987), 6.6 mg g⁻¹ (Hedrick *et al.*, 1991a), 13.4 mg g⁻¹ (Hedrick *et al.* 1991a) and 38 mg g⁻¹ (Pauly & Van Vleet, 1986a), giving a mean value of 12.5 mg g⁻¹ and a coefficient of variation (CV) of 120 %. Similarly, the ether lipid content of *Methanospirillum hungatei* had a mean of 38 mg g⁻¹ and a CV of 17 % between different research groups (Hedrick *et al.*, 1991a; Pauly & Van Vleet, 1986a). Possible reasons for these differences in the ether lipid content within the same methanogenic species which have been encountered between different research groups could include:

1. different routes of calculation.
2. different solvent extraction techniques, which can have a significant effect on the yield of ether lipid (Hedrick *et al.*, 1991a; Nishihara & Koga, 1987; Koga *et al.*, 1993b).
3. or natural variation within the species due to differences in growth conditions between the different research groups. Incubation temperature has been found to effect the amount of ether lipid in thermophilic methanogens (Sprott *et al.*, 1991). Differences in ether lipid content over different growth pressures and for different growth phases for the mesophile *Methanosarcina acetivorans* were not significant at the 95 % confidence interval (see chapter 4). However, a reduction in the ether lipid content was observed from the log to the stationary growth phase of a thermophilic methanogen (Morii & Koga, 1993) though it was uncertain whether this difference was simply due to different extraction yields. Data on changes in ether lipid content due to changes in physical or chemical parameters for mesophilic species of methanogens has not been reported.

By using the mean ether lipid values for *Methanosarcina barkeri* (*i.e.* 12.5 mg g⁻¹), *Methanospirillum hungatei* (*i.e.* 38 mg g⁻¹) and *Methanosarcina acetivorans* (*i.e.* 13.9 mg g⁻¹), together with data from 8 other mesophilic species of methanogen (Hedrick *et al.*, 1991a; Pauly & Van Vleet, 1986a) then a mean value of 23.5 (SD = 14.9) mg ether lipid per gram dry weight of methanogenic cells can be approximated.

Having estimated an approximate ether lipid content per dry gram of methanogenic cells it was necessary to convert this value to a mean ether lipid content per cell. The mean number of bacterial cells to make up one gram in dry weight is a conversion factor that has been widely used when converting concentrations of cell constituent bioindicators to cell numbers (Balkwill

et al., 1988; Bratbak & Dundas, 1984; Nichols *et al.*, 1987). The following is a list of such conversion factors that have been used from the current literature: 6.4×10^{11} cells per dry gram, 2.5×10^{12} cells g^{-1} (Balkwill *et al.*, 1988), 2.08 (SD = 1.7) $\times 10^{12}$ cells g^{-1} (Bratbak & Dundas, 1984) and 5.9×10^{12} cells g^{-1} (Nichols *et al.*, 1987). From the growth experiment using *Methanosarcina acetivorans* (see chapter 4) approximately 2.7 (SD = 1.1) $\times 10^{12}$ cells g^{-1} was determined. By taking all of these conversion factors quoted then a mean value of 3×10^{12} cells g^{-1} (dry weight) can be approximated with limits of 1.2 and 4.8×10^{12} .

By using this conversion factor then an estimate of $(23.5 \times 10^{-3} \div 3 \times 10^{12}) 7.8 \times 10^{-15}g$ ether lipid per methanogenic cell can be approximated with limits of $(8.6 \times 10^{-3} \div 4.8 \times 10^{12}) 1.8 \times 10^{-15}$ to $(38.4 \times 10^{-3} \div 1.2 \times 10^{12}) 3.2 \times 10^{-14}g$ ether lipid per cell. Although the ether lipid concentration per dry weight of cells appeared to vary, an attempt was made to use these conversion factors, with the appropriate limits, to obtain order of magnitude values for the percentage of ether lipids accounted for by the estimated number of methanogens by MPN.

Table 5.4. shows MPN and total ether lipid results for Holyhead cores A and D and the intertidal core. Also by using the conversion factors given it was possible to obtain an estimation of the numbers of methanogens that would be expected, if all the ether lipid was attributed to viable methanogens, as well as an estimate of the percentage ether lipids accounted for by the numbers of viable methanogens determined by the MPN technique.

The proportion of ether lipids represented by viable methanogens appeared to be very small in both the Holyhead and intertidal cores (table 5.4). Mean percentages of ether lipid due to viable methanogens for the Holyhead cores ranged from 0.00007 % (with limits of 0.00002 to 0.0003 %) to 0.00207 % (limits of 0.00048 to 0.00848 %). Proportions of the total ether lipid content for the intertidal core were low but generally greater than the Holyhead cores and ranged from 0.0001% (with limits of 0.00002 to 0.0004 %) to 0.1 % (with limits of 0.02 to 0.4 %).

The MPN technique has inherent shortcomings due to the growth media exerting selective pressures on the bacterial populations and thereby causing only part of the population to grow. Jørgensen (1978) showed that for sulphate reducing bacteria underestimations of 3 orders of magnitude of the true population size was typical for the MPN technique. Other determinations have shown that MPN underestimations of the total natural bacterial population in sediments by direct counts range from 0.0001 % to 10 % (Van Es & Meyer-Reil, 1982) and 0.0000087 % to 0.03 % (Parkes *et al.*, 1990). However, methanogens are known to be comparatively difficult to culture due to their extreme sensitivity to oxygen which may cause greater underestimations of the methanogenic population in marine sediments by the MPN technique. Typical underestimations of the MPN technique on the methanogenic population of sediments have not been determined in the current literature.

Table 5.4. Percentage of ether lipid attributed to the viable methanogens in Holyhead cores A and D and the intertidal core with upper and lower limits estimated from conversion factors calculated from the current literature (Hedrick *et al.*, 1991a; Pauly & Van Vleet, 1986a) and chapter 4. Also given is the expected methanogen numbers if all of the ether lipids could be attributed to viable biomass.

Depth (cm) <i>a</i>	Number of Viable Methanogens per gram (MPN g ⁻¹)	Total Ether Lipid (µg g ⁻¹)	Expected MPN g ⁻¹ if <i>b</i> Ether Lipids were due to Viable Methanogens (with upper and lower limits)			Percentage of Ether <i>c</i> Lipid due to Viable Methanogens (MPN) (with upper and lower limits)		
			LOWER	MEAN	UPPER	LOWER	MEAN	UPPER
Holyhead Core A								
18	614	6.37	2.0 x10 ⁸	8.2 x10 ⁸	3.5 x10 ⁹	0.00002	0.00008	0.00031
38	1276	7.49	2.3 x10 ⁸	9.6 x10 ⁸	4.2 x10 ⁹	0.00003	0.00013	0.00055
78	9279	5.41	1.7 x10 ⁸	6.9 x10 ⁸	3.0 x10 ⁹	0.00031	0.00134	0.00549
118	614	2.77	8.7 x10 ⁷	3.6 x10 ⁸	1.5 x10 ⁹	0.00004	0.00017	0.00071
158	6149	2.32	7.3 x10 ⁷	3.0 x10 ⁸	1.3 x10 ⁹	0.00048	0.00207	0.00848
Holyhead Core D								
6	614	5.37	1.7 x10 ⁸	6.9 x10 ⁸	3.0 x10 ⁹	0.00002	0.00009	0.00037
46	1124	3.93	1.2 x10 ⁸	5.0 x10 ⁸	2.2 x10 ⁹	0.00005	0.00022	0.00092
106	230	2.44	7.6 x10 ⁷	3.1 x10 ⁸	1.4 x10 ⁹	0.00002	0.00007	0.00030
146	6149	4.51	1.4 x10 ⁸	5.8 x10 ⁸	2.5 x10 ⁹	0.00025	0.00106	0.00436
Intertidal Core								
17	15960	0.88	2.8 x10 ⁷	1.1 x10 ⁸	4.9 x10 ⁸	0.00326	0.01415	0.05804
27	114530	0.86	2.7 x10 ⁷	1.1 x10 ⁸	4.8 x10 ⁸	0.02397	0.10388	0.42616
37	610	0.86	2.7 x10 ⁷	1.1 x10 ⁸	4.8 x10 ⁸	0.00013	0.00055	0.00227
47	130	1.04	3.3 x10 ⁷	1.3 x10 ⁸	5.8 x10 ⁸	0.00002	0.00010	0.00040
57	610	1.04	3.3 x10 ⁷	1.3 x10 ⁸	5.8 x10 ⁸	0.00011	0.00046	0.00188
67	610	3.93	1.2 x10 ⁸	5.0 x10 ⁸	2.2 x10 ⁹	0.00003	0.00012	0.00050
77	3590	2.30	7.2 x10 ⁷	2.9 x10 ⁸	1.3 x10 ⁹	0.00028	0.00122	0.00499

a. MPN and ether lipid values taken from the nearest sediment depth.

b. Expected number of methanogens if all the ether lipids present in the sediment were due to viable methanogens. Using data from the current literature for ether lipid per dry cell weight (*i.e.* mean = 23.5 mg g⁻¹, SD = 14.9 mg g⁻¹), and assuming 3.0 x10¹² (SD = 1.8 x10¹²) cells per dry gram, then 7.9 x10⁻¹⁵ g ether lipid per methanogen cell can be approximated, with limits of 1.8x10⁻¹⁵ to 3.2 x10⁻¹⁴.

c. Percentage ether lipid due to viable methanogens were determined using an estimated conversion factor of 7.9 x10⁻¹⁵ g ether lipid per cell (with limits of 1.8 x10⁻¹⁵ to 3.2 x10⁻¹⁴). Therefore a typical mean calculation for the 18 cm depth of Holyhead core A was:

$$(614 \div (6.37 \times 10^{-6} \div 7.9 \times 10^{-15})) \times 100 = 0.00008.$$

However, if the viable methanogens present in the sediment were to account for a large proportion of the total ether lipid content (*i.e.* >50 %) then typical underestimations of the MPN technique of between 4 and 6 orders of magnitude for the Holyhead sediments and 2 and 6

orders of magnitude for the intertidal sediments would be expected. These typical MPN underestimations for the methanogenic population are certainly within the limits determined by van Es and Meyer-Reil (1982) and Parkes *et al.* (1990). If these underestimations were correct then expected counts of methanogens would range from approximately 3×10^8 to 5×10^9 per dry gram of sediment for the Holyhead cores and 1×10^8 to 3×10^9 per dry gram for the intertidal core (see table 5.4). Values of this order of magnitude have never been reported in marine sediments by the MPN technique before. Typical numbers of viable methanogens determined using the MPN technique in other marine (*i.e.* 10^2 to 10^3 g⁻¹, Warford & Kosiur, 1979) and estuarine (*i.e.* 10^3 to 10^6 g⁻¹, Jones & Paynter, 1978) sediments are generally comparable to the MPN values determined for the Holyhead and intertidal cores. However, these published MPN values will also be significantly lower than the true methanogenic population present.

Comparisons of methanogen numbers between the MPN technique and the fluorescent antibody technique in sediments have identified some interesting results (Strayer & Tiedje, 1978; Ward & Frea, 1979). The fluorescent antibody technique is a direct count that appears to be both species and strain specific (Strayer & Tiedje, 1978; Ward & Frea, 1979). It determines viable, dormant and dead intact methanogenic cells and as such is not directly comparable to the MPN technique. However, in a freshwater harbour sediment that supported active methanogenesis numbers of intact *Methanobrevibacter ruminantium* cells were determined at 7×10^{10} per dry gram by the fluorescent antibody technique yet this methanogen population could not be enriched using suitable media (Ward & Frea, 1979). It was possible that the *M. ruminantium* cells detected may have lost viability which has been observed in a study *Methanospirillum hungatei* after energy sources were removed for a period (Brevil & Patel, 1980), however, Ward and Frea (1979) suggest that viability may be lost by; not maintaining anaerobic conditions during sampling or due to the species not growing at all in mixed culture when compared to pure culture. Novitsky (1987) has shown that over 90 % of the sediment-water community was not actively growing. Also, numbers of one species of methanogen detected by the fluorescent antibody technique in lake sediments were found to be between one and two orders of magnitude greater than numbers determined using the MPN technique, which was supposed to be selective for most methanogenic species present (Strayer & Tiedje, 1978).

An attempt was made to count the methanogens washed from the sediment samples using ultra-violet stimulation of the methanogenic fluorescing coenzymes but proved unsuccessful due to the auto fluorescence fading quickly and generally being too faint to distinguish from the sediment particles. Photography of the field of view may have overcome the problem of fading fluorescence but on application it only proved successful on methanogenic cultures.

Therefore the information suggests that it is not possible to determine whether most of the ether lipid is present as non-viable necromass or biomass because the expected methanogenic numbers

estimated from the lipid data potentially falls within the large underestimation errors of the MPN technique which have been determined in other studies. The amount of bacterial growth in the most dilute positive MPN tube (*i.e.* containing methane) was not sufficient from the experiences with the methanogen growth culture experiments to perform an ether lipid determination. The long extraction, purification and derivatisation reactions involved in the ether lipid determination meant that numbers of methanogens of the order of 10^5 to 10^6 were required to provide a detectable ether lipid concentration. Attempts to further culture the most dilute positive MPN tube proved unsuccessful as detailed in section 2.1.3.

Hence either the most probable number technique caused a vast underestimation of the total viable methanogens present in the sediment, or the concentration of ether lipids in the sediment due to viable methanogenic biomass was negligible and most of the ether lipids could be attributed to methanogenic necromass, or more probably a combination of the two explanations.

The large variations of ether lipid per methanogenic dry weight suggests that these conversion factors should only be made on the basis of ether lipid information taken from the samples in question. Attempts to include all possible errors associated with the conversion factors from the literature do not provide positive results when applied to the data. In fact, after this extensive search, there is no way as yet to determine unequivocally what is the viable, or active biomass, or necromass of methanogenic bacteria in a marine sediment.

5.9.2. Comparison of Ether Lipid with Phospholipid Phosphate Concentration.

Attempts to count the total bacterial numbers washed from the sediment proved unsuccessful due to the acridine orange staining much of the detrital material which caused a lack of contrast in order to distinguish the cells. Therefore lipid phosphate was used as an indicator of the biomass within the sediments. Phospholipid phosphate has proved to be an accurate measure of the microbial biomass due to it remaining constant in diverse bacterial monocultures over a variety of different conditions which are comparable to stresses found in nature (Wilkinson *et al.*, 1972, White *et al.*, 1979b). Phospholipid phosphate has been favourably compared with ATP content as a means of estimating sediment biomass (White *et al.*, 1979a,b). It also has greater extraction efficiencies than total cell counts which can underestimate the true cell number due to sediment-cell interactions (Findlay *et al.*, 1989). Lipid phosphate has previously been used to estimate microbial biomass in marine sediments (Findlay *et al.*, 1989), estuarine sediments (Martz *et al.*, 1983; White *et al.*, 1979a,b) and sewage digesters (Henson *et al.*, 1985; Nichols *et al.*, 1987).

Typical half lives of phospholipid phosphate in anaerobically incubated sediment samples have been reported at 12 to 16 days (White *et al.*, 1979c) and 24 days (Parkes, 1987) which is

measurably longer than for aerobic sediments at 2 days (White *et al.*, 1979c) and 0.8 days (Parkes, 1987). Therefore the residence of phospholipid phosphate in marine sediments is likely to be more than 8 to 30 times greater for anaerobic relative to aerobic sediments. The significance of longer periods for degradation under anaerobic conditions may question the use of phospholipid phosphate as an indicator of biomass under these conditions. However, the frequency and period for cells to divide will also have a significant effect on whether the phospholipid phosphate reflects living biomass or mainly necromass.

Parkes *et al.* (1990) showed that 3 % of cells in the total bacterial community of a marine sediment were dividing and the percentage changed little with sediment depth. However, the bacteria may remain attached after division for long periods of time which can lead to large overestimates of the bacterial growth rate in sediments from such counts of frequency of dividing cells (Fallon *et al.*, 1983). If the rate of production of phospholipid phosphate from newly formed bacterial cells was greater than the rate of degradation of phospholipid phosphate then there could be expected to be a net increase in the phospholipid phosphate concentration with increasing sediment depth. Phospholipid phosphate was shown to decrease with increasing sediment depth (see table A8.1 of appendix VIII) suggesting that it was probably degraded quicker than it was formed though it is also possible that the concentrations input from the water column had been increasing significantly over recent years.

Phospholipid phosphate values were generally comparable between Holyhead cores and also within the anaerobic sediments of another study (White *et al.*, 1979b,c). Significantly higher phosphate values were found to occur in aerobic surface sediments of the study of White *et al.* (1979b) which probably reflected the greater biomass. The phosphate concentrations of the Holyhead cores generally decreased by half down the entire core length (*i.e.* 160-210 cm) which was also similar to the trends reported over the anaerobic sediment depths of an estuarine sediment (White *et al.*, 1979b). Comparison of the phospholipid phosphate content between the study areas showed that there was greater biomass in the Holyhead sediments than the intertidal site by a factor of 15 to 60 in the surface sediments (*i.e.* 18 cm) and a factor of 15 to 40 at 80 cm depth. However, for the ether lipids the contrast between the two sites was not as great with Holyhead having more by a factor of 4 to 10 for surface sediments and 1.5 to 3 at greater depth (*i.e.* 80 cm).

The mean concentration of phospholipid phosphate per dry gram of cells has been determined for a range of bacterial species at 50 $\mu\text{moles gram}^{-1}$ (White *et al.*, 1979a,b). The growth experiment using *M. acetivorans* (see chapter 4) gave a mean value of 48.9 μmoles (SD = 24) phosphate per dry gram of cells. Lipid phosphate concentrations of a thermophilic methanogen have been reported at 14.6 $\mu\text{moles per gram}$ (dry weight) (Martz *et al.*, 1983), but the proportion of lipid phosphate has been found to increase in thermophilic methanogens with

increasing incubation temperature (Sprott *et al.*, 1991). By using an approximate conversion factor to convert the weight of dry cells to cell numbers (*i.e.* 5.9×10^{12} cells per dry gram) as used by Nichols *et al.* (1987) then an estimate of the total number of cells in the sediments can be made on the basis of the phosphate data. Table 5.5. shows the phospholipid phosphate concentrations for the Holyhead and intertidal cores with estimations of the microbial cell number represented by the phospholipid phosphate.

By using the appropriate conversion factors given then the estimated total numbers of microbial cells showed a general decrease from 1×10^{10} cells per dry gram in the more surface sediments to 3×10^9 cells per gram at greater depth. Comparison of these estimated total microbial cell numbers as determined from the phospholipid phosphate data with the expected numbers of methanogens determined from the ether lipid data suggested that between 13 and 39 % (mean=21 %, SD = 8.7) of the estimated total microbial population would be expected to be methanogens throughout the Holyhead cores. The estimated numbers of viable methanogens from the ether lipid data for the intertidal core were approximately 13 to 420 % (mean=141 %, SD=151 %) of the total numbers of microbial cells as estimated from the lipid phosphate data.

There has been very few publications on the proportions of certain bacterial classes in anaerobic marine sediments. Parkes *et al.* (1990) determined numbers of heterotrophic, nitrate-reducing, sulphate reducing, methanogenic and hexadecane oxidising bacteria by selective MPN procedures in a marine sediment core of high organic loading. Proportions of methanogens rose below a band of elevated sulphate reduction to 24 % of the total MPN count though proportions over much of the remaining depths were generally negligible. It must be noted, however, that porewater sulphate concentrations were non-limiting to SRB over most of the sediment depths analysed in Parkes *et al.* (1990) which may question whether these results can be considered typical of near-shore sediments.

The use of conversion factors to approximate whether the methanogenic ether lipids represented viable or active biomass or necromass within the sediment profiles is prone to errors. Although these approximations are based on using averaged conversion factors to obtain order of magnitude values for the total microbial cell number of the sediment samples, it does suggest that much of the ether lipid content is unlikely to be due to viable methanogenic bacteria, especially for the 66 cm depth of the intertidal core. This could suggest that the sediments received an input of relic ether lipid material or, more likely, that the non-viable ether lipid represents methanogens that have lost their viability after *in-situ* growth within the sediments. Loss of viability after energy sources have been removed for a period has been demonstrated in methanogens (Brevil & Patel, 1980).

Table 5.5. Phospholipid phosphate data for the Holyhead Harbour and intertidal sediment cores used as a basis to estimate total microbial cell numbers. The methanogenic ether lipid data was converted to methanogen number, by assuming that all of the the lipid represented viable biomass (see table 5.4). The percentage numbers of methanogens (*i.e.* from ether lipid data) of the total cell number (*i.e.* from lipid phosphate data) is given from the conversion factors used.

Depth Mean (cm) <i>a</i>	Lipid Phosphate (nmoles g ⁻¹)	Estimated Cell Number due to Lipid Phosphate <i>b</i>	Percentage of methanogens of total cell number. Taken from the assumptions and conversion factors stated in footnote <i>c</i>		
			LOWER	MEAN	UPPER
Holyhead Core A					
5	79.6	4.8 x10 ⁹	-	-	-
10	85.2	5.1 x10 ⁹	-	-	-
25	81.4	4.9 x10 ⁹	4	17	72
45	71.5	4.3 x10 ⁹	5	22	97
65	57.8	3.5 x10 ⁹	-	-	-
85	29.5	1.8 x10 ⁹	10	39	170
105	28.0	1.7 x10 ⁹	-	-	-
125	36.6	2.2 x10 ⁹	4	16	70
145	26.0	1.6 x10 ⁹	-	-	-
165	24.6	1.5 x10 ⁹	5	20	87
Holyhead core D					
3	86.4	5.2 x10 ⁹	3	13	58
10	111.7	6.7 x10 ⁹	-	-	-
35	74.1	4.5 x10 ⁹	-	-	-
55	65.7	3.9 x10 ⁹	3	13	55
75	63.1	3.8 x10 ⁹	-	-	-
95	34.2	2.1 x10 ⁹	-	-	-
115	29.3	1.7 x10 ⁹	4	18	77
135	27.5	1.7 x10 ⁹	-	-	-
155	30.8	1.9 x10 ⁹	8	31	136
Intertidal Core					
6	14.5	8.7 x10 ⁸	3	13	56
18	3.8	2.3 x10 ⁸	12	49	211
30	5.8	3.5 x10 ⁸	8	32	137
42	2.9	1.7 x10 ⁸	19	77	334
56	1.7	1.0 x10 ⁸	32	131	570
66	2.0	1.2 x10 ⁸	103	424	1838
78	1.8	1.1 x10 ⁸	67	273	1183

a. Parameters given to the nearest sediment depths

b. Using 50 µmoles phosphate per dry gram of cells (White *et al.*, 1979a), and 3.0 x10¹² cells per dry gram *i.e.* 8.47 x10⁻¹⁸ moles phosphate per cell.

c. Percentage numbers of methanogens (assuming the ether lipids represent viable biomass and using conversion factors given in table 5.4) of the total cell number (as estimated from the lipid phosphate data).

5.10. Estimated Total Methane Produced From Concentrations of Ether Lipid Present

Conversion factors for the amount of methane produced per unit ether lipid synthesised have been previously estimated as a possible means of setting limits on total methane production in paleoenvironmental reconstructions (Pauly & Van Vleet, 1986a). Indirect calculations via ratios of methane per dry cell weight, total lipid per dry cell weight, and total lipid per ether lipid of a range of methanogens were solved simultaneously to estimate the methane produced per given concentration of ether lipid synthesised. Using the combined data of Pauly & Van Vleet (1986a), which included three sources of variation, it was possible to estimate that between 3,268 and 12,867 moles of methane are produced per mole of diether. The mean value of 8039 moles CH₄ per mole DPGE was equivalent to 12.3 moles CH₄ per gram ether lipid.

Data from the growth experiments involving *Methanobolus tindarius*, *Methanococcoides methylutens* and *Methanosarcina acetivorans* in chapter 4 revealed that the amount of methane produced per unit diether lipid synthesised was within one order of magnitude for the three methanogenic monocultures tested. The methane/ether lipid ratios did not appear to change between the lag, exponential and stationary growth phases of the growth culture experiments. Mean values for each growth experiment were measured to range from 12826 to 72638 moles of methane per mole of diether membrane lipid, with a mean of 44749 (see chapter 4). The mean ratios for the total 43 data points of the three growth experiments were also similar (*i.e.* 45218) with a standard deviation comparable to the mean limits given (*i.e.* 29939). These values equated to 68.6 moles CH₄ per gram of ether lipid. Assuming that this ratio can be applied to tetraether lipids then 68.6 moles CH₄ per gram ether lipid is equivalent to 89361 moles CH₄/mole tetraether with limits of 25650 and 145276 moles/mole.

If it can be assumed that these ratios can be applied to environmental samples and that the ether lipids present are from methanogenic origins, then the ether lipid to methane ratios can be used to estimate the total amount of methane that would have been expected to be produced from the total ether lipid concentration measured in the sediment samples. However, such an estimation of the total methane produced will include both; the amount of *in-situ* methane produced within the sediments, as well as the total interpreted amount of methane produced by relic methanogenic material (*i.e.* biomass and necromass) produced before deposition to the sediment.

Table 5.6 includes both the found methane concentrations and the estimated proportion that this represents of the total calculated methane from the ether lipid/methane ratios. The ether lipid/methane ratios were taken from both the growth experiments (chapter 4) and also from the ratios indirectly calculated from Pauly and Van Vleet (1986a). The upper and lower limits are calculated using the extreme ratios given at the beginning of this section.

Table 5.6. Estimated total methane produced from the concentrations of ether lipid present using conversion factors estimated from chapter 4 and Pauly and Van Vleet (1986a).

Depth Mean (cm)	Total ether lipid nmol g ⁻¹		Found <i>b</i> Methane Conc. μmol g ⁻¹	Estimated methane <i>c</i> Calculated from ether lipids Found/Estimated (%)			Estimated methane <i>d</i> Calculated from ether lipids Found/Estimated (%)		
	C20	C40 <i>a</i>		Mean	Upper	Lower	Mean	Upper	Lower
Holyhead Core A									
5	0.83	3.49	<i>e</i>	0.003	0.010	0.002	0.016	0.040	0.010
10	0.89	3.34	<i>e</i>	0.003	0.010	0.002	0.016	0.040	0.010
25	0.89	4.44	0.1	0.001	0.005	0.001	0.008	0.019	0.005
45	1.12	5.18	0.1	0.002	0.007	0.001	0.011	0.027	0.007
65	0.86	2.38	3.4	0.136	0.473	0.084	0.753	1.853	0.471
85	0.86	3.72	10.9	0.294	1.026	0.182	1.634	4.020	1.021
105	0.74	1.57	14.9	0.859	2.997	0.531	4.777	11.750	2.984
125	0.92	1.66	11.7	0.616	2.150	0.381	3.426	8.427	2.140
145	1.35	1.51	16.3	0.834	2.910	0.516	4.639	11.411	2.898
165	1.64	0.96	12.7	0.798	2.785	0.494	4.440	10.921	2.774
Holyhead Core B									
6	1.72	2.38	0.1	0.003	0.012	0.002	0.019	0.047	0.012
20	1.64	2.15	0.0	0.002	0.005	0.001	0.008	0.021	0.005
40	n.m.	n.m.	6.1						
60	1.60	1.00	12.3	0.763	2.663	0.472	4.245	10.442	2.652
80	2.47	3.02	6.6	0.173	0.605	0.107	0.964	2.373	0.603
100	1.58	1.85	15.0	0.636	2.219	0.393	3.537	8.700	2.210
120	1.75	2.22	21.6	0.782	2.728	0.483	4.347	10.693	2.716
140	3.53	4.73	13.0	0.224	0.781	0.138	1.245	3.062	0.778
160	2.79	4.16	<i>e</i>	0.262	0.914	0.162	1.456	3.582	0.910
Holyhead Core C									
3	0.81	2.61	0.0	0.001	0.004	0.001	0.006	0.015	0.004
20	0.75	1.96	0.1	0.006	0.022	0.004	0.035	0.085	0.022
45	0.72	3.87	0.1	0.003	0.009	0.002	0.015	0.036	0.009
65	1.04	2.96	0.7	0.022	0.078	0.014	0.125	0.308	0.078
83	1.30	5.28	13.8	0.260	0.908	0.161	1.446	3.557	0.903
103	0.95	2.05	14.8	0.656	2.290	0.406	3.648	8.975	2.279
125	0.52	1.53	12.9	0.804	2.806	0.497	4.471	10.999	2.793
150	0.43	1.34	16.7	1.200	4.187	0.742	6.672	16.413	4.169
170	0.46	1.86	15.4	0.826	2.882	0.511	4.592	11.296	2.869
190	0.51	2.01	18.8	0.930	3.244	0.575	5.169	12.715	3.229
209	0.74	2.62	<i>e</i>	0.703	2.454	0.435	3.910	9.617	2.443
Holyhead Core D									
3	1.12	3.56	<i>e</i>	0.003	0.009	0.002	0.015	0.037	0.009
10	1.50	5.86	0.1	0.002	0.006	0.001	0.009	0.023	0.006
35	1.26	4.48	0.1	0.002	0.008	0.001	0.012	0.030	0.008
55	0.89	2.55	3.2	0.119	0.417	0.074	0.664	1.633	0.415
75	0.78	2.52	7.2	0.276	0.964	0.171	1.537	3.780	0.960
95	0.77	1.40	8.8	0.553	1.930	0.342	3.076	7.568	1.922
115	0.64	1.55	11.3	0.676	2.357	0.418	3.756	9.240	2.347
135	0.52	1.74	19.7	1.101	3.842	0.681	6.122	15.059	3.825
155	0.81	3.05	<i>e</i>	0.637	2.223	0.394	3.543	8.715	2.213

Table 5.6. *cont...*

Depth Mean (cm)	Total ether lipid nmol g ⁻¹		Methane ^b Conc. (measured) μmol g ⁻¹	Estimated methane ^c Calculated from ether lipids Found/Estimated (%)			Estimated methane ^d Calculated from ether lipids Found/Estimated (%)		
	C20	C40 ^a		Mean	Upper	Lower	Mean	Upper	Lower
Intertidal Core									
18	0.51	0.42	0.004	0.001	0.002	0.000	0.004	0.009	0.002
30	0.55	0.38	0.002	0.000	0.001	0.000	0.002	0.005	0.001
42	0.40	0.60	0.003	0.000	0.001	0.000	0.002	0.006	0.001
56	0.52	0.54	0.004	0.001	0.002	0.000	0.003	0.008	0.002
66	1.78	2.12	0.004	0.000	0.001	0.000	0.001	0.002	0.001
78	0.92	1.30	0.069	0.004	0.015	0.003	0.024	0.060	0.015

(a) C40 lipid concentration is the pooled acyclic and cyclic tetraether lipids of each sample.

(b) Measured methane concentration determined by gas chromatography.

(c) Estimated methane concentration using ether lipid:methane ratios taken from the growth experiments of chapter 4, *i.e.* 44749 moles methane per mole of diether (diether limits of 12825 to 72638) and 89361 moles methane per mole of tetraether (tetraether limits of 25650 to 145276). These ratios for the diether and tetraether lipids are also equivalent to a ratio of 68.6 moles of methane per gram of total ether lipids. Upper and lower estimated methane limits were taken from the limits of the ether lipid:methane ratios.

(d) Estimated methane concentration using data from Pauly and Van Vleet, (1986a), *i.e.* 8039 moles methane per mole of diether (with limits of 3268 to 12867) and 16014 moles of methane per mole of tetraether (with limits of 6510 to 25633). These ratios were also equivalent to 12.3 moles of methane per gram of total ether lipids with limits of 5.0 to 19.7 moles CH₄ per gram of total ether lipid.

(e) Methane value taken from nearest depth. (n.d.) = not determined.

Using the molar ratio of methane produced per diether lipid of 44749:1 (with limits; 12826 to 72368) from the growth experiments of chapter 4, and 89361:1 for the tetraether lipids (with limits; 25613 to 144514) it was evident that the proportion of methane measured within the sediments is a small fraction of the total methane that would have been expected on the basis of the amount of ether lipids present. The found methane concentrations at a given depth can therefore be readily accounted for by a biogenic source as inferred from the ether lipid concentration, at the same depth.

Less than 0.02 % of the estimated total methane expected was present in the upper, relatively gas-free sediments of the Holyhead cores. Similar results were also found throughout the entire intertidal core (*i.e.* <0.02 %). Also by using the ratios calculated by Pauly and Van Vleet (1986a) the measured methane results were still much lower than 0.1 % of the expected values in these samples (see table 5.6, column *d*).

Within the acoustically turbid sediments of Holyhead Harbour (*i.e.* >50 cm), the amount of measured methane corresponded to between 0.1 and 4 % of the expected CH₄ value using the ratios given in this report (see table 5.6, column *c*), and between 2 and 16 % using the ratios calculated from Pauly and Van Vleet (1986a)(see table 5.6). This suggested that either most of the ether lipids were present from relic methanogens of a source prior to deposition or, more likely, that most of the methane produced had either oxidised or migrated out of the sediment.

5.11. Observation of Trends in the Isopranyl Ether Lipids

The diether and tetraether lipids were analysed in this study to give an indication of the methanogenic biomass/necromass in acoustically turbid marine sediments. To date there has only been one other major survey of the concentrations of diether and tetraether lipid species in marine sediments, which was primarily concerned with observing the diagenetic removal of the lipids at greater sediment depths (Pauly & Van Vleet, 1986b). A range of ether lipids including diether and cyclic and acyclic tetraether lipids have not previously been determined in near shore marine sediments. Therefore from this work it was also possible to highlight some of the more interesting results that were observed from the types of ether lipid species detected and also from the observed concentrations and distributions.

5.11.1. Trends in the Concentrations of the Ether Lipids with Depth

The concentrations of the diether and acyclic and cyclic tetraethers in the sediment profiles of the Holyhead cores and intertidal core are given in table A8.1 of appendix VIII and are shown in figures A8.1 and A8.2 of appendix VIII, respectively. The ether lipid concentrations were observed to rise slightly towards the bottom of Holyhead cores B, C and D but the change in ether lipid concentration with increasing depth was not consistent between the Holyhead sediment cores. Correlation analysis of lipid concentration versus depth revealed that the individual ether lipid species generally reflected the changes observed in the total ether lipid concentration. Total ether lipid concentrations were observed to decrease with increasing sediment depth in Holyhead cores A, C and D ($r = -0.75$, -0.36 and -0.70 , respectively) and increase with increasing sediment depth in Holyhead core B only ($r = +0.63$).

The two cores that were located the closest to each other in Holyhead Harbour were cores B and C (*i.e.* 11 m apart, see figure 5.4). Cores B and C demonstrated both contrasting depths of maximum ether lipid concentration and contrasting changes in concentration with increasing sediment depth. This indicated that there was considerable variation in the ether lipids existed over short distances in the Harbour sediments (see figure A8.1, appendix VIII).

The rate of methanogenesis has been observed to increase below the SRZ, as detailed in section 1.5 of Chapter 1, which may also be expected to cause an increase in the methanogenic turnover

or biomass at such a depth. In a limited number of abyssal sediment samples the ether lipid content was observed to increase significantly by a factor of ten from surface sediments (*i.e.* 5 m, <1 Ma) to deeper sediments which coincided with the base of the SRZ (*i.e.* 95 m, 2 Ma) (Pauly & Van Vleet, 1986b). Ether lipid removal through diagenesis was only apparent at significantly greater depths (Pauly & Van Vleet, 1986b). The sedimentation rate in the abyssal sediments is expected to be significantly less than the near-shore Holyhead sediments, therefore the sediment depths sampled in the Holyhead cores represent a very small fraction of the time that similar depths of the abyssal sediments represent. This might suggest that the underlying trend is for the ether lipid content to rise in concentration with increasing sediment depth, as was observed in the samples of Pauly and Van Vleet (1986b). However, this trend may, due to local variations in the inputs of ether lipids or organic matter to the sediment, not be apparent from the shallow sediment depths sampled in Holyhead Harbour. The types of ether lipid input to the sediments are discussed in section 5.12.

5.11.2. Changes in the Proportions of Ether Lipids with Increasing Sediment Depth

Some methanogens are capable of utilising alternative substrates not competed for by the sulphate reducing bacteria, such as methyl amines and methanol, and are thought to be responsible for the low rates of methanogenesis detected within the shallower sediment depths of the SRZ, as detailed in section 1.5 (Ward & Winfrey, 1985). From table 1.2 it is apparent that the methanogens capable of metabolising methyl amines and methanol belong to the *Methanosarcinaceae* family of the order *Methanomicrobiales*. There are approximately 20 mesophilic methanogens of the *Methanosarcinaceae* family isolated to date and most of these have been found to contain predominantly diether lipids in their membranes. The mesophilic methanogens from the *Methanococcaceae* family (order *Methanococcales*) also contain predominantly diether lipids in their membranes, but do not have the ability to metabolise alternative substrates that are not competed for by the SRB. Other methanogens such as *Methanosphaera stadtmaniae* and *Methanocorpusculum* from recently defined families can also metabolise methanol but require hydrogen to do so (see table 1.2 and 1.1).

Therefore it could be hypothesised that a greater proportion of methanogens from the *Methanosarcinaceae* family relative to the total population might be expected in the SRZ of the Holyhead cores relative to greater sediment depths. This could, under certain conditions, cause an increase in the proportion of diether lipids in the SRZ. Due to the very late completion of the ether lipid methodology for the determination of the tetraether lipids this hypothesis could not be tested on laboratory prepared samples. *is why mention it?*

The SRZ appeared to range from surface sediments to approximately 30/70 cm for the Holyhead cores, and beyond the maximum depth of the intertidal core (see section 5.4). From table 5.7 it

is evident that the proportion of diether lipids is higher in the sulphate reducing depths relative to the deeper sediments in Holyhead core B only. In cores A, C and D the greater proportion of diether lipids generally occurred in the sediments below the SRZ. However, it can be noted from table 5.7 that the standard deviation associated with the diether proportions overlap in all cases and therefore none of the changes with depth are significant. This hypothesis should be checked in laboratory samples before attempting to speculate further information from the data included in these sediment cores.

Table 5.7. Mean proportions of diether lipid relative to the total ether lipid concentration (%) within sediments of the sulphate reduction zone (SRZ) and at greater sediment depth below the SRZ.

Sediment Core	Maximum depth of Sulphate Reduction Zone ^a	Mean Diether Lipid Proportion C20 / Total Lipid (%) ^b	
		Within SRZ	Below SRZ
Holyhead Core A	45 cm	10.3 (1.1)	23.9 (12.9)
Holyhead Core B	80 cm	31.8 (8.3)	27.6 (2.0)
Holyhead Core C	83 cm	12.8 (3.1)	13.6 (2.9)
Holyhead Core D	55 cm	13.0 (1.5)	15.4 (4.0)
Intertidal Core	>78 cm	32.1 (6.6)	-

a. The maximum depth was determined as the depth where the sulphate concentration fell below 1 mM for cores A, C and D. For Core B the sulphate concentration never fell below 2.7 mM (see table 5.1) therefore this depth was used as the maximum interpreted depth of the SRZ.

b. Mean percentage of diether of the total ether lipid concentration are given with standard deviations given in parentheses.

5.11.3. Significant Proportions of Cyclic Tetraether Lipids

Tetraether lipids containing 1, 2, 3 and 4 cyclopentyl rings (cyclic tetraethers) in the C40 side chain derivatives (see figure 1.1) appear to be most abundant in the thermoacidophiles of the archaeobacteria (Tornabene & Langworthy, 1978; Smith 1988; De Rosa *et al.*, 1986a). Concentrations and distributions of tetraether lipids containing cyclopentyl ring structures have been partially studied in thermoacidophile species such as *Sulpholobus solfataricus* and *Caldariella acidophila* (De Rosa *et al.*, 1980a; b; 1983; 1986a). It is expected that the *in-situ* temperatures of the Holyhead and intertidal cores would not be high enough for growth or enrichment of thermoacidophilic archaeobacteria. Tornabene and Langworthy (1978) analysed ether lipids from nine species of methanogenic archaeobacteria and found no evidence of ether lipids containing cyclopentyl rings in any of the isolates studied.

Correlation of the cyclic ether lipids with the acyclic diether and tetraether lipids which are expected to be of methanogenic origin was high (*i.e.* $r = 0.92$, $n = 44$, $p \ll 0.001$), suggesting that the acyclic ether lipids were also probably of methanogenic origin. Cyclic tetraether lipids have been found in high proportions in one thermophilic methanogen (*i.e.* $>30\%$ in *Methanothermobacter feravidus*, Pauly & Van Vleet, 1986b) though another methanogenic thermophile, *Methanobacterium thermoautotrophicum*, was found not to contain any cyclic tetraethers (Tornabene & Langworthy, 1978). Proportions of cyclic tetraether lipids of up to 3% in some cultured methanogens have also been suggested (Pauly & Van Vleet, 1986b). Studies by De Rosa *et al.* (1986b) have shown that trace amounts of cyclopentyl ring tetraether lipids can be formed by the methanogen *Methanosarcina barkeri* (strain DSM 800). However, Nishihara and Koga (1991) discount this in studies made on the same strain of methanogen. Morii and Koga (1993) have shown that the proportions of acyclic diether to tetraether lipid can change over the growth phase of a thermophilic methanogen from 80% tetraether during log growth to 93% during the stationary phase. This information may collectively suggest that not only the proportions of certain ether lipids may change but also the presence of certain ether lipids (*i.e.* cyclopentyl ring tetraether lipids) may be formed as a consequence of changing growth conditions. Research is required on the possible changes in lipid composition in response to changes in the growth conditions of mesophilic methanogenic bacteria. This could not be attempted in this present study due to the very late development of the analytical method to quantitatively analyse the tetraether lipids.

From this information on laboratory grown methanogens it might therefore be anticipated that the cyclic tetraether lipids should be found in low concentrations in mesophilic marine sediments and also form a small proportion of the total ether lipids present. The concentrations of cyclic ether lipids in the sediments of Holyhead Harbour and the intertidal site were found to be significant and made up a large proportion of the total ether lipid concentration (*i.e.* 30 to 40%).

An undefined cyclic ether lipid was also found in significant concentrations in these sediments. The undefined cyclic tetraether lipid determined in this study (*i.e.* C40,[?] see section 3.3.3.1) is probably the same as the undefined cyclic tetraether lipid which has also been found in other marine sediments of other studies. The unknown of this study (*i.e.* C40,[?]) had a comparable retention time to the unknown determined in other studies (*i.e.* C40,^{2'}) (Pauly & Van Vleet, 1986b; Chappe *et al.*, 1982). Comparison of the known C40,² with the uncharacterised C40,[?] lipid showed that they were present in similar concentrations (*i.e.* 1.09 : 1, respectively) and varied in a similar manner throughout the total data set (*i.e.* $r = 0.98$, $n = 44$, $p \ll 0.001$, see section 3.3.3.1).

The high concentration of cyclic ether lipids within both near-shore and off-shore sediments was unexpected on the basis of the data gathered from laboratory cultured methanogens. The

concentrations and proportions of these cyclic ether lipids therefore warranted further study by comparing the data between these sites. Concentrations of the total cyclic tetraether lipids in this study (*i.e.* 0.6 - 3.6 $\mu\text{g g}^{-1}$) were significantly lower than the much older abyssal sediments of the study of Pauly and Van Vleet (1986b) (*i.e.* 20 - 176 $\mu\text{g g}^{-1}$ over first 100 m depth, 1 to 5 Ma). Concentrations of cyclic ether lipids in the intertidal core (0.46 $\mu\text{g g}^{-1}$, SD = 0.29) were also significantly lower than each of the Holyhead cores, *i.e.* Core A= 1.82 $\mu\text{g g}^{-1}$, SD= 0.90, Core B= 1.95 $\mu\text{g g}^{-1}$, SD= 0.86, Core C= 1.68 $\mu\text{g g}^{-1}$ SD = 0.73, Core D= 1.93 $\mu\text{g g}^{-1}$, SD = 0.88. The significance of these concentrations between the sites can be appreciated when compared to the total ether lipid concentration. Figure 5.23 illustrates the proportions of the cyclic ether lipids in the intertidal and Holyhead cores and also in one abyssal core of the study of Pauly and Van Vleet (1986b). From figure 5.23 it is apparent that the proportion of the cyclic lipids of the total ether lipids are significant in all sediment sites. Also, these proportions were similar between the Holyhead cores (42.3 % SD = 5.0 %) and the abyssal (43.8 % SD = 4.9 %) sediments of Pauly and Van Vleet (1986b). However, the proportions of cyclic ether lipids were lower in the intertidal core (*i.e.* 28.7 % SD = 4.5 %) than each of the Holyhead and abyssal cores.

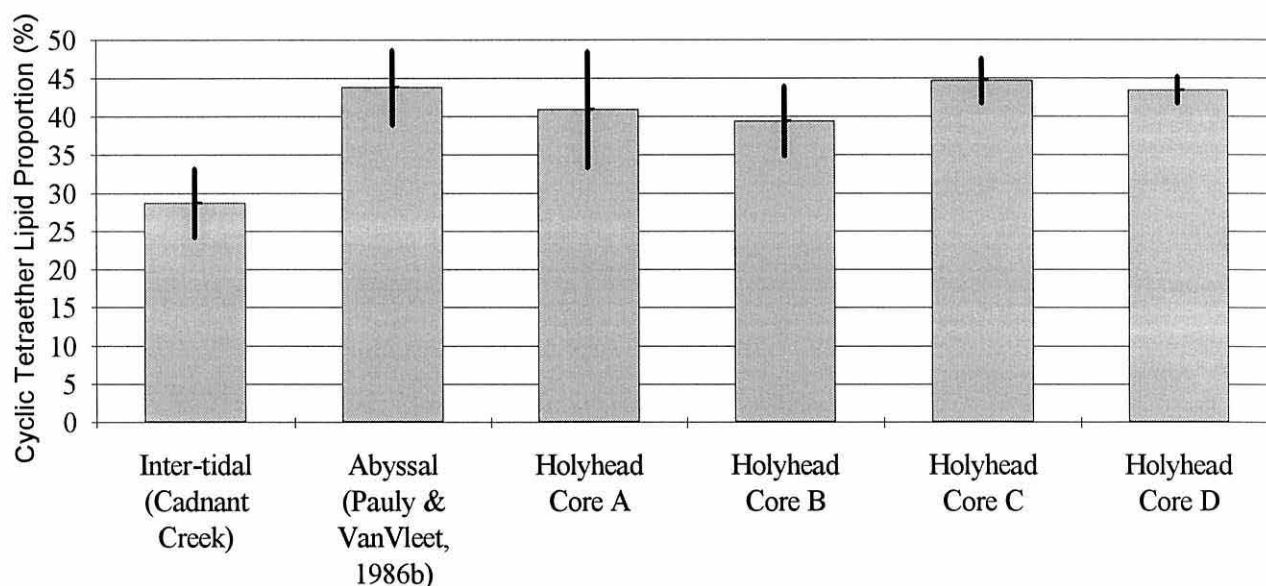


Figure 5.23. Proportions of cyclic tetraether lipids of the total ether lipid concentration (with standard deviation error bars) for selected sediment samples.

The type and amount of organic matter that is expected to be deposited to the Holyhead Harbour, intertidal and abyssal sediments is expected to differ significantly (Rheinheimer, 1991). Therefore it is interesting that the mean proportions of certain cyclic ether lipids of the total ether lipid concentration were not dissimilar between these sites. The proportion of C_{40,2} and C_{40,?} of the total ether lipid were respectively; 19 and 20 % for Holyhead Harbour, 14 and 13 % for the intertidal, and 17 and 17 % for the abyssal sediments. Because the cyclic ether lipid

C40,2 is rare and C40,? not characterised in laboratory cultured methanogens the significance of these results has yet to be determined.

Due to the greater age of the sediments in the studies of abyssal sediments when compared to the Holyhead or intertidal sediments it could be suggested that the cyclopentyl ring structures are formed via diagenetic processes (Pauly & Van Vleet, 1986b). It has been discounted that these cyclic ether lipids may result from the acyclic ether lipids as an artifact of the preparation procedure (Pauly & Van Vleet, 1986b). There was not a consistent change in the proportion of the cyclic lipids of the total ether lipid with increasing depth in any of the cores analysed (*i.e.* regression analysis of cyclic ether lipid proportion *versus* depth showed that the 95 % confidence intervals for the slope incorporated zero). This information suggests that the cyclisation is therefore, unlikely to be a response to diagenetic changes because the proportions for the deepest sediments were comparable to the shallowest sediments of Holyhead Harbour and was also comparable to the geologically dated abyssal sediments of Pauly and Van Vleet (1986b).

The significance of these cyclic ether lipid results is uncertain as it has yet to be determined whether the large proportions of these cyclic ether lipids in marine sediments represent unknown mesophilic methanogens which have high proportions of cyclic ether lipids in their membranes, or whether the proportions of cyclic ether lipids may increase in a particular species in response to environmental conditions. The possibility that there could be a significant number of marine methanogenic bacteria that have yet to be characterised and which contain predominantly cyclic ether lipids would seem unlikely. Therefore, this information could suggest that the production of cyclic ether lipids in the membranes of methanogenic bacteria may occur in known species as a result of conditions found in the sediment. Furthermore, if the presence of cyclic ether lipids is brought on by certain conditions in the sediment that are not recreated in the laboratory cultures then these conditions are expected to occur soon after deposition in Holyhead Harbour due to the significant sedimentation rate.

why as are
isolate a very
small % of
total population

5.11.4. Correlation of Ether Lipid Species

Polar lipid fatty acids have been extensively used in eubacterial taxonomy and in ecological studies as measures of eubacterial biomass, community structure, and metabolic status, as reviewed by Parkes (1987) and White (1983). The polar ether lipids of the archaeobacteria show much less structural diversity than eubacterial polar lipid fatty acids, being dominated by the diether (C20) and tetraether (C40) lipids. Although there is some variation in the isoprenoid chain length (Mancuso *et al.*, 1985) and cyclisation (De Rosa *et al.*, 1986b), there is generally insufficient diversity to relate ether lipids to specific groups of methanogens in ecological samples. However, the determination of the intact phospho- and glyco- ether lipid chains of methanogenic species by supercritical fluid chromatography has been used to increase the information content of the archaeobacterial lipid profile (Hedrick *et al.*, 1991a). Koga and

colleagues (1993a, b) found the presence of certain phospho and glyco- ether lipid component parts, regardless of their arrangement in the lipid molecules, was characteristic of methanogen taxonomic groups at a family or genus level.

5.12. The Ether Lipid Concentration Anomaly;

A Possible Explanation

Methane concentrations in Holyhead Harbour were found to increase significantly below the SRZ, which on a previous study of this site was also found to coincide with net methane production from incubation experiments (Jones *et al.*, 1986). It might therefore be expected for an indicator lipid of methanogenic biomass to show an increase at the point where methane concentrations were shown to rise, and, due to the recalcitrant nature of these lipids, to perhaps show an increase with increasing sediment depth. The ether lipid profiles did not show a consistent and significant increase below the sulphate - methane transition. Possible reasons why the ether lipid profile showed only a small change in concentration with depth over the total length of the cores relative to the methane profile which demonstrated a two order of magnitude change across the sulphate - methane transition are considered:

1. A comparable amount of methane may have been produced in the SRZ as was detected below the SRZ but was subsequently removed by methane oxidation. As discussed in section 5.4 the rate of methanogenesis below the SRZ in marine sediments is expected to be significantly greater than within the SRZ. Anaerobic methane consumption was inferred to exist in the SRZ of the Holyhead sediments from simple modelling of the methane profiles (see section 5.6.2). Therefore if large rates of methanogenesis were present in the SRZ the evidence from the methane detected could be negligible. However, the rate of methanogenesis in sediments where anaerobic methane consumption was also observed was found to be greater below the SRZ than above (Kosiur & Warford, 1979). This, together with the slow degradation rate of the ether lipids in anaerobic sediments (Harvey *et al.*, 1986) would suggest that the ether lipid concentration should increase with increasing sediment depth, especially across the sulphate - methane transition. However, the effect of increasing inputs of raw sewage over recent years may have contributed to increases of *in-situ* methanogenesis in surface sediments of the SRZ relative to deeper sediments which may have received a lower input of organic matter at the time of deposition. Kosiur and Warford (1979) showed that methanogenesis was more than a factor of 30 greater for sediments receiving raw untreated sewage compared to the effects of aerobically treating the sewage, though how this change compared below the SRZ was not reported. The organic matter content of the sediments of Holyhead Harbour would have provided an answer to this question. Censor data for Holyhead showed a 14 % increase in the populace from 1981 to 1991 to 11,782 (M. Venables, *pers. comm.*, 1996). Increasing amounts of *in-situ* methanogenesis as a result of the increasing input of raw sewage over more recent years cannot therefore be disregarded.

2. The ether lipids present may be mainly from other non-methanogenic bacteria. However, information on the required growth conditions of halophiles and thermoacidophiles (König & Stetter, 1989) would suggest that the conditions present in Holyhead Harbour are more optimum for methanogenic bacteria than the other ether lipid containing classes of archaeobacteria.

3. Methanogens may be producing methane without increasing cell biomass under these sediment conditions. There would appear to be little information available on the cell division rates of methanogenic bacteria within marine sediments, but increases in activity (*i.e.* methane production) may be expected to also cause an increase in cell division and hence increase the ether lipid concentration. Increases in methanogenic activity can be reflected in the methanogenic biomass of bioreactors as measured by the ether lipid content (Hedrick *et al.*, 1991b).

4. Sediment erosion from the large passenger ferries which frequent the harbour and rapid re-deposition from nearby dredging operations may confuse any relationships between ether lipid profiles and other parameters studied. The re-suspension of sediment from ferries might be expected to cause the smoothing of any sharp changes in the ether lipid content over the shallower sediment depths. This is, however, unlikely to effect the sediment once it has reached depths approaching the bottom of the SRZ (*i.e.* 30-70 cm). The bathymetric survey of Holyhead Harbour (see table A10.2 of appendix X) showed that the seabed in this area was composed of flat plateaux (*i.e.* differences in depth of 0.1 m between sampling points) and showed little evidence of deep erosion in localised areas that would correspond to recent ferry passages. Therefore ferry traffic is not expected to be the main factor controlling the observed ether lipid profiles.

5. It is possible that there could be a significant ether lipid input from the water column as river run-off of methanogenic biomass and/or necromass. The water column input is expected to include river run-off, sewage input, sediment rapidly deposited from dredging and a small input from the productivity in the 8-10 m of overlying water. Therefore any changes in the biomass from actively dividing methanogens within the sediment may be small relative to the concentration of the ether lipids deposited to the sediment. Ether lipids are expected to show slower degradation rates under certain anaerobic conditions (Harvey *et al.*, 1986) therefore the reason why the ether lipid profiles did not show an increase in concentration with increasing sediment depth may be due to an increased water column input over more recent years.

The most appropriate hypotheses would appear to postulate an increased amount of water column input over more recent years causing an increase in either the *in-situ* methanogenesis or the ether lipid content of the material deposited. Therefore the types of material input to the water column before deposition to the sediment also requires consideration to assess the possible sources of the ether lipids to the sediment:

1. Re-suspension of sediment into the water column from nearby areas through dredging will cause a relatively rapid deposition to the study area of Holyhead Harbour. However the ultimate source of the sediment and ether lipids contained within will still be unknown.

2. Viable methanogens have been shown to be present in the guts of zooplankton (Oremland, 1979; Bianchi *et al.*, 1992) and particulate matter associated with faecal waste (Bianchi *et al.*, 1992). Other methanogens of the *Methanosarcinaceae* family have also been isolated from open ocean water column samples (Cynar & Yayanos, 1991) and Angelis and Lee (1994) have shown that the concentrations of trimethylamine in the gut contents of zooplankton are sufficient to account for all of the methanogenesis in zooplankton samples. Ether lipids associated with faecal particulate matter of a hyper saline marine basin were shown to be of diether origin though the presence of tetraether lipids was not ascertained at this site (Dickins and Van Vleet, 1992). The 8 to 10 m depth of overlying water in Holyhead Harbour is, however, considered to be insufficient to provide a significant input of viable methanogens from the guts of zooplankton and associated faecal matter.

3. Methanogenic biomass/necromass may be associated with river run-off into Holyhead Harbour. Antibody probes have shown that new immunotype methanogenic strains of the family *Methanosarcinaceae* were present and viable within the oxygenated water column samples taken from Chesapeake Bay (Sieburth *et al.*, 1993). Viable methanogens were mainly associated with the particulate matter of the riverine input to the water column of Chesapeake Bay and numbers of up to 35 per litre via the MPN technique were reported (Sieburth *et al.*, 1993). Particulate matter originates from sewage and river run-off in Chesapeake Bay and can result in significant methanogenesis in these sediments forming areas of acoustic turbidity (Hill *et al.*, 1992). Methanogens of the *Methanosarcinaceae* family may be more oxygen tolerant than other families (Pauly & Van Vleet, 1986b) and they are the only methanogens to metabolise methanol and methylamines and also contain predominantly diether membrane lipids (see table 1.2). From this information on the types of methanogens enriched from the water column it could suggest that diether membrane lipids would predominate in the water column and surface sediments. The diether lipid proportion of the total ether lipid content did not show an increase in the more surface sediments of Holyhead Harbour, though this, as a test, has yet to be proven in laboratory studies.

Anaerobic digesters are known to promote bacterial activity including methanogenesis (Hedrick *et al.*, 1991b,c). Significant concentrations of ether lipid at $8.9 \pm 4.5 \mu\text{g g}^{-1}$ DPGE have been reported in sewage sludge taken from a digester. The sewage of Holyhead Harbour is, however, not treated in this way but arrives as raw comminuted (mixed) sewage with an ether lipid content not expected to be significantly different from when it passed through the human gut. The significant raw sewage input to the water column of Holyhead Harbour is detailed in Jones (1977) and the sites of the outputs and approximate volumes discharged for the area are shown in figure 5.1. Research into methanogens present in the human gut has shown that not all people have methanogens in their gut but for those who do *Methanobrevibacter smithii* is by far the

most abundant and is typically enriched in the large bowel (Nottingham & Hungate, 1968; Miller & Wollin, 1982). *Methanobrevibacter smithii* has been shown to contain 55 % tetraether lipids (see table 1.2). The methanogen numbers range from extremely low (a few cells per gram) to as high as 10^{10} per dry gram faecal weight and in some individuals can be equal to 10 % of the total concentration of viable anaerobic bacteria (König & Stetter, 1989). It was shown in a large survey that only one third of US citizens had methanogens in their faeces and the concentration was generally low (10^4 to 10^7 per dry gram) (D.C. White, *Pers. comm.*, 1994). Using the ether lipid content per methanogenic cell conversion factor determined in section 5.9.1 this cell number equated to $<0.1 \text{ ng g}^{-1}$ to $<0.1 \text{ } \mu\text{g g}^{-1}$ for the values given by White (*pers. comm.*, 1994). These ether lipid concentrations were too low to affect the ether lipid profiles of Holyhead Harbour even when allowing for the errors associated with the conversion factors. Therefore, considering only a proportion of the population contain methanogens this information suggests that the input of human faeces is unlikely to directly provide the major source of the ether lipids to the sediments of Holyhead Harbour or the intertidal site.

Methanogens are known to be very concentrated in the rumen of cattle (König & Stetter, 1989) which may be a potential source of the ether lipids to the sediments. Holyhead was once an important port for the transport of cattle from Ireland to Wales and England at the rate of up to 600,000 head per year at its peak in the early 1960's (Jackson, 1969). Cattle were typically walked off the ships along tracks to cattle pens (lairages) which were located on the edges of the inner harbour. The faecal matter was frequently washed from the pens and tracks into the harbour (J. Cave, *pers. comm.* 1996) where it would have been distributed by water currents.

Methanogens isolated from the rumen of cattle have been shown to contain large proportions tetraether lipids when in pure culture with proportions ranging up to 89 % tetraether lipids. Studies using fluorescent antibody techniques have shown that numbers of *Methanobrevibacter ruminantium* in the sediment of an aquatic harbour were in excess of 1×10^{10} per dry gram but could not be enriched by MPN techniques (Ward & Frea, 1979). Since such species have not been isolated from sediments (König & Stetter, 1989) it may suggest that they have been washed from the fields where cattle or sheep graze to the rivers and finally to the lake in this particular study (Ward & Frea, 1979). The concentration of methanogens in the rumen chamber of cattle and sheep are typically 10^{10} per ml and the turnover of bacteria including methanogens is understood to be significant (D Lloyd, *pers. comm.* 1996). Methanogen concentrations of this size could provide a significant ether lipid input to the sediment. It has not been reported whether the ether lipids are degraded under the conditions present within the rumen and hind gut of ruminants therefore it is not known whether the ether lipid concentration is likely to rise with the increasing turnover of methanogenic bacteria in the gut. A study of the ether lipid content within the faecal matter would provide some interesting information in this area.

However, the cattle trade through Holyhead Harbour finally finished in 1975 after its demise since the late 1960's (J. Cave, *pers. comm.* 1996) and would therefore not be expected to provide much of the input to the depths of sediment sampled in this study assuming that the

sedimentation rate calculated at 13 cm y^{-1} has continued over more recent years. Also the ether lipid concentration of the intertidal core (*i.e.* 0.88 to $3.93 \mu\text{g g}^{-1}$) which would not have received a large input from the cattle trade described here was lower but of a similar order of magnitude to the Holyhead sediments (*i.e.* 2.03 to $8.62 \mu\text{g g}^{-1}$). Therefore, if the ether lipids are from ruminant animals it would suggest that the input is mainly from run-off from fields into the streams and is occurring to the present day. It should also be noted that the abyssal sediments would be expected to receive a negligible input from river run-off but had significantly higher concentrations of total ether lipid at $41 \mu\text{g g}^{-1}$ though the age of these sediments was considerably older (*i.e.* $\approx 1 \text{ Ma}$).

There are two streams which pass through farmland on Holy Island and finally enter Holyhead Harbour through the Turkeyshore and Porthfelin sewage outfalls (T. Gant, *pers. comm.*, 1996, see figure 5.1). Current numbers of ruminant animals on Holy Island have risen by approximately a factor of 3 over the last 10 years to 2000 cattle and 3000 sheep (G. Morris, *pers. comm.*, 1996). This information therefore suggests that an increased ether lipid input to the sediments from ruminant faecal matter could be occurring through run-off from agricultural land.

Therefore possible reasons why the ether lipid concentrations do not show an increase with increasing sediment depth especially across the sulphate - methane transition where methane concentrations increase by two orders of magnitude include:

- a. The increased organic matter being deposited to the Holyhead sediments via increased sewage over recent years is causing *in-situ* methanogenesis to increase thus increasing the *in-situ* methanogenic biomass.
- b. The ether lipids present may be directly from the increasing inputs of faecal waste of ruminant animals in the area which arrives via run-off into streams and finally into the harbour via the sewage outfalls.

It is not possible to compare the ether lipid data to other recently deposited near-shore marine sediments because the concentrations of both diether and cyclic and acyclic tetraether lipids are not available in the current literature. The sediments of the Menai Strait, like Holyhead Harbour, also receive inputs of both river run-off as well as raw sewage and therefore it is not possible to ascertain from these two environments whether the ether lipids are predominantly from *in-situ* methanogenesis or from the faecal waste of ruminants from river run-off. The viable methanogens enriched through the MPN technique showed contrasting profiles to the ether lipid data for cores A and D and the intertidal core which may therefore suggest that the ether lipids were present from non-viable methanogenic sources. Whether the methanogens would have lost their viability after growth within the sediment or whether this indicates a relic ether lipid input can not be ascertained from the information gathered. Methanogens have been found to lose their viability after energy sources were removed for a period of time (Brevil & Patel, 1980).

The cyclic ether lipid isomer (C40,1') of the C40,1 lipid (see figure 1.1) has been shown to be a discrete indicator of freshwater environments (Pauly & Van Vleet, 1986a,b; Chappe *et al.*, 1982) in a similar way that the C40,2' isomer of C40,2 (*i.e.* C40,? in this study) is a discrete indicator of marine depositional environments (Pauly & Van Vleet, 1986b; Chappe *et al.*, 1982). The presence of C40,1' in the sediments of rivers would therefore be expected which when eroded could be transported to the sea. This C40,1' lipid was not detected in the marine environment of this study where there is expected to be some riverine input. It could therefore be argued that this ether lipid could become degraded on route to the sea but this would also suggest that the total ether lipid input from the freshwater environments would also be expected to be negligible. The lack of C40,1' in the Holyhead and intertidal sediments may therefore provide evidence of a negligible riverine input to these study sites, though further study is required to substantiate this. However, the run-off from fields of ruminant faecal matter may be a significantly greater ether lipid input than that of terrestrial methanogen inputs to rivers, and the presence of either C40,1' or C40,? in the guts of ruminant animals has yet to be proven.

Mesophilic methanogens have not been shown to produce significant proportions of cyclic ether lipids (*i.e.* < 3 %) in laboratory studies. However, cyclic ether lipids were present in significant proportions over all depths in the Holyhead and intertidal sediments. The proportions of cyclic ether lipids in Holyhead Harbour were comparable to the deep sea sediments of Pauly and Van Vleet (1986b). The study area of Pauly and Van Vleet (1986b) was the Benguela upwelling system in the south-eastern Atlantic Ocean which is expected to receive methanogens and organic matter from sinking faecal waste from the productivity in the water column. The input from riverine or sewage outfalls is expected to be comparatively negligible. Therefore the contrasting depositional environments of the study of Pauly and Van Vleet (1986b) and Holyhead Harbour suggests the input of these cyclic ether lipids is not likely to be from methanogenic sources formed prior to deposition. This might suggest that the cyclic ether lipids have been formed as a result of physiological changes in mesophilic methanogens that are actively growing within the sediments. Changes in the ether lipid composition of mesophilic marine methanogens therefore requires further study. The fact that the cyclic ether lipids accounted for approximately 30 to 40 % of the total ether lipids present in these studies suggested that most of the ether lipids are probably from a similar origin. Measurements of the rate of methanogenesis via radioactive labelled substrates over the total core lengths may confirm this hypothesis of increased methanogenesis in the more surface sediments. Similarly the determination of organic matter content could have provided evidence of an increased input of organic matter over more recent years.

5.13. Conclusions

The sediments of Holyhead Harbour showed similar patterns of sulphate and methane within the cores. These patterns were typified by a decreasing sulphate concentration with increasing depth, indicating the SRZ, to a point where the methane concentration was shown to increase by two orders of magnitude. However, the concentration of sulphate over the depth of the SRZ appeared to vary significantly between cores which may suggest a variable depositional environment to the sediments within Holyhead Harbour.

The methane concentration was calculated to exceed the solubility limit of the pore water in the sediments below the SRZ in Holyhead Harbour. The presence of gas voids, caused by undissolved gas, was also confirmed using sound velocity and X-ray analysis, and was shown to extend beyond the base of all cores studied. The results found by the three techniques were in good agreement. Changes in sound velocity could be used to indicate the presence of undissolved gas, while the sediment was still located within the core barrel. This technique could therefore be used to quickly determine the depth where the undissolved gas began, and whether it extended beyond the base of the sediment cores. The X-ray analysis showed the gas voids to have an elongated shape and were oriented in the vertical plane. Elongated, rather than spherical gas voids, suggested a possible mechanism for gas migration. The elongated gas fissures were present below the SRZ but did not extend up into the SRZ, suggesting that the rate of removal of methane within the SRZ was greater than the rate of gas migration via the fissures.

Modelling the methane distributions within the Holyhead cores suggested that the profiles could not be described by diffusion and depositional advection alone, even when the high sedimentation rates that were calculated for the area, were taken into account. The model which came closest to predicting the found methane profile, above the calculated point of methane saturation, incorporated a methane removal term which could be interpreted as anaerobic methane oxidation. The error associated with the 20 cm depth sampling resolution suggested that the rate constant for methane consumption was approximately $2.5 \times 10^{-7} \text{ s}^{-1}$. Surprisingly there was not a consistent increase in sulphide at the base of the SRZ which would have been predicted as a result of methane oxidation with sulphate as electron acceptor. The concentration of soluble sulphide was also unexpectedly low in Holyhead Harbour. The reason for this is not known, but may be due to increased scavenging by iron present in discarded coal ash from steam ships, which was deposited before the anaerobic sediments built up.

The relationship between ether lipid and methane concentration that was tentatively suggested in the freshwater and estuarine sediments of the study of Martz *et al.* (1983) was not shown to exist in Holyhead Harbour. A relationship appeared to exist between methane and the limited MPN counts in the Holyhead cores but not in the intertidal core. The ether lipid concentration and the MPN counts, however, changed in an unrelated manner in all cores studied. This was in sharp contrast to the findings in chapter 4 with pure cultures.

The yield of the internal standard from the ether lipid determination of the entire four day procedure of extraction, purification, derivatisation and analysis was low at 27 %. However, this procedure showed good reproducibility for replicate sediment samples. Very little additional ether lipid was recovered by, more rigorous, extraction of the pre-extracted sediment residue.

The MPN determination may provide information on the distribution of the active methanogenic population within the sediment but cannot be used to directly relate whether much of the ether lipid represents active, viable biomass or necromass because of the large and variable underestimates of the true population that are evident for the MPN technique.

A conversion factor to relate ether lipid synthesised to the total methane produced was taken from the literature and also calculated from experiments in chapter 4. The concentration of methane that was calculated to be in the sediments as a result of the ether lipids was shown to be significantly greater than the methane found in the sediments. This suggested that all of the methane found in the sediments could be readily accounted for by methanogenic lipids from within the same depths of sediment analysed. The reasons why the methane calculated from the ether lipid concentration was significantly greater than the methane found in the sediment are twofold. Firstly, most of the ether lipids may originate from a source prior to deposition, and/or secondly, that most of the methane calculated to be in the sediments has been removed by oxidation or migration. It is strongly recommended that more research into the variation of these conversion factors be made in an environment that reflects, more naturally, the conditions in marine sediments.

Cyclic tetraether lipids are not commonly reported in laboratory grown mesophilic methanogens, therefore, the presence of large concentrations, and high proportions of cyclic tetraether lipids was not expected in these marine sediments. Cyclic ether lipids have been detected in geologically dated abyssal sediments (Pauly and Van Vleet, 1986b) which suggested they may be formed as a result of diagenetic changes after long periods of deposition. The proportions of cyclic ether lipids in the near-shore sediments of this study showed little change relative to the total ether lipid concentration with increasing sediment depth suggesting that cyclisation is not likely to be a response to diagenetic changes. The cyclic ether lipids correlated very highly with the acyclic tetraether lipids, which are more common in methanogenic bacteria, and this may suggest that the cyclic ether lipids were also expected to be of methanogenic origin in these near-shore sediments.

The cyclic ether lipids made up 30 to 40 % of the total ether lipid concentration. It is unlikely that the cyclic ether lipids represent a new methanogenic group of organisms that have yet to be characterised in marine sediments. The presence of small concentrations of cyclic ether lipids in the same strain of methanogen grown at different laboratories has been disputed in the literature. Therefore it is hypothesised that the cyclic tetraether lipids are formed by known methanogenic

species as a result of changing conditions in the sediment and from this study it could be suggested that these conditions are expected to occur soon after deposition.

Contrary to the findings of Pauly and Van Vleet (1986b) an increase in the total ether lipid concentration was not consistently observed below the SRZ in the sediments of Holyhead Harbour. Possible explanations may include changes in the types/amount of input of either relic methanogenic material or the organic matter over recent periods.

Holyhead Harbour and the intertidal area receives inputs from both riverine and sewage sources. The raw sewage and the faecal waste from the large cattle trade through Holyhead in the 1960's were not expected to make a significant contribution of relic ether lipid to the total ether lipid content of the sediments of this study. Recently deposited faecal matter from ruminant animals in the fields of the surrounding areas could provide a source of ether lipids via river run-off, though further study is required on the types of ether lipids in faecal waste.

The types of water column input of relic methanogenic material to the sediments of Holyhead and the abyssal site of Pauly and Van Vleet (1986b) are expected to be significantly different. However, the proportions of ether lipids between these sites were found to be similar with significant concentrations of cyclic ether lipids which are not common in laboratory grown methanogens. Because the potential sources of relic ether lipid material to the sediment was so contrasting between these sites this information may suggest that much of the ether lipids in the sediments were from methanogenic biomass created *in-situ* in the sediments. This would suggest that the organic loading to the sediments has been increasing over recent years thus causing the high concentrations of ether lipid in the SRZ. Further research is required to study the production of ether lipids in methanogens grown under conditions that are typical for marine sediments, with more detailed analysis of the sources of ether lipids to the sediments.

*and measure organic carbon content of
the sediment*

CHAPTER 6. ARTIFICIALLY PREPARED CONSOLIDATED SEDIMENTS USING METHANOGENIC BACTERIA TO CREATE ACOUSTIC TURBIDITY.

6.1. Introduction

Undissolved gas can be identified in marine sediments by changes in the geoacoustic properties of the sediment, and can be detected remotely using high resolution seismic profiling (Hovland & Judd, 1988). This technique can usually only detect the horizontal extent, and not the vertical extent (*i.e.* depth), of the gas charged sediment (Yuan *et al.*, 1992). If there is a significant vertical depth of undissolved gas which is trapped beneath comparatively impermeable sediment layers then there is a risk of unexpected blowouts within 10 m of the seabed during drilling operations (Stat-Oil Newsletter, 1989; Judd, 1991). It has been suggested that it would be useful to develop an acoustic probe for *in-situ* sound velocity measurements, with the interpretation that low velocity compression waves would indicate the presence of undissolved gas (Sills & Wheeler, 1992).

Compression waves pass through the pore water of the sediment and are controlled by the porosity of the sediment. Shear waves, however, pass through the sediment frame. In fine grained muddy sediments the velocity of shear waves (*i.e.* 20 to 100 ms⁻¹) is typically much slower than the velocity of compression waves (*i.e.* 1300 to 1600 ms⁻¹) (Yuan *et al.*, 1992). Compression waves can be used to indicate undissolved gas in sediments whereas shear waves can not (Yuan *et al.*, 1992).

Undissolved gas can also have a significant effect on the undrained strength and the compressibility of the sediment. These effects can cause undermining of offshore foundation structures (Hovland & Judd, 1988). A general overview of the various effects of undissolved gas on the geotechnical behaviour of fine-grained sediments is given in Sills *et al.* (1991). Therefore the effects of undissolved gas on the geoacoustic and geotechnical properties of the sediment should be considered when designing foundations for offshore structures (Sills & Wheeler, 1992).

Sediment samples recovered from the seabed undergo decompression due to changes in pressure. In acoustically turbid sediments this decompression would be expected to cause the

undissolved gas to expand and some of the dissolved gas to come out of solution. The period during which this expansion would take place is expected to be a function of the sediment. The outer edges of the acoustically turbid sediments recovered from Holyhead Harbour were observed to bubble due to escaping gas. Changes to the sediment caused by decompression will therefore effect the sediment structure. For this reason, mechanical tests on the engineering properties of recovered sediments is of limited value due to the structural changes imposed on the sediment when recovered from the *in-situ* environment. Improvements in sampling techniques have reduced the impact that the sampling has on the properties of the sediment by keeping the sediment sample pressurized during the coring operation (Denk *et al.*, 1981). By using these techniques it is possible to carry out basic testing of the sediment after transferring the sample from the corer to the testing apparatus in a hyperbaric chamber but this is expensive due to the requirement of complex equipment and a research vessel.

An alternative approach has been proposed by Sills & Wheeler (1992), whereby the undissolved gas is artificially created in the sediment from methane which has been impregnated into gas adsorbent particles known as zeolite. The zeolite can be mixed into a sediment slurry before the consolidation apparatus is set up. Sills and Wheeler (1992) have demonstrated using electron micrographs that void structures in artificially prepared gassy cores are similar to those observed in retrieved, gassy sediments of the western Irish Sea (Yuan *et al.*, 1992).

However, the process of artificially creating undissolved gas in the sediment using zeolite is relatively rapid when compared to the natural process of methane build up from methanogenesis. The maximum time for the zeolite to discharge the methane into the sediment has been estimated at a few hours (Wheeler, 1990). Therefore there is a risk that the zeolite may discharge most of the methane before significant consolidation has occurred. In marine sediments significant consolidation can occur before the formation of undissolved methane, due to the pressure of the overlying sediment and water, and also due to the time taken for the whole process to occur. The use of alternative gassing methods that would allow sufficient consolidation to take place before the gas voids were formed might ameliorate this problem. One example of an alternative method involves flushing the sediment with methane saturated water at elevated pressures before the pressure is reduced at a given time (Sills & Wheeler, 1992). However, this technique can only be practiced on sandy sediments and not on fine grained sediments of low permeability (Sills & Wheeler, 1992).

For these reasons there was a need to determine whether the gassing of the sediment could be simulated more naturally using laboratory prepared methanogenic cultures.

The aims of this chapter were to determine whether acoustic turbidity could be artificially created in prepared sediment cores using methanogenic bacteria. The experiment was designed to compare the effect of undissolved biogenic gas on the consolidation of the sediment (*i.e.* biological and physical processes) relative to killed control cores (*i.e.* physical processes only) in the consolidation set-up. Changes in the incubation temperature was also used to determine the effect of the rate of formation of acoustic turbidity on the sediment cores (*i.e.* 8 and 30 °C). The presence of undissolved gas can be determined in the sediment in a number of ways during the course of the experiment and also by sectioning the cores at the end of the experiment.

Observations through the clear acrylic liner of the consolidation apparatus could identify gas voids on the outer edge of the sediment surface. The velocity of compression waves can be indicative of undissolved gas (section 5.5.1) and the change in the length of the cores can suggest an amount of undissolved gas relative to control cores. Further analyses of the sediment required subsamples of the sediment cores to be taken at the end of the experimental period. X-ray photographs provided a means of assessing the abundance and shape of the gas voids within the sediment and could be directly compared to the X-ray photographs of the Holyhead cores. The solubility limit for methane in the sediment pore waters for the conditions was calculated to determine whether the found methane would be expected to form undissolved gas voids.

The change in concentration of ether lipids can also be used to indicate the change in the biomass/necromass of the methanogenic material between the cores. The conversion factors of the ether lipid formed per methane produced for the methanogen *M. tindarius* are given in the growth experiment of section 4.4. The ether lipid concentration in the consolidation cores was therefore converted to a concentration of methane that would be expected to be present on the basis of the conversion factors given. Comparison of the expected methane with the measured methane concentration and the calculated solubility limits was made to determine whether the ether lipids could be used as an indirect means of estimating the methane that is expected to have been produced in artificially consolidated sediment cores.

6.2. Results and Discussion

The materials and methods used to prepare the sediment cores are given in section 2.9 and the consolidation apparatus is illustrated in figure 2.1 of chapter 2. A total of four cores were prepared each having an applied load of approximately 2770 g, which was equivalent to a pressure of 1.125 (*i.e.* 1+1/8th) atmospheres (atm). Two cores were incubated at 30 °C (*i.e.* cores 1 and 2) and two at 8 °C (*i.e.* cores 3 and 4). One core from each incubation temperature contained methanogenic bacteria (*i.e.* *M. tindarius*) and growth media to stimulate methanogenesis (*i.e.* active cores 1 and 3). To the other core of each incubation temperature a mixture of antibiotics was added to inhibit eubacterial growth (see section 2.9) and 2-bromoethanesulphonic acid was added to inhibit methanogenesis (Oremland, 1988) (*i.e.* killed control cores 2 and 4). The changes in the parameters monitored from the killed control cores could be considered to be due to the physical processes of consolidation with a negligible contribution from active biological processes. Whereas the changes to the active sediment cores (*i.e.* 1 and 3) could be expected to be due to the effects of both physical and biological processes.

6.2.1. Sediment Parameters Determined During the Consolidation Experiment

The length of the sediment cores, visual appearance of the sediment surface against the acrylic liner and the sound velocity were all monitored at intervals during the period of the experiment as the consolidation increased. Table 6.1 shows the core lengths determined during the 235 hour period. The change in sediment length relative to the value recorded at time zero is presented as percentages from time zero (*i.e.* 100 %) in figure 6.1. The error associated with the length measurement was estimated at 0.05 cm and the appropriate error bars are given in figure 6.1.

Table 6.1. Length measurements determined over time for the four sediment cores that were located in the consolidation apparatus.

Time (hours)	Sediment Core Length (cm)			
	Core1 30°C Active	Core 2 30°C Control	Core 3 8°C Active	Core 4 8°C Control
0	13.40	12.95	13.80	13.70
10	13.20	12.00	13.30	12.85
38	13.15	10.80	12.50	12.25
62	12.30	10.25	11.90	11.90
94	12.05	10.15	11.30	11.40
135	12.00	10.10	11.15	11.15
157	11.50	10.00	10.90	11.00
235	11.15	9.90	10.95	10.85

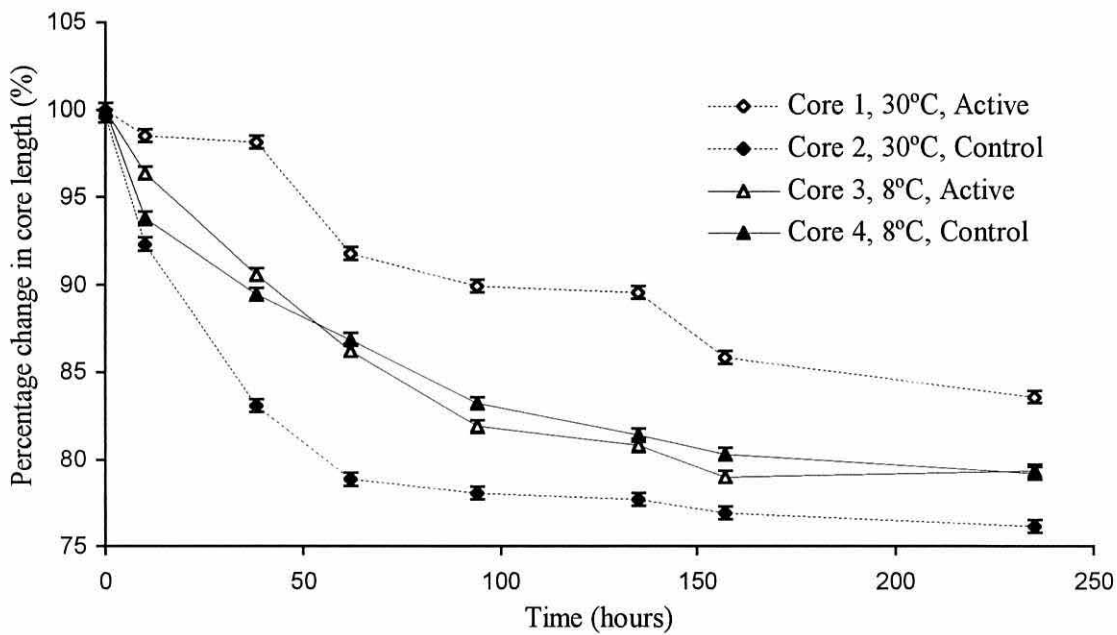


Figure 6.1. Percentage change in core length from time zero for the four sediments located in the consolidation apparatus. The error bars represent the 0.05 cm error for the length determination.

The greatest reduction in core length over the 235 hour period was observed in killed control core 2 incubated at 30 °C (*i.e.* 100 - 76 = 24 % reduction). The active sediment core incubated at 30 °C (core 1) showed the least change in core length over the experimental period (*i.e.* 15 %). Cores 3 and 4 were incubated at the lower temperature of 8 °C and showed a similar reduction in the core length of 21 % and could generally not be distinguished from each other over the experimental period.

The sound velocity was also measured during the period of the consolidation experiment at three locations in the sediment; the top section, the mid section and the bottom section. Specimen outputs from the sonic viewer, which was used to measure the passage time of the sound wave across the core, are given in figure A4.1 of appendix IV. Five sound velocity determinations were taken from each sediment section at each sampling period. The mean sound velocity with the upper and lower 95 % confidence limits are given in table 6.2. Due to the sound wave velocity being inversely proportional to the temperature (Keen, 1968) the consolidation apparatus was removed from the incubators and kept at room temperature for one hour before the sound velocities and core lengths were determined. As the acrylic plunger moved down inside the consolidation liners (see figure 2.1) over time the sampling position at the top sediment section became obscured for sound velocity determinations in cores 2, 3 and 4 (see n.d. in table 6.2).

Table 6.2. Sound velocities determined across the four consolidated cores at top, mid and bottom sections. Five replicate determinations were taken for each measurement. The mean sound velocities and the 95 % confidence intervals are presented.

TIME (hours)	Sound Velocity (m s ⁻¹) with 95% confidence limits								
	Top Section			Mid Section			Bottom Section		
	-95%	MEAN	+95%	-95%	MEAN	+95%	-95%	MEAN	+95%
Core 1, 30°C, Active									
0	1471	1491	1512	1472	1483	1493	1466	1487	1509
10	1433	1466	1499	1415	1433	1451	1381	1401	1422
38	1422	1441	1460	1432	1445	1457	1398	1417	1435
62	1398	1417	1435	1440	1453	1466	1373	1405	1438
94	1408	1445	1483	1416	1436	1456	1386	1401	1416
135	1402	1417	1432	1417	1437	1457	1401	1413	1425
157	1401	1401	1401	1423	1433	1443	1379	1393	1408
235	1391	1409	1427	1393	1405	1417	1386	1397	1409
Core 2, 30°C, Killed Control									
0	1451	1470	1489	1448	1461	1475	1456	1478	1501
10	1426	1455	1486	1449	1466	1482	1422	1441	1460
38	1457	1470	1483	1447	1457	1468	1447	1457	1468
62	1417	1433	1448	1403	1429	1455	1396	1425	1454
94	n.d.	n.d.	n.d.	1404	1433	1462	1393	1417	1441
135	n.d.	n.d.	n.d.	1406	1425	1444	1395	1417	1439
157	n.d.	n.d.	n.d.	1449	1449	1449	1393	1405	1417
235	n.d.	n.d.	n.d.	1424	1437	1449	1407	1417	1427
Core 3, 8°C, Active									
0	1460	1474	1488	1464	1478	1493	1464	1478	1493
10	1418	1441	1464	1392	1421	1451	1417	1437	1457
38	n.d.	n.d.	n.d.	1425	1445	1466	1398	1417	1435
62	n.d.	n.d.	n.d.	1409	1425	1440	1383	1417	1453
94	n.d.	n.d.	n.d.	1424	1437	1449	1424	1437	1449
135	n.d.	n.d.	n.d.	1441	1457	1474	1398	1417	1435
157	n.d.	n.d.	n.d.	1449	1449	1449	1440	1451	1461
235	n.d.	n.d.	n.d.	1393	1405	1417	1407	1417	1427
Core 4, 8°C, Killed Control									
0	1441	1470	1500	1462	1474	1486	1446	1457	1469
10	1396	1429	1463	1401	1452	1507	1402	1433	1465
38	1436	1466	1497	1446	1466	1486	1441	1461	1483
62	1420	1449	1479	1424	1437	1449	1394	1425	1456
94	n.d.	n.d.	n.d.	1425	1445	1466	1411	1437	1463
135	n.d.	n.d.	n.d.	1431	1457	1484	1417	1437	1457
157	n.d.	n.d.	n.d.	1440	1453	1466	1425	1441	1457
235	n.d.	n.d.	n.d.	1424	1437	1449	1401	1425	1449

n.d. = not determined due to the piston part of the apparatus obstructing the sound wave.

The mean sound velocity of the sediment was shown to generally decrease over time for all core sections analysed with the greatest reduction noticed in the active cores (*i.e.* cores 1 and 3). Regression analysis of sound velocity *versus* time showed that this decrease was significant at the 95 % confidence level for the mid and top sections of core 1 and for the bottom section of core 2, *i.e.* the 95 % error for the slope did not incorporate zero. The greatest rate of decrease in mean sound velocity occurred within the initial 10 hours for core incubated at 30 °C and 62 hours for cores at 8 °C (*i.e.* from $>1490 \text{ ms}^{-1}$ to $<1417 \text{ ms}^{-1}$). The velocities recorded before significant consolidation had occurred to the sediment were comparable to the values typically found for water, *i.e.* approximately 1500 ms^{-1} (Keen, 1968). After 62 hours the decrease in sound velocity with increasing time was much less.

The mean sound velocity was generally lower in the methanogenically active cores when compared to the killed controls, for the corresponding incubation temperature (see table 6.2). However, the resolution of the time intervals measured on the sonic viewer (section 2.9) was $0.2 \mu\text{s}$. For a 5 cm diameter core this equated to a resolution of approximately 8.3 ms^{-1} intervals on the velocity determinations. This large error associated with the sound velocity determinations caused the 95 % confidence intervals to be large. Therefore the sound velocity results could not be distinguished between the active and killed control cores at the 95 % confidence level in this experiment. A smaller resolution (*i.e.* higher frequency) on the sonic viewer might therefore be expected to provide results that were significant at the 95 % confidence level.

The diameter of the cores in the consolidation apparatus (*i.e.* 5 cm) was smaller than the core barrel used to measure the sound velocity in the sediments from Holyhead Harbour (*i.e.* 10 cm). The error associated with the sound velocity of the Holyhead cores was therefore less for two reasons. Firstly, due to the difference in the distances that the sound wave travelled between the two set-ups, the $0.2 \mu\text{s}$ sampling resolution equated to a lower error of sound velocity in the Holyhead core barrel (*i.e.* 5.4 ms^{-1}) relative to the error determined for the consolidation apparatus (*i.e.* 8.3 ms^{-1}). Secondly, due to the sound wave also passing through the material used to house the sediments the range of sound velocities available will also be a function of the core barrel size and the material used. The sound velocities measured across an empty (*i.e.* air only) core barrel were found to be comparable to the velocities determined for gas charged sediments. Therefore lower sound velocities are expected for the gas charged sediments than those quoted in table 6.2. The range of sound velocities determined across the Holyhead sediments in the larger core barrel was significantly greater (*i.e.* $1667 - 1492 = 175 \text{ ms}^{-1}$) than the range of sound velocities determined across the smaller consolidation apparatus (*i.e.* $1498 - 1389 = 69 \text{ ms}^{-1}$). Therefore the reason why the 95 % confidence limits for the consolidation apparatus showed large errors relative to the Holyhead determinations is expected to be a function of the core barrel used to house the cores.

The velocity of the compression wave through fine-grained, gas-free sediments is expected to increase as the pressure and also the consolidation increases (Yuan *et al.*, 1992). However, the sound velocity in fine grained sediments which contain undissolved gas has been shown to decrease as the pressure and also consolidation increases (Yuan *et al.*, 1992). The gas charged sediments of the active cores 1 and 3 showed this expected relationship of decreased sound velocity with increasing time, *i.e.* consolidation (see table 6.2). However, the killed control cores 2 and 4, which contained insufficient methane to form undissolved gas voids (as discussed later in this section), also showed a general decrease in sound velocity with increasing time, *i.e.* consolidation. The reason for this result would appear to be due to the presence of some gas voids introduced during the procedure of preparing the cores. Some gas voids were evident in the X-ray photographs of the killed control cores given in figure 6.2, but were of a different shape to those in the gas charged, active cores (section 6.6.2). These gas voids are expected to form an increasing proportion of the pore water by volume as the consolidation (*i.e.* time) increases. The acoustic properties of sediments have been shown to be affected by as little as 1 % undissolved gas (Hovland & Judd, 1992).

6.2.2. Sediment Parameters Determined at the End of the Consolidation Experiment

Following determination of the core length and sound velocity during the experimental period the sediment was removed from the consolidation apparatus. Sediment samples were taken from the top and bottom of the cores approximately 2 to 4 cm from the ends. The sediments were analysed for water content (section 2.6), methane (section 2.4) and DPGE ether lipid (section 2.13) and the results are presented in table 6.3. X-ray analyses were also performed on the sectioned sediments (see section 2.8) and are presented in figure 6.2.

The active sediment cores were shown to have a lower water content than the killed control cores. The water content had reduced in all cores at the end of the 235 hour period relative to value determined at time zero (*i.e.* 62 %). The water content in the active cores was lower than the corresponding killed control cores. This result was most significant in the 30 °C incubation. *M. tindarius* require water (1 mole) to metabolise the trimethylamine carbon substrate (2 moles) in this experiment. The calculated loss of water as a result of this metabolism was, however, negligible compared to the water content of these sediments. The reduction in water content in the active cores may therefore have been due to the gas voids providing a preferential route for pore water evaporation, up the edges of the sediment inside the acrylic liner.

Methane concentration in units of $\mu\text{g g}^{-1}$ was converted to units of mM using the water content data and by assuming that the gas voids present displace both pore water and sediment in equal amounts (see calculation in section 5.4.1).

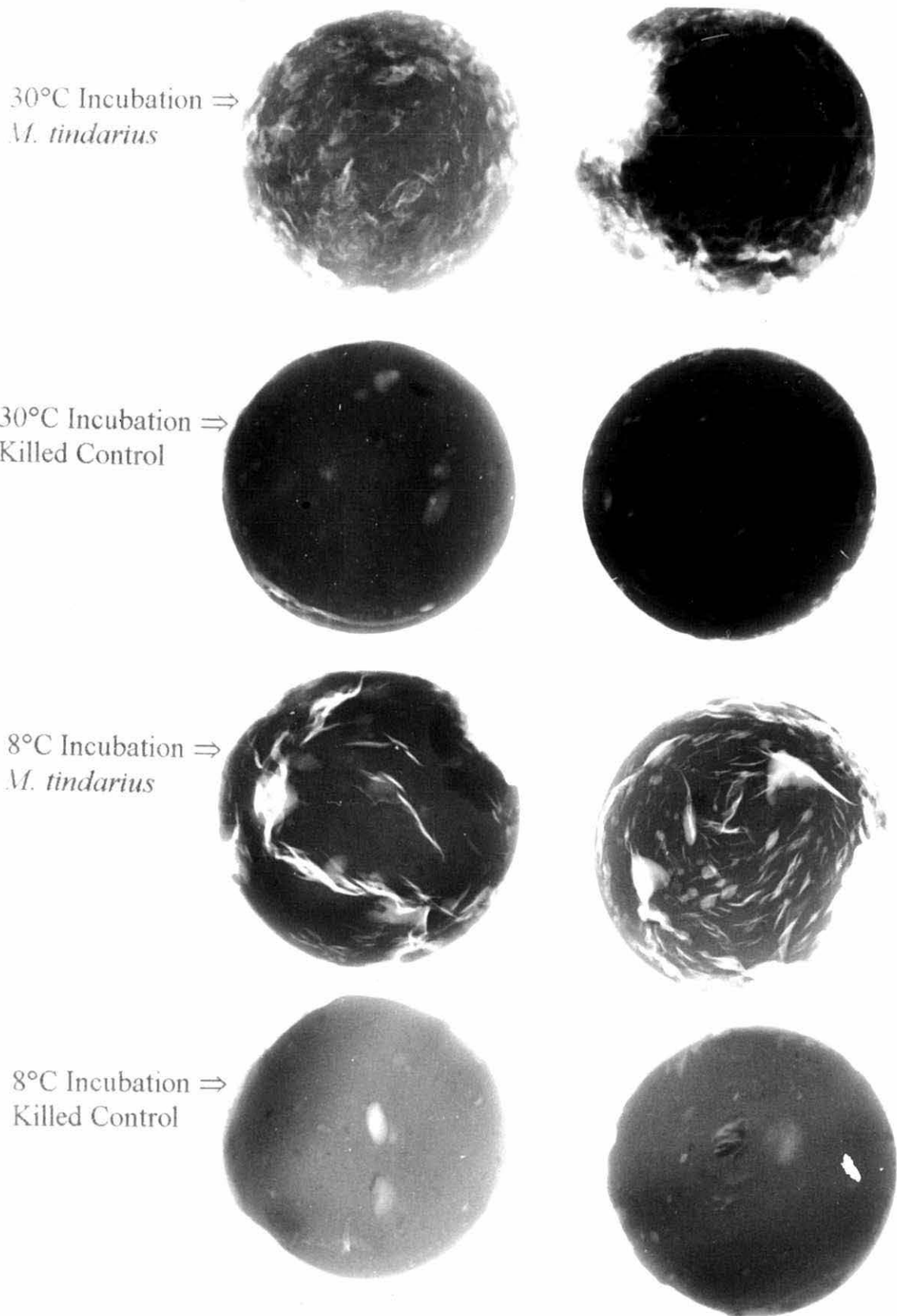


Figure 6.2. X-ray photograph of sections removed from the four consolidation cores at the end of the experiment. The core sections, taken from the top and bottom of each core, include from the top: Active core 1 at 30 °C, Killed control core 2 at 30 °C, Active core 3 at 8 °C, and Killed control core 4 at 8 °C.

Table 6.3. Water, methane and DPGE ether lipid content of the consolidation cores, determined at the end of the experiment. Expected methane was calculated from the ether lipid data using the conversion factor given for *M. tindarius* in section 4.4.

Sediment Determination for the top and bottom sections	Consolidation Core			
	Core 1 30°C Active	Core 2 30°C Control	Core 3 8°C Active	Core 4 8°C Control
WATER CONTENT				
Top (%)	43.4	56.8	42.8	45.7
Bottom (%)	42.1	57.4	40.6	45.0
METHANE				
Top ($\mu\text{g g}^{-1}$)	6.4	0.2	2.7	0.4
Bottom ($\mu\text{g g}^{-1}$)	4.8	0.4	2.6	0.3
Top (mM)	8.4 *	0.1	3.6 *	0.5
Bottom (mM)	6.6 *	0.3	3.8 *	0.4
Top ($\mu\text{moles g}^{-1}$)	0.403	0.011	0.167	0.027
Bottom ($\mu\text{moles g}^{-1}$)	0.301	0.023	0.164	0.021
DPGE ETHER LIPID ^a				
Top (μM)	1.69	0.02	0.52	0.08
Bottom (μM)	1.38	-0.05	0.55	-0.02
ESTIMATED METHANE (mM) ^b				
Top (upper limit)	39.8	0.5	12.3	1.9
Top (mean conversion)	21.7	0.3	6.7	1.0
Top (lower limit)	5.7	0.1	1.8	0.3
Bottom (upper limit)	32.5	-	13.0	-
Bottom (mean conversion)	17.7	-	7.0	-
Bottom (lower limit)	4.7	-	1.9	-

* Methane values are above the calculated maximum solubility for methane at the temperatures (*i.e.* 8 and 30 °C) and pressure (*i.e.* 1.125 atm) given (*i.e.* 1.9 mM methane at 8 °C and 1.1 mM at 30 °C).

^a DPGE ether lipid concentration was determined by gas chromatography in the top and bottom sections of the consolidation cores after the experiment had finished (*i.e.* after 235 hours) and also in an aliquot of the sediment taken before the experiment began. The difference in the concentration of the DPGE lipid since the beginning of the experiment is presented in the table 6.3 in nmoles ml⁻¹ (*i.e.* μM).

^b Estimated methane concentration was calculated using the ether lipid to methane conversion factors given in the growth experiment of *M. tindarius* in section 4.4. The mean conversion factor (*i.e.* 12825 moles methane per mole DPGE ether lipid) with upper (23568 moles/mole) and lower (3398 moles/mole) limits have been calculated.

- The ether lipid concentration determined after the experiment was less than the value determined at the start of the consolidation experiment.

The solubility of methane at the temperatures (8 and 30 °C) and pressure (1.125 atm) of the cores was calculated from the equation given in section 5.5.2 (Weisenburg & Guinasso, 1979; Atkinson & Richards, 1967). The maximum concentration of dissolved methane in the pore waters was calculated at 1.9 mM for the 8 °C incubation and 1.1 mM for 30 °C.

It can be shown from table 6.3 that the active cores (*i.e.* cores 1 and 3) had significant concentrations of methane present which were calculated to exceed the solubility limit of the pore water and therefore would be expected to form undissolved gas voids (see * in table 6.3). Conversely, the lower methane concentrations in the killed control cores were below the solubility limit at their respective temperatures and would therefore be expected to be dissolved in the pore water. These results were also corroborated from the X-ray analyses given in figure 6.2.

The active cores were shown to contain significant quantities of elongated gas voids in the X-ray photograph (*i.e.* white gas voids on a black sediment background, figure 6.2). However, the killed control cores were generally gas-free in the X-ray photographs besides a few larger bubbles which would have been introduced during the mixing of the sediment before the start of the experiment. The gas voids could also be viewed through the side of the acrylic consolidation apparatus. It was noticed over the period of the experiment that the gas voids in active core 1 (*i.e.* 30 °C) formed very quickly (*i.e.* < 10 hours) relative to active core 3 (*i.e.* ~ 50 hours) but the extent of the cracks diminished towards the end of the experiment in core 1. This may have reflected the methane escaping from the consolidation apparatus. The gas voids in core 3 (*i.e.* 8 °C) formed much slower than core 1 but appeared to be more apparent in the X-ray photograph at the end of the experimental period (see figure 6.2). The methane concentration in core 1 was, however, significantly greater than core 3 (table 6.3).

The elongated gas voids did not appear to have any overall direction of penetration in the vertical plane from the surfaces of the acrylic liners that were visible. This was contrary to the acoustically turbid marine sediments reported by Hill *et al.* (1992). However, this might be explained by the fact that the pore water was observed to escape from the sediment by moving to the edge of the core and then passing up the sides that were in contact with the acrylic liner (see figure 2.1 in Chapter 2). This water movement would not be expected to represent what happens in marine sediments and therefore might be the reason why the elongated voids did not appear to be oriented with the long axis in the vertical plane.

The gas voids were observed through the sides of the apparatus to be of both elongated and spherical shapes but in the X-ray photograph the gas voids appeared to be predominantly elongated (figure 6.2). X-ray analysis detects gas voids that are overlaid (*i.e.* 3-dimensional) in the sediment structure and presents the information in 2-dimensions in the photograph.

Therefore the appearance of spherical gas voids that are superimposed may appear elongated by X-ray analysis. Further tests are required to substantiate this.

The concentration of DPGE ether lipids in the sediments at time zero represented relic ether lipids from the sediment before the experiment began as well as ether lipid in the *M. tindarius* culture that was added to the sediment. The concentration of the DPGE lipid in the sediment - culture slurry was therefore determined at the beginning of the experiment at 1.45 nmoles g⁻¹ (2.36 μM). The concentration of DPGE lipid presented in table 6.3 represents the difference in concentration over the experimental period. The change in ether lipid concentration for the killed control cores (*i.e.* cores 2 and 4) over the experiment was small (*i.e.* -0.05 to 0.08 μM) relative to the change in ether lipid for active cores 1 and 3 (*i.e.* 0.52 to 1.69 μM).

Conversion factors of methane produced per ether lipid synthesised have been determined in a growth experiment of the methanogen *M. tindarius* in section 4.4. A mean conversion factor of 12825 moles methane per mole DPGE, with limits of 3398 and 23568 were calculated. Comparison of the increase in ether lipid concentration over the experiment with the methane found in the cores showed a strong relationship. Approximately 5123 moles methane per mole of ether lipid was determined from the data with a correlation coefficient of $r = 0.98$. However, the consolidation apparatus was not a closed system and therefore methane was expected to escape during the 235 hour experimental period. The conversion factor was therefore expected to be greater than 5123 moles of methane per mole of ether lipid. Therefore the conversion factors determined in the closed system experiment of section 4.4 of chapter 4 were applied to the ether lipid data and the results are presented in table 6.3.

The estimated methane values for the active cores were approximately 5 to 40 mM for core 1 and 2 to 13 mM for core 3. The range of calculated methane values included the methane concentrations that were found in these cores, *i.e.* 6.6 to 8.4 mM for core 1 and 3.6 to 3.8 mM for core 3. It is important to note that all of the estimated methane values were greater than the calculated solubility limit of methane in the pore waters and would, on the basis of the ether lipid data, be expected to form undissolved gas voids. The mean estimated methane concentration was shown to be greater than the methane found in the active cores, which may reflect methane that had escaped from the sediment cores during the 235 hour experimental period.

The estimated methane concentrations calculated for the killed control cores were, however, significantly lower than the active cores at 0 to 0.5 mM for core 2 and 0 to 1.9 mM for core 4. The concentration of ether lipid in the sediment slurry at the start of the experiment was significant relative to the concentration at the end of the experimental period for the experiment. Therefore the errors associated with the estimated methane concentration for the

cores were expected to be large, especially for the killed control cores. The estimated methane values for the killed control cores were, however, less than the calculated solubility limit for methane in the pore waters. The upper limit estimate for core 4 was reported to be at the solubility limit for methane at 8 °C (i.e. 1.9 mM, table 6.3). Therefore on the basis of the ether lipid concentrations and the conversion factors the concentration of methane estimated in the killed control cores were predicted to not exceed the methane solubility limit in the pore waters. Further work on the use of ether lipid to methane conversion factors is required to determine whether these inferences from the ether lipid data are appropriate.

Therefore in conclusion it would appear that the methanogenic bacteria can be used to generate acoustic turbidity in artificially consolidated sediment cores. However, there are some improvements to the existing experimental set-up that need to be made for subsequent experiments:

1. The incorporation of gas bubbles when homogenizing the sediment at the start of the experiment was part of the reason why the killed control cores showed some geoacoustical properties that were characteristic of gas charged sediments (*i.e.* decreasing velocity of compression sound wave with increasing consolidation). The small methane concentrations also signified that the inhibitors did not prevent methanogenesis immediately, though methane concentrations were still well below the solubility limit.
2. The size and shape of the consolidation apparatus should be improved so that the time for the sound wave to pass around the material of the apparatus is much longer compared to the time for the sound wave to pass through the sediment. Ideally, the consolidation apparatus should be designed with a gas tight joint to prevent the sound wave from continuing around the material of the apparatus to the receiver part of the sonic viewer. A sonic viewer with a greater sampling resolution (*i.e.* greater frequency) than 0.2 μ s would also improve the significance of the sound velocity data.
3. The concentration of ether lipids introduced at the start of the experiment should be significantly reduced relative to the expected increase during the period of the experiment. Additions of very dilute methanogenic cultures would also have the advantage of introducing a lag period before the population and the methane concentration build up.
4. The gas voids observed through the acrylic liner appeared in less than 10 hours for the active core at 30 °C and up to 50 hours in the active core at 8 °C. If a greater period of consolidation is required before the formation of significant quantities of methane gas then it is recommended that lower starting temperatures of 3 °C be used.

5. The use of a pressure tight consolidation apparatus would help to contain the methane produced. Therefore it could be possible to compare whether the estimated methane concentration (*i.e.* using the ether lipid concentration and conversion factors) reflected the methane found at the end of the experiment.

6. The acrylic piston which applied the load to the sediment allowed some pore water to escape from around the edges of the sediment core up the sides of the piston. The transport of pore water up the edges of the liner therefore provided a preferential route that would not be considered characteristic of the consolidation process in marine sediments.

6.3. Summary

In order to study the effects that undissolved gas has on the geoacoustic and geotechnical properties of marine sediments it is necessary to prepare artificially consolidated acoustically turbid sediment cores. Geophysical researchers currently use gassing methods that cause unrealistically rapid methods to generate acoustic turbidity. It would appear from the results presented in this chapter that methanogenic bacteria, that have been prepared in the laboratory, can be used as an alternative gassing method to generate acoustic turbidity. The determination of whether the generation of acoustic turbidity by methanogenic bacteria has a different and more realistic effect on the geoacoustic and geotechnical properties of the sediment compared to the existing artificial gassing methods has yet to be determined.

The presence of undissolved gas on the outer edges of the sediment was observed through the clear acrylic liner of the consolidation apparatus. The gas voids appeared to consist of both spherical and elongated gas voids. The presence of undissolved gas was also detected in the sediment using X-ray photography. The gas voids shown in the X-ray photographs were mainly of an elongated shape. This discrepancy might therefore be an artifact caused by superimposing the X-ray of the 3-dimensional sediment structure onto a 2-dimensional photograph. Further tests are required to substantiate this.

Differences in the length of the cores were apparent between the methanogenically active and killed control cores in the high temperature incubation but not in the low temperature incubation. The consolidation apparatus used in this experiment would appear to be inappropriate for the indication of undissolved gas by the measurement of sound velocity. Although the averaged sound velocity data for the methanogenically active cores were generally lower than the killed control cores at each incubation temperature, the 95 % confidence limits determined with this present set-up were large and therefore the sound velocity results could not be significantly differentiated between active and killed control cores.

The increase in the concentration of ether lipids was shown to reflect the increase in methane detected at the end of the experiment. The ether lipid concentration was used to calculate the methane expected on the basis of conversion factors determined in chapter 4. Good agreement was shown to exist between the methane calculated from the ether lipid concentration and the methane found at the end of the experiment. For this experiment the presence of undissolved gas could be predicted on the basis of the change in ether lipid concentration and the appropriate conversion factors. Further work on the use of ether lipid to methane conversion factors is required to determine whether these inferences from the ether lipid data are appropriate under other conditions and with other methanogenic species.

Various improvements to the existing consolidation apparatus can now be recommended from these experiments

CHAPTER 7. CONCLUSIONS AND SUGGESTIONS FOR FURTHER RESEARCH.

Methanogens form part of the archaeobacteria kingdom and therefore possess some unique features which distinguish them from eubacteria. The membranes of archaeobacteria comprise of predominantly ether linked membrane lipids and are very rarely found in eubacterial species, which tend to possess ester linked membrane lipids. In certain marine sediments, such as the Holyhead and intertidal sites of this study, the concentration of ether lipids are expected to reflect a predominantly methanogenic source. The sediments in Holyhead Harbour have been shown to contain significant concentrations of methane of biogenic origin which can result in the characteristic geoacoustic signature known as acoustic turbidity. This study was established to compare how well the concentration of ether linked membrane lipids compared to the biomass of methanogenic bacteria, and to determine whether the concentration of ether lipids correlated with the counts of viable methanogens and methane concentration in sediments showing acoustic turbidity.

It can be concluded that the concentration of ether lipids, estimated by the technique in this thesis, is a good criterion for the determination of methanogenic biomass in pure culture, since it correlates well with other biomass determinants, including the dry weight of organism. However, because of the recalcitrant nature of the lipid, especially under anaerobic conditions, the problem of estimating the fraction of the material measured that is from moribund organisms, is a major drawback especially in old cultures.

The procedure to determine ether lipids in marine sediments was found to be a very time consuming process, requiring approximately four days of full analyst time to process six samples through the numerous stages of extraction, clean-up, derivatisation and analysis by gas chromatography. The alkane derivatives gave the most quantitative results of the isoprenoid chains that were representative of the larger ether lipid molecules. This method gave good reproducibility from replicate samples of an homogenised sediment, with coefficients of variation of 5 % for diether and 10 % for tetraether derivatives. Very little additional ether lipid was recovered by, more rigorous, extraction of the pre-extracted sediment residue. The preparation of a halogenated derivative of the diether was also demonstrated and this is expected to offer a significant improvement to the sensitivity of the method with final analysis by electron capture detection on the gas chromatograph.

The ether lipid derivatives identified in all of the Holyhead and intertidal sediment samples included; acyclic phytane (C₂₀) from the diether lipid and acyclic biphytane (C₄₀) from the tetraether, as well as significant concentrations of three biphytane derivatives, also from tetraethers, that contained different configurations of cyclopentyl rings structures (C₄₀,1 C₄₀,2 C₄₀,?). All of these derivatives have previously been detected in abyssal sediments, but this was the first study to identify these compounds in near-shore sediments.

The uncharacterised derivative identified in these sediments (C₄₀,?) had a comparative retention time to the uncharacterised derivative (C₄₀,2') determined in two other studies, and both derivatives are believed to be the same. It was suggested by Chappe and colleagues (1982) that the unknown might be an isomer of the two cyclopentyl ring derivative. However, the mass spectral information of the uncharacterised derivative (*i.e.* C₄₀,?) would suggest, in this study, that it was an isomer of the 3-cyclopentyl ring biphytane derivative, and is very susceptible to ionisation close to the middle of the molecule. The concentrations of the uncharacterised derivative and the 2 cyclopentyl ring derivative were very similar in all sediments analysed and the correlation coefficient was highly significant, suggesting a possible common source of these two derivatives to the sediments. The uncharacterised ether lipid (C₄₀,?) has not been detected in methanogens to date, and the 2 cyclopentyl ring derivative (C₄₀,2) has only been detected in very low concentrations in a very limited number of methanogens. Further study is required to determine from what larger ether lipids, and what species, these derivatives may originate.

Cyclic tetraether lipids are not commonly reported in laboratory grown mesophilic methanogens, therefore, the presence of large concentrations, and high proportions of cyclic tetraether lipids was not expected in these marine sediments. Cyclic ether lipids have been detected in geologically dated abyssal sediments (Pauly and Van Vleet, 1986b) which suggested they may be formed as a result of diagenetic changes after long periods of deposition. The proportions of cyclic ether lipids in the near-shore sediments of this study showed little change relative to the total ether lipid concentration with increasing sediment depth suggesting that cyclisation is not likely to be a response to diagenetic changes. The cyclic ether lipids correlated very highly with the acyclic tetraether lipid, which is more common in methanogenic bacteria, and this may suggest that the cyclic ether lipids were also expected to be of methanogenic origin in these near-shore sediments.

The cyclic ether lipids made up 30 to 40 % of the total ether lipid concentration. It is unlikely that the cyclic ether lipids represent a new methanogenic group of organisms that has yet to be characterised in marine sediments. The presence of small concentrations of cyclic ether lipids in the same strain of methanogen grown at different laboratories has been disputed in the literature. Therefore, it is hypothesised that the cyclic tetraether lipids are formed by known methanogenic species as a result of changing conditions in the sediment, and from this study it could be suggested that these conditions would be expected to occur soon after deposition.

The sediments of Holyhead Harbour showed similar patterns of sulphate and methane within the cores. These patterns were typified by a decreasing sulphate concentration with increasing depth, indicating the sulphate reduction zone (SRZ), to a point where the methane concentration was shown to increase by two orders of magnitude. However, the concentration of sulphate over the depth of the SRZ appeared to vary significantly between cores which may suggest a variable depositional environment to the sediments within Holyhead Harbour.

doubt
full!

The methane concentration was calculated to exceed the solubility limit of the pore water in the sediments below the SRZ in Holyhead Harbour. The presence of gas voids, caused by undissolved gas, was also confirmed using sound velocity and X-ray analysis, and was shown to extend beyond the base of all cores studied. The results found by the three techniques were in good agreement. Changes in sound velocity could be used to indicate the presence of undissolved gas, while the sediment was still located within the core barrel. This technique could therefore be used to quickly determine the depth where the undissolved gas began, and whether it extended beyond the bottom of the sediment cores. The X-ray analysis showed the gas voids to have an elongated shape and were oriented in the vertical plane. Elongated, rather than spherical gas voids, suggested a possible mechanism for gas migration. The elongated gas fissures were present below the SRZ but did not extend up into the SRZ, possibly suggesting that the rate of removal of methane within the SRZ was greater than the rate of gas migration via the fissures.

Modelling of the methane distributions within the Holyhead cores suggested that the profiles could not be described by diffusion and depositional advection alone, even when the high sedimentation rates, that were calculated for the area, were taken into account. The model which came closest to predicting the found methane profile, above the calculated point of methane saturation, incorporated a methane removal term which could be interpreted as anaerobic methane oxidation. The error associated with the 20 cm depth sampling resolution suggested that the rate constant for methane consumption was approximately $2.5 \times 10^{-7} \text{ s}^{-1}$. Surprisingly, there was not a consistent increase in sulphide at the base of the SRZ which would have been predicted as a result of methane oxidation with sulphate as electron acceptor. The concentration of soluble sulphide was also unexpectedly low in Holyhead Harbour. The reason for this is not known, but may be due to increased scavenging by iron present in discarded coal ash from steam ships, which was deposited before the anaerobic sediments built up.

The numbers of viable methanogens in the sediments of Holyhead Harbour could be shown, from the limited data, to be significantly greater at increased depths compared to the surface sediments and to also show similar profiles to the methane data. However, the ether lipid concentration profiles were not consistent in the cores taken from Holyhead Harbour. Although, there were localised maxima in the ether lipid concentration at the depth where methane was shown to increase markedly, a relationship between these two parameters was shown to not exist. Similarly, the ether lipid data did not reflect the numbers of viable

methanogens in the sediments of Holyhead Harbour. Because this was the first study of ether lipid profiles in near-shore marine sediments it is not possible to determine whether these variable concentrations of ether lipid with increasing depth are typical for marine sediments or, whether they reflect a significant variation in the depositional conditions over short distances in Holyhead Harbour. Rheinheimer (1991) suggested that where sediments are layered unevenly, zones of low bacterial content may be followed by zones with a higher content, and this is usually limited to within the top 100 cm.

The MPN determination may provide information on the distribution of the active, viable methanogenic population within the sediment but, from this data, cannot be used to directly relate whether much of the ether lipid represents active, viable biomass or necromass because of the large and variable underestimates of the true population that are evident for the MPN technique.

Methane is the product of all energy producing reactions in methanogens. It has been suggested that the amount of ether lipid synthesised is proportional to the total concentration of methane produced. Some work has also been made towards estimating the total concentration of methane to have been produced in sediments simply from the concentration of ether lipid present in paleoenvironmental reconstructions (Pauly & Van Vleet, 1986a). From the growth experiments given in this thesis it was possible to directly calculate the amount of methane produced for a given increase in the ether lipid content. Conversion factors for methane produced per diether lipid synthesised showed neither increasing nor decreasing trends with time over the lag, exponential and stationary growth phase for three species of methanogens investigated. Application of the conversion factors to a sediment in a consolidation apparatus, which had been mixed with media and a methanogenic culture, showed some interesting results. The change in ether lipid concentration was shown, via the appropriate conversion factors, to correctly infer whether sufficient methane had been formed in order to exceed the solubility limit of the methane in the pore water and form undissolved gas voids.

Application of these ratios to the ether lipid data of the Holyhead and intertidal sediments suggested that all of the methane present in the sediment could be readily accounted for by a biogenic source from within the same depths of sediment analysed. Also, the significant concentrations of ether lipid suggested that the concentration of methane remaining in the sediment was only a small proportion of what would have been expected from these conversion factors. This information may suggest that much of the ether lipid represents a relic source of methanogenic material formed prior to deposition to the sediments or, more likely, that most of the methane that was expected on the basis of the ether lipids present had been removed by either migration or oxidation.

It is strongly recommended that more research be carried out with cultures that are well into their stationary growth phases to simulate, more naturally, the growth of methanogens in the

sediments. Also, these conversion factors should be tested for a range of different carbon substrates to determine whether the proportion of substrate that is converted to cell carbon changes significantly in methanogens.

Contrary to the findings of Pauly and Van Vleet (1986b) an increase in the total ether lipid concentration was not consistently observed below the SRZ in the sediments of Holyhead Harbour. Possible explanations may include changes in the types/amount of input of either relic methanogenic material or the organic matter, over recent periods.

Holyhead Harbour and the intertidal area receives inputs from both riverine and sewage sources. The raw sewage and the faecal waste from the large cattle trade through Holyhead in the 1960's were not expected to make a significant contribution of relic ether lipid to the total ether lipid content of the sediments in this study. Recently deposited faecal matter from ruminant animals in the fields of the surrounding areas could provide a source of ether lipids via river run-off, though further study is required on the types of ether lipids in faecal waste.

The types of water column input of relic methanogenic material to the sediments of Holyhead and the abyssal site of Pauly and Van Vleet (1986b) are expected to be significantly different. However, the proportions of ether lipids between these sites were found to be similar with significant concentrations of cyclic ether lipids which are not common in laboratory grown methanogens. Because the potential sources of relic ether lipid material to the sediment was so contrasting between these sites this information may suggest that much of the ether lipids in the sediments were from methanogenic biomass created *in-situ* in the sediments. This would suggest that the organic loading to the sediments has been increasing over recent years thus causing the high concentrations of ether lipid in the SRZ. Further research is required to study the production of ether lipids in methanogens grown under conditions that are typical for marine sediments, with more detailed analysis of the sources of ether lipids to the sediments.

Source of
organic
Carbon?

The study of acoustic turbidity in marine sediments is a relatively recent scientific discipline, and therefore research into the effects that acoustic turbidity may have on the geoacoustical and geotechnical properties of the sediment is a contemporary science. Presently, there is a need to prepare artificially consolidated acoustically turbid sediment cores in order to study the effects that undissolved gas has on the geoacoustic and geotechnical properties of marine sediments. Geophysical researchers currently use gassing methods that cause unrealistically rapid periods to generate acoustic turbidity. It would appear from the results presented in this study that methanogenic bacteria, that have been prepared in the laboratory, can be used as an alternative gassing method to generate acoustic turbidity.

REFERENCES

Alperin M.J., D.B. Albert & C.S. Martens (1994) Seasonal variations in production and consumption rates of dissolved organic carbon in an organic-rich coastal sediment. *Geochimica et Cosmochimica Acta*, **58**, 4909-4930.

Alperin M.J. & W.S. Reeburgh (1985) Inhibition experiments on anaerobic methane oxidation. *Applied and Environmental Microbiology*, **50**, 940-945.

Anderson A.L. & W.R. Bryant (1990) Gassy sediment occurrence and properties: Northern Gulf of Mexico. *Geo-Marine Letters*, **10**, 209-220.

Archer D.B. (1984) Detection and quantitation of methanogens by enzyme-linked immunosorbent assay. *Applied and Environmental microbiology*, **48**, 797-801.

Archer D.B. & J.E. Harris (1986) Methanogenic bacteria and methane production in various habitats, p185-208. In: *Anaerobic Bacteria in Habitats Other Than Man*. E.M. Barnes and G.C. Mead (eds.). The Society of Applied Bacteriology, Symposium Series No. 13, Blackwell Scientific Publication, London.

Atkinson & Richards (1967) The occurrence and distribution of methane in the marine environment. *Deep Sea Research*, **14**, 673-684.

Balch W.E., G.E. Fox, L.J. Magrum, C.R. Woese & R.S. Wolfe (1979) Methanogens: Reevaluation of a unique biological group. *Microbiological Reviews*, **43**, 260-296.

Balkwill D.L., F.R. Leach, J.T. Wilson, J.F. McNabb & D.C. White (1987) Equivalence of microbial biomass measures based on membrane lipid and cell wall components, adenosine triphosphate, and direct counts in subsurface aquifer sediments. *Microbial Ecology*, **16**, 73-84.

Banat I.M. & D.B. Nedwell (1983) Mechanism of turnover of C₂ - C₄ fatty acids in high sulphate and low sulphate anaerobic sediments. *FEMS Microbiological Letters*, **17**, 107-110.

Bennell J. (1994) School of Ocean Sciences, University of Wales; Bangor, *pers. comm.*

Barrow G.M. (1988) Physical properties of gases, p3-22. In: *Physical Chemistry*. McGraw-Hill Book Company, London.

Bernard B.B. (1979) Methane in marine sediments. *Deep Sea Research*, **26**, 429-443.

Berner R.A. (1974) Kinetic models for the early diagenesis of nitrogen, sulfur, phosphorous and silicon in anoxic marine sediments, p.427-450. In: *The Sea*, Vol. 5, E.D. Goldberg (Ed.), Wiley, London.

Bianchi M., D. Marty, J.L. Teyssie & S.W. Fowler (1992) Strictly aerobic and anaerobic bacteria associated with sinking particulate matter and zooplankton fecal pellets. *Marine Ecology Progress Series*, **88**, 55-60.

Blake D.R., E.W. Mayer, S.C. Tyler, Y. Makide, D.C. Montague & F.S. Rowland (1982) Global increase in atmospheric methane concentrations between 1978 and 1980. *Geophysical Research Letters*, **9**, 477-480.

Blau K. & G. King (1978) Electron capturing ability and chemical structure. In: *Handbook of Derivatives for Chromatography*. Heyden, London, 576 pp.

Bligh E.G. & W.J. Dyer (1959) A rapid method of total lipid extraction and purification. *Canadian Journal of Biochemistry and Physiology*, **37**, 911-917.

Bratbak G. & I. Dundas (1984) Bacterial dry matter content and biomass estimations. *Applied and Environmental Microbiology*, **48**, 755-757.

Brevil C. & G.B. Patel (1980) Composition of *Methanospirillum hungatei* during growth on different media. *Canadian Journal of Microbiology*, **26**, 577-582.

Brock T.D. & M.T. Madigan (eds.) (1991) Archaeobacteria. In: *Biology of Microorganisms*. Chapter. 20. Prentice Hall, New Jersey, USA.

Bruggen J.J.A. van, K.B. Zwart, J.G.F. Hermans, E.M. van Hove, C.K. Strumm & G.D. Vogels. (1986) Isolation & characterisation of *Methanoplanus endosymbiosus* sp. nov. an endosymbiont of the marine sapropelic ciliate *Metopus contortus*. *Archives of Microbiology*, **144**, 367-374.

Bu'lock J.D., M. DeRosa & A. Gambacorta (1983) Isoprenoid biosynthesis in archaebacteria. In: *Biosynthesis of Isoprenoid Compounds*. J.W. Porter & S.L. Spurgeon (eds.), John Wiley & Sons, Chichester, Chapter 3, pp. 159-189.

Burke R.A. & W.M. Sackett (1986) Stable hydrogen and carbon isotopic compositions of biogenic methanes from several shallower aquatic environments. In: *Organic Marine Geochemistry*, M.L. Sohn (ed.), ACS Symposium Series 305, American Chemical Society, Washington, pp. 297-313.

Burke Jr. R.A., D.F. Reid, J.M. Brooks & D.M. Lavoie (1983) Upper water column methane geochemistry in the eastern tropical North Pacific. *Limnology and Oceanography*, **28**, 19-32.

Cappenburg T.E. & E. Jongejan (1978) Microenvironments of Sulphate reduction and methane production in freshwater sediments. In: *Biogeochemistry of Defined Microenvironments in Aquatic and Terrestrial Systems*. Proceedings of a third International Symposium of the Environmental Biogeochemistry, W.E. Krumbein (ed.), Ann Arbor Press, London pp, 129-138.

Carvel C. (1996) Eastbourne Port Authority, *pers. comm.*

Cave J. (1996) Holyhead Historian, *pers. comm.*

Chappe B., P. Albrecht & W. Michaelis (1982) Polar lipids of archaebacteria in sediments and petroleum. *Science*, **217**, 65-66.

Christofi N., A. Farrar, G.R. Henderson & A. Macleoda. (1986) Most probable number - A mathematical determination, *Binary*, April.

Cline J.D. (1969) Spectrophotometric determination of hydrogen sulphide in natural waters. *Limnology and Oceanography*, **14**, 454-458.

Comita P.B. & R.B. Gagosian (1983) Membrane lipid from deep-sea hydrothermal vent methanogen: a new macrocyclic glycerol diether. *Science*, **222**, 1329-1331.

Corder R.E., L.A. Hook, J.M. Larkin & J.I. Frea (1983) Isolation and characterisation of two new methane producing cocci: *Methanogenium olentangyi*, sp.nov., and *Methanococcus deltae*, sp.nov. *Archives of Microbiology*, **134**, 28-32.

Craig H. & C.C. Chou (1982) Methane: the record in polar ice cores. *Geophysical Research Letters*, **9**, 1221-1224.

Cranston R.E. (1992) Estimating methane releases from marine sediments. *Shallow Gas Newsletter*. A. Judd (ed.), No. 6, Sept.

Cynar F.J. & A.A. Yayanos (1991) Enrichment and characterisation of a methanogenic bacterium from the oxic upper layer of the ocean. *Current Microbiology*, **23**, 89-96.

Dando P.R., M.C. Austen, R.A. Burke, M.A. Kendall, M.C. Kennicutt II, A.G. Judd, D.C. Moore, S.C.M. O'Hara, R. Schmaljohann & A.J. Southward (1991) Ecology of a North Sea pockmark with an active methane seep. *Marine Ecology Progressive Series*, **70**, 49-63.

Davis A.M. (ed.) (1992) Methane in Marine Sediments. *Continental Shelf Research*, Vol.12, No. 10, Pergamon Press, Oxford, 1264 pp.

Davies J.B. & R.M. Squires (1954) Detection of microbially produced gaseous hydrocarbons other than methane. *Science*, **119**, 381-382.

Davis J.B. & Yarborough (1966) Anaerobic oxidation of hydrocarbons by *Desulfovibrio desulfuricans*. *Chemical Geology*, **1**, 137-146.

De Angelis M.A. & C. Lee (1994) Methane production during zooplankton grazing on marine phytoplankton. *Limnology and Oceanography*, **39**, 1298-1308.

Denk E.M., W.A. Dunlap, W.R. Bryant, L.J. Milberger & T.J. Whelan (1981) A pressurized core barrel for sampling gas-charged marine sediments. *Proceedings of the 13th Offshore Technology Conference 1*, Paper No. 4120, Richardson, pp 43-52.

De Rosa M., A. Gambacorta & B. Nicolaus (1980a) Regularity of isoprenoid biosynthesis in the ether lipids of archaebacteria. *Phytochemistry*, **19**, 791-793.

De Rosa M., A. Gambacorta, B. Nicolaus, S. Sodano & J.D. Bu'Lock (1980b) Structural regularities in tetraether lipids of *Caldariella* and their biosynthetic and phyletic implications. *Phytochemistry*, **19**, 833-836.

De Rosa M., E. Esposito, A. Gambacorta, Nicolaus, B & J.D. Bu'Lock (1980c) Effects of temperature on ether lipid composition of *Caldariella acidophila*. *Phytochemistry*, **19**, 827-831.

De Rosa M., A. Gambacorta, B. Nicolaus, B. Chappe & P. Albrecht (1983) Isoprenoid ethers; backbone of complex lipids of the archaebacterium *Sulfolobus soflataricus* *Biochimica et Biophysica Acta*, **753**, 249-256.

De Rosa M., A. Gambacorta & A. Gliozzi (1986a) Structure, biosynthesis and physiochemical properties of archaebacterial lipids. *Microbiological Reviews*, **50**, 70-80.

De Rosa M., A. Gambacorta, V. Lanzotti, A. Trincone, J.E. Harris & W.D. Grant (1986b) A range of ether core lipids from the methanogenic archaebacterium *Methanosarcina barkeri*. *Biochimica et Biophysica Acta*, **875**, 487-492.

Devol A.H., J.J. Anderson, K. Kuivila & J.W. Murray (1984) A model for coupled sulphate reduction and methane oxidation in the sediments of Saanich inlet. *Geochimica et Cosmochimica Acta*, **48**, 993-1004.

Dickins H.D. & E.S. Van Vleet (1992) Archaebacterial activity in the Orca Basin determined by the isolation of characteristic isopranyl ether -linked lipids. *Deep Sea Research*, **39**, 521-536.

Doddema H.J. & G.D. Vogels (1978) Improved identification of methanogenic bacteria by fluorescence microscopy. *Applied and Environmental Microbiology*, **36**, 752-754.

Edwards T. & B.C. McBride (1974) New method for the isolation and identification of methanogenic bacteria. *Journal of Applied Microbiology*, **29**, 540-545.

Fallon R.D., S.Y. Newell & C.S. Hopkinson (1983) Bacterial production in marine sediments: Will cell-specific measures agree with whole-system metabolism? *Marine Ecology Progress Series*, **11**, 119-127.

Ferrante G, I. Eikel, G.B. Patel & G.D. Sprott (1988) Structure of the major polar lipids isolated from the acetoclastic methanogen, *Methanotheroxiphilium concilii* GP6. *Biochimica et Biophysica Acta*, **963**, 162-172.

Fiebig K. & G. Gottschak (1983) Methanogenesis from choline by a coculture of *Desulfovibrio* sp. and *Methanosarcina barkeri*. *Applied and Environmental Microbiology*, **45**, 161-168.

Findlay R.H., G.M. King & L. Watling (1989) Efficacy of phospholipid analysis in determining microbial biomass in sediments. *Applied and Environmental Microbiology*, **55**, 2888-2893.

Floodgate G.D., G.B. Jones & M.R. Yarrington (1984) Chemical and microbiological aspects of acoustically turbid sediments. *Deuxieme Colloque International de Bacteriologie Marine* - C.N.R.S. Brest, France, pp. 35-42.

Fry J.C. (1988) Determination of biomass. In: *Methods in Aquatic Bacteriology*. B. Austin (ed.), John Wiley & sons Ltd., London, pp. 27-72.

Fuchs G. & E. Stupperich (1984) Carbon dioxide reduction to all carbon in methanogens. In: *Microbial Growth on C1 Compounds*, R.L. Crawford & R.S. Hanson (eds.), Proceedings of the 4th International Symposium, American Society for Microbiology, Washington DC, U.S.A., pp. 199-202.

Gant T. (1996) Anglesey Borough Council, *pers. comm.*

Gerrard W. & M.F. Lappert (1952) Fission of mixed ethers by boron trichloride. *Journal of the Chemical Society*, pp. 1486-1490.

Grant W.D., G. Pinch, J.E. Harris, M. De Rosa & A. Gambacorta (1985) Polar lipids in methanogen taxonomy. *Journal of General Microbiology*, **131**, 3277-3286.

Guezennec J. & A. Fiala-Medioni (1996) Bacterial abundance and diversity in the Barbados Trench determined by phospholipid analysis. *FEMS Microbial Ecology*, **19**, 83-93.

Gunnarsson L.A.H. & P.H. Ronnow (1982) Interrelationships between sulphate reducing and methane producing bacteria in coastal sediments with intense sulphide production. *Marine Biology*, **69**, 121-128.

Gunsalus R.P., J.A. Rommesser & R.S. Wolfe (1978) Preparation of coenzyme M analogues and their activity in the methyl coenzyme M reductase system of *Methanobacterium thermoautotrophicum*. *Biochemistry*, **17**, 2374-2377.

Guyer K.E., W.A. Hoffman L.A. Horrocks and D.G. Cornwell (1963) Studies on the composition of glycerol ethers and their preparation from diacyl glycerol ethers in liver oils. *Journal of Lipid Research*, **4**, 385-391.

Harris J.E. (1985) Gelrite as an agar substitute for the cultivation of mesophilic *Methanobacterium* and *Methanobrevibacter* species. *Applied and Environmental Microbiology*, **50**, 1107-1109.

Harris J.E., P.A. Pinn & R.P. Davis (1984) Isolation and characterisation of a novel thermophilic fresh water methanogen. *Applied and Environmental Microbiology*, **48**, 1123-1128.

Hartzell P.L., G. Zvilius, J.C. Escalante-Semerena & M.I. Donnelly (1985) Coenzyme F₄₂₀ dependence on the methylene tetrahydro methanopterin dehydrogenase of *Methanobacterium thermoautotrophicum*. *Biochimica et Biophysica Resumae (Commun.)*, **133**, 884-890.

Harvey H.R., R.D. Fallon & J.S. Patton (1986) The effect of organic matter and oxygen on the degradation of bacterial membrane lipids in marine sediments. *Geochimica et Cosmochimica Acta*, **50**, 795-804.

Hedrick D.B., J.B. Guckert & D.C. White (1991a) Archaeobacterial ether lipid diversity analysed by supercritical fluid chromatography: integration with a bacterial lipid protocol. *Journal of Lipid Research*, **32**, 659-666.

Hedrick D.B., B. Richards, W. Jewell, J.B. Guckert & D.C. White (1991b) Disturbance, starvation, and overfeeding stresses detected by microbial lipid biomarkers in high-solids high-yield methanogenic reactors. *Journal of Industrial Microbiology*, **8**, 91-98.

Hedrick D.B., A. Vass, B. Richards, W. Jewell, J.B. Guckert & D.C. White (1991c) Starvation, and overfeeding stress on high yield methanogenic digestors. *Biomass and Bioenergy*, **1**, 75-82.

Hedrick D.B., T. White J.B. Guckert W.J. Jewell & D.C. White (1992) Microbial biomass and community structure of a phase-separated methanogenic reactor determined by lipid analysis. *Journal of Industrial Microbiology*, **9**, 193-199.

Heine-Dobbernack E., S.M. Schoberth & H. Sahm (1988) Relationship of intracellular coenzyme F₄₂₀ content to growth and metabolic activity of *Methanobacterium bryanti* and *Methanosarcina barkeri*. *Applied and Environmental Microbiology*, **54**, 454-459.

Henson J.M., P.H. Smith & D.C. White (1985) Examination of thermophilic methane producing digestors by analysis of bacterial lipids. *Applied and Environmental Microbiology*, **50**, 1428-1433.

Hill J.M., J.P. Halka, R. Conkwright, K. Koczot & S. Coleman (1992) Distribution and effects of shallow gas on bulk estuarine sediment properties. *Continental Shelf Research*, **12**, 1219-1230.

Hines M.E. & J.D. Buck (1982) Distribution of methanogenic and sulphate-reducing bacteria in near-shore marine sediments. *Applied and Environmental Microbiology*, **43**, 447-453.

Holzappel-Pschorn A. & W. Seiler (1986) Methane emissions during a cultivation period from an Italian rice paddy. *Journal Geophysical Research*, **91**, 11803-11814.

Hovland M (1992) Pockmarks and gas-charged sediments in the eastern Skagerrak. *Continental Shelf Research*, **12**, 1111-1120.

Hovland M. & A.G. Judd (1988) *Seabed Pockmarks and Seepages*. Graham and Trotman Ltd, London, pp. 285.

Hovland M., M. Talbot, H. Quale, S. Olausson & L. Aasberb (1987) Methane related carbonate cements in pockets of the North Sea. *Journal Sedimentology and Petrology*, **57**: 881-892.

Howarth R.W. (1978) A rapid and precise method for determining sulphate in seawater, estuarine waters and sediment pore waters. *Limnology and Oceanography* **23**, 1066-1069.

Huser B.A., K. Wuhrmann & A.J.B. Zehnder (1982) *Methanothrix soehngenii* gen. nov. sp. nov., a new acetotrophic non-hydrogen oxidising methane bacterium. *Archives of Microbiology*, **132**, 1-9.

Iversen N. & T.H. Blackburn (1981) Seasonal rates of methane oxidation in anoxic marine sediments. *Applied and Environmental Microbiology*, **41**, 1295-1300.

Iversen N. & B.B. Jorgensen (1985) Anaerobic methane oxidation rates at the sulfate-methane transition in marine sediments from Kattegat & Skagerrak. *Limnology and Oceanography*, **30**, 944-955.

Iversen N. & B.B. Jorgensen (1985) Diffusion coefficients of sulfate and methane in marine sediments: Influence of porosity. *Geochimica et Cosmochimica Acta*, **57**, 571-578.

Jackson L. (1969) Article in Rail News 26th September 1969 on the shipping of cattle from Dublin.

Jones P.W. (1977) Holyhead sewage system, Welsh Water, Bangor, North Wales, pp. 12.

Jones J.G. (1979) *A Guide to Methods for Estimating Microbial Numbers and Biomass in Freshwater*. Freshwater Biological Association, Scientific Publication No. 39. Titus Wilson and Son Ltd, Kendal, 109pp.

Jones W.J. & M.J.B. Paynter (1980) Populations of methane producing bacteria and *in-vitro* methanogenesis in saltmarsh and estuarine sediments. *Applied and Environmental Microbiology*, **39**, 864-871.

Jones G.B., J.D. Bennell & G.D. Floodgate (1986) Chemical and microbiological aspects of acoustically turbid sediments: preliminary investigations. *Marine Geotechnology*, **6**, 315-332.

Jones S.R. & T.M. Jeffs (1991) Near surface sea temperatures in coastal waters of the North Sea, English channel and Irish Sea. *Fisheries Research Data Report No 24*, MAFF, Lowestoff, pp.53.

Jones W.J., D.P. Nagle & W.B. Whitman (1987) Methanogens and the diversity of archaeobacteria. *Microbiological Reviews*, **51**, 135-177.

Jones W.J., J.A. Leigh, F. Mayer, C.R. Woese & R.S. Wolfe (1983a) *Methanococcus jannaschii* sp. nov., an extremely thermophilic methanogen from a submarine hydrothermal vent. *Archives of Microbiology*, **136**, 254-261.

Jones W.J., W.B. Whitman, R.D. Fields & R.S. Wolfe (1983b) Growth and plating efficiency of methanococci on agar media. *Applied and Environmental Microbiology*, **46**, 220-226.

Jørgensen B.B. (1977) The sulfur cycle of a coastal marine sediment (Limfjorden, Denmark). *Limnology and Oceanography*, **22**, 814-832.

Jørgensen B.B. (1978) A comparison of methods for the quantification of bacterial sulphate reduction in coastal marine sediments. III. Estimation from chemical and bacteriological field data. *Journal of Geomicrobiology*, **1**, 49-64.

Jørgensen N.O. (1976) Recent high magnesium calcite/aragonite cementations of beach and submarine sediments from Denmark. *Journal of Sedimentary Petrology*, **46**, 940-951.

Jørgensen N.O. (1992) Methane-derived carbonate cementation of Holocene marine sediments from Kattegat, Denmark. *Continental Shelf Research*, **12**, 1209-1218.

Jørgensen N.O., T. Laier, B. Buchardt & T. Cederberg (1990) Shallow hydrocarbon gas in the northern Jutland-Kattegat region, Denmark. *Bulletin of the Geological Society of Denmark*, **38**, 69-76.

Judd A.G. (1991) Shallow Gas Group Newsletter, No.4, January, pp.11..

Judd A.G. & M. Hovland (1992) The evidence of shallow gas in marine sediments. *Continental Shelf Research*, **12**, 1081-1096.

Kadam P.C., D.R. Ranade, L. Mandelco & D.R. Boone (1994) Isolation and characterisation of *Methanobrevibacterium bombayensis* sp. nov., a methylotrophic methanogen that requires high concentrations of divalent cations. *International Journal of Systematic Bacteriology*, **44**, 603-607.

Karl D.M. & B.D. Tilbrook (1994) Production and transport of methane in oceanic particulate organic matter. *Nature*, **368**, 732-734.

Kates M. (1992) Faculty of Science, University of Ottawa, *pers. comm.*

Kates M. (1964) Simplified procedures for hydrolysis or methanolysis of lipids. *Journal of Lipid Research*, **5**, 132-135.

Kates M. (1972) Techniques of lipidology. In: *Laboratory Techniques in Biochemistry and Molecular Biology*, T.S. Work & E. Work (eds.), North-Holland Publishing Company, London, Volume 3 Part II.

Kates M., L.S. Yengoyan & P.S. Sastry (1964) A diether analog of phosphatidyl glycerophosphate in *Halobacterium cutirubrum*. *Biochimica et Biophysica Acta*, **98**, 252-268.

Keen M.J. (1968) *An Introduction to Marine Geology*. Pergamon Press Ltd, Oxford, pp. 218.

Kiene R.P., R.S. Oremland, A. Catena, L.G. Miller & D.G. Capone (1986) Metabolism of reduced methylated sulfur compounds by anaerobic sediments and a pure culture of an estuarine methanogen. *Applied and Environmental Microbiology*, **52**, 1037-1045.

King G.M. (1984) Metabolism of trimethylamine, choline and glycine betaine by sulphate reducing and methanogenic bacteria in marine sediments. *Applied Environmental Microbiology*, **48**, 719-725.

King G.M., M.J. Klug & D.R. Lovley (1983) Metabolism of acetate, methanol and methylated amines in intertidal sediments of Lowes Cove, Maine. *Applied Environmental Microbiology*, **45**, 1848-1853.

Kirsop B.H. (1984) Methanogenesis. *CRC Critical Reviews in Biotechnology*, **1**, issue 2, 109-159.

Koga, Y, M.A. Matsushita, M. Ohga & M. Nishihara (1993a) Taxonomic significance of the distribution of component parts of polar ether lipids in methanogens. *Systematics of Applied Microbiology*, **16**, 342-351.

Koga, Y, M. Nishihara, H. Morii & M.A. Matsushita (1993b) Ether polar lipids of methanogenic bacteria: structures, comparative aspects, and biosyntheses. *Microbiological Reviews*, **57**, 164-182.

König, H. & K.O. Stetter (1982). Isolation and characterisation of *Methanlobus tindarius* sp.nov., a coccoid methanogen growing only on methanol and methylamines. *Zentralblatt für Bakteriologie, Mikteriologie und Hygeine., I. Abt. Orig.*, **C3**, 478-490.

König, H. and K.O. Stetter (1989) Archaeobacteria. In: *Bergley's Manual of Systematic Bacteriology*, J.T. Staley, M.P. Bryant, N. Pfennig & J.G. Holt (eds.), Volume 3, section 25, Williams and Wilkins, Baltimore, pp. 2171-2220.

Kosior D.R. & A.L. Warford (1979) Methane production and oxidation in Santa Barbara basin sediments. *Estuarine and Coastal Science*, **8**, 379-385.

Kristjansson J.K., P. Schönheit & R.K. Thauer (1982) Different K_s values for hydrogen of methanogenic bacteria and sulfate-reducing bacteria: An explanation for the apparent inhibition of methanogenesis by sulfate. *Archives of Microbiology*, **131**, 278-282.

Kuivila K.M., J.W. Murray & A.H. Devol (1990) Methane production in the sulphate depleted sediments of two marine basins. *Geochimica et Cosmochimica Acta*, **54**, 403-411.

Kulm L.D. & E. Suess (1990) Relationship between carbonate deposits and fluid venting: Oregon accretionary prism. *Journal of Geophysical Research* **95**: 8899-8915.

- Kurr M., R. Huber, H. Koenig, H.W Jannasch, H. Fricke, K.O. Stetter & J.K. Kristjansson (1991) *Methanopyrus kandleri*, gen. and sp. nov. represents a novel group of hyperthermophilic methanogens, growing at 110°C. *Archives of Microbiology*, **156**, 239-247.
- Lacis A., J. Hansen, P. Lee, T. Mitchell & S. Lebedeff (1981) Greenhouse effect of trace gases 1970-1980. *Geophysical Research Letters*, **8**, 1035-1038.
- Laier T., N.O. Jørgensen, B. Buchardt, T. Cederberg & A. Kuijpers (1992) Accumulation and seepages of biogenic gas in Northern Denmark. *Continental Shelf Research*, **12**, 1173-1186.
- Lamontagne R.A., J.W. Swinnerton & V.J. Linnenbom (1971) Non-equilibrium of carbon monoxide and methane at the air-sea interface. *Journal of Geophysical Research*, **76**, 5117-5121.
- Langworthy T.A. (1985) Lipids in Archaeobacteria. In: *The Bacteria*, C.R. Woese & R.S. Wolfe (eds.), Academic Press, London. pp. 459-491.
- Langworthy T.A., G. Holzer, J. G. Zeikus & T. G. Tornabene (1983) Iso and anteiso-branched glycerol diethers of the thermophilic anaerobe. *Thermodesulfobacterium commune*. *Systematics and Applied Microbiology*, **4**, 1-17.
- Lidstrom M.E. (1983) Methane consumption in Framvaren, an anoxic marine fjord. *Limnology and Oceanography*, **28**, 1247-1251.
- Lloyd D., K. Hillman, N. Yarlett & A.G. Williams (1989) Hydrogen production by holtrich protooa: effects of oxygen and implications for metabolic control by in-situ conditions. *Journal of Protozoology*, **36**, 205-213.
- Lloyd, D (1996) Dept. of Microbiology, U.C. Wales; Cardiff, *pers. comm.*
- Lovelock J.E. & A.J. Watson (1978) Electron capture detector - Theory and practice II. *Journal of Chromatography*, **158**, 123-138.
- Lovley D.R. & M.J. Klug (1983) Methanogenesis from methanol and methylamines and acetogenesis from hydrogen and carbon dioxide in the sediments of a eutrophic lake. *Applied and Environmental Microbiology*, **45**, 1310-1315.
- Lyman & Flemming (1940) Artificial preparation of seawater. *Journal of Marine Research*, **3**, 134-138.

Macario A. & Conway de Macario E. (eds.) (1985) In: *Monoclonal Antibodies against Bacteria*. Academic Press, London, pp.213-249.

MacDonald G.J (1983) The many origins of natural gas. *Journal of Petroleum Geology*, **5**, 341-362.

Mancuso C.A., G. Odham, G. Westendahl, J. Reeve & D.C. White (1985) C₁₅, C₂₀ and C₂₅ isoprenoid homologues in glycerol diether phospholipids of methanogenic bacteria. *Journal of Lipid Research*, **26**, 1120-1125.

Manheim F.T. & L.S. Waterman (1974) Diffusimetry (diffusion coefficient estimation) on sediment cores by resistivity probe. In: *Initial report DSDP* (ed C.C. Von der Borch *et al*). **22**, pp. 663-670.

Martens C.S. & R.A. Berner (1974) Methane production in the interstitial waters of sulphate-depleted marine sediments, *Science*, **185**, 1167-1169.

Martens C.S. & R.A. Berner (1977) Interstitial water chemistry of anoxic Long Island Sound Sediments. I. Dissolved gases. *Limnology and Oceanography*, **22**, 11-25.

Martens C.S. & J. Val Klump (1980) Biogeochemical cycling in an organic-rich coastal marine basin 1. Methane sediment-water exchange processes. *Geochimica et Cosmochimica Acta*, **44**, 471-490.

Martz R.F., D.I. Sebacher & D.C. White (1983) Biomass measurement of methane forming bacteria in environmental samples. *Journal of Microbiological Methods*, **1**, 53-61.

Miller T.L. & M.J. Wollin (1982) Enumeration of *Methanobrevibacter smithii* in human faeces. *Archives of Microbiology*, **131**, 14-18.

Moldowan J.M. & W.K. Seifert (1979) Head to head linked isoprenoid hydrocarbons in petroleum. *Science*, **204**, 169-171.

Moore W.E.C. (1966) Techniques for routine culture of fastidious anaerobes. *International Journal of Systematic Bacteriology*, **16**, 173-190.

Morii H. & Y. Koga (1993) Tetraether type polar lipids increase after logarithmic growth phase of *Methanobacterium thermoautotrophicum* in compensation for the decrease of diether lipids. *FEMS Microbiology Letters*, **109**, 283-288.

Morris G. (1996) Farm Manager, Anglesey Aluminium, *pers. comm.*

Mountfort D.O. & R.A. Asher (1981) Role of sulphate reduction *versus* methanogenesis in terminal carbon flow in polluted intertidal sediment of Waimea Inlet, Nelson, New Zealand. *Applied and Environmental Microbiology*, **42**, 252-258.

Moura I., J.J.G. Moura, H. Santos, A.V. Xavier, G. Burch, H.D. Peck & J. LeGall (1983) Proteins containing the factor F₄₂₀ from *Methanosarcina barkeri* and *Methanobacterium thermoautotrophicum*: Isolation and properties. *Biochimica et Biophysica Acta*, **742**, 84-90.

Mullin M.D., C.M. Pochini, S. McCrindle, M. Romkes, S.H. Safe & L.M. Safe (1984) High resolution PCB analysis: Synthesis and chromatographic properties of all 209 PCB congeners. *Environmental Science and Technology*, **18**, 468-476.

Murray J.W., V. Grundmanis & W.J. Smethie (1978) Interstitial water chemistry in the sediments of Saanich Inlet. *Geochimica et Cosmochimica Acta*, **42**, 1011-1026.

Nedwell D.B. (1969) The microbial ecology of an intertidal sediment. PhD Thesis University of Wales, Bangor.

Nichols P.D., C.A. Mancuso & D.C. White (1987) Measurement of methanotroph and methanogen signature phospholipids for use in assessment of biomass and community structure in model systems. *Organic Geochemistry*, **11**, 451-461.

Nichols P.D. & P.D. Franzmann (1992) Unsaturated diether phospholipids in the Antarctic methanogen *Methanococoides burtonii*. *FEMS Microbiology Letters*, **98**, 205-208.

Nishihara M. (1991) Dept of Chemistry, University of Occupational and Environmental Health, Kitakyushu, Japan (*pers. comm.*).

Nishihara M. & Y. Koga (1987) Extraction and composition of polar lipids from the archaeobacterium, *Methanobacterium thermoautotrophicum*: Effective extraction of tetraether lipids by an acidified solvent. *Journal of Biochemistry*, **101**, 997-1005.

Nishihara M. & Y. Koga (1988) Quantitative conversion of diether or tetraether phospholipids to glycerophosphoesters by dealkylation with BCl₃: a tool for structural analysis of archaeobacterial lipids. *Journal of Lipid Research*, **29**, 384-388.

Nishihara M. & Y. Koga (1991) Hydroxyarchaetidylserine and hydroxyarchaetidyl-myoinositol in *Methanosarcina barkeri*: polar lipids with a new core portion. *Biochimica et Biophysica Acta*, **1082**, 211-217.

Nishihara M., M. Akagawa-Matsushita, Y. Toga & Y. Koga (1995) Inference to methanogenic bacteria in wastewater digester sludges by lipid component analysis. *Journal of Fermentation Bioengineering*, **79**, 400-402.

Nottingham P.M. & R.E. Hungate (1968) Isolation of methanogenic bacteria from faeces of man. *Journal of Bacteriology*, **96**, 2178-2179.

Novitsky J.A. (1987) Microbial growth rates and biomass production in a marine sediment: Evidence for a vary active but mostly nongrowing community. *Applied Environmental Microbiology*, **53**, 2368-2372.

Ohtsubo S., M. Kanno, H. Miyahara, S. Kohno, Y. Koga & I. Miura (1993) A sensitive method for quantification of acetoclastic methanogens and estimation of total methanogenic cells in natural environments based on an analysis of ether-linked glycerolipids. *FEMS Microbiol Ecology*, **12**, 39-50.

Oremland R.S. (1979) Methanogenic activity in plankton samples and fish intestines: A mechanism for *in situ* methanogenesis in oceanic surface waters. *Limnology and Oceanography*, **24**, 1136-1141.

Oremland R.S. (1988) Biogeochemistry of methanogenic bacteria. In: *Biology of Anaerobic Micro-organisms*. A.J.B. Zehnder (ed.), Wiley, New York, pp. 641-705.

Oremland R.S. & S. Polcin (1982) Methanogenesis and sulphate reduction in marine sediments. *Geochimica et Cosmochimica Acta*, **42**, 209-214.

Oremland R.S. & B.F. Taylor (1978) Sulphate reduction and methanogenesis in marine sediments. *Geochimica et Cosmochimica Acta*, **47**, 209-214.

Oremland R.S., L.M. Marsh & S. Polcin (1982) Methane production and simultaneous sulphate reduction in anoxic, salt marsh sediments. *Nature*, **296**, 143-145.

Parkes R.J. (1987) Analysis of microbial communities within sediments using biomarkers. In: Society of General Microbiology, vol.41. *Ecology of Microbial Communities*, University Press, Cambridge, 147-177.

- Parkes R.J., B.A. Gragg., J.C. Fry, R.A. Herbert & J.T. Winspenny (1990) Bacterial biomass and activity in deep sediment layers from the Peru margins. *Philosophical Transactions of the Royal Society of London* **A331**: 139-153.
- Parsons T.R., Y. Maita and C.M. Lalli (1984) *A Manual Of Chemical And Biological Methods For Seawater Analysis*. Pergamon Press, Oxford, 114 pp.
- Pauly G.G. & S. Van Vleet (1986a) Acyclic archaeobacterial ether lipids in swamp sediments. *Geochimica et Cosmochimica Acta*, **50**, 1117-1125.
- Pauly G.G. & S. Van Vleet (1986b) Archaeobacterial ether lipids: Natural tracers of biogeochemical processes. *Advances in Organic Geochemistry*, **10**, 859-867.
- Pease T.K., E.S. Van Vleet & J.S. Barre (1992) Diphytanyl glycerol ether distributions in sediments of the Orca Basin. *Geochimica et Cosmochimica Acta*, **56**, 3469-3479.
- Pedersen D. & G.S. Sayler (1980) Methanogenesis in freshwater sediments: inherent variability and effects of environmental contaminants. *Canadian Journal of Microbiology*, **27**, 198-205.
- Perry J.H. (1963) *Chemical Engineers' Handbook*. Fourth edition, R.H. Perry, C.H. Chilton & S.D. Kirkpatrick (Eds), McGraw-Hill Book Company, London, chapt.9, pp. 2-3.
- Peters A. (1988) Methanogenesis in Holyhead harbour: A study in microbial ecology. BSc Project, pp. 26.
- Postgate J.R. (1969) Methane as a minor product of pyruvate metabolism by sulphur reducing and other bacteria. *Journal of General Microbiology*, **57**, 293-302.
- Premchitt J., N.S. Rad, P. To, R. Shaw & J.W.C. James (1992) A study of gas in marine sediments in Hong Kong. *Continental Shelf Research*, **12**, 1251-1264.
- Rasmussen R.A. & M.A.K. Khalil (1984) Atmospheric methane in the recent and ancient atmospheres: Concentration, trends and interhemispheric gradient. *Journal of Geophysical Research*, **89**, 11599-11605.
- Reeburgh W.S. (1967) An improved interstitial water sampler. *Limnology and Oceanography*, **2**, 163-165.

Reeburgh W.S. (1980) Anaerobic methane oxidation: Rate depth distributions in Skan Bay sediments. *Earth Planetary and Science Letters*, **15**, 334-337.

Rheinheimer G. (1991) *Aquatic Microbiology*. 4th Edition, pp.363. John Wiley & Sons, Chichester.

Rice D.R. & G.E. Claypool (1981) Generation, accumulation and resource potential of biogenic gas. *The American Association of Petroleum Geologists Bulletin*, **65**, pp. 5-25.

Roberts D. (1994) Anglesey Aluminium Ltd, Holyhead, *pers. comm.*

Robinson R.W. (1986) Life cycles in the methanogenic archaeobacterium *Methanosarcina mazei*. *Applied and Environmental Microbiology*, **52**: 17-27.

Robinson J.A. & J.M. Tiedje (1982) Kinetics of hydrogen consumption by rumen fluid, anaerobic digester sludge and sediment. *Applied and Environmental Microbiology*, **44**, 1374-1384.

Ronnow P.H. & L.A.H. Gunnarsson (1981) Sulfide-dependent methane production and growth of a thermophilic methanogenic bacterium. *Applied and Environmental Microbiology*, **42**, 580-584.

Rowe R., R. Todd & J. Waide (1977). Microtechnique for the most probable number analysis. *Applied and Environmental Microbiology*, **33**, 675-680.

Rudd J.W.M. & C.D. Taylor (1980) Methane cycling in aquatic environments. In: *Advances in Aquatic Microbiology*, M.R. Droop & H.W. Jannason (eds.), **2**, 77-150.

Sansome F.J. & C.S. Martens (1981) Methane production from acetate and associated methane fluxes from anoxic coastal sediments. *Science*, **211**, 707-709.

Schonheit P., J.K. Kristjansson & R.K. Thauer (1982) Kinetic mechanism for the ability of sulphate reducers to out-compete methanogens for acetate. *Archives of Microbiology*, **132**, 285-288.

Schubel J.R. (1974) Gas bubbles and the acoustically impenetrable or turbid character of some estuarine sediments. In: *Natural Gases in Marine Sediments*, I.R. Kaplan (ed.), Plenum Press, New York, 324 pp.

Scott R.I., N. Yarlett, K. Hillman, T.N. Williams, A.G. Williams & D. Lloyd (1983) The pressure of oxygen in rumen liquor and its effects on methanogenesis. *Journal of Applied Bacteriology*, **55**, 143-149.

Scranton M.I. & P.G. Brewer (1977) Occurrence of methane in near surface waters of the western subtropical North Atlantic. *Deep Sea Research*, **24**, 127-138.

Senior E., E.B. Lindstrom, I.M. Banat & D.B. Nedwell (1982) Sulphate reduction and methanogenesis in the sediment of a saltmarsh on the east coast of the U.K. *Applied and Environmental Microbiology*, **43**, 987-996.

Seyfried P.L. & A.R.G. Owen (1978) Evaluation of the most probable number technique for the enumeration of faecal coliforms and *Pseudomonas aeruginosa* in sediments. In: *Methodology for Biomass Determinations and Microbial Activities in Sediments*, ASTM STP 673. C.D. Litchfield & P.L. Seyfried (eds.), American Society for Testing Materials, Philadelphia, pp. 52-63.

Sieburth J.McN (1993) C₁ bacteria in the water column of Chesapeake Bay, USA. I. Distribution of sub-populations of oxygen tolerant, obligately anaerobic, methylotrophic methanogens that occur in microniches reduced by their bacterial consorts. *Marine Ecology Progress Series*, **95**, 67-80.

Sieburth J.McN., P.W. Johnson, A.J.L. Macario & E.C. de Macario (1993) C₁ bacteria in the water column of Chesapeake Bay, USA. II. The dominant oxygen and hydrogen sulphide-tolerant methylotrophic methanogens, coenriched with their oxidative and sulphate reducing bacterial consorts, are all new immunotypes and probably include new taxa. *Marine Ecology Progress Series*, **95**, 81-89.

Sills G.C. & Wheeler S.J. (1992) The significance of gas for offshore operations. *Continental Shelf Research*, **12**, 1239-1250.

Sills G.C. & Wheeler S.J., S.D. Thomas & T.N. Gardner (1991) The behaviour of offshore soils containing gas bubbles. *Geotechnique*, **41**, 227-242.

Smith P.F. (1988) Archaeobacteria and other specialized bacteria. In: *Microbial Lipids*. Vol I, C. Ratledge (ed.), Academic Press, New York pp. 499-537.

Smith G.C. & G.D. Floodgate (1992) A chemical method for estimating methanogenic biomass, *Continental Shelf Research*, **12**, 1187-1196.

Smith P.H. & R.E. Hungate (1958) Isolation and Characterisation of *Methanobacterium ruminantium* sp., *Journal of Bacteriology*, **75**, 713-718.

Smith M.R., S.H. Zinder & R.A. Mah (1980) Microbial methanogenesis from acetate. *Processes in Biochemistry*, **15**, 34-39.

Sokal R.R. & F.J. Rohlf (1969) *Biometry*. W.H. Freeman and Company, San Francisco, U.S.A., pp. 776.

Sorensen J., D. Christensen & B.B. Jorgensen (1981) Volatile fatty acids and hydrogen as substrates for sulphate reducing bacteria in anaerobic marine sediments. *Applied and Environmental Microbiology*, **42**, 5-11.

Sowers K.R., S.F. Baron & J.G. Ferry (1984) *Methanosarcina acetivorans* sp. nov., an actotrophic methane-producing bacterium isolated from marine sediments. *Applied and Environmental Microbiology*, **47**, 971-978.

Sprott G.D., M. Meloche & J.C. Richards (1991) Proportions of diether, macrocyclic diether, and tetraether lipids in *Methanococcus jannaschii* grown at different temperatures. *Journal of Bacteriology*, **173**, 3907-3910.

Stat-Oil News letter (1989) Stat-Oil, Stavanger, Norway.

Strayer R.F., & J.M. Tiedje (1978) Application of the fluorescent-antibody technique to the study of a methanogenic bacterium in lake sediments. *Applied and Environmental Microbiology*, **35**, 192-198.

Streitwieser A. & C.H. Heathcock (1985) *Introduction to Organic Chemistry*. 3rd edition Macmillan Publishing Company, New York, pp1197.

Stetter K.O., M. Thomin, J. Winter, G. Wildgruber, H. Huber, W. Zillig, D. Janecovic, H. Konig, P. Palm, S. Wunderl (1981) *Methanothermus fervidus* sp. nov. a novel thermophilic methanogen isolated from as Icelandic hot spring. *Zentralblatt fur Bakteriologie, Mikteriologie und Hygeine.*, I. Abt. Orig., **C2**, 166-178.

Taylor G.T. & S.J. Pirt (1977) Nutrition and factors limiting the growth of a methanogenic bacterium (*Methanobacterium thermoautotrophicum*), *Archives of Microbiology*, **133**, 17-22.

Teixidor P. & J.O. Grimalt (1992) Gas chromatographic determination of isoprenoid alkylglycerol diethers in archaeobacterial cultures and environmental samples. *Journal of Chromatography*, **607**, 253-259.

Tilbrook B.D. & D.M. Karl (1995) Methane sources, distributions and sinks from California coastal waters to the oligotrophic North Pacific gyre. *Marine Chemistry*, **49**, 51-64.

Tornabene T.G. & T.A. Langworthy (1978) Diphytanyl and Dibiphytanyl glycerol ethers in methanogenic bacteria. *Science*, **203**, 51-53.

Ullman W. & R.C. Aller (1982) Diffusion coefficients in nearshore marine sediments. *Limnology and Oceanography*, **27**, 552-555.

Van Es F.B. & L.A. Meyer-Reil (1982) Biomass and metabolic activity of heterotrophic marine bacteria. *Advances in Microbial Ecology*, **6**, 111-170.

Van Veldhoven P.P. & G.P. Mannaerts (1987) Inorganic and organic phosphate measurements in the nanomolar range. *Analytical Biochemistry*, **161**, 45-48.

Velji M.I. & L.J. Albright (1986) Microscopic enumeration of attached marine bacteria of seawater, marine sediment, fecal matter and kelp blade samples following pyrophosphate and ultrasound treatments. *Canadian Journal of Microbiology*, **32**, 121-125.

Vella A.J. & G. Holzer (1990) Ether-derived alkanes from sedimentary organic matter. *Organic Geochemistry*, **15**, 209-214.

Venables M. (1996) Archives Dept, Anglesey Borough Council, Llangefni, Anglesey, *pers comm*.

Wakeham S.G., C. Lee, J.W. Farrington & R.B. Gagosian (1984) Biogeochemistry of particulate matter in the oceans: results from sediment trap experiments. *Deep Sea Research*, **31**, 509-528.

Ward T.E. & J.I. Frea (1979) Estimation of microbial activities in lake sediments by measurement of sediment gas evolution. In: *Methodology for biomass determinations and microbial activities in sediments*, ASTM STP 673. C.D. Litchfield & P.L. Seyfried (eds.), American Society for Testing and Materials, Philadelphia, U.S.A., pp. 156-166.

Ward D.M. & Winfrey M.R. (1985) Interactions between methanogenic and sulphate-reducing bacteria in sediments. *Advances in Aquatic Microbiology*, **3**, 141-179.

Warford A.N. & D.R. Kosiur (1979) The effect of wastewater treatment on methanogenesis in marine outfall. *Journal of the Water Pollution control Federation*, **51**, 37-42.

Watson E. & S. Wilk (1974) Derivatization and gas chromatographic determination of some biologically important acids in cerebrospinal fluid. *Analytical Biochemistry*, **59**, 441-451.

Weisenburg D.A. & N.L. Guinasso (1979) Equilibrium solubilities of methane, carbon monoxide and hydrogen in water and seawater. *Journal of Chemical Engineering Data*, **24**, 356-360.

Wheeler S.J. (1990) Movement of large gas bubbles in unsaturated fine grained sediments. *Marine Geotechnology*, **9**, 113-129.

Wheeler S.J., G.C. Sills, W.K. Shaw, S.M. Duffy & D.G. Boden (1991) The influence of shallow gas on geotechnical properties. *Journal of the Society of Underwater Technology*, **17**, 11-16.

Whitaker M.J., E. Faber & M. Schoell (1986) Biogenic methane formation in marine and freshwater environments: carbon dioxide reduction *versus* acetate fermentation-isotopic evidence. *Geochimica et Cosmochimica Acta*, **50**, 693-709.

White D.C. (1983) Analysis of Microorganisms in terms of quantity and activity in natural environments. In: *Microbes in their Natural Environments* J.H. Slater (ed.) Cambridge University Press, Cambridge, pp. 37-66.

White D.C., R.J. Bobbie, J.S. Herron, J.D. King & S.J. Morrison (1979a) Biochemical measurements of microbial mass and activity from environmental samples. In: *Native Aquatic Bacteria: Enumeration, Activity, and Ecology*, ASTM STP 695, J.W. Costerton and R.R. Colwell, Eds., American Society for testing and materials, 69-81.

White D.C., R.J. Bobbie, J.D. King, J. Nickels & P. Amoe (1979b) Lipid analysis of sediments for microbial biomass and community structure. In: *Methodology for Biomass Determination and Microbial Activities in Sediments* ASTM STP 673. S.D. Litchfield & P.C. Seyfried (Eds.), American Society for testing and materials, 87-103.

White D.C., W.M. Davis, J.S. Nickels, J.D. King & R.J. Bobbie (1979c) Determination of the sedimentary microbial biomass by extractable lipid phosphate. *Oecologia*, **40**, 51-62.

White D.C. (1994) *Pers. comm.*, 1994

Wiesenburg D.A. & N.L. Guinasso (1979) Equilibrium solubilities of methane, carbon monoxide and hydrogen in water and seawater. *Journal of Chemical and Engineering Data*, **24**, 356-360.

Wilkinson B.J., M.R. Morman & D.C. White (1972) Phospholipid composition and metabolism of *Micrococcus denitrificans*. *Journal of Microbiology*, **112**, 1288-1294.

Winfrey M.R., D.G. Marty, A.J.M. Bianchi & D.M. Ward (1981) Vertical distribution of sulfate reduction, methane production, and bacteria in marine sediments. *Geomicrobiology Journal*, **2**, 341-362.

Woese C.R. (1977) A Comment on the methanogenic bacteria and the primitive ecology. *Journal of Molecular Evolution*, **9**, 369-371.

Woese C.R. (1981) Archaeobacteria. *Scientific American*, **244**, 94-107.

Woese C.R., L.J. Magrum & G.E. Fox (1978) Archaeobacteria. *Journal of Molecular Evolution*, **11**, 245-252.

Wood R. & F. Snyder (1966) Gas-liquid chromatographic analysis of long chain isomeric glyceryl monoethers. *Lipids*, **1**, 62-72.

Yancey P.H., M.E. Clark, S.C. Hand, R.D. Bowlus & G.N. Somero (1982) Living with water stress: evolution of osmolyte systems. *Science*, **217**, 1214-1222.

Yarrington M (1990) formerly of School of Ocean Sciences, University of Wales; Bangor, *pers. comm.*

Yuan F., J.D. Bennel & A.M. Davis (1992) Acoustic and physical characteristics of gassy sediments in the western Irish Sea. *Continental Shelf Research*, **12**, 1121-1134.

Zehnder A.J.B. & T.D. Brock (1979) Methane formation and methane oxidation by methanogenic bacteria. *Journal of Bacteriology*, **137**, 420-432.

Zeikus J.G. (1977) The biology of methanogenic bacteria. *Bacteriological Reviews*, **1**, 514-541.

APPENDIX I.**Media for the Culture of Methanogenic Bacteria****A1.1. Medium No.3 as described by Balch *et al.*, (1979).**Medium (g l⁻¹)

NaCl	18.0	Fe(NH ₄)(SO ₄) ₂ .7H ₂ O	0.002
NaHCO ₃	5.0	Sodium acetate	1.0
Yeast extract (Difco)	2.0	Trypticase (Difco)	2.0
L-Cysteine-HCl	0.5	Na ₂ S.9H ₂ O	0.5
Na ₂ MoO ₄ .2H ₂ O	4.84	(Alperin & Reeburgh, 1985)	

Mineral Solution (3d)

KCl	0.67	MgCl ₂ .6H ₂ O	8.52
MgSO ₄ .7H ₂ O	6.90	NH ₄ Cl	0.50
CaCl ₂ .2H ₂ O	0.28	K ₂ HPO ₄	0.28

Mineral solution (3d) was made up to 1 litre with distilled water and 500 ml was taken for every 1 litre of total media required.

Trace Mineral Solution (e)

H ₃ BO ₃	0.01	Na ₂ MoO ₄ .2H ₂ O	0.01
CaCl ₂ .2H ₂ O	0.1	Nitrilotriacetic acid	1.5
MgSO ₄ .7H ₂ O	3.0	MnSO ₄ .2H ₂ O	0.5
NaCl	1.0	FeSO ₄ .2H ₂ O	0.1
CoCl ₂ .6H ₂ O	0.183	Na ₂ SeO ₃	0.01
Na ₂ WO ₄ .2H ₂ O	0.01	(Van Bruggen <i>et al.</i> , 1986)	

The nitrilotriacetic acid was initially dissolved in potassium hydroxide to a pH = 5.5. The minerals were then added and the pH adjusted to 7.0 using KOH. Trace mineral solution (e) (Balch *et al.*, 1979) was supplemented further with:

Trace Vitamin Solution (f) (mg l⁻¹)

Biotin	2.0	Folic acid	2.0
Pyridoxine HCl	10.0	Thiamine hydrochloride	5.0
Riboflavin	5.0	Nicotinic acid	5.0
DL-calcium pantothenate	5.0	Vitamin B12	0.1
p-aminobenzoic acid	5.0	Lipoic (thioctic) acid	5.0

A1.2. Growth Media for *Methanococcoides methylutens*

Methanococcoides methylutens was received from Dr K Sowers (UCLA). Trimethylamine and methanol were the only carbon substrates to be metabolised by this methanogen. Trimethylamine HCl (3.0 g l⁻¹) was used as the substrate in all preparations of this species. Media is prepared under 80 % nitrogen and 20 % carbon dioxide to a final pH = 7.0 - 7.2. Incubation temperature 30 °C.

Growth Media (g l⁻¹)

KCl	0.34	MgCl ₂ ·6H ₂ O	4.0
MgSO ₄ ·7H ₂ O	3.45	NH ₄ Cl	0.25
CaCl ₂ ·2H ₂ O	0.14	K ₂ HPO ₄	0.14
NaCl	18.0	Fe(NH ₄) ₂ (SO ₄) ₂ ·7H ₂ O	0.002
NaHCO ₃	5.0	Yeast Extract (Difco)	2.0
Trypticase	2.0	Resasurin	0.001
Vitamin Solution	10.0 ml	(Balch <i>et al.</i> , 1979)	
Trace Minerals	10.0 ml	(Balch <i>et al.</i> , 1979)	
Cysteine HCl	0.5	Sodium sulphide	0.5

A1.3. Growth media for *Methanosarcina acetivorans*

This medium was similar to that for *Methanococcoides methylutens* (Appendix A1.2) and was supplemented with 1.64 g l⁻¹ of sodium acetate.

A1.4. Growth Media for *Methanolobus tindarius*

The medium for *Methanolobus tindarius* was prepared using most of the ingredients of medium No.3 of Balch *et al.* (1979), except instead of using sodium acetate, yeast extract and trypticase, the media was supplemented with the following:

Trimethylamine (100%)	5.3 ml l ⁻¹
Methanol	5.0 ml l ⁻¹
Rumen fluid	10 ml l ⁻¹

The pH was adjusted to 6.2 before autoclaving at 2 Bar nitrogen/carbon dioxide which was recommended to prevent the pH shift from neutral to alkaline. However, the alternative method of section 2.1.2 of Chapter 2 also prevented the shift in pH.

A1.5. Media used for the Most Probable Number (MPN) Determination

The medium described below was based on medium No.3 of Balch *et al*, (1979) and was used as a suitable growth medium for the most probable number determination of all marine sediment methanogens.

Media (g l⁻¹)

KCl	0.34	MgCl ₂ .6H ₂ O	4.26
MgSO ₄ .7H ₂ O	3.45	NH ₄ Cl	0.25
CaCl ₂ .2H ₂ O	0.14	K ₂ HPO ₄	0.14
Fe(NH ₄)(SO ₄) ₂ .7H ₂ O	0.002	NaHCO ₃	5.0
NaCl	18.0	NaMoO ₄ .2H ₂ O	4.84
Trypticase	2.0	Yeast Extract	2.0
Rumen Fluid	10.0 ml	Sediment Extract	10.0 ml
Trace minerals	10.0 ml	Trace vitamins	10.0 ml
Trimethylamine	3.0 ml	Sodium acetate	1.0
Methanol	1.0 ml	Resasurin	0.0001
Distilled water	1000 ml		

APPENDIX II**Comparison of Peak Height and Peak Area units of Measurement for the GC Determination of Methane by Regression Analysis**

Regression analysis of peak area and peak height units *versus* the concentration of methane injected on to the chromatograph revealed that peak area ($r^2 = 0.99$) gave more consistent results than peak height ($r^2 = 0.95$).

Table A2.1. Comparison of peak height and peak area units of measurement for the gas chromatographic determination of methane by regression analysis.

Moles of Methane Injected ($\times 10^{-16}$)	Peak Area	Peak Height
1.79	47001	3779
1.79	72525	3408
1.79	81297	5183
4.48	155449	7960
4.48	124799	6723
4.48	79462	6757
22.4	208415	17984
22.4	198683	10155
22.4	188005	18851
44.8	450883	11472
44.8	439641	14859
44.8	412567	21029
89.5	1046212	66637
89.5	1010216	36779
89.5	1002097	104157
448	4781122	317227
448	5285582	572443
448	4802006	308792
1340	11821440	836085
1340	11630904	834165
1340	11383111	834392
	$r^2 = 0.99$ $p \ll 0.001$	$r^2 = 0.95$ $p \ll 0.001$

APPENDIX III**Statistical equation used to determine 95% confidence intervals of the methane data.**

Estimation of X (log₁₀ moles of methane) from Y (log₁₀ GC peak area) using the following regression equations which are given in more detail in section 14.7 of Sokal and Rohlf, (1969).

$$H = \frac{t_{0.05 [n-2]}}{D} \sqrt{S_{y.x}^2 \left[D \left(\frac{1}{\bar{a}} + \frac{1}{\bar{n}} \right) + \frac{(Y_i - \bar{Y})^2}{\sum x^2} \right]}$$

where

$$D = b_{y.x}^2 - t_{0.05 [n-2]}^2 S_b^2$$

and the 95 % confidence intervals are:

$$L_1 = \bar{X} + \frac{b_{y.x} (Y_i - \bar{Y})^2}{D} - H$$

$$L_2 = \bar{X} + \frac{b_{y.x} (Y_i - \bar{Y})^2}{D} + H$$

where n = the number of calibration points

a = number of groups in the anova

$b_{y.x}$ = slope of the calibration line (*i.e.* $\Sigma xy / \Sigma x^2$) (regression coefficient).

$\Sigma \hat{y}^2 = (\Sigma xy)^2 / \Sigma x^2$ (the explained sum of squares).

$\Sigma d^2_{yx} = \Sigma y^2 - \Sigma \hat{y}^2$ (the unexplained sum of squares).

$s^2_{y.x} = (\Sigma d^2_{yx}) / n - 2$

$s_b = \sqrt{(s^2_{y.x} / \Sigma x^2)}$ (standard error of the regression coefficient).

\bar{Y} = mean Y point in the calibration line.

Y_i = log₁₀ GC peak area of the sample.

\bar{X} = mean X point in the calibration line.

$t_{0.05 [n-2]}$ = two tailed t distribution for n-2 degrees of freedom.

APPENDIX IV**Typical outputs from the sonic viewer when determining the sound velocity through the sediment sections**

The outputs from the sonic viewer using a signal of 250 KHz through the consolidation apparatus are given below. The two printouts show the time elapsed from time zero to the time taken for the signal to pass through a gas-free (A) and gas-charged (acoustically turbid) (B) sediment. The time elapsed from sending the signal to receiving it was accurately measured using the cross-hairs on the sonic viewer. The divisions on the printouts between time zero and the signal are in 5 micro-second (μs) intervals. Typical values of $61 \mu\text{s}$ (*i.e.* 1639 ms^{-1}) for the gas-free sediments and $68 \mu\text{s}$ (*i.e.* 1471 ms^{-1}) for the gas-charged sediments of Holyhead Harbour were recorded across the 10 cm diameter of the core barrel. Values of $34.8 \mu\text{s}$ (*i.e.* 1437 ms^{-1}) for gas free and $37.4 \mu\text{s}$ (*i.e.* 1337 ms^{-1}) for gas charged sediments across the 5 cm core barrel of the consolidation apparatus. The 95 % confidence limits of the sound velocities were small for the Holyhead determinations (section 5.5.1) and large for the determinations made for the consolidation apparatus (section 6.2) which is expected to be a function of the material used to house the sediment.

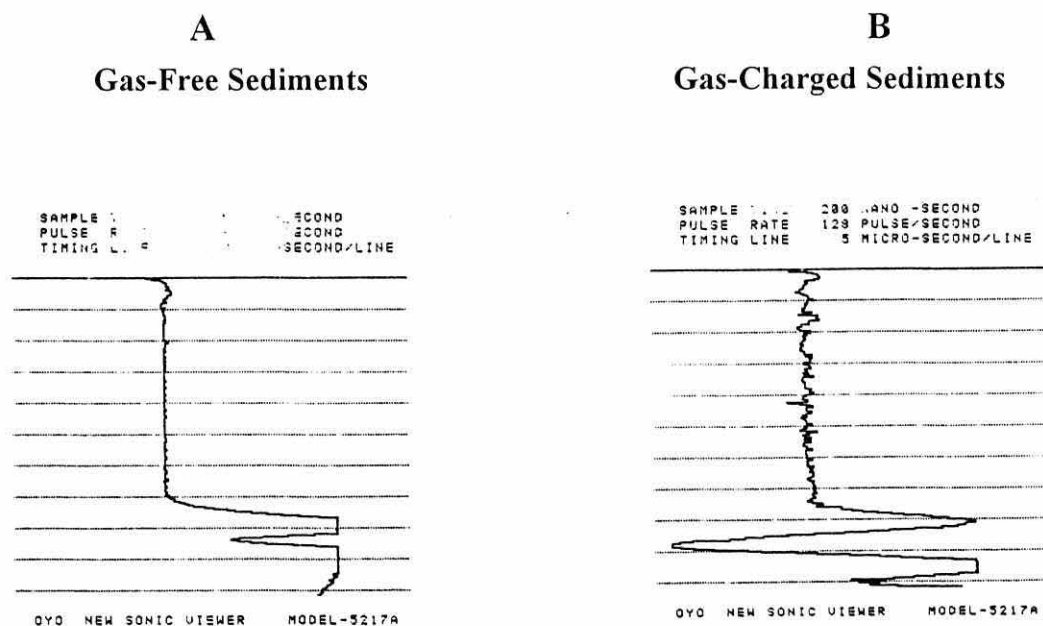


Figure A1. Specimen oscilloscope print-outs of gas free (A) and acoustically turbid (B) sediments prepared in the consolidation apparatus.

APPENDIX V**A5.1 Phospholipid Phosphate Calibration**

The method for the spectrophotometric determination of phospholipid phosphate is given in Findlay *et al.* (1989). The phospholipid used in the calibration experiment was phosphatidylcholine dipentadecanoyl (PPCDPD) and the range of phosphate equivalent molar concentrations that were used are given in table A5.1.1. Potassium persulphate in sulphuric acid was the oxidising agent to release the phosphate from the phospholipids. This reaction was also completed on an inorganic phosphate (KH_2PO_4).

For the methanogenic ether lipids extract the phospholipid phosphate determination required the removal of an aliquot of the total sample. However, it was anticipated that for certain samples with a low ether lipid concentration this aliquot could reduce the ether lipid concentration to below the detection limit for the method. Therefore the aqueous products of the acid methanolysis (*i.e.* ether lipids chemically removed) were also used for the determination of phospholipid phosphate for samples with a low ether lipid concentration (see section 2.13.3 of chapter 2). The aqueous products were evaporated down before adopting the method of Findlay *et al.* (1989). Calibration results for the organic phosphate, inorganic phosphate and the phosphate released after acid methanolysis are given in table A5.1.1 and are also represented in figure A5.1.2.

Table A5.1.1. Calibration data of organic, inorganic and acid methanolysis phosphate using the method of Findlay *et al.* (1989).

ABSORBANCE at 610 nm			Equivalent Concentration of Phosphate (nmoles PO_4)
Inorganic Phosphate (KH_2PO_4)	Organic Phosphate (PPCDPD)*	Aqueous Products of Methanolysis	
0.00	0.00	0.00	0.00
-	0.09	-	0.75
-	0.17	-	1.50
0.20	-	-	2.75
-	0.22	-	4.50
0.37	-	0.40	5.51
-	0.62	0.69	9.10
0.80	-	-	11.02
-	-	0.83	13.60
1.31	-	-	16.53
-	1.21	1.23	18.20
-	1.52	-	22.70

*PPCDPD = phosphatidyl choline dipentadecanoyl.

"-" non equivalent phosphate concentrations were used.

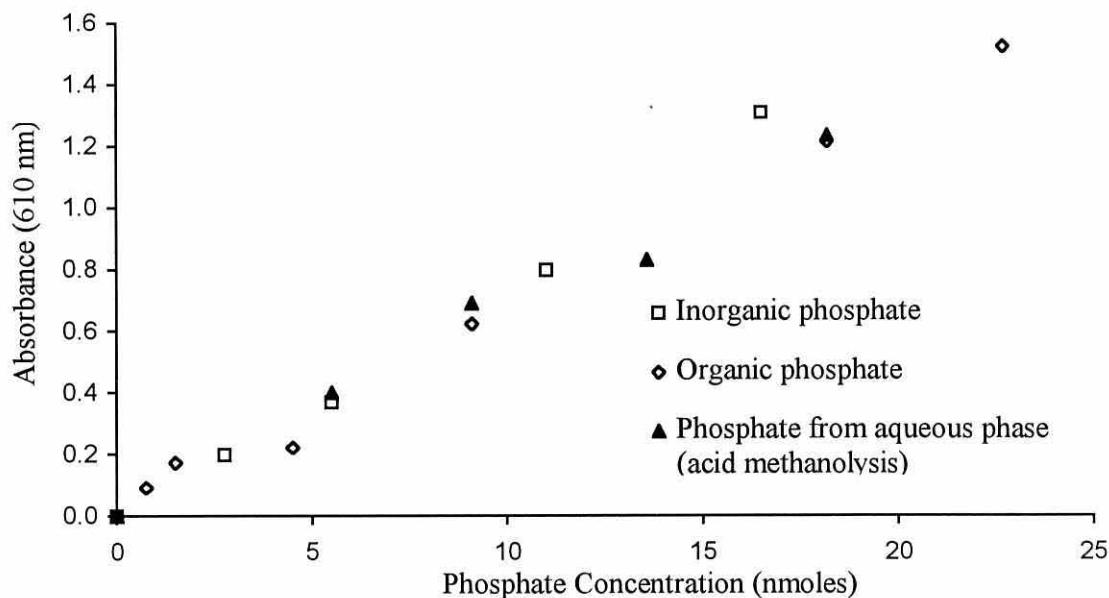


Figure A5.1.2. Phosphate calibration graphs for inorganic, organic and acid methanolysis phosphate products using the method of Findlay *et al.* (1989).

Regression analysis gave a high correlation between the phosphate concentration and absorbance at 610 nm for the inorganic phosphate ($r = 0.997$, $p < 0.001$), the organic phosphate ($r = 0.997$, $p < 0.001$) and for the phosphate product of the aqueous phase collected after acid methanolysis ($r = 0.968$, $p < 0.01$). The slopes were all comparable at the 95% confidence level.

A5.2 Sulphate Calibration

The concentration of dissolved sulphate in the pore waters of the sediment was determined using the method of Howarth (1978). Table A5.2.1 shows the sulphate calibration data which was linear and demonstrated a high correlation coefficient (*i.e.* $r = 0.996$, $p < 0.001$). A summary of the method is given in section 2.11 of chapter 2.

A5.3. Sulphide Calibration

The concentration of the dissolved sulphide in the pore waters of the sediment was determined using the method of Cline (1969). Calibration data for the three sulphide concentration ranges are given in table A5.3.1. The following correlation coefficients were reported for each concentration range: 3-40 μM , $r = 0.954$; 40-250 μM , $r = 0.979$; 250-1000 μM , $r = 0.992$, all of which were significant at $p < 0.001$. In practice all sediment sulphide concentrations required the lowest calibration concentration range, *i.e.* 3-40 μM . See section 2.12 of chapter 2 for a summary of the method.

Table A5.2.1. Calibration data for the method of determining sulphate concentrations in sediment pore waters (Howarth, 1978).

Sulphate Concentration (mM)	Volume of titrant (MgCl ₂ , 0.025M) Added (ml)	Volume of mean blank minus volume of standards (ml)
0	2.11	0.00
6.0	1.81	0.30
10.3	1.76	0.35
16.2	1.46	0.65
22.1	1.19	0.92
29.7	0.88	1.23

Table A5.3.1. Calibration data for the method of determining sulphide concentrations in sediment pore waters (Cline, 1969).

3-40 μ M		40-250 μ M		250-1000 μ M	
Sulphide Concentration (μ M)	Absorbance minus the blank (670 nm)	Sulphide Concentration (μ M)	Absorbance minus the blank (670 nm)	Sulphide Concentration (μ M)	Absorbance minus the blank (670 nm)
10	0.100	51	0.091	307	0.166
10	0.151	51	0.090	307	0.158
10	0.120	51	0.089	307	0.174
20	0.143	102	0.171	512	0.272
20	0.151	102	0.137	512	0.253
20	0.154	102	0.144	512	0.236
31	0.247	154	0.253	717	0.336
31	0.267	154	0.206	717	0.318
31	0.266	154	0.203	717	0.341
41	0.315	205	0.322	922	0.382
41	0.339	205	0.302	922	0.396
41	0.389	205	0.305	922	0.416
		256	0.347	1024	0.445
		256	0.317	1024	0.444
		256	0.343	1024	0.431

APPENDIX VI**Ether Lipid Data Collected by Gas Chromatography**

Peak area and retention time data of all ether lipids including internal and external standards analysed by gas chromatography from Holyhead and intertidal sediment samples. Calculations of the ether lipid concentrations were made following the procedure given in Appendix VII. Calculations include the independent quantification of the non-methanogenic dihydrophytol lipid and subsequent subtraction from the diether lipid (C₂₀, DPGE) which it can interfere with during this method.

Ether lipids include; C₂₀ = C₂₀H₄₂ ; C_{40,0} = C₄₀H₈₂ ; C_{40,1} = C₄₀H₈₀ ;
C_{40,2} = C₄₀H₇₈ ; C_{40,?} = C₄₀H_?

Sample No17A T Depth 3-8cm Vol.Inj:1µL/500 Spl.Fract: ¹⁹ / ₄₀	C ₁₆ H ₃₄ Int. Std.	C ₁₉ H ₄₀ Ext. Std.	C ₂₀ H ₄₂ DPGE + Phytol	C ₄₀ H ₈₂ (0xC ₅ ring)	C ₄₀ H ₈₀ (1xC ₅ ring)	C ₄₀ H ₇₈ (2xC ₅ ring)	C ₄₀ H _? (3xC ₅ ring)
Ret.time (mins)	11.88	13.99	15.77	38.05	39.19	40.41	41.11
Peak Area (PA) (x10 ³ units)	1677	1972	173.9	635.2	53.17	284.2	323.9
Conc.(µg) per sample (50.86g)			27.69	102.1	8.55	45.68	52.07
Conc. C ₂₀ , C ₄₀ derivatives per dry gram (µg/g)			0.54 -0.07* 0.47	2.01	0.17	0.90	1.02
Conc. DPGE, bi- DPGE per dry gram (µg/g)			0.54	2.32	0.19	0.99	1.13
Moles (nano) per dry gram (nmoles/g)			0.83	1.79	0.15	0.80	0.92
Dihydrophytol Determination PA x10 ³ Vol. Injected: 1µL of 300 Phytanyl acetate Rt=21.74 PA= 134.3 Heneicosanyl acetate Rt=26.45 PA= 1825 *Concentration per gram = 0.07 µg/g Sample fraction: 19/40 Yield = 46 %							

Sample No17A B Depth 8-13cm Vol.Inj:1µL/500 Spl.Fract: ¹⁹ / ₄₀	C ₁₆ H ₃₄ Int. Std.	C ₁₉ H ₄₀ Ext. Std.	C ₂₀ H ₄₂ DPGE + Phytol	C ₄₀ H ₈₂ (0xC ₅ ring)	C ₄₀ H ₈₀ (1xC ₅ ring)	C ₄₀ H ₇₈ (2xC ₅ ring)	C ₄₀ H ₇₆ (3xC ₅ ring)
Ret.time (mins)	11.88	13.97	15.79	38.04	39.18	40.40	41.41
Peak Area (PA) (x10 ³ units)	1390	1897	160.5	716.3	61.55	183.7	124.0
Conc.(µg) per sample (53.43g)			30.82	138.9	11.93	35.62	24.04
Conc. C ₂₀ , C ₄₀ derivatives per dry gram (µg/g)			0.58				
			-0.05*				
			0.53	2.60	0.22	0.67	0.45
Conc. DPGE, bi- DPGE per dry gram (µg/g)			0.58	2.87	0.25	0.74	0.50
Moles (nano) per dry gram (nmoles/g)			0.94	2.31	0.20	0.60	0.40
Dihydrophytol Determination PA= x10 ³ Vol. Injected: 1µL of 300 Phytanyl acetate Rt=21.67 PA= 59.7 Heneicosanyl acetate Rt=26.37 PA= 1274 *Concentration per gram = 0.05µg/g Sample fraction: 19/40 Yield = 40 %							

Sample No. 15A Depth 20-30cm Vol.Inj:1µL/500 Spl.Fract: ¹⁹ / ₄₀	C ₁₆ H ₃₄ Int. Std.	C ₁₉ H ₄₀ Ext. Std.	C ₂₀ H ₄₂ DPGE + Phytol	C ₄₀ H ₈₂ (0xC ₅ ring)	C ₄₀ H ₈₀ (1xC ₅ ring)	C ₄₀ H ₇₈ (2xC ₅ ring)	C ₄₀ H ₇₆ (3xC ₅ ring)
Ret.time (mins)	11.90	14.01	15.81	38.03	39.19	40.40	41.11
Peak Area (PA) (x10 ³ units)	1230	2080	126.8	560.2	47.58	243.1	273.7
Conc.(µg) per sample (49.50g)			27.52	122.8	10.43	53.28	60.01
Conc. C ₂₀ , C ₄₀ derivatives per dry gram (µg/g)			0.56				
			-0.06*				
			0.50	2.48	0.21	1.08	1.21
Conc. DPGE, bi- DPGE per dry gram (µg/g)			0.58	2.88	0.25	1.25	1.41
Moles (nano) per dry gram (nmoles/g)			0.89	2.21	0.19	0.97	1.09
Dihydrophytol Determination PA x10 ³ Vol. Injected: 1µL of 300 Phytanyl acetate Rt=21.70 PA= 73.91 Heneicosanyl acetate Rt=26.39 PA= 1699 *Concentration per gram = 0.06 µg/g Sample fraction:19/40 Yield = 33 %							

Sample No.13A Depth 40-50cm Vol.Inj:1μL/500 Spl.Fract:19/40	C ₁₆ H ₃₄ Int. Std.	C ₁₉ H ₄₀ Ext. Std.	C ₂₀ H ₄₂ DPGE + Phytol	C ₄₀ H ₈₂ (0xC ₅ ring)	C ₄₀ H ₈₀ (1xC ₅ ring)	C ₄₀ H ₇₈ (2xC ₅ ring)	C ₄₀ H ₇₆ (3xC ₅ ring)
Ret.time (mins)	11.92	14.01	15.81	38.02	39.18	40.37	41.09
Peak Area (PA) (x10 ³ units)	1308	1681	161.6	719.3	98.03	291.8	330.2
Conc.(μg) per sample (50.82g)			32.97	148.2	20.20	60.12	68.02
Conc. C ₂₀ , C ₄₀ derivatives per gram (μg/g)			0.65 -0.02* 0.63	2.92	0.40	1.18	1.34
Conc. DPGE, bi- DPGE per dry gram (μg/g)			0.73	3.38	0.46	1.37	1.55
Moles (nano) per dry gram (nmoles/g)			1.11	2.59	0.35	1.06	1.20
Dihydrophytol Determination PA x10 ³ Vol. Injected: 1μL of 300 Phytanyl acetate Rt=21.69 PA= 30.9 Heneicosanyl acetate Rt=26.33 PA= 1301 *Concentration per gram = 0.02 μg/g Sample fraction:19/40 Yield = 41 %							

Sample No. 11A Depth 60-70cm Vol.Inj:1μL/500 Spl.Fract:19/40	C ₁₆ H ₃₄ Int. Std.	C ₁₉ H ₄₀ Ext. Std.	C ₂₀ H ₄₂ DPGE + Phytol	C ₄₀ H ₈₂ (0xC ₅ ring)	C ₄₀ H ₈₀ (1xC ₅ ring)	C ₄₀ H ₇₈ (2xC ₅ ring)	C ₄₀ H ₇₆ (3xC ₅ ring)
Ret.time (mins)	11.93	14.03	15.81	38.03	39.19	40.40	41.11
Peak Area (PA) (x10 ³ units)	1754	2201	173.0	444.1	38.32	201.0	223.0
Conc.(μg) per sample (52.14g)			26.33	68.27	5.89	30.91	34.28
Conc. C ₂₀ , C ₄₀ derivatives per dry gram (μg/g)			0.50 -0.02* 0.48	1.31	0.11	0.59	0.66
Conc. DPGE, bi- DPGE per dry gram (μg/g)			0.56	1.52	0.13	0.69	0.76
Moles (nano) per dry gram (nmoles/g)			0.86	1.16	0.10	0.53	0.59
Dihydrophytol Determination PA x10 ³ Vol. Injected: 1μL of 300 Phytanyl acetate Rt=21.65 PA= 31.15 Heneicosanyl acetate Rt=26.35 PA= 1271 *Concentration per gram = 0.02 μg/g Sample fraction:19/40 Yield = 44 %							

Sample No. 9A Depth 80-90cm Vol.Inj:1μL/500 Spl.Fract: ¹⁹ / ₄₀	C ₁₆ H ₃₄ Int. Std.	C ₁₉ H ₄₀ Ext. Std.	C ₂₀ H ₄₂ DPGE + Phytol	C ₄₀ H ₈₂ (0xC ₅ ring)	C ₄₀ H ₈₀ (1xC ₅ ring)	C ₄₀ H ₇₈ (2xC ₅ ring)	C ₄₀ H ₇₆ (3xC ₅ ring)
Ret.time (mins)	11.91	14.01	15.78	38.04	39.17	40.40	41.10
Peak Area (PA) (x10 ³ units)	1530	2019	157.5	636.9	58.39	312.1	278.4
Conc.(μg) per sample (54.19g)			27.49	112.3	10.29	55.01	49.06
Conc. C ₂₀ , C ₄₀ derivatives per gram (μg/g)			0.51 -0.02* 0.49	2.07	0.22	1.18	1.05
Conc. DPGE, bi- DPGE per dry gram (μg/g)			0.56	2.40	0.22	1.18	1.05
Moles (nano) per dry gram (nmoles/g)			0.86	1.84	0.17	0.91	0.81
Dihydrophytol Determination $\frac{PA \times 10^3}{Vol. \text{ Injected: } 1\mu\text{L of } 300}$ Phytanyl acetate Rt=21.64 PA= 30.3 Heneicosanyl acetate Rt=26.33 PA= 1307 *Concentration per gram = 0.02 μg/g Sample fraction:19/40 Yield = 42 %							

Sample No. 7A i Depth 100-110cm Vol.Inj:1μL/500 Spl.Fract: ¹⁹ / ₄₀	C ₁₆ H ₃₄ Int. Std.	C ₁₉ H ₄₀ Ext. Std.	C ₂₀ H ₄₂ DPGE + Phytol	C ₄₀ H ₈₂ (0xC ₅ ring)	C ₄₀ H ₈₀ (1xC ₅ ring)	C ₄₀ H ₇₈ (2xC ₅ ring)	C ₄₀ H ₇₆ (3xC ₅ ring)
Ret.time (mins)	11.86	13.97	15.75	37.96	39.12	40.32	41.01
Peak Area (PA) (x10 ³ units)	1034	1878	86.12	170.9	11.41	78.35	90.27
Conc.(μg) per sample (51.95g)			22.22	44.52	2.97	20.42	23.52
Conc. C ₂₀ , C ₄₀ derivatives per dry gram (μg/g)			0.43 -0.02* 0.41	0.86	0.06	0.39	0.45
Conc. DPGE, bi- DPGE per dry gram (μg/g)			0.48	0.99	0.07	0.46	0.53
Moles (nano) per dry gram (nmoles/g)			0.73	0.76	0.05	0.35	0.41
Dihydrophytol Determination $\frac{PA \times 10^3}{Vol. \text{ Injected: } 1\mu\text{L of } 300}$ Phytanyl acetate Rt=21.65 PA= 31.15 Heneicosanyl acetate Rt=26.35 PA= 1271 *Concentration per gram = 0.02 μg/g Sample fraction:19/40 Yield = 15 %							

Sample No. 5A Depth 120-130cm Vol.Inj:1 μ L/500 Spl.Fract:19/40	C ₁₆ H ₃₄ Int. Std.	C ₁₉ H ₄₀ Ext. Std.	C ₂₀ H ₄₂ DPGE + Phytol	C ₄₀ H ₈₂ (0xC ₅ ring)	C ₄₀ H ₈₀ (1xC ₅ ring)	C ₄₀ H ₇₈ (2xC ₅ ring)	C ₄₀ H ₇₆ (3xC ₅ ring)
Ret.time (mins)	11.85	13.99	15.75	37.97	39.15	40.32	41.03
Peak Area (PA) (x10 ³ units)	517.1	1874	52.83	67.43	14.98	49.47	48.25
Conc.(μ g) per sample (54.19g)			27.27	35.15	7.81	25.79	25.15
Conc. C ₂₀ , C ₄₀ derivatives per gram (μ g/g)			0.54 -0.02* 0.52	0.70	0.16	0.51	0.50
Conc. DPGE, bi- DPGE per dry gram (μ g/g)			0.60	0.81	0.18	0.60	0.58
Moles (nano) per dry gram (nmoles/g)			0.92	0.62	0.14	0.46	0.45
Dihydrophytol Determination PA x10³ Vol. Injected: 1 μ L of 300 Phytanyl acetate Rt=21.64 PA= 30.3 Heneicosanyl acetate Rt=26.33 PA= 1307 *Concentration per gram = 0.02 μ g/g Sample fraction:19/40 Yield = 15 %							

Sample No. 3A Depth 140-150cm Vol.Inj:1 μ L/500 Spl.Fract:19/40	C ₁₆ H ₃₄ Int. Std.	C ₁₉ H ₄₀ Ext. Std.	C ₂₀ H ₄₂ DPGE + Phytol	C ₄₀ H ₈₂ (0xC ₅ ring)	C ₄₀ H ₈₀ (1xC ₅ ring)	C ₄₀ H ₇₈ (2xC ₅ ring)	C ₄₀ H ₇₆ (3xC ₅ ring)
Ret.time (mins)	11.86	14.00	15.78	37.97	N.D.	40.35	41.06
Peak Area (PA) (x10 ³ units)	299.7	1832	46.65	48.12	N.D.	29.16	22.89
Conc.(μ g) per sample (53.08g)			41.56	43.28	N.D.	26.23	20.59
Conc. C ₂₀ , C ₄₀ derivatives per dry gram (μ g/g)			0.78 -0.02* 0.76	0.82	N.D.	0.50	0.39
Conc. DPGE, bi- DPGE per dry gram (μ g/g)			0.88	0.95	N.D.	0.57	0.45
Moles (nano) per dry gram (nmoles/g)			1.34	0.73	N.D.	0.44	0.35
Dihydrophytol Determination PA x10³ Vol. Injected: 1 μ L of 300 Phytanyl acetate Rt=21.65 PA= 31.15 Heneicosanyl acetate Rt=26.35 PA= 1271 *Concentration per gram = 0.02 μ g/g Sample fraction:19/40 Yield = 9 %							

Sample No. 1A Depth 160-170cm Vol.Inj:1 μ L/500 Spl.Fract: ¹⁹ / ₄₀	C ₁₆ H ₃₄ Int. Std.	C ₁₉ H ₄₀ Ext. Std.	C ₂₀ H ₄₂ DPGE + Phytol	C ₄₀ H ₈₂ (0xC ₅ ring)	C ₄₀ H ₈₀ (1xC ₅ ring)	C ₄₀ H ₇₈ (2xC ₅ ring)	C ₄₀ H ₇₆ (3xC ₅ ring)
Ret.time (mins)	11.84	13.99	15.77	38.00	N.D.	40.38	41.09
Peak Area (PA) (x10 ³ units)	384.1	1949	72.72	42.84	N.D.	25.40	25.62
Conc.(μ g) per sample (53.97g)			50.55	30.07	N.D.	17.83	17.98
Conc. C ₂₀ , C ₄₀ derivatives per gram (μ g/g)			0.94 -0.02* 0.92	0.56	N.D.	0.33	0.33
Conc. DPGE, bi- DPGE per dry gram (μ g/g)			1.07	0.65	N.D.	0.38	0.39
Moles (<i>nano</i>) per dry gram (<i>nmoles</i> /g)			1.63	0.50	N.D.	0.30	0.30
Dihydrophytol Determination PA x10 ³ Vol. Injected: 1 μ L of 300 Phytanyl acetate Rt=21.64 PA= 30.3 Heneicosanyl acetate Rt=26.33 PA= 1307 *Concentration per gram = 0.02 μ g/g Sample fraction:19/40 Yield = 10 %							

Sample No.17B Depth 0-10cm Vol.Inj:1µL/500 Spl.Fract: ¹⁹ / ₈₀	C ₁₆ H ₃₄ Int. Std.	C ₁₉ H ₄₀ Ext. Std.	C ₂₀ H ₄₂ DPGE + Phytol	C ₄₀ H ₈₂ (0xC ₅ ring)	C ₄₀ H ₈₀ (1xC ₅ ring)	C ₄₀ H ₇₈ (2xC ₅ ring)	C ₄₀ H ₇₆ (3xC ₅ ring)
Ret.time (mins)	11.85	14.01	15.80	38.01	N.D.	40.41	41.13
Peak Area (PA) (x10 ³ units)	212.7	1973	41.62	44.44	N.D.	31.40	26.88
Conc.(µg) per sample (48.95g)			52.24	56.33	N.D.	39.81	34.07
Conc. C ₂₀ , C ₄₀ derivatives per dry gram (µg/g)			1.07 -0.10* 0.97	1.15	N.D.	0.81	0.70
Conc. DPGE, bi- DPGE per dry gram (µg/g)			1.12	1.34	N.D.	0.95	0.81
Moles (nano) per dry gram (nmoles/g)			1.72	1.02	N.D.	0.73	0.62
Dihydrophytol Determination PA x10 ³ Vol. Injected: 1µL of 100 Phytanyl acetate Rt=21.35 PA= 14.98 Heneicosanyl acetate Rt=26.16 PA= 190.2 *Concentration per gram = 0.10 µg/g Sample fraction:19/40 Yield = 12 %							

Sample No. 15B Depth 15-25cm Vol.Inj:1µL/500 Spl.Fract: ¹⁹ / ₈₀	C ₁₆ H ₃₄ Int. Std.	C ₁₉ H ₄₀ Ext. Std.	C ₂₀ H ₄₂ DPGE + Phytol	C ₄₀ H ₈₂ (0xC ₅ ring)	C ₄₀ H ₈₀ (1xC ₅ ring)	C ₄₀ H ₇₈ (2xC ₅ ring)	C ₄₀ H ₇₆ (3xC ₅ ring)
Ret.time (mins)	11.84	13.99	15.78	37.99	N.D.	40.36	41.06
Peak Area (PA) (x10 ³ units)	122.5	1943	33.25	20.23	N.D.	20.32	18.04
Conc.(µg) per sample (51.99g)			72.43	44.50	N.D.	41.71	39.70
Conc. C ₂₀ , C ₄₀ derivatives per dry gram (µg/g)			1.39 -0.47* 0.92	0.86	N.D.	0.80	0.76
Conc. DPGE, bi- DPGE per dry gram (µg/g)			1.07	0.99	N.D.	0.93	0.89
Moles (nano) per dry gram (nmoles/g)			1.64	0.76	N.D.	0.72	0.68
Dihydrophytol Determination PA x10 ³ Vol. Injected: 1µL of 100 Phytanyl acetate Rt=21.68 PA= 45.0 Heneicosanyl acetate Rt=26.38 PA= 185.6 *Concentration per gram = 0.47 µg/g Sample fraction:19/40 Yield = 7 %							

Sample No. 11B Depth 55-65cm Vol.Inj:1µL/500 Spl.Fract: ¹⁹ / ₈₀	C ₁₆ H ₃₄ Int. Std.	C ₁₉ H ₄₀ Ext. Std.	C ₂₀ H ₄₂ DPGE + Phytol	C ₄₀ H ₈₂ (0xC ₅ ring)	C ₄₀ H ₈₀ (1xC ₅ ring)	C ₄₀ H ₇₈ (2xC ₅ ring)	C ₄₀ H ₇₆ (3xC ₅ ring)
Ret.time (mins)	11.97	14.09	15.90	38.10	N.D.	40.45	41.20
Peak Area (PA) (x10 ³ units)	196.1	1916	37.66	18.83	N.D.	11.56	11.90
Conc.(µg) per sample (51.58g)			51.27	25.89	N.D.	15.89	16.37
Conc. C ₂₀ , C ₄₀ derivatives per dry gram (µg/g)			0.99 -0.09* 0.90	0.50	N.D.	0.31	0.32
Conc. DPGE, bi- DPGE per dry gram (µg/g)			1.04	0.58	N.D.	0.36	0.37
Moles (nano) per dry gram (nmoles/g)			1.59	0.45	N.D.	0.28	0.28
Dihydrophytol Determination PA x10 ³ Vol. Injected: 1µL of 100 Phytanyl acetate Rt=21.38 PA= 15.97 Heneicosanyl acetate Rt=26.16 PA= 207.0 *Concentration per gram = 0.09 µg/g Sample fraction: 19/40 Yield = 11 %							

Sample No. 9B Depth 75-85cm Vol.Inj:1µL/500 Spl.Fract: ¹⁹ / ₈₀	C ₁₆ H ₃₄ Int. Std.	C ₁₉ H ₄₀ Ext. Std.	C ₂₀ H ₄₂ DPGE + Phytol	C ₄₀ H ₈₂ (0xC ₅ ring)	C ₄₀ H ₈₀ (1xC ₅ ring)	C ₄₀ H ₇₈ (2xC ₅ ring)	C ₄₀ H ₇₆ (3xC ₅ ring)
Ret.time (mins)	11.85	13.97	15.78	37.99	39.16	40.37	41.04
Peak Area (PA) (x10 ³ units)	203.9	1829	58.05	62.44	3.84	31.71	33.37
Conc.(µg) per sample (51.23g)			75.99	82.54	5.08	41.92	44.11
Conc. C ₂₀ , C ₄₀ derivatives per dry gram (µg/g)			1.48 -0.09* 1.39	1.61	0.10	0.82	0.86
Conc. DPGE, bi- DPGE per dry gram (µg/g)			1.61	1.87	0.12	0.95	0.10
Moles (nano) per dry gram (nmoles/g)			2.46	1.43	0.09	0.73	0.77
Dihydrophytol Determination PA x10 ³ Vol. Injected: 1µL of 100 Phytanyl acetate Rt=21.67 PA= 14.54 Heneicosanyl acetate Rt=26.37 PA= 172.7 *Concentration per gram = 0.09 µg/g Sample fraction:19/40 Yield = 12 %							

Sample No. 7B Depth 95-105cm Vol.Inj:1µL/500 Spl.Fract: ¹⁹ / ₈₀	C ₁₆ H ₃₄ Int. Std.	C ₁₉ H ₄₀ Ext. Std.	C ₂₀ H ₄₂ DPGE + Phytol	C ₄₀ H ₈₂ (0xC ₅ ring)	C ₄₀ H ₈₀ (1xC ₅ ring)	C ₄₀ H ₇₈ (2xC ₅ ring)	C ₄₀ H ₇₆ (3xC ₅ ring)
Ret.time (mins)	11.85	13.97	15.78	37.98	39.13	40.36	41.40
Peak Area (PA) (x10 ³ units)	258.3	1872	51.33	46.61	3.09	25.15	30.18
Conc.(µg) per sample (52.78g)			53.04	48.64	3.23	26.24	31.50
Conc. C ₂₀ , C ₄₀ derivatives per dry gram (µg/g)			1.00				
			-0.11*				
			0.89	0.92	0.06	0.50	0.60
Conc. DPGE, bi- DPGE per dry gram (µg/g)			1.03	1.07	0.07	0.58	0.69
Moles (nano) per dry gram (nmoles/g)			1.57	0.82	0.05	0.45	0.53
Dihydrophytol Determination PA x10 ³ Vol. Injected: 1µL of 100 Phytanyl acetate Rt=21.67 PA= 28.12 Heneicosanyl acetate Rt=26.37 PA= 217.0 *Concentration per gram = 0.11 µg/g Sample fraction:19/40 Yield = 15 %							

Sample No. 5B Depth 115-125cm Vol.Inj:1µL/500 Spl.Fract: ¹⁹ / ₈₀	C ₁₆ H ₃₄ Int. Std.	C ₁₉ H ₄₀ Ext. Std.	C ₂₀ H ₄₂ DPGE + Phytol	C ₄₀ H ₈₂ (0xC ₅ ring)	C ₄₀ H ₈₀ (1xC ₅ ring)	C ₄₀ H ₇₈ (2xC ₅ ring)	C ₄₀ H ₇₆ (3xC ₅ ring)
Ret.time (mins)	11.85	13.97	15.78	37.99	39.13	40.38	41.06
Peak Area (PA) (x10 ³ units)	289.7	2018	61.63	69.15	3.49	32.35	40.83
Conc.(µg) per sample (54.69g)			56.81	64.36	3.25	30.11	37.99
Conc. C ₂₀ , C ₄₀ derivatives per dry gram (µg/g)			1.04				
			-0.05*				
			0.99	1.17	0.06	0.55	0.70
Conc. DPGE, bi- DPGE per dry gram (µg/g)			1.14	1.37	0.07	0.64	0.81
Moles (nano) per dry gram (nmoles/g)			1.75	1.05	0.05	0.49	0.62
Dihydrophytol Determination PA x10 ³ Vol. Injected: 1µL of 100 Phytanyl acetate Rt=21.65 PA= 11.03 Heneicosanyl acetate Rt=26.35 PA= 175.4 *Concentration per gram = 0.05 µg/g Sample fraction:19/40 Yield = 16 %							

Sample No. 3B Depth 135-145cm Vol.Inj:1μL/500 Spl.Fract: ⁹ / ₈₀	C ₁₆ H ₃₄ Int. Std.	C ₁₉ H ₄₀ Ext. Std.	C ₂₀ H ₄₂ DPGE + Phytol	C ₄₀ H ₈₂ (0xC ₅ ring)	C ₄₀ H ₈₀ (1xC ₅ ring)	C ₄₀ H ₇₈ (2xC ₅ ring)	C ₄₀ H ₇₆ (3xC ₅ ring)
Ret.time (mins)	11.86	14.01	15.79	38.00	39.19	40.39	41.09
Peak Area (PA) (x10 ³ units)	110.1	1968	41.74	48.78	2.47	26.58	30.84
Conc.(μg) per sample (50.07g)			101.2	119.4	6.04	65.07	75.50
Conc. C ₂₀ , C ₄₀ derivatives per dry gram (μg/g)			2.02 -0.04* 1.98	2.39	0.12	1.30	1.51
Conc. DPGE, bi- DPGE per dry gram (μg/g)			2.30	2.77	0.14	1.51	1.75
Moles (nano) per dry gram (nmoles/g)			3.50	2.12	0.11	1.16	1.35
Dihydrophytol Determination PA x10 ³ Vol. Injected: 1μL of 100 Phytanyl acetate Rt=21.73 PA= 7.72 Heneicosanyl acetate Rt=26.44 PA= 209.9 *Concentration per gram = 0.04 μg/g Sample fraction:19/40 Yield = 12 %							

Sample No. 1B Depth 155-165cm Vol.Inj:1μL/500 Spl.Fract: ⁹ / ₈₀	C ₁₆ H ₃₄ Int. Std.	C ₁₉ H ₄₀ Ext. Std.	C ₂₀ H ₄₂ DPGE + Phytol	C ₄₀ H ₈₂ (0xC ₅ ring)	C ₄₀ H ₈₀ (1xC ₅ ring)	C ₄₀ H ₇₈ (2xC ₅ ring)	C ₄₀ H ₇₆ (3xC ₅ ring)
Ret.time (mins)	11.91	14.03	15.84	38.06	39.23	40.43	41.14
Peak Area (PA) (x10 ³ units)	146.1	1857	46.99	61.97	4.30	33.80	35.84
Conc.(μg) per sample (53.71g)			85.85	114.3	7.92	62.35	66.11
Conc. C ₂₀ , C ₄₀ derivatives per dry gram (μg/g)			1.60 -0.03* 1.57	2.13	0.15	1.16	1.23
Conc. DPGE, bi- DPGE per dry gram (μg/g)			1.82	2.47	0.17	1.35	1.43
Moles (nano) per dry gram (nmoles/g)			2.79	1.89	0.13	1.04	1.10
Dihydrophytol Determination PA x10 ³ Vol. Injected: 1μL of 100 Phytanyl acetate Rt=21.66 PA= 6.833 Heneicosanyl acetate Rt=26.37 PA= 185.2 *Concentration per gram = 0.03 μg/g Sample fraction:19/40 Yield = 17 %							

Sample No. 21C Depth 0-5 cm Vol.Inj:1µL/500 Spl.Fract: ¹⁹ / ₄₀	C ₁₆ H ₃₄ Int. Std.	C ₁₉ H ₄₀ Ext. Std.	C ₂₀ H ₄₂ DPGE + Phytol	C ₄₀ H ₈₂ (0xC ₅ ring)	C ₄₀ H ₈₀ (1xC ₅ ring)	C ₄₀ H ₇₈ (2xC ₅ ring)	C ₄₀ H ₇₆ (3xC ₅ ring)
Ret.time (mins)	11.99	14.07	15.87	38.05	39.19	40.41	41.13
Peak Area (PA) (x10 ³ units)	1779	1889	190.9	511.1	44.09	244.7	269.4
Conc.(µg) per sample (55.36g)			28.64	77.43	6.68	37.07	40.82
Conc. C ₂₀ , C ₄₀ derivatives per dry gram (µg/g)			0.52				
			-0.06*				
			0.46	1.40	0.12	0.67	0.74
Conc. DPGE, bi- DPGE per dry gram (µg/g)			0.53	1.62	0.14	0.78	0.86
Moles (nano) per dry gram (nmoles/g)			0.81	1.24	0.11	0.60	0.66
Dihydrophytol Determination PA x10 ³ Vol. Injected: 1µL of 300 Phytanyl acetate Rt=21.69 PA= 80.63 Heneicosanyl acetate Rt=26.39 PA= 1927 *Concentration per gram = 0.06 µg/g Sample fraction:19/80 Yield = 52 %							

Sample No. 19C Depth 15-25cm Vol.Inj:1µL/500 Spl.Fract: ¹⁹ / ₄₀	C ₁₆ H ₃₄ Int. Std.	C ₁₉ H ₄₀ Ext. Std.	C ₂₀ H ₄₂ DPGE + Phytol	C ₄₀ H ₈₂ (0xC ₅ ring)	C ₄₀ H ₈₀ (1xC ₅ ring)	C ₄₀ H ₇₈ (2xC ₅ ring)	C ₄₀ H ₇₆ (3xC ₅ ring)
Ret.time (mins)	11.99	14.10	15.87	38.05	39.21	40.42	41.13
Peak Area (PA) (x10 ³ units)	1195	1932	103.2	237.7	17.76	110.6	129.9
Conc.(µg) per sample (50.77g)			23.06	53.62	4.01	24.94	29.30
Conc. C ₂₀ , C ₄₀ derivatives per dry gram (µg/g)			0.45				
			-0.03*				
			0.42	1.06	0.08	0.49	0.58
Conc. DPGE, bi- DPGE per dry gram (µg/g)			0.49	1.23	0.09	0.57	0.67
Moles (nano) per dry gram (nmoles/g)			0.75	0.94	0.07	0.44	0.52
Dihydrophytol Determination PA x10 ³ Vol. Injected: 1µL of 300 Phytanyl acetate Rt=21.69 PA= 18.56 Heneicosanyl acetate Rt=26.38 PA= 1568 *Concentration per gram = 0.03 µg/g Sample fraction:19/80 Yield = 34 %							

Sample No. 17C Depth 40-50cm Vol.Inj:1μL/500 Spl.Fract:19/40	C ₁₆ H ₃₄ Int. Std.	C ₁₉ H ₄₀ Ext. Std.	C ₂₀ H ₄₂ DPGE + Phytol	C ₄₀ H ₈₂ (0xC ₅ ring)	C ₄₀ H ₈₀ (1xC ₅ ring)	C ₄₀ H ₇₈ (2xC ₅ ring)	C ₄₀ H ₇₆ (3xC ₅ ring)
Ret.time (mins)	11.84	13.93	15.71	37.94	39.09	40.30	40.99
Peak Area (PA) (x10 ³ units)	1625	2109	167.1	718.6	46.29	304.6	330.9
Conc.(μg) per sample (53.53g)			27.44	119.2	7.68	50.52	54.88
Conc. C ₂₀ , C ₄₀ derivatives per dry gram (μg/g)			0.51				
			-0.09*				
			0.42	2.23	0.14	0.94	1.02
Conc. DPGE, bi- DPGE per dry gram (μg/g)			0.47	2.58	0.17	1.10	1.19
Moles (nano) per dry gram (nmoles/g)			0.72	1.98	0.13	0.85	0.92
Dihydrophytol Determination PA x10 ³ Vol. Injected: 1μL of 300 Phytanyl acetate Rt=21.73 PA= 130.2 Heneicosanyl acetate Rt=26.39 PA= 1292 *Concentration per gram = 0.09 μg/g Sample fraction:19/40 Yield = 42 %							

Sample No. 15C Depth 60-70cm Vol.Inj:1µL/500 Spl.Fract: ¹⁹ / ₄₀	C ₁₆ H ₃₄ Int. Std.	C ₁₉ H ₄₀ Ext. Std.	C ₂₀ H ₄₂ DPGE + Phytol	C ₄₀ H ₈₂ (0xC ₅ ring)	C ₄₀ H ₈₀ (1xC ₅ ring)	C ₄₀ H ₇₈ (2xC ₅ ring)	C ₄₀ H ₇₆ (3xC ₅ ring)
Ret.time (mins)	11.82	13.95	15.75	37.96	39.11	40.30	41.02
Peak Area (PA) (x10 ³ units)	970.9	1972	120.4	331.5	370.2	125.6	127.3
Conc.(µg) per sample (51.73g)			33.09	92.05	10.28	34.88	35.34
Conc. C ₂₀ , C ₄₀ derivatives per dry gram (µg/g)			0.64				
			-0.05*				
			0.59	1.78	0.20	0.67	0.68
Conc. DPGE, bi- DPGE per dry gram (µg/g)			0.68	2.06	0.23	0.78	0.79
Moles (nano) per dry gram (nmoles/g)			1.04	1.58	0.18	0.60	0.61
Dihydrophytol Determination PA x10 ³ Vol. Injected: 1µL of 300							
Phytanyl acetate Rt=21.74 PA= 47.12 Heneicosanyl acetate Rt=26.41 PA= 1317							
*Concentration per gram = 0.05 µg/g Sample fraction:19/40 Yield = 27 %							

Second Extraction of the 15C sample with HCl

Sample No. 15C Depth 60-70cm Vol.Inj:1µL/500 Spl.Fract: ¹⁹ / ₄₀	C ₁₆ H ₃₄ Int. Std.	C ₁₉ H ₄₀ Ext. Std.	C ₂₀ H ₄₂ DPGE + Phytol	C ₄₀ H ₈₂ (0xC ₅ ring)	C ₄₀ H ₈₀ (1xC ₅ ring)	C ₄₀ H ₇₈ (2xC ₅ ring)	C ₄₀ H ₇₆ (3xC ₅ ring)
Ret.time (mins)	11.75	13.90	15.72	37.93	n.d.	n.d.	n.d.
Peak Area (PA) (x10 ³ units)	70.4	2001	43.7	34.8	-	-	-
Conc.(µg) per sample (51.73g)			31.98	89.02	-	-	-
Conc. C ₂₀ , C ₄₀ derivatives per dry gram (µg/g)			0.62				
			-0.05*				
			0.56	1.72	-	-	-
Conc. DPGE, bi- DPGE per dry gram (µg/g)			0.65	2.00	-	-	-
Difference in lipid concentration relative to initial extraction			-4.4 %	-2.9 %	-	-	-
Dihydrophytol Determination PA x10 ³ Vol. Injected: 1µL of 300							
Phytanyl acetate Rt=21.74 PA= 47.12 Heneicosanyl acetate Rt=26.41 PA= 1317							
*Concentration per gram = 0.05 µg/g Sample fraction:19/40 Yield = 3.4 %							

Sample No. 13C Depth 80-85cm Vol.Inj:1µL/500 Spl.Fract: ¹⁹ / ₄₀	C ₁₆ H ₃₄ Int. Std.	C ₁₉ H ₄₀ Ext. Std.	C ₂₀ H ₄₂ DPGE + Phytol	C ₄₀ H ₈₂ (0xC ₅ ring)	C ₄₀ H ₈₀ (1xC ₅ ring)	C ₄₀ H ₇₈ (2xC ₅ ring)	C ₄₀ H ₇₆ (3xC ₅ ring)
Ret.time (mins)	11.87	13.96	15.76	37.99	39.13	40.35	40.04
Peak Area (PA) (x10 ³ units)	1347	1973	207.0	801.0	65.54	328.6	365.8
Conc.(µg) per sample (52.63g)			41.01	160.3	13.11	65.75	73.20
Conc. C ₂₀ , C ₄₀ derivatives per dry gram (µg/g)			0.78 -0.05* 0.73	3.05	0.25	1.25	1.39
Conc. DPGE, bi- DPGE per dry gram (µg/g)			0.85	3.53	0.29	1.45	1.62
Moles (nano) per dry gram (nmoles/g)			1.30	2.71	0.22	1.12	1.25
Dihydrophytol Determination PA x10 ³ Vol. Injected: 1µL of 300							
Phytanyl acetate Rt=21.73 PA= 57.16 Heneicosanyl acetate Rt=26.37 PA= 1328							
*Concentration per gram = 0.05 µg/g Sample fraction:19/40 Yield = 37 %							

Second Extraction of the 13C sample with HCl

Sample No. 13C Depth 80-85cm Vol.Inj:1µL/500 Spl.Fract: ¹⁹ / ₄₀	C ₁₆ H ₃₄ Int. Std.	C ₁₉ H ₄₀ Ext. Std.	C ₂₀ H ₄₂ DPGE + Phytol	C ₄₀ H ₈₂ (0xC ₅ ring)	C ₄₀ H ₈₀ (1xC ₅ ring)	C ₄₀ H ₇₈ (2xC ₅ ring)	C ₄₀ H ₇₆ (3xC ₅ ring)
Ret.time (mins)	11.83	13.97	15.76	37.80	n.d.	n.d.	n.d.
Peak Area (PA) (x10 ³ units)	56.5	2054	42.7	16.8	-	-	-
Conc.(µg) per sample (52.63g)			41.1	157.0	-	-	-
Conc. C ₂₀ , C ₄₀ derivatives per dry gram (µg/g)			0.78 -0.05* 0.73	2.98	-	-	-
Conc. DPGE, bi- DPGE per dry gram (µg/g)			0.85	3.46	-	-	-
Difference in lipid concentration relative to initial extraction			0 %	-1.9 %	-	-	-
Dihydrophytol Determination PA x10 ³ Vol. Injected: 1µL of 300							
Phytanyl acetate Rt=21.73 PA= 57.16 Heneicosanyl acetate Rt=26.37 PA= 1328							
*Concentration per gram = 0.05 µg/g Sample fraction:19/40 Yield = 2 %							

Sample No. 11C Depth 100-105cm Vol.Inj:1µL/500 Spl.Fract: ¹⁹ / ₄₀	C ₁₆ H ₃₄ Int. Std.	C ₁₉ H ₄₀ Ext. Std.	C ₂₀ H ₄₂ DPGE + Phytol	C ₄₀ H ₈₂ (0xC ₅ ring)	C ₄₀ H ₈₀ (1xC ₅ ring)	C ₄₀ H ₇₈ (2xC ₅ ring)	C ₄₀ H ₇₆ (3xC ₅ ring)
Ret.time (mins)	11.92	14.02	15.81	38.00	39.15	40.37	41.08
Peak Area (PA) (x10 ³ units)	1228	2012	129.8	256.9	24.03	120.2	118.4
Conc.(µg) per sample (49.67g)			28.22	56.41	5.28	26.38	25.99
Conc. C ₂₀ , C ₄₀ derivatives per dry gram (µg/g)			0.57				
			-0.03*				
			0.54	1.14	0.11	0.53	0.52
Conc. DPGE, bi- DPGE per dry gram (µg/g)			0.62	1.32	0.12	0.62	0.61
Moles (<i>nano</i>) per dry gram (<i>n</i> moles/g)			0.95	1.01	0.09	0.48	0.47
Dihydrophytol Determination PA x10 ³ Vol. Injected: 1µL of 300 Phytanyl acetate Rt=21.71 PA= 29.91 Heneicosanyl acetate Rt=26.40 PA= 1262 *Concentration per gram = 0.03 µg/g Sample fraction: 19/40 Yield = 33 %							

Second Extraction of the 11C sample with HCl

Sample No. 11C Depth 100-105cm Vol.Inj:1µL/500 Spl.Fract: ¹⁹ / ₄₀	C ₁₆ H ₃₄ Int. Std.	C ₁₉ H ₄₀ Ext. Std.	C ₂₀ H ₄₂ DPGE + Phytol	C ₄₀ H ₈₂ (0xC ₅ ring)	C ₄₀ H ₈₀ (1xC ₅ ring)	C ₄₀ H ₇₈ (2xC ₅ ring)	C ₄₀ H ₇₆ (3xC ₅ ring)
Ret.time (mins)	12.33	14.47	16.64	38.53	n.d.	n.d.	n.d.
Peak Area (PA) (x10 ³ units)	73.1	2271	40.0	36.4	-	-	-
Conc.(µg) per sample (49.67g)			28.45	56.49	-	-	-
Conc. C ₂₀ , C ₄₀ derivatives per dry gram (µg/g)			0.57				
			-0.03*				
			0.54	1.14	-	-	-
Conc. DPGE, bi- DPGE per dry gram (µg/g)			0.63	1.32	-	-	-
Difference in lipid concentration relative to initial extraction			+1.5 %	0 %			
Dihydrophytol Determination PA x10 ³ Vol. Injected: 1µL of 300 Phytanyl acetate Rt=21.71 PA= 29.91 Heneicosanyl acetate Rt=26.40 PA= 1262 *Concentration per gram = 0.03 µg/g Sample fraction: 19/40 Yield = 2.8 %							

Sample No. 9C Depth 120-130cm Vol.Inj:1 μ L/500 Spl.Fract: ¹⁹ / ₄₀	C ₁₆ H ₃₄ Int. Std.	C ₁₉ H ₄₀ Ext. Std.	C ₂₀ H ₄₂ DPGE + Phytol	C ₄₀ H ₈₂ (0xC ₅ ring)	C ₄₀ H ₈₀ (1xC ₅ ring)	C ₄₀ H ₇₈ (2xC ₅ ring)	C ₄₀ H ₇₆ (3xC ₅ ring)
Ret.time (mins)	11.95	14.07	15.85	38.03	39.20	40.40	41.12
Peak Area (PA) (x10 ³ units)	1330	1988	79.55	203.6	15.76	100.2	109.6
Conc.(μ g) per sample (50.59g)			15.97	41.27	3.19	20.32	22.22
Conc. C ₂₀ , C ₄₀ derivatives per dry gram (μ g/g)			0.32 -0.02* 0.30	0.82	0.06	0.40	0.44
Conc. DPGE, bi- DPGE per dry gram (μ g/g)			0.34	0.95	0.07	0.47	0.51
Moles (nano) per dry gram (nmoles/g)			0.53	0.73	0.06	0.36	0.39
Dihydrophytol Determination PA x10 ³ Vol. Injected: 1 μ L of 300 Phytanyl acetate Rt=21.70 PA= 12.22 Heneicosanyl acetate Rt=26.37 PA= 1457 *Concentration per gram = 0.02 μ g/g Sample fraction:19/80 Yield = 36 %							

Sample No. 7C Depth 145-155cm Vol.Inj:1 μ L/500 Spl.Fract: ¹⁹ / ₄₀	C ₁₆ H ₃₄ Int. Std.	C ₁₉ H ₄₀ Ext. Std.	C ₂₀ H ₄₂ DPGE + Phytol	C ₄₀ H ₈₂ (0xC ₅ ring)	C ₄₀ H ₈₀ (1xC ₅ ring)	C ₄₀ H ₇₈ (2xC ₅ ring)	C ₄₀ H ₇₆ (3xC ₅ ring)
Ret.time (mins)	12.00	14.09	15.87	38.06	39.22	40.41	41.11
Peak Area (PA) (x10 ³ units)	1288	2053	70.25	166.4	12.83	89.67	97.99
Conc.(μ g) per sample (51.06g)			14.56	34.84	2.69	18.77	20.52
Conc. C ₂₀ , C ₄₀ derivatives per dry gram (μ g/g)			0.29 -0.05* 0.24	0.68	0.05	0.37	0.40
Conc. DPGE, bi- DPGE per dry gram (μ g/g)			0.28	0.79	0.06	0.43	0.47
Moles (nano) per dry gram (nmoles/g)			0.42	0.61	0.05	0.33	0.36
Dihydrophytol Determination PA x10 ³ Vol. Injected: 1 μ L of 300 Phytanyl acetate Rt=21.68 PA= 27.64 Heneicosanyl acetate Rt=26.33 PA= 1466 *Concentration per gram = 0.05 μ g/g Sample fraction:19/80 Yield = 34 %							

Sample No. 5C Depth 165-175cm Vol.Inj:1 μ L/500 Spl.Fract: ¹⁹ / ₄₀	C ₁₆ H ₃₄ Int. Std.	C ₁₉ H ₄₀ Ext. Std.	C ₂₀ H ₄₂ DPGE + Phytol	C ₄₀ H ₈₂ (0xC ₅ ring)	C ₄₀ H ₈₀ (1xC ₅ ring)	C ₄₀ H ₇₈ (2xC ₅ ring)	C ₄₀ H ₇₆ (3xC ₅ ring)
Ret.time (mins)	11.95	14.06	15.85	38.05	39.23	40.42	41.13
Peak Area (PA) (x10 ³ units)	1473	1977	79.83	260.7	18.26	170.6	157.5
Conc.(μ g) per sample (53.06g)			14.47	47.71	3.34	31.23	28.83
Conc. C ₂₀ , C ₄₀ derivatives per dry gram (μ g/g)			0.27 -0.02* 0.25	0.90	0.06	0.59	0.54
Conc. DPGE, bi- DPGE per dry gram (μ g/g)			0.30	1.04	0.07	0.68	0.63
Moles (nano) per dry gram (nmoles/g)			0.45	0.80	0.06	0.53	0.49
Dihydrophytol Determination PA x10 ³ Vol. Injected: 1 μ L of 300 Phytanyl acetate Rt=21.69 PA= 10.64 Heneicosanyl acetate Rt=26.35 PA= 1175 *Concentration per gram = 0.02 μ g/g Sample fraction:19/80 Yield = 40 %							

Sample No. 3C Depth 185-195cm Vol.Inj:1 μ L/500 Spl.Fract: ¹⁹ / ₄₀	C ₁₆ H ₃₄ Int. Std.	C ₁₉ H ₄₀ Ext. Std.	C ₂₀ H ₄₂ DPGE + Phytol	C ₄₀ H ₈₂ (0xC ₅ ring)	C ₄₀ H ₈₀ (1xC ₅ ring)	C ₄₀ H ₇₈ (2xC ₅ ring)	C ₄₀ H ₇₆ (3xC ₅ ring)
Ret.time (mins)	11.93	14.03	15.82	38.04	39.19	40.43	41.15
Peak Area (PA) (x10 ³ units)	996.1	2038	64.99	201.6	15.92	93.44	104.2
Conc.(μ g) per sample (49.68g)			17.42	54.56	4.31	25.29	28.19
Conc. C ₂₀ , C ₄₀ derivatives per dry gram (μ g/g)			0.35 -0.07* 0.28	1.10	0.09	0.51	0.57
Conc. DPGE, bi- DPGE per dry gram (μ g/g)			0.33	1.27	0.10	0.59	0.66
Moles (nano) per dry gram (nmoles/g)			0.50	0.98	0.08	0.46	0.51
Dihydrophytol Determination PA x10 ³ Vol. Injected: 1 μ L of 300 Phytanyl acetate Rt=21.65 PA= 30.18 Heneicosanyl acetate Rt=26.33 PA= 1474 *Concentration per gram = 0.07 μ g/g Sample fraction:19/80 Yield = 27 %							

Sample No.C1(i) Depth 205-213cm Vol.Inj:1µL/500 Spl.Fract: ¹⁹ / ₄₀	C ₁₆ H ₃₄ Int. Std.	C ₁₉ H ₄₀ Ext. Std.	C ₂₀ H ₄₂ DPGE + Phytol	C ₄₀ H ₈₂ (0xC ₅ ring)	C ₄₀ H ₈₀ (1xC ₅ ring)	C ₄₀ H ₇₈ (2xC ₅ ring)	C ₄₀ H ₇₆ (3xC ₅ ring)
Ret.time (mins)	11.89	14.01	15.80	38.01	39.19	40.42	41.11
Peak Area (PA) (x10 ³ units)	914.6	1796	78.71	291.6	22.44	133.8	144.2
Conc.(µg) per sample (53.01g)			22.97	85.96	6.61	39.43	42.51
Conc. C ₂₀ , C ₄₀ derivatives per dry gram (µg/g)			0.43				
			-0.03*				
			0.40	1.62	0.12	0.74	0.80
Conc. DPGE, bi- DPGE per dry gram (µg/g)			0.47	1.88	0.14	0.86	0.93
Moles (nano) per dry gram (nmoles/g)			0.71	1.44	0.11	0.67	0.72
Dihydrophytol Determination PA x10³ Vol. Injected: 1µL of 300 Phytanyl acetate Rt=21.74 PA= 26.62 Heneicosanyl acetate Rt=26.43 PA= 1951 *Concentration per gram = 0.03 µg/g Sample fraction:19/80 Yield = 28 %							

Sample No.C1 ii Depth 205-213cm Vol.Inj:1µL/500 Spl.Fract: ¹⁹ / ₄₀	C ₁₆ H ₃₄ Int. Std.	C ₁₉ H ₄₀ Ext. Std.	C ₂₀ H ₄₂ DPGE + Phytol	C ₄₀ H ₈₂ (0xC ₅ ring)	C ₄₀ H ₈₀ (1xC ₅ ring)	C ₄₀ H ₇₈ (2xC ₅ ring)	C ₄₀ H ₇₆ (3xC ₅ ring)
Ret.time (mins)	11.91	14.04	15.83	38.04	39.19	40.41	41.11
Peak Area (PA) (x10 ³ units)	701.5	2044	60.98	179.9	14.46	85.53	90.26
Conc.(µg) per sample (53.53g)			23.21	69.15	5.56	32.87	34.68
Conc. C ₂₀ , C ₄₀ derivatives per dry gram (µg/g)			0.43				
			-0.03*				
			0.40	1.29	0.10	0.61	0.65
Conc. DPGE, bi- DPGE per dry gram (µg/g)			0.47	1.50	0.12	0.71	0.75
Moles (nano) per dry gram (nmoles/g)			0.72	1.15	0.09	0.55	0.58
Dihydrophytol Determination PA x10³ Vol. Injected: 1µL of 300 Phytanyl acetate Rt=21.69 PA= 12.55 Heneicosanyl acetate Rt=26.38 PA= 1841 *Concentration per gram = 0.03 µg/g Sample fraction:19/80 Yield = 19 %							

Sample No.C1iii Depth 205-213cm Vol.Inj:1µL/500 Spl.Fract: ¹⁹ / ₄₀	C ₁₆ H ₃₄ Int. Std.	C ₁₉ H ₄₀ Ext. Std.	C ₂₀ H ₄₂ DPGE + Phytol	C ₄₀ H ₈₂ (0xC ₅ ring)	C ₄₀ H ₈₀ (1xC ₅ ring)	C ₄₀ H ₇₈ (2xC ₅ ring)	C ₄₀ H ₇₆ (3xC ₅ ring)
Ret.time (mins)	11.93	14.07	15.86	38.04	39.21	40.41	41.13
Peak Area (PA) (x10 ³ units)	914.6	1796	78.71	277.5	20.9	135.1	133.3
Conc.(µg) per sample (52.44g)			23.76	74.43	5.61	36.24	35.74
Conc. C ₂₀ , C ₄₀ derivatives per dry gram (µg/g)			0.45				
			-0.03*				
			0.42	1.42	0.11	0.69	0.68
Conc. DPGE, bi- DPGE per dry gram (µg/g)			0.50	1.65	0.12	0.80	0.79
Moles (<i>nano</i>) per dry gram (<i>n</i> moles/g)			0.76	1.26	0.10	0.62	0.61
Dihydrophytol Determination PA x10 ³ Vol. Injected: 1µL of 300 Phytanyl acetate Rt=21.69 PA= 20.63 Heneicosanyl acetate Rt=26.38 PA= 2275 *Concentration per gram = 0.03 µg/g Sample fraction:19/80 Yield = 29 %							

Sample No.15D T Depth 0-5cm Vol.Inj:1µL/500 Spl.Fract: ¹⁹ / ₄₀	C ₁₆ H ₃₄ Int. Std.	C ₁₉ H ₄₀ Ext. Std.	C ₂₀ H ₄₂ DPGE + Phytol	C ₄₀ H ₈₂ (0xC ₅ ring)	C ₄₀ H ₈₀ (1xC ₅ ring)	C ₄₀ H ₇₈ (2xC ₅ ring)	C ₄₀ H ₇ (3xC ₅ ring)
Ret.time (mins)	11.94	14.05	15.86	38.05	39.22	40.43	41.13
Peak Area (PA) (x10 ³ units)	770.2	1911	119.4	307.0	20.53	128.5	145.1
Conc.(µg) per sample (52.52g)			41.39	107.5	7.18	44.98	50.79
Conc. C ₂₀ , C ₄₀ derivatives per dry gram (µg/g)			0.79 -0.16* 0.63	2.05	0.14	0.86	0.97
Conc. DPGE, bi- DPGE per dry gram (µg/g)			0.73	2.37	0.16	0.99	1.12
Moles (nano) per dry gram (nmoles/g)			1.11	1.82	0.12	0.77	0.87
Dihydrophytol Determination PA x10 ³ Vol. Injected: 1µL of 300 Phytanyl acetate Rt=21.73 PA=95.81 Heneicosanyl acetate Rt=26.46 PA=2179 *Concentration per gram = 0.16 µg/g Sample fraction:19/80 Yield = 22 %							

Sample No.15D B Depth 5-15cm Vol.Inj:1µL/500 Spl.Fract: ¹⁹ / ₄₀	C ₁₆ H ₃₄ Int. Std.	C ₁₉ H ₄₀ Ext. Std.	C ₂₀ H ₄₂ DPGE + Phytol	C ₄₀ H ₈₂ (0xC ₅ ring)	C ₄₀ H ₈₀ (1xC ₅ ring)	C ₄₀ H ₇₈ (2xC ₅ ring)	C ₄₀ H ₇ (3xC ₅ ring)
Ret.time (mins)	11.94	14.07	15.85	38.05	39.21	40.43	41.13
Peak Area (PA) (x10 ³ units)	401.7	1864	66.70	216.8	16.33	85.94	93.99
Conc.(µg) per sample (42.10g)			44.32	145.5	10.96	57.67	63.07
Conc. C ₂₀ , C ₄₀ derivatives per dry gram (µg/g)			1.05 -0.20* 0.85	3.46	0.26	1.37	1.50
Conc. DPGE, bi- DPGE per dry gram (µg/g)			0.98	4.01	0.30	1.59	1.74
Moles (nano) per dry gram (nmoles/g)			1.50	3.07	0.23	1.23	1.34
Dihydrophytol Determination PA x10 ³ Vol. Injected: 1µL of 300 Phytanyl acetate Rt=21.79 PA=40.80 Heneicosanyl acetate Rt=26.47 PA=1709 *Concentration per gram = 0.20 µg/g Sample fraction:19/80 Yield = 12 %							

Sample No. 13D Depth 30-40cm Vol.Inj:1μL/500 Spl.Fract: ¹⁹ / ₈₀	C ₁₆ H ₃₄ Int. Std.	C ₁₉ H ₄₀ Ext. Std.	C ₂₀ H ₄₂ DPGE + Phytol	C ₄₀ H ₈₂ (0xC ₅ ring)	C ₄₀ H ₈₀ (1xC ₅ ring)	C ₄₀ H ₇₈ (2xC ₅ ring)	C ₄₀ H ₇₆ (3xC ₅ ring)
Ret.time (mins)	11.95	14.07	15.86	38.06	39.22	40.44	41.14
Peak Area (PA) (x10 ³ units)	535.9	1951	87.76	275.2	19.31	118.1	122.5
Conc.(μg) per sample (53.60g)			43.72	138.5	9.71	59.41	61.65
Conc. C ₂₀ , C ₄₀ derivatives per dry gram (μg/g)			0.82				
			-0.11*				
			0.71	2.58	0.18	1.11	1.15
Conc. DPGE, bi- DPGE per dry gram (μg/g)			0.82	3.00	0.21	1.29	1.34
Moles (nano) per dry gram (nmoles/g)			1.25	2.30	0.16	0.99	1.03
Dihydrophytol Determination PA x10³ Vol. Injected: 1μL of 300 Phytanyl acetate Rt=21.65 PA= 55.61 Heneicosanyl acetate Rt=26.33 PA= 1366 *Concentration per gram = 0.11 μg/g Sample fraction:19/80 Yield = 30 %							

Sample No. 11D Depth 50-60cm Vol.Inj:1μL/500 Spl.Fract: ¹⁹ / ₄₀	C ₁₆ H ₃₄ Int. Std.	C ₁₉ H ₄₀ Ext. Std.	C ₂₀ H ₄₂ DPGE + Phytol	C ₄₀ H ₈₂ (0xC ₅ ring)	C ₄₀ H ₈₀ (1xC ₅ ring)	C ₄₀ H ₇₈ (2xC ₅ ring)	C ₄₀ H ₇₆ (3xC ₅ ring)
Ret.time (mins)	12.00	14.08	15.88	38.08	32.23	40.46	41.17
Peak Area (PA) (x10 ³ units)	1226	1992	137.8	321.7	25.03	152.4	172.9
Conc.(μg) per sample (51.50g)			29.99	70.72	5.50	33.51	38.02
Conc. C ₂₀ , C ₄₀ derivatives per dry gram (μg/g)			0.58				
			-0.09*				
			0.49	1.37	0.11	0.65	0.74
Conc. DPGE, bi- DPGE per dry gram (μg/g)			0.57	1.59	0.12	0.76	0.86
Moles (nano) per dry gram (nmoles/g)			0.88	1.22	0.10	0.58	0.66
Dihydrophytol Determination PA x10³ Vol. Injected: 1μL of 300 Phytanyl acetate Rt=21.73 PA= 71.54 Heneicosanyl acetate Rt=26.47 PA= 1999 *Concentration per gram = 0.09 μg/g Sample fraction:19/80 Yield = 33 %							

Sample No. 9D Depth 70-80cm Vol.Inj:1µL/500 Spl.Fract: ¹⁹ / ₄₀	C ₁₆ H ₃₄ Int. Std.	C ₁₉ H ₄₀ Ext. Std.	C ₂₀ H ₄₂ DPGE + Phytol	C ₄₀ H ₈₂ (0xC ₅ ring)	C ₄₀ H ₈₀ (1xC ₅ ring)	C ₄₀ H ₇₈ (2xC ₅ ring)	C ₄₀ H ₇₆ (3xC ₅ ring)
Ret.time (mins)	11.96	14.07	15.87	38.10	39.27	40.47	41.20
Peak Area (PA) (x10 ³ units)	845.6	1968	72.41	194.1	15.66	97.32	107.6 2
Conc.(µg) per sample (46.50g)			22.86	61.87	4.99	31.02	34.31
Conc. C ₂₀ , C ₄₀ derivatives per dry gram (µg/g)			0.49 -0.05* 0.44	1.33	0.11	0.67	0.74
Conc. DPGE, bi- DPGE per dry gram (µg/g)			0.51	1.54	0.12	0.77	0.86
Moles (nano) per dry gram (nmoles/g)			0.79	1.18	0.10	0.60	0.66
Dihydrophytol Determination PA x10 ³ Vol. Injected: 1µL of 300 Phytanyl acetate Rt=21.71 PA= 27.12 Heneicosanyl acetate Rt=26.39 PA=2221 *Concentration per gram = 0.05 µg/g Sample fraction:19/80 Yield = 23 %							

Sample No. 7D Depth 90-100cm Vol.Inj:1µL/500 Spl.Fract: ¹⁹ / ₄₀	C ₁₆ H ₃₄ Int. Std.	C ₁₉ H ₄₀ Ext. Std.	C ₂₀ H ₄₂ DPGE + Phytol	C ₄₀ H ₈₂ (0xC ₅ ring)	C ₄₀ H ₈₀ (1xC ₅ ring)	C ₄₀ H ₇₈ (2xC ₅ ring)	C ₄₀ H ₇₆ (3xC ₅ ring)
Ret.time (mins)	11.95	14.07	15.87	38.07	39.25	40.46	41.16
Peak Area (PA) (x10 ³ units)	903.0	1951	79.38	129.5	10.11	61.44	68.66
Conc.(µg) per sample (51.35g)			23.47	38.67	3.02	18.34	20.50
Conc. C ₂₀ , C ₄₀ derivatives per dry gram (µg/g)			0.46 -0.03* 0.43	0.75	0.06	0.36	0.40
Conc. DPGE, bi- DPGE per dry gram (µg/g)			0.50	0.87	0.07	0.42	0.46
Moles (nano) per dry gram (nmoles/g)			0.76	0.67	0.05	0.32	0.36
Dihydrophytol Determination PA x10 ³ Vol. Injected: 1µL of 300 Phytanyl acetate Rt=21.75 PA=16.77 Heneicosanyl acetate Rt=26.44 PA=2036 *Concentration per gram = 0.03 µg/g Sample fraction:19/80 Yield = 25 %							

Sample No. 5D Depth 110-120cm Vol.Inj:1µL/500 Spl.Fract: ¹⁹ / ₄₀	C ₁₆ H ₃₄ Int. Std.	C ₁₉ H ₄₀ Ext. Std.	C ₂₀ H ₄₂ DPGE + Phytol	C ₄₀ H ₈₂ (0xC ₅ ring)	C ₄₀ H ₈₀ (1xC ₅ ring)	C ₄₀ H ₇₈ (2xC ₅ ring)	C ₄₀ H ₇₆ (3xC ₅ ring)
Ret.time (mins)	11.97	14.07	15.86	38.07	39.27	40.46	41.16
Peak Area (PA) (x10 ³ units)	972.6	1716	72.71	157.3	11.84	72.78	82.74
Conc.(µg) per sample (51.55g)			19.96	43.59	3.28	20.17	22.93
Conc. C ₂₀ , C ₄₀ derivatives per dry gram (µg/g)			0.39 -0.02* 0.37	0.85	0.06	0.39	0.44
Conc. DPGE, bi- DPGE per dry gram (µg/g)			0.42	0.98	0.07	0.45	0.52
Moles (nano) per dry gram (nmoles/g)			0.65	0.75	0.06	0.35	0.40
Dihydrophytol Determination PA x10 ³ Vol. Injected: 1µL of 300 Phytanyl acetate Rt=21.73 PA=15.95 Heneicosanyl acetate Rt=26.44 PA=1925 *Concentration per gram = 0.02 µg/g Sample fraction: 19/80 Yield = 31 %							

Sample No. 3D Depth 130-140cm Vol.Inj:1µL/500 Spl.Fract: ¹⁹ / ₄₀	C ₁₆ H ₃₄ Int. Std.	C ₁₉ H ₄₀ Ext. Std.	C ₂₀ H ₄₂ DPGE + Phytol	C ₄₀ H ₈₂ (0xC ₅ ring)	C ₄₀ H ₈₀ (1xC ₅ ring)	C ₄₀ H ₇₈ (2xC ₅ ring)	C ₄₀ H ₇₆ (3xC ₅ ring)
Ret.time (mins)	12.02	14.10	15.91	38.10	39.24	40.47	41.17
Peak Area (PA) (x10 ³ units)	1199	1964	76.91	231.2	17.97	104.7	118.6
Conc.(µg) per sample (54.17g)			17.12	51.96	4.04	23.53	26.65
Conc. C ₂₀ , C ₄₀ derivatives per dry gram (µg/g)			0.32 -0.02* 0.30	0.96	0.07	0.43	0.49
Conc. DPGE, bi- DPGE per dry gram (µg/g)			0.34	1.11	0.09	0.50	0.57
Moles (nano) per dry gram (nmoles/g)			0.53	0.85	0.07	0.39	0.44
Dihydrophytol Determination PA x10 ³ Vol. Injected: 1µL of 300 Phytanyl acetate Rt=21.77 PA=10.57 Heneicosanyl acetate Rt=26.47 PA=1300 *Concentration per gram = 0.02 µg/g Sample fraction: 19/80 Yield = 33 %							

Sample No. 1D Depth 150-160cm Vol.Inj:1 μ L/500 Spl.Fract:19/40	C ₁₆ H ₃₄ Int. Std.	C ₁₉ H ₄₀ Ext. Std.	C ₂₀ H ₄₂ DPGE + Phytol	C ₄₀ H ₈₂ (0xC ₅ ring)	C ₄₀ H ₈₀ (1xC ₅ ring)	C ₄₀ H ₇₈ (2xC ₅ ring)	C ₄₀ H ₇₆ (3xC ₅ ring)
Ret.time (mins)	11.87	13.99	15.79	38.03	39.17	40.39	41.09
Peak Area (PA) (x10 ³ units)	1298	1817	120.7	418.0	35.26	199.9	202.0
Conc.(μ g) per sample (51.69g)			24.82	86.78	7.32	41.51	41.94
Conc. C ₂₀ , C ₄₀ derivatives per dry gram (μ g/g)			0.48				
			-0.03*				
			0.45	1.68	0.14	0.80	0.81
Conc. DPGE, bi- DPGE per dry gram (μ g/g)			0.53	1.95	0.16	0.93	0.94
Moles (<i>nano</i>) per dry gram (<i>nmoles</i> /g)			0.80	1.49	0.13	0.72	0.73
Dihydrophytol Determination PA x10 ³ Vol. Injected: 1 μ L of 300 Phytanyl acetate Rt=21.64 PA=32.59 Heneicosanyl acetate Rt=26.32 PA= 1292 *Concentration per gram = 0.03 μ g/g Sample fraction:19/40 Yield = 39 %							

Sample No.INT2 Depth 12-24cm Vol.Inj:1μL/500 Spl.Fract: ¹⁹ / ₄₀	C ₁₆ H ₃₄ Int. Std.	C ₁₉ H ₄₀ Ext. Std.	C ₂₀ H ₄₂ DPGE + Phytol	C ₄₀ H ₈₂ (0xC ₅ ring)	C ₄₀ H ₈₀ (1xC ₅ ring)	C ₄₀ H ₇₈ (2xC ₅ ring)	C ₄₀ H ₇₆ (3xC ₅ ring)
Ret.time (mins)	11.97	14.07	15.85	38.05	39.21	40.45	41.16
Peak Area (PA) (x10 ³ units)	1078	2040	64.62	52.16	4.87	22.06	21.83
Conc.(μg) per sample (54.34g)			15.99	13.04	1.22	5.51	5.46
Conc. C ₂₀ , C ₄₀ derivatives per dry gram (μg/g)			0.29				
			-0.01*				
			0.28	0.24	0.02	0.10	0.10
Conc. DPGE, bi- DPGE per dry gram (μg/g)			0.33	0.28	0.03	0.12	0.12
Moles (nano) per dry gram (nmoles/g)			0.50	0.21	0.02	0.09	0.09
Dihydrophytol Determination				Vol.Injected: 1μL of 300			
Phytanyl acetate Rt=21.69 PA=10.95				Heneicosanyl acetate Rt=26.41 PA=2760			
*Concentration per gram = 0.01 μg/g				Sample fraction:19/80 Yield = 29 %			

SampleNo.INT3 Depth 24-36cm Vol.Inj:1μL/500 Spl.Fract: ¹⁹ / ₄₀	C ₁₆ H ₃₄ Int. Std.	C ₁₉ H ₄₀ Ext. Std.	C ₂₀ H ₄₂ DPGE + Phytol	C ₄₀ H ₈₂ (0xC ₅ ring)	C ₄₀ H ₈₀ (1xC ₅ ring)	C ₄₀ H ₇₈ (2xC ₅ ring)	C ₄₀ H ₇₆ (3xC ₅ ring)
Ret.time (mins)	11.99	14.08	15.89	38.07	N.D.	40.46	41.15
Peak Area (PA) (x10 ³ units)	923.7	1966	58.89	47.36	N.D.	15.47	15.62
Conc.(μg) per sample (52.56g)			17.02	13.82	N.D.	4.52	4.56
Conc. C ₂₀ , C ₄₀ derivatives per dry gram (μg/g)			0.32				
			-0.01*				
			0.31	0.26	N.D.	0.09	0.09
Conc. DPGE, bi- DPGE per dry gram (μg/g)			0.36	0.30	N.D.	0.10	0.10
Moles (nano) per dry gram (nmoles/g)			0.55	0.23	N.D.	0.08	0.08
Dihydrophytol Determination				Vol. Injected: 1μL of 300			
Phytanyl acetate Rt=21.43 PA=10.00				Heneicosanyl acetate Rt=26.15 PA=2274			
*Concentration per gram = 0.01 μg/g				Sample fraction:19/80 Yield = 25 %			

Sample No.INT4 Depth 36-48cm Vol.Inj:1μL/500 Spl.Fract: ¹⁹ / ₄₀	C ₁₆ H ₃₄ Int. Std.	C ₁₉ H ₄₀ Ext. Std.	C ₂₀ H ₄₂ DPGE + Phytol	C ₄₀ H ₈₂ (0xC ₅ ring)	C ₄₀ H ₈₀ (1xC ₅ ring)	C ₄₀ H ₇₈ (2xC ₅ ring)	C ₄₀ H ₇₆ (3xC ₅ ring)
Ret.time (mins)	11.89	13.99	15.77	37.95	39.09	40.28	40.98
Peak Area (PA) (x10 ³ units)	1588	2063	75.20	121.5	6.81	43.20	43.86
Conc.(μg) per sample (54.91g)			12.64	20.62	1.16	7.33	7.45
Conc. C ₂₀ , C ₄₀ derivatives per dry gram (μg/g)			0.23 -0.01* 0.22	0.38	0.02	0.13	0.14
Conc. DPGE, bi- DPGE per dry gram (μg/g)			0.26	0.44	0.02	0.16	0.16
Moles (nano) per dry gram (nmoles/g)			0.40	0.33	0.02	0.12	0.12
Dihydrophytol Determination				Vol. Injected: 1μL of 300			
Phytanyl acetate Rt=21.45 PA=7.43				Heneicosanyl acetate Rt=26.17 PA= 2082			
*Concentration per gram = 0.01 μg/g				Sample fraction:19/80 Yield = 42 %			

SampleNo.INT5 Depth 48-60cm Vol.Inj:1μL/500 Spl.Fract: ¹⁹ / ₄₀	C ₁₆ H ₃₄ Int. Std.	C ₁₉ H ₄₀ Ext. Std.	C ₂₀ H ₄₂ DPGE + Phytol	C ₄₀ H ₈₂ (0xC ₅ ring)	C ₄₀ H ₈₀ (1xC ₅ ring)	C ₄₀ H ₇₈ (2xC ₅ ring)	C ₄₀ H ₇₆ (3xC ₅ ring)
Ret.time (mins)	11.83	13.93	15.71	37.87	39.03	40.23	40.92
Peak Area (PA) (x10 ³ units)	1171	2395	73.05	80.20	3.55	32.53	26.50
Conc.(μg) per sample (55.48g)			16.65	18.46	0.82	7.49	6.10
Conc. C ₂₀ , C ₄₀ derivatives per dry gram (μg/g)			0.30 -0.01* 0.29	0.33	0.01	0.13	0.11
Conc. DPGE, bi- DPGE per dry gram (μg/g)			0.34	0.39	0.02	0.16	0.13
Moles (nano) per dry gram (nmoles/g)			0.52	0.30	0.01	0.12	0.10
Dihydrophytol Determination				Vol. Injected: 1μL of 300			
Phytanyl acetate Rt=21.68 PA=9.021				Heneicosanyl acetate Rt=26.37PA=2389			
*Concentration per gram = 0.01 μg/g				Sample fraction:19/80 Yield = 27 %			

Sample No.INT6 Depth 60-72cm Vol.Inj:1µL/500 Spl.Fract: ¹⁹ / ₄₀	C ₁₆ H ₃₄ Int. Std.	C ₁₉ H ₄₀ Ext. Std.	C ₂₀ H ₄₂ DPGE + Phytol	C ₄₀ H ₈₂ (0xC ₅ ring)	C ₄₀ H ₈₀ (1xC ₅ ring)	C ₄₀ H ₇₈ (2xC ₅ ring)	C ₄₀ H ₇₆ (3xC ₅ ring)
Ret.time (mins)	11.90	14.03	15.82	38.05	N.D.	40.45	41.17
Peak Area (PA) (x10 ³ units)	199.5	1915	42.42	64.14	N.D.	17.54	13.31
Conc.(µg) per sample (53.85g)			56.75	86.66	N.D.	23.69	17.98
Conc. C ₂₀ , C ₄₀ derivatives per dry gram (µg/g)			1.05				
			-0.05*				
			1.00	1.61	N.D.	0.44	0.33
Conc. DPGE, bi- DPGE per dry gram (µg/g)			1.16	1.87	N.D.	0.51	0.39
Moles (nano) per dry gram (nmoles/g)			1.78	1.43	N.D.	0.39	0.30
Dihydrophytol Determination				Vol. Injected: 1µL of 300			
Phytanyl acetate Rt=21.66 PA=7.00				Heneicosanyl acetate Rt=26.38 PA= 1932			
*Concentration per gram = 0.05 µg/g				Sample fraction:19/80 Yield = 6 %			

SampleNo.INT7 Depth 72-84cm Vol.Inj:1µL/500 Spl.Fract: ¹⁹ / ₄₀	C ₁₆ H ₃₄ Int. Std.	C ₁₉ H ₄₀ Ext. Std.	C ₂₀ H ₄₂ DPGE + Phytol	C ₄₀ H ₈₂ (0xC ₅ ring)	C ₄₀ H ₈₀ (1xC ₅ ring)	C ₄₀ H ₇₈ (2xC ₅ ring)	C ₄₀ H ₇₆ (3xC ₅ ring)
Ret.time (mins)	11.88	14.03	15.82	38.04	39.21	40.41	41.14
Peak Area (PA) (x10 ³ units)	577.4	1924	58.63	87.98	6.08	30.97	31.51
Conc.(µg) per sample (50.03g)			27.11	41.08	2.84	14.46	14.71
Conc. C ₂₀ , C ₄₀ derivatives per dry gram (µg/g)			0.54				
			-0.02*				
			0.52	0.82	0.06	0.29	0.29
Conc. DPGE, bi- DPGE per dry gram (µg/g)			0.60	0.95	0.07	0.34	0.34
Moles (nano) per dry gram (nmoles/g)			0.92	0.73	0.05	0.26	0.26
Dihydrophytol Determination				Vol. Injected: 1µL of 300			
Phytanyl acetate Rt=21.65 PA=9.25				Heneicosanyl acetate Rt=26.39 PA= 2054			
*Concentration per gram = 0.02 µg/g				Sample fraction:19/80 Yield = 17 %			

APPENDIX VII**TYPICAL LIPID CALCULATIONS****Example calculations from Holyhead sample 17A (top), i.e. Core A, 5 cm (3 - 8 cm)****(See Appendix VI for raw ether lipid data)**

Internal Standard (1,2-di-*O*-hexadecyl *rac* glycerol) Added = 315 µg
 (equivalent to 262.5 µg C₁₆H₃₄ derivative)

External Standard (Pristane C₁₉H₄₀) Added = 137.3 ng µl⁻¹
 (68.65 µg in 500 µL)

From gas chromatographic analysis of different carbon chain length hydrocarbons it was evident that longer hydrocarbons gave proportionately less signal (peak area) for the same given mass analysed. Therefore multiplication factors relative to the internal standard (unity) were required.

Internal Standard (C ₁₆ H ₃₄)	: Factor = 1
External Standard (C ₁₉ H ₄₀), C ₂₀ H ₄₂	: Factor = 1.017
C ₄₀ H ₈₂ , C ₄₀ H ₈₀ , C ₄₀ H ₇₈ , C ₄₀ H ₇₆	: Factor = 1.027

1/20 th of the total sample was used for phospholipid phosphate determination and the remaining 19/20 ths was usually split into 2 equal portions for

- (i) Methanogenic lipid determination (19/40 ths)
- (ii) Dihydrophytol (plant lipid) determination (19/40 ths)

The sample fraction volume (*i.e.* 19/40 ths) is given on each of the result sheets (see Appendix VI).

Determination of Yield

Peak area of 137.3 ng External standard (C₁₉H₄₀) = 1972336
 Multiplication factor = 1.017
 2005866

Peak area of 262.5 µg Internal standard (C₁₆H₃₄) = 1677228
 (which is 19/40 ths of the original sample)
 ÷ 19/40
 = 3531006

$$\begin{aligned} \therefore \text{Concentration internal standard (C}_{16}\text{H}_{34}) &= \left(\frac{3531006}{2005866} \right) \times 137.3 \times 10^{-9} \\ &= 241.7 \text{ ng per } \mu\text{l} \\ &= 120.85 \text{ } \mu\text{g per } 500 \mu\text{l (total sample)} \end{aligned}$$

Concentration of internal standard added is 262.5 μg

$$\therefore \text{Yield} = \frac{120.8}{262.5} \times 100 = 46.0 \%$$

Dihydrophytol Determination

$$\begin{aligned} \text{Peak area of } 33.3 \text{ ng per } \mu\text{l external standard} &= 1825195 \\ \text{(Heneicosanyl acetate)} \end{aligned}$$

$$\begin{aligned} \text{Peak area of phytanyl acetate} &= 134336 \\ \text{(dihydrophytol derivative)} \end{aligned}$$

$$\begin{aligned} \therefore \text{Concentration of phytanyl acetate} &= \left(\frac{134336}{1825195} \right) \times 33.3 \times 10^{-9} \\ &= 2.45 \text{ ng per } \mu\text{l} \end{aligned}$$

1 μl from 300 μl was injected. This represents 19/40 ths of the original sample.

$$\begin{aligned} \therefore \text{Concentration of phytanyl acetate per sample} &= 2.45 \times 10^{-9} \times \left(\frac{300}{19/40} \right) \\ &= 1.55 \text{ } \mu\text{g} \end{aligned}$$

Assuming that the yield of the dihydrophytol determination is similar to that of the internal standard (1,2-di-*O*-hexadecyl *rac* glycerol) *i.e.* 46.0%.

$$\therefore \text{Concentration of dihydrophytol per gram of sediment} = 1.55 \times 10^{-6} \times \left(\frac{1}{0.46} \right)$$

$$\begin{aligned} \text{(Weight of sediment extracted} &= 50.86 \text{ g)} &= 3.365 \times 10^{-6} \div 50.86 \text{ g} \\ &= \underline{\underline{66.17 \text{ ng g}^{-1} (\approx 0.07 \text{ } \mu\text{g g}^{-1})}} \end{aligned}$$

DPGE (C20) Determination

$$\text{Peak area of } 262.5\mu\text{g internal standard} = 1677228$$

$$\text{Peak area of } C_{20}H_{42} \text{ (DPGE (C20) derivative plus dihydrophytol derivative)} = 173943$$

$$\therefore \text{Concentration of } C_{20}H_{42} = \left(\frac{173942}{1677228} \right) \times 262.5 \times 10^{-6}$$

$$= 27.22 \times 10^{-6}$$

$$\text{Multiplication factor} = 1.017$$

$$= 27.69 \mu\text{g } C_{20}H_{42} \text{ per sample}$$

$$\therefore \text{Concentration of } C_{20}H_{42} \text{ per gram (DPGE + dihydrophytol derivative)} = 27.69 \times 10^{-6} \div 50.86 \text{ g}$$

$$= 0.54 \mu\text{g g}^{-1}$$

$$\therefore \text{Concentration of DPGE derivative only (concentration of dihydrophytol} = 0.07 \mu\text{g g}^{-1}) = 0.54 - 0.07$$

$$= 0.47 \mu\text{g/g}$$

Molecular weight (Mol.wt) of $C_{20}H_{42}$ (C20) = 282.6 (see figure 1.1 of chapter 1)

Molecular weight of DPGE (C20) = 653.2

(N.B. 2 moles of $C_{20}H_{42}$ in 1 mole DPGE)

$$\therefore \text{Conc. DPGE} = \text{Conc. } C_{20}H_{42} \times \left(\frac{\text{Mol.wt.DPGE}}{\text{Mol.wt.}C_{20}H_{42} \times 2} \right)$$

$$\therefore \text{Concentration of DPGE (C20) (C}_{43}\text{H}_{88}\text{O}_3) = 0.47 \times \left(\frac{653.2}{282.6 \times 2} \right) = \underline{\underline{0.54 \mu\text{g g}^{-1}}}$$

$$\therefore \text{Molar concentration of DPGE (DPGE Mol.wt.}=653.2) = 0.56 \div 653.2$$

$$= \underline{\underline{0.83 \text{ nmoles g}^{-1}}}$$

Bi-DPGE (acyclic, C40,0) Determination

$$\begin{aligned}
 \text{Peak area of } C_{40}H_{82} \text{ acyclic bi-DPGE derivative} &= 635177 \\
 \therefore \text{Concentration of } C_{40}H_{82} &= \left(\frac{635177}{1677228} \right) \times 262.5 \times 10^{-6} \\
 &= 99.41 \times 10^{-6} \\
 \text{Multiplication factor} &= 1.027 \\
 &= 102.09 \mu\text{g } C_{40}H_{82} \text{ per sample} \\
 \therefore \text{Concentration of bi-DPGE derivative} &= 102.09 \times 10^{-6} \div 50.86 \text{ g} \\
 (C_{40}H_{82}) &= 2.01 \mu\text{g g}^{-1} \\
 \text{Molecular weight of } C_{40}H_{82} &= 563 \\
 \text{Molecular weight of acyclic bi-DPGE} &= 1302 \\
 \text{(N.B. 2 moles of } C_{40}H_{82} \text{ in 1 mole acyclic bi-DPGE (} C_{86}H_{172}O_6 \text{))} \\
 \therefore \text{Conc. bi-DPGE} = \text{Conc. } C_{40}H_{82} \times \left(\frac{\text{Mol.wt. bi-DPGE}}{\text{Mol.wt. } C_{40}H_{82} \times 2} \right) \\
 \therefore \text{Concentration of acyclic bi-DPGE} &= 2.01 \times 10^{-6} \times \left(\frac{1302}{2 \times 563} \right) \\
 (C_{86}H_{172}O_6) \\
 \therefore \text{Molar concentration of acyclic bi-DPGE} &= 2.32 \times 10^{-6} \div 1302 \\
 (i.e. C40,0) &= \underline{\underline{1.79 \text{ nmoles g}^{-1}}}
 \end{aligned}$$

The calculations given for the acyclic bi-DPGE lipid and derivatives are similar to those for the cyclic bi-DPGE lipids since the difference in molecular weight is negligible.

$$\begin{aligned}
 \text{Molecular weight of } C_{40}H_{80} \text{ derivative (1 ring)} &= 561 \\
 \text{Molecular weight of bi-DPGE (2 x 1 ring, C40,1)} &= 1298 \\
 \text{Molecular weight of } C_{40}H_{78} \text{ derivative (2 ring)} &= 559 \\
 \text{Molecular weight of bi-DPGE (2 x 2 ring, C40,2)} &= 1294
 \end{aligned}$$

The molecular weight of the unknown bi-DPGE lipid (*i.e.* C40,?) was determined as that of the 2 pentacyclic ring derivative (*i.e.* C40,2).

APPENDIX VIII.

Table A8.1. Concentrations of diether (C20) and acyclic (C40,0) and cyclic (C40,1, C40,2, C40,?) tetraether lipids and phospholipid phosphate in sediments of Holyhead Harbour and an intertidal core (n.m. = not measured, sample lost).

Depth Mean (cm)	Diether C20 µg g ⁻¹	Tetraether				Sum of Ethers µg g ⁻¹	Lipid Phosphate (nmoles g ⁻¹)
		C40,0 µg g ⁻¹	C40,1 µg g ⁻¹	C40,2 µg g ⁻¹	C40,? µg g ⁻¹		
Holyhead Core A							
5	0.54	2.01	0.19	0.99	1.13	4.86	79.6
10	0.58	2.87	0.25	0.74	0.50	4.94	85.2
25	0.58	2.88	0.25	1.25	1.41	6.37	81.4
45	0.73	3.38	0.46	1.37	1.55	7.49	71.5
65	0.56	1.52	0.13	0.69	0.76	3.66	57.8
85	0.56	2.40	0.22	1.18	1.05	5.41	29.5
105	0.48	0.99	0.07	0.46	0.53	2.53	28.0
125	0.60	0.81	0.18	0.60	0.58	2.77	36.6
145	0.88	0.95	0.00	0.57	0.45	2.85	26.0
165	1.07	0.65	0.00	0.30	0.30	2.32	24.6
Holyhead Core B							
6	1.12	1.34	0.00	0.95	0.81	4.22	99.6
20	1.07	0.99	0.00	0.93	0.89	3.88	58.4
40	n.m.	n.m.	n.m.	n.m.	n.m.	n.m.	44.8
60	1.04	0.58	0.00	0.36	0.37	2.35	55.5
80	1.61	1.87	0.12	0.95	1.00	5.55	41.3
100	1.03	1.07	0.07	0.58	0.69	3.44	48.7
120	1.14	1.37	0.07	0.64	0.81	4.03	54.1
140	2.30	2.77	0.14	1.51	1.75	8.47	47.5
160	1.82	2.47	0.17	1.35	1.43	7.24	45.8
Holyhead Core C							
3	0.53	1.62	0.14	0.78	0.86	3.93	138.7
20	0.49	1.23	0.09	0.57	0.67	3.05	127.9
45	0.47	2.58	0.17	1.10	1.19	5.51	98.5
65	0.68	2.06	0.23	0.78	0.79	4.54	69.3
83	0.85	3.53	0.29	1.45	1.62	7.74	82.2
103	0.62	1.32	0.12	0.62	0.61	3.29	52.4
125	0.34	0.95	0.07	0.47	0.51	2.34	30.2
150	0.28	0.79	0.06	0.43	0.47	2.03	28.0
170	0.30	1.04	0.07	0.68	0.63	2.72	23.1
190	0.33	1.27	0.10	0.59	0.66	2.95	26.3
209	0.48	1.68	0.13	0.79	0.82	3.90	26.2
Holyhead Core D							
3	0.73	2.37	0.16	0.99	1.12	5.37	86.4
10	0.98	4.01	0.30	1.59	1.74	8.62	111.7
35	0.82	3.00	0.21	1.29	1.34	6.66	74.1
55	0.58	1.59	0.12	0.76	0.86	3.91	65.7
75	0.51	1.54	0.12	0.77	0.86	3.80	63.1
95	0.50	0.87	0.07	0.42	0.46	2.32	34.2
115	0.42	0.98	0.07	0.45	0.52	2.44	29.3
135	0.34	1.11	0.09	0.50	0.57	2.61	27.5
155	0.53	1.95	0.16	0.93	0.94	4.51	30.8
Intertidal Core						6 cm =	14.5
18	0.33	0.28	0.03	0.12	0.12	0.88	3.8
30	0.36	0.30	0.01	0.10	0.10	0.86	5.8
42	0.26	0.44	0.02	0.16	0.16	1.04	2.9
56	0.34	0.39	0.02	0.16	0.13	1.04	1.7
66	1.16	1.87	0.01	0.51	0.39	3.93	2.0
78	0.6	0.95	0.07	0.34	0.34	2.3	1.8

APPENDIX VIII.

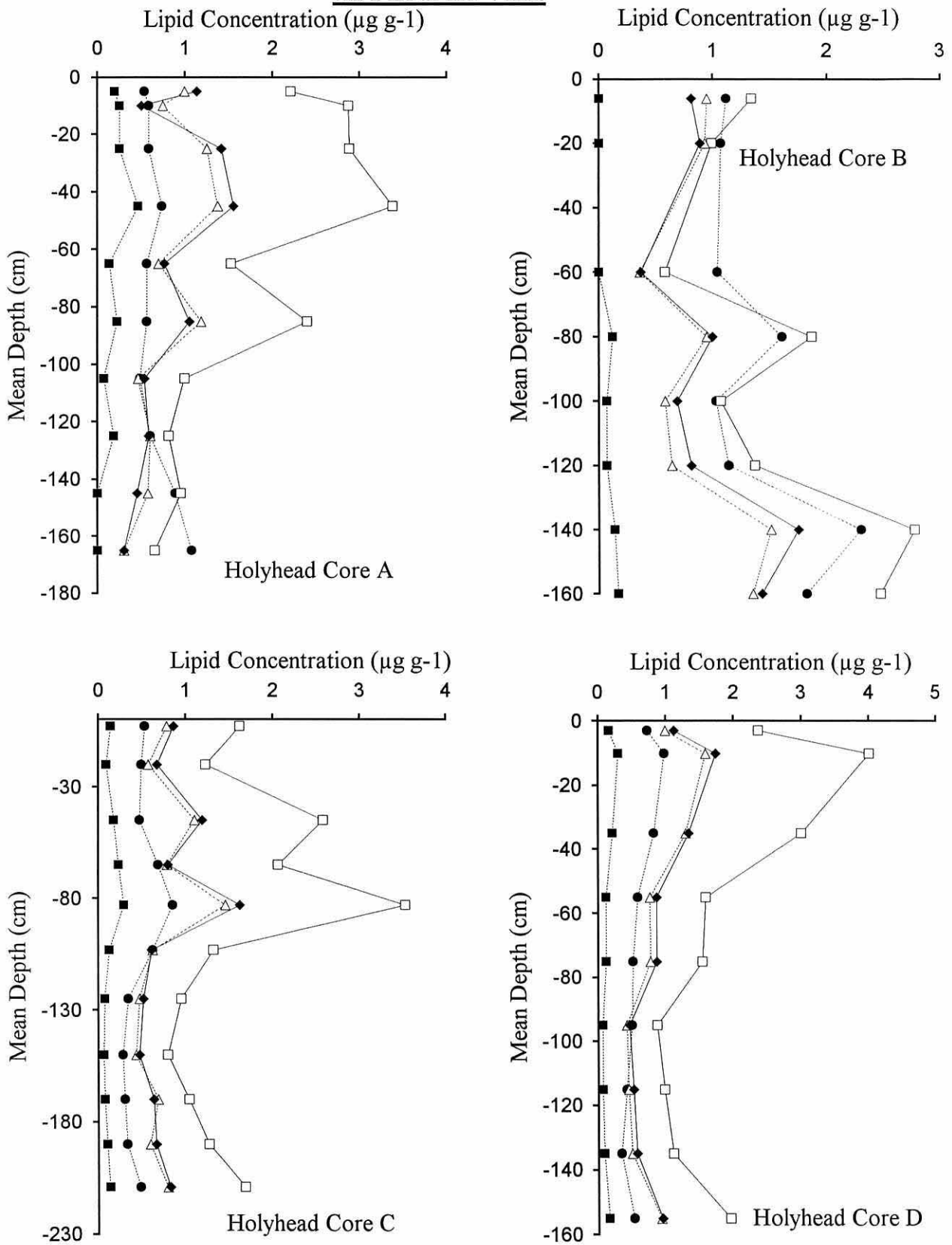


Figure A8.1. Ether lipid concentrations of the Holyhead Harbour cores showing diether C20 (.....●.....) and acyclic C40,0 (—□—) and cyclic C40,1 (.....■.....), C40,2 (.....△.....), C40,? (—◆—) tetraether lipids.

APPENDIX VIII.

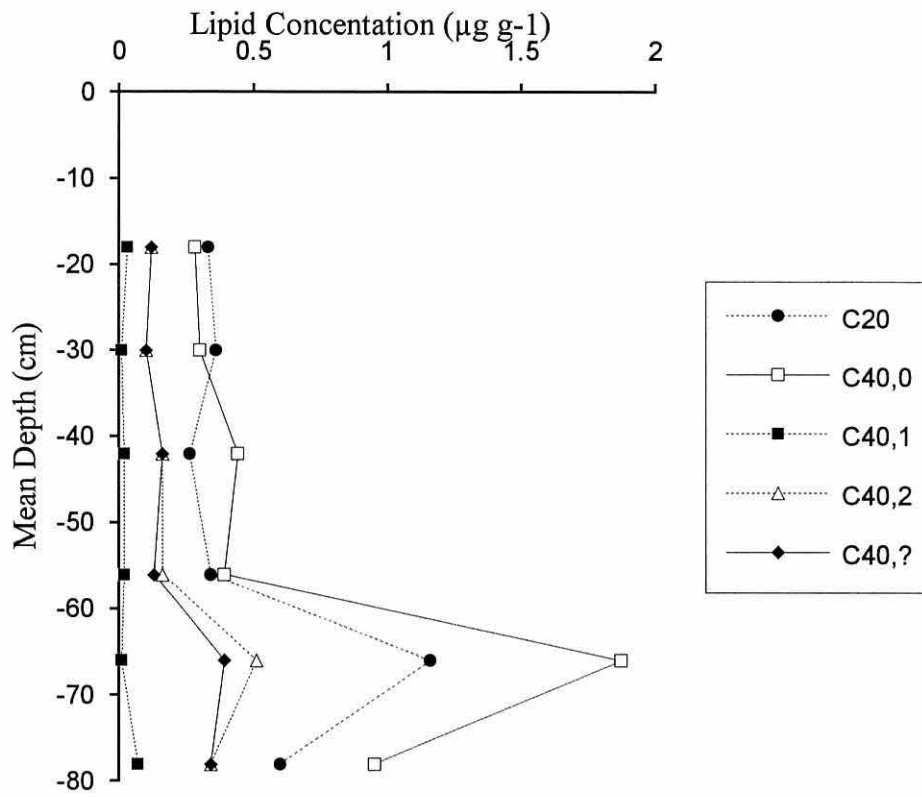


Figure A8.2. Ether lipid concentrations of the intertidal core showing diether (C20) and acyclic (C40,0) and cyclic (C40,1 C40,2 C40,?) tetraether lipids.

A chemical method for estimating methanogenic biomass

G. C. SMITH* and G. D. FLOODGATE*

(Received 17 October 1990; in revised form 20 September 1991; accepted 15 January 1992)

Abstract—Methane-forming bacteria belong to the archaeobacterial kingdom and as such possess unique membrane lipids in that phytanyl ether linked phospholipids replace the more usual ester linked analogues. A common methanogenic membrane ether lipid (Di-Phytanyl Glycerol Ether; DPGE) can be extracted using solvents, chemically broken down, derivatized, purified using thin layer chromatography, and finally analysed quantitatively by capillary gas chromatography. In order to evaluate the concentration of DPGE as a means of estimating the biomass of methanogens, this membrane lipid was compared with cell numbers, methane production and turbidity at 578 nm in a controlled growth experiment of a marine methanogenic monoculture of *Methanobolus tindarius*. It was found that the DPGE lipid data produced similar growth curves to the other measured parameters. All the parameters used to monitor the growth experiment showed an interesting change at a point in the growth cycle of *M. tindarius* where cell division slowed down and the growth of individual cells appeared to be the major mechanism of increasing the biomass. Preliminary environmental samples taken from both a marine inter-tidal and a freshwater site were analysed for the DPGE lipid and the results are discussed.

INTRODUCTION

APPROXIMATELY 50% of the total organic carbon degraded by the anaerobic microbiota in the biosphere results in the formation of methane (HIGGINS *et al.*, 1981). The biogenesis of methane under controlled conditions has the potential to become a source of renewable energy, and might be of major significance in a future of predicted limited resources. However, not all the effects of methane are beneficial to mankind. Biogenic methane formed under pressure in landfill sites can be dangerous if the capping material has insufficient strength to contain the pressure of gas generated. Methane formed close to the surface in marine sediments can present drilling operations with potentially dangerous high pressure sources of methane, generally referred to as "shallow gas" (HOVLAND and JUDD, 1988).

Methane is biologically generated by a diverse group of bacteria called methanogens. These together with certain thermoacidophilic, thermophilic and halophilic bacteria constitute a separate kingdom of bacteria known as the archaeobacteria, a distinction that is made due to the possession of a number of unique biochemical features that clearly differentiate them from all other prokaryotic and eukaryotic life (BALCH *et al.*, 1979). The membrane lipids of the archaeobacteria are one such distinguishing feature where the usual ester linked phospholipids are replaced by ether linked analogues.

*School of Ocean Sciences, University College of Wales, Bangor, Menai Bridge, Gwynedd LL59 5EY, U.K.

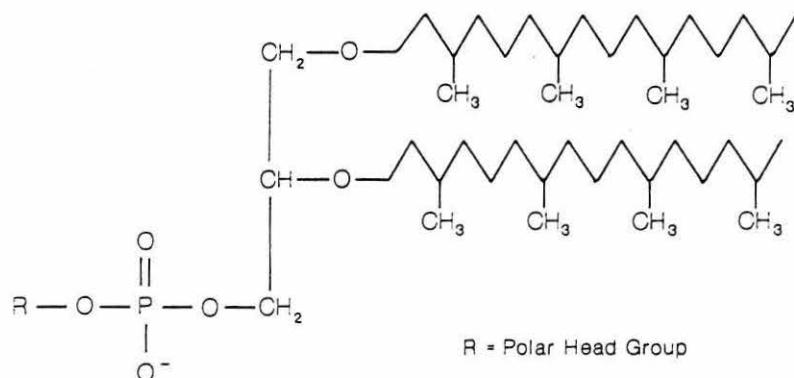


Fig. 1. Methanogenic Diether Phospholipid Di-phytanyl Glycerol Ether (DPGE).

In most cases, the membrane lipids of archaeobacteria are based on two principal structures. These consist of two 20 carbon saturated isoprenoid hydrocarbons ether linked to a glycerol backbone (di-*O*-phytanyl glycerol ether; DPGE) (Fig. 1) or two 40 carbon isoprenoid hydrocarbons ether linked to two glycerol molecules [tetra-*O*-di(biphytanyl glycerol ether); biDPGE] in a "monolayer" type membrane configuration (JONES *et al.*, 1987). Although DPGE and biDPGE are the predominant constituents of archaeobacterial polar lipids, diversity exists within these characteristic structures (DE ROSA *et al.*, 1986).

Thermoacidophilic and thermophilic archaeobacteria, found in hot springs and hydrothermal vents, tend to possess a significant proportion of the stronger tetraether lipid in what is believed to reflect a more extreme environment. WOESE *et al.* (1978) postulated that such archaeobacteria are similar to those early life forms when primordial earth was a hot, acidic, anaerobic environment. Halophiles and methanogens occupy comparatively less extreme environments and as a result contain relatively less tetraether and more of the diether phospholipid component (Fig. 1) than thermoacidophiles and thermophiles (JONES *et al.*, 1987).

Methanogens occupy some very varied ecosystems which include ruminant animals, termite guts, paddy fields, landfill sites, marine and freshwater sediments. Methanogens isolated from marine and freshwater sediments principally contain diether (DPGE) and uncyclized tetraether (biDPGE) lipids in various proportions (KONIG and STETTER, 1988, PAULY and VAN VLEET, 1986). Quantification of such lipids has been used effectively as a means of differentiating methanogenic from nonarchaeobacterial biomass in both water column particulate material and sediment samples taken from an Antarctic lake (MANCUSO *et al.*, 1990).

Therefore since the thermoacidophiles, thermophiles and halophiles are unlikely to form a significant biomass in such mesophilic sediments the diether lipid (DPGE) could be an ideal signature lipid for the determination of methanogenic biomass and growth.

MATERIALS AND METHODS

All solvents used in the experiments described below were purchased from Rathburn Chemicals Ltd (Walkerburn, Scotland). Other chemicals came from Sigma Chemicals Ltd (Dorset, England). Spectrophotometric determinations were made on a diode array spectrophotometer (Hewlett Packard, Vectra ES/12).

Growth of the bacterium

One hundred millilitres of monoculture were grown in 200 ml medical flasks fitted with modified suba seals and a metal screw top to facilitate head space sampling. The monoculture *Methanobus tindarius* is a marine, mesophilic, coccoidal or lobal, monotrichous flagellated methanogen isolated from a marine sediment at Tindari in Sicily (KONIG and STETTER, 1982). The culture was grown at 25°C and pH = 6.2 on Medium No. 3 (BALCH *et al.*, 1979) without acetate, yeast extract or trypticase and was supplemented with 123 mmol l⁻¹ methanol and 59 mmol l⁻¹ trimethylamine.

Bacterial direct counts

Cells were first immersed in tetrasodium pyrophosphate (0.001 M), a deflocculent used in conjunction with a sonic probe to gently disperse the cells in an even manner (VELJI and ALBRIGHT, 1986). Using the method of PARSONS *et al.* (1984) the bacteria were stained with acridine orange and diluted with formalin (40%) before being filtered on to a prestained irglan black nucleopore filter. Enumeration was made with a Leitz (Ortholux, 8667-51) UV microscope using BG38 and BG12 excitation filters and a K510 barrier filter on setting 2.

Lipid extraction

The gas headspace, cell number and turbidity analyses were completed before the lipid extraction commenced. Each 100 ml of growth culture was then centrifuged at 30,000 rpm (10,000 g) for 20 min before discarding the supernatant.

Environmental samples (approximately 90 g or wet weight) were collected using a hand held corer from approximately 40 cm below the surface for the marine inter-tidal sample (collected from the Menai Strait, N. Wales) and 15 cm for the freshwater sample (from Llyn Maelog Lake, Rhosneigr, N. Wales).

The lipid extraction technique of BLIGH and DYER (1959) was completed for all samples and modified with 5% trichloroacetic acid aqueous phase for increased yield from bound proteins (NISHIHARA and KOGA, 1988). Sonication also helped to break up particles and aid in lipid-solvent interaction. An addition of 50 µg internal standard 1,2-di-O-hexadecyl *rac* glycerol ensured that extraction losses were accounted for. Each single phase organic/aqueous extraction was maintained for 2 h for the growth culture experiments and 6 h for the environmental samples. The latter samples were then filtered and the residue re-extracted and filtered before the chloroform fraction was rotary evaporated to dryness in a reacti-vial.

Cleavage and substitution of the ether lipids

Approximately 2.5 ml of 47% hydriodic acid was added to each rotary evaporated sample and refluxed in the reacti-vial for 12 h at 100°C with intermittent shaking. Addition of deionized water facilitated the transfer of lipid into a petroleum ether (40–60°) phase which was subsequently washed with saturated sodium thiosulphate solution. The alkyl iodides were substituted with an acetate group by further blowing down of the organic phase in a reacti-vial and adding 2.5 ml glacial acetic acid in an excess of silver acetate. This

was refluxed at 100°C for 24 h with intermittent shaking (GUYER *et al.*, 1963). Lipid extraction using deionized water and petroleum ether was again repeated before washing the sample with saturated sodium hydrogen carbonate solution, to remove excess acid and anhydrous sodium sulphate solution to dry the sample.

Purification of the alkyl acetates

The dried sample was blown down and taken up in 100 μ l of chloroform and spotted on a TLC plate. A hexane/ether (95:5) mobile phase was used in a continuous coelution tank for 50 min. Coelution of the phytanyl acetate standard together with exposure to iodine vapour showed the location of the alkyl acetates, which were scraped off and eluted with chloroform and methanol (1:1) through a glass wool plug. The sample was blown down under nitrogen and taken up in 200 μ l of *n*-hexane. The phytanyl acetate standard was prepared from phytol using platinum dioxide (Adams' Catalyst) and the method of GUYER *et al.* (1963).

Gas-liquid chromatography

Phytanyl acetate was analysed on a Carlo Erba (HRGC 5160) gas chromatograph equipped with an SE30 capillary column (0.3 mm \times 25 m) (Alltech Associates Inc., Lancashire), using a nitrogen carrier gas and a flame ionisation detector (FID). A temperature program from 50 to 300°C at 10°C min⁻¹ gave a phytanyl acetate retention time of approximately 20 min for a 70 kPa carrier gas pressure. The internal standard gave a retention time of 19 min (hexadecanyl acetate; C₁₆H₃₃-O-COCH₃). Typical chromatograms of both the sample and standard peaks are given in Fig. 2. Headspace gas was analysed for methane using a DANI (3800) gas chromatograph with a 1.5 m \times 3 mm packed (Porapak Q) column, nitrogen carrier gas and an FID.

RESULTS AND DISCUSSION

Growth experiment

The cell number growth curve (Fig. 3) shows negligible lag phase immediately after culture inoculation. Over the 8 to 56 h experimental period, the bacterial cell numbers increased in an exponential manner reaching the final stationary phase after approximately 56 h. Observations made using epifluorescent microscopy over the 8 to 56 h time period showed that *M. tindarius* tended to devote more energy towards cell division rather than individual cell growth, with mean cell diameters of approximately 0.3 μ m. During the stationary phase which began after 56 h the growth of individual cells became the more dominant process, with bacterial cells reaching 1 μ m in diameter. Turbidity which was measured as absorbance at 578 nm also showed this change in the growth phase after approximately 48/56 h (Fig. 3).

Good correlation was found between the DPGE lipid concentration and total methane produced over time (Fig. 4). This result might be expected in such a closed system growth experiment during relatively early growth phases since methane production is directly related to the cell energy. During this log phase the energy produced would be used both

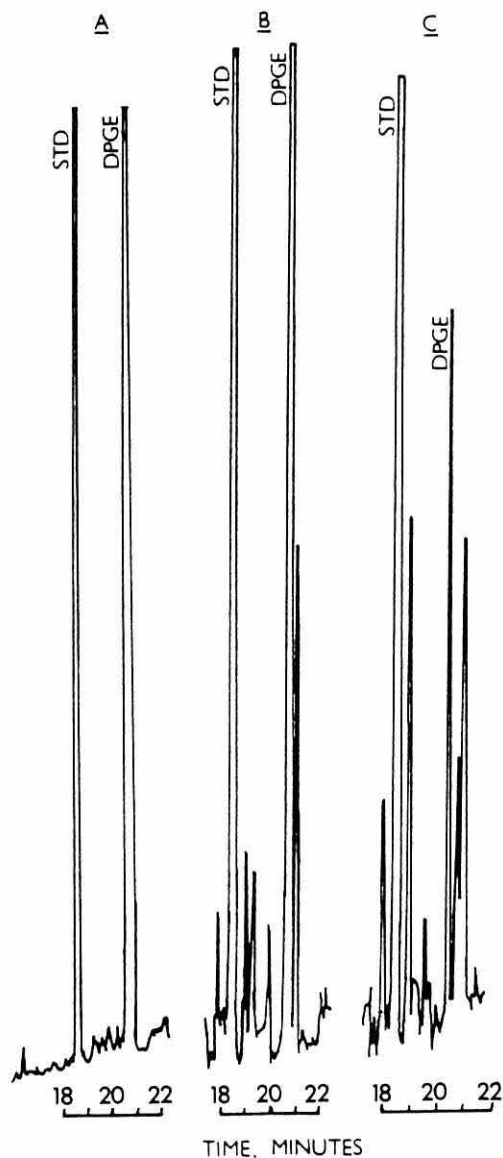


Fig. 2. Gas chromatograms representing internal standard (STD) and diether phospholipid (DPGE) for: (A) growth experiment; (B) freshwater; and (C) marine samples.

for cell division and also for increasing the cell size, both of which will contribute to the membrane lipid concentration.

The relationship between total membrane produced and the membrane DPGE lipid concentration is also shown in Fig. 5. By using a log scale of methane produced versus the lipid concentration (Fig. 5) the change in the growth phase at 48/56 h can be observed more clearly.

Figure 6 again shows this relatively abrupt change in the results of the growth experiment after approximately 48 h. This result could either be totally due to the noticeable change in the cell size during the growth phase or due to a change in the diether

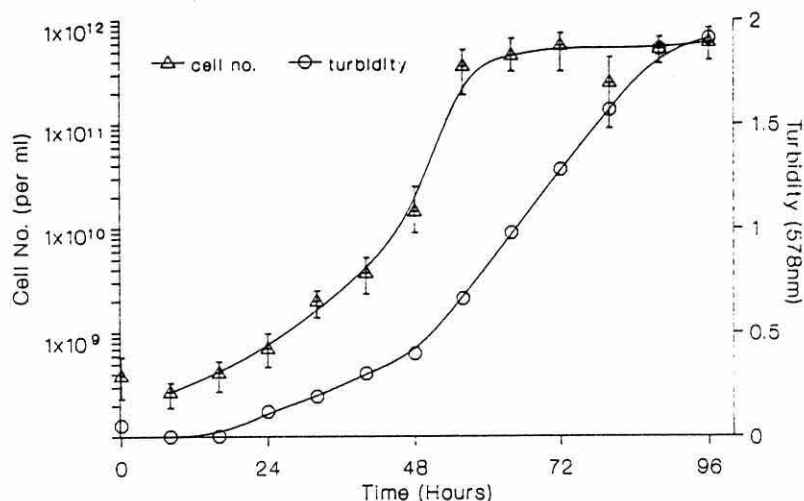


Fig. 3. Growth experiment showing *M. tindarius* cell number and turbidity at 578 nm over time.

lipid composition over this period. A further experiment will need to be conducted using the additional parameter of cell volume in order to conclude whether the phospholipid composition does change during the growth phase of *M. tindarius*.

Preliminary environmental results

Table 1 shows that the concentration of DPGE lipid in the freshwater sample was an order of magnitude greater than that of the marine sample, a result that was expected due to the higher concentration of sulphate in the marine environment. This allowed the sulphate reducing bacteria to predominate by out-competing the methanogens for electron acceptors (LOVLEY *et al.*, 1982).

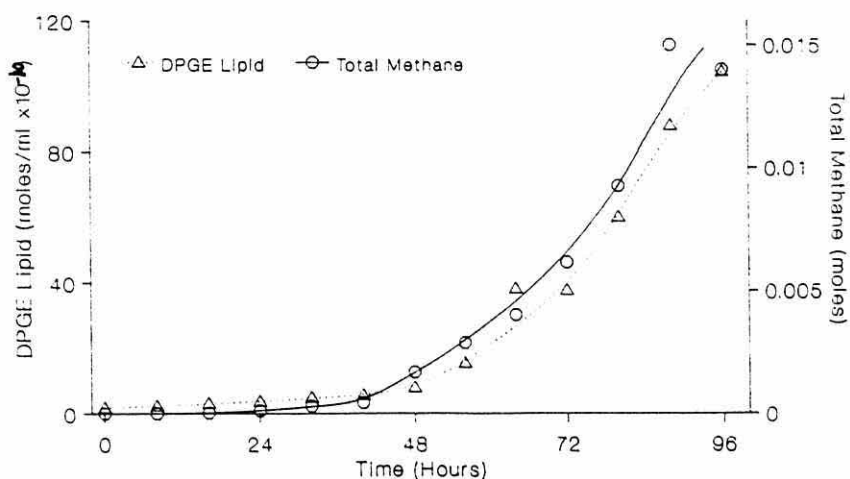


Fig. 4. Growth experiment showing DPGE lipid concentration and total methane produced over time for *M. tindarius*.

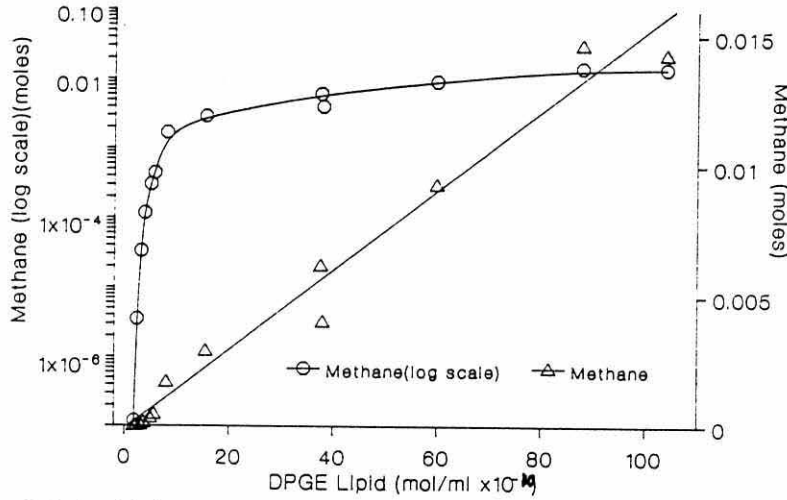


Fig. 5. Relationship between total methane produced (linear and log scale) and DPGE concentration for *M. tindarius*.

MARTZ *et al.* (1983) used a different method of DPGE lipid analysis using high performance liquid chromatography (HPLC). They found a freshwater value of 8.7 nmoles DPGE/dry g sediment which is comparable to the 3.23 nmoles DPGE/dry g measured from the single site and single depth in Llyn Maelog Lake. MARTZ *et al.* (1983) also quoted an estuarine concentration of 70 pmoles DPGE/dry g sediment. This is almost an order of magnitude less than the Menai Strait sample (454 pmoles), a difference possibly attributable to the greater sewage loading of the Menai Strait. A combination of both a high organic loading and high sedimentation rate has the effect of causing a more rapid sediment redox change, due to the scavenging of oxygen associated with aerobic organic matter breakdown. This process provides the anaerobic microbiota with more

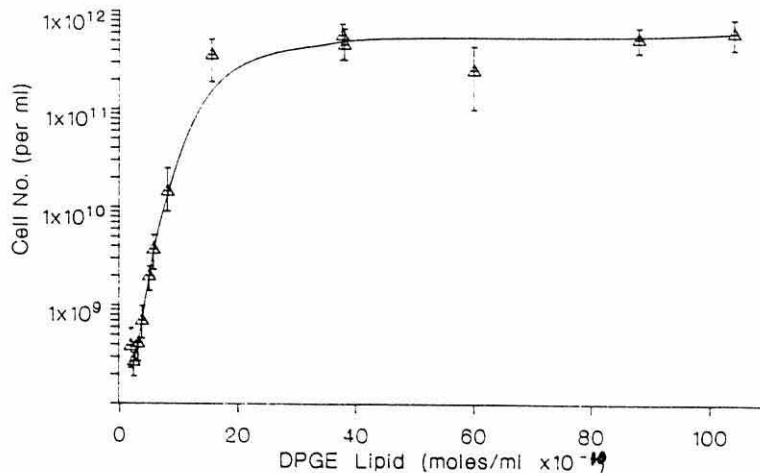


Fig. 6. Relationship between cell number and DPGE phospholipid during the growth experiment of *M. tindarius*.

Table 1. Diether (DPGE) lipid concentrations for environmental samples

	Concentration DPGE lipid per dry gram sediment
Freshwater sample (Llyn Maelog Lake)	2.20 μg DPGE/dry g 3.23 nmoles DPGE/dry g
Marine sample (Menai Strait)	303 ng DPGE/dry g 454 pmoles DPGE/dry g

organic substrates which are either directly or indirectly utilizable by the methanogenic bacteria.

Detection limit

By using capillary gas chromatography with a flame ionization detector, a detection limit of 1.6×10^{-9} g phytanyl acetate was achieved. This corresponds to 2.35×10^{-12} moles DPGE lipid. From dry weight measurements it was calculated that the detection limit corresponds to 1.21×10^{-7} g bacteria.

This sensitivity in terms of the number of bacteria clearly depends very closely on the mean size of the organism. The methanogen *M. tindarius* used in the growth experiment had a mean size of $0.7 \mu\text{m}$ diameter ($0.17 \mu\text{m}^3$). Hence 10^7 cells would be required to detect this small methanogen. However, other methanogens found in marine sediments, such as *Methanosarcina*, *Methanogenium*, *Methanomicrobiales* and *Methanobacterium* species tend to be much larger in size, with cell volumes ranging from 0.52 up to $14.2 \mu\text{m}^3$ ($3.0 \mu\text{m}$ diameter), and therefore the number required for detection will decrease. By using a typical bacterial size at $3 \times 1 \mu\text{m}$, with a cell volume of $2.36 \mu\text{m}^3$ and a dry weight of 1.1×10^{-12} g cell $^{-1}$, a total of 110,000 cells would be required for detection and quantification. MARTZ *et al.* (1983) quote a sensitivity of 7×10^{-14} moles DPGE but peak resolution is not fully achieved.

CONCLUSIONS

All parameters used to monitor the growth experiment show an interesting change in the growth curve of *M. tindarius*. Cell division is the initial, most dominant process of increasing the biomass, with cell sizes not increasing to more than $0.3 \mu\text{m}$ in diameter. After approximately 48 h into the growth experiment the rate of cell division decreases and the growth of individual bacterial cells becomes the major process of increasing methanogenic biomass. This is reflected in the cell sizes increasing to more than $1 \mu\text{m}$ in diameter. The relationship between the total methane produced and the DPGE lipid concentration also illustrates this change in the growth phase as well as possibly suggesting a change in the DPGE lipid composition early in the growth phase of *M. tindarius*.

The DPGE lipid concentration appears to be an adequate indication of methanogenic biomass in a controlled closed system growth experiment. The total methane produced also reflects the biomass of *M. tindarius* which is expected in such an experiment where methane is produced directly from all energy associated processes, and is subsequently not

chemically or biologically oxidized. The DPGE lipid concentration however, together with total substrate availability, has the added advantage of possibly differentiating between methane produced at a particular point in a sediment, and methane migration to that point. This technique would appear to have an advantage over the Most Probable Number (MPN) method, which can be seriously limited due to the media exerting selective growth of the population (ROWE *et al.*, 1977). However, when the methanogenic population is relatively small and increased sediment size is an impractical means of extracting sufficient DPGE lipid then the MPN technique would be a more appropriate technique to use.

Preliminary environmental results show that the DPGE lipid can be both detected and quantified at levels as low as 2.35×10^{-12} moles DPGE using this method. Both marine and freshwater sediment samples gave typical DPGE concentrations of 454 pmoles and 3.23 nmoles per dry gram of sediment, respectively. This is comparable to other environmental DPGE results made using high performance liquid chromatography (MARTZ *et al.*, 1983).

Acknowledgements—The authors wish to thank Dr M. Blaut for the methanogenic monoculture of *Methanobus tindarius*. This work was supported by grant No. GR/E/9746.3 from the Science and Engineering Research Council with a linked case award from ESSO Petroleum Company Ltd.

REFERENCES

- BALCH W. E., G. E. FOX, L. J. MAGRUM, C. R. WOESE and R. S. WOLFE (1979) Methanogens: reevaluation of a unique biological group. *Microbiological Reviews*, **43**, 260–296.
- BLIGH E. G. and W. J. DYER (1959) A rapid method of total lipid extraction and purification. *Canadian Journal of Biochemistry and Physiology*, **37**, 911–917.
- DE ROSA M., A. GAMBACORTA and A. GLIOZZI (1986) Structure, biosynthesis, and physicochemical properties of archaeobacterial lipids. *Microbiological Reviews*, **50**, 70–80.
- GUYER K. E., W. A. HOFFMAN, L. A. HORROCKS and D. G. CORNWELL (1963) Studies on the composition of glycerol ethers and their preparation from diacyl glycerol ethers in liver oils. *Journal of Lipid Research*, **4**, 385–391.
- HIGGINS I. F., D. J. BEST, R. C. HAMMOND and D. SCOTT (1981) Methane-oxidizing microorganisms. *Microbiological Reviews*, **45**, 556–590.
- HOVLAND M. and A. G. JUDD (1988) *Seabed pockmarks and seepages*. Graham and Trotman Ltd, London, 285 pp.
- JONES W. J., D. P. NAGLE and W. B. WHITMAN (1987) Methanogens and the diversity of archaeobacteria. *Microbiological Reviews*, **51**, 135–177.
- KONIG H. and K. O. STETTER (1982) Isolation and characterization of *Methanobus tindarius* sp. nov., a coccoid methanogen growing only on methanol and methylamines. *Zentralblatt für Bakteriologie, Mikteriologie und Hygiene*, I. Abt. Orig. C3, 478–490.
- KONIG H. and K. O. STETTER (1988) Archaeobacteria. In: *Bergey's manual of systematic bacteriology*, J. T. STALEY, M. P. BRYANT, N. PFFENNIG and J. G. HOLT, editors. Vol. 3, Willimans and Wilkins, Baltimore, pp. 2171–2220.
- LOVLEY D. R., D. F. DWYER and M. J. KLUG (1982) Kinetic analysis of competition between sulphate reducers and methanogens for hydrogen in sediments. *Applied and Environmental Microbiology*, **43**, 1373–1379.
- MANCUSO C. A., P. D. FRANZMANN, H. R. BURTON and P. D. NICHOLS (1990) Microbial community structure and biomass estimates of a methanogenic Antarctic lake ecosystem as determined by phospholipid analyses. *Microbial Ecology*, **19**, 73–95.
- MARTZ R. F., D. I. SEBACHER and D. C. WHITE (1983) Biomass measurement of methane forming bacteria in environmental samples. *Journal of Microbiological Methods*, **1**, 53–61.
- NISHIHARA M. and Y. KOGA (1988) Quantitative conversion of diether or tetraether phospholipids to glycerol-

- phosphoesters by dealkylation with BCl_3 : a tool for structural analysis of archaeobacterial lipids. *Journal of Lipid Research*, **29**, 384–388.
- PARSONS T. R., Y. MAITA and C. M. LALLI (1984) *A manual of chemical and biological methods for seawater analysis*, Pergamon Press, Oxford, 130 pp.
- PAULY G. G. and E. S. VAN VLEET (1986) Archaeobacterial ether lipids: Natural tracers of biogeochemical processes. *Organic Geochemistry*, **10**, 859–867.
- ROWE R., R. TODD and J. WAIDE (1977) Microtechnique for most probable number analysis. *Applied and Environmental Microbiology*, **33**, 675–680.
- TORNABENE T. G. and T. A. LANGWORTHY (1979) Diphytanyl and dibiphytanyl glycerol ether lipids of methanogenic archaeobacteria. *Science*, **203**, 51–53.
- VELJI M. I. and L. J. ALBRIGHT (1986) Microscopic enumeration of attached marine bacteria of seawater, marine sediment, fecal matter and kelp blade samples following pyrophosphate and ultrasound treatments. *Canadian Journal of Microbiology*, **32**, 121–126.
- WOESE C. R., L. J. MAGRUM and G. E. FOX (1978) Archaeobacteria. *Journal of Molecular Evolution*, **11**, 245–252.

Table A10.1. Water depth soundings taken from the bathymetry survey of Holyhead Harbour in 1985.

Longitude coordinate (4°37')	7.8"	7.5"	7.3"	7.0"	6.8"	6.5"	6.3"	6.0"	5.8"	5.5"	5.3"	5.0"	4.8"	4.5"	4.3"	4.0"	3.8"	3.5"	3.3"	3.0"	2.8"	2.5"	2.3"	2.0"	
Longitude distance (m)	116	120	125	130	134	139	143	148	153	157	162	167	171	176	180	185	190	194	199	204	208	213	217	222	
Latitude distance (m)																									
Latitude coordinate																									
0m 53°19'36.0"	10.9	11.3	11.4	11.4	11.5	11.5	11.6	11.7	11.7	11.8	11.6	11.5	11.6	11.6	11.6	11.6	11.6	11.6	11.6	11.6	11.7	11.7	11.8	11.9	12.0
6 53°19'36.2"	10.8	11.2	11.5	11.5	11.5	11.5	11.5	11.6	11.6	11.5	11.2	11.3	11.5	11.6	11.6	11.6	11.6	11.6	11.6	11.6	11.6	11.7	11.9	12.0	12.0
12 53°19'36.4"	10.7	11.2	11.6	11.6	11.4	11.4	11.5	11.5	11.5	11.3	11.2	11.4	11.5	11.5	11.5	11.6	11.7	11.7	11.7	11.7	11.8	11.9	11.9	11.9	
18 53°19'36.6"	10.7	11.2	11.6	11.6	11.3	11.3	11.4	11.4	11.4	11.2	11.2	11.4	11.5	11.5	11.5	11.6	11.7	11.7	11.7	11.8	11.8	11.8	11.9	12.0	
25 53°19'36.8"	10.6	11.1	11.6	11.6	11.3	11.4	11.3	11.3	11.2	11.2	11.2	11.4	11.5	11.5	11.7	11.6	11.7	11.8	11.8	11.8	11.8	11.8	11.8	12.1	
31 53°19'37.0"	10.5	11.0	11.5	11.5	11.4	11.4	11.2	11.4	11.2	11.2	11.3	11.4	11.5	11.5	11.7	11.8	11.8	11.8	11.9	11.8	11.9	11.8	11.8	12.2	
37 53°19'37.2"	10.4	10.9	11.5	11.5	11.5	11.3	11.0	11.4	11.2	11.3	11.3	11.4	11.6	11.6	11.7	11.8	11.9	11.9	11.9	11.9	11.9	11.9	11.8	12.0	12.3
43 53°19'37.4"	10.3	11.2	11.4	11.4	11.4	11.2	11.0	11.3	11.2	11.3	11.4	11.4	11.6	11.6	11.8	11.9	11.9	11.9	11.9	11.8	11.9	11.9	11.9	12.1	12.4
49 53°19'37.6"	10.2	11.4	11.4	11.4	11.4	11.1	11.0	11.3	11.2	11.4	11.4	11.4	11.6	11.7	11.8	11.9	11.9	11.9	11.9	11.8	11.9	12.0	12.2	12.5	
55 53°19'37.8"	10.2	11.0	11.4	11.4	11.3	11.0	11.0	11.2	11.2	11.4	11.4	11.4	11.6	11.7	11.9	11.9	11.9	11.9	11.9	11.9	12.2	12.1	12.3	12.6	
62 53°19'38.0"	10.5	10.9	11.3	11.2	11.1	11.0	11.1	11.2	11.3	11.4	11.4	11.4	11.7	11.8	11.9	12.0	11.9	11.9	11.9	12.1	12.2	12.2	12.4	12.7	
68 53°19'38.2"	10.7	11.2	11.2	11.2	11.0	11.0	11.2	11.2	11.3	11.3	11.4	11.4	11.6	11.9	12.0	12.0	12.0	12.0	12.0	12.1	12.2	12.2	12.4	12.8	
74 53°19'38.4"	10.9	11.1	11.1	11.1	11.0	11.0	11.2	11.2	11.4	11.3	11.3	11.4	11.7	11.9	11.9	12.0	12.0	12.0	12.0	12.1	12.2	12.3	12.6	12.7	
80 53°19'38.6"	11.0	11.0	11.1	11.0	11.0	11.1	11.2	11.2	11.4	11.3	11.3	11.5	11.6	11.8	11.8	11.9	12.0	12.0	12.1	12.2	12.3	12.3	12.5	12.6	
86 53°19'38.8"	11.0	11.0	11.0	11.0	11.1	11.1	11.2	11.3	11.3	11.2	11.3	11.4	11.5	11.7	11.7	11.8	11.9	11.6	12.3	12.3	12.4	12.5	12.5	12.5	
92 53°19'39.0"	11.0	11.0	11.0	11.1	11.1	11.2	11.2	11.3	11.3	11.4	11.4	11.4	11.5	11.6	11.6	11.7	11.7	11.8	12.1	12.4	12.4	12.4	12.4	12.4	

* Data points in shaded boxes refer to the reported depth soundings whereas the remaining points were estimated from contour diagrams.

Table A10.2. Water depths taken from the bathymetry survey of Holyhead Harbour in 1993.

Longitude	4°37'	14.0"	13.8"	13.5"	13.3"	13.0"	12.8"	12.5"	12.3"	12.0"	11.8"	11.5"	11.3"	11.0"	10.8"	10.5"	10.3"	10.0"
Latitude	Distance	0	5	9	14	19	23	28	32	37	42	46	51	56	60	65	69	74
53°19'	metres																	
36.0"	0	7.1	7.1	7.1	7.2	7.3	7.3	7.3	7.3	7.2	7.2	7.2	7.2	7.2	7.2	7.4	7.5	7.4
36.2"	6	7.1	7.1	7.2	7.2	7.3	7.3	7.3	7.2	7.2	7.2	7.2	7.2	7.2	7.2	7.3	7.4	7.4
36.4"	12	7.1	7.2	7.3	7.2	7.2	7.3	7.2	7.2	7.2	7.2	7.1	7.1	7.1	7.1	7.2	7.3	7.3
36.6"	19	7.2	7.2	7.3	7.2	7.2	7.2	7.1	7.1	7.1	7.1	7.1	7.1	7.1	7.1	7.1	7.2	7.2
36.8"	25	7.2	7.2	7.3	7.1	7.1	7.1	7.1	7.1	7.1	7.1	7.1	7.1	7.1	7.1	7.0	7.2	7.2
37.0"	31	7.2	7.2	7.2	7.0	7.0	7.0	7.1	7.1	7.1	7.1	7.1	7.1	7.1	7.1	6.9	7.0	7.2
37.2"	37	7.1	7.1	7.1	6.9	7.0	7.1	7.1	7.0	7.1	7.0	7.0	7.0	7.1	7.0	7.0	7.0	7.1
37.4"	43	7.0	7.0	7.0	6.9	6.9	7.0	7.1	7.0	7.0	7.0	7.0	7.1	7.1	7.0	7.0	7.0	7.0
37.6"	49	7.0	7.0	7.0	6.9	6.9	7.0	7.0	6.9	7.0	7.0	7.0	7.0	7.0	7.0	7.0	7.1	7.0
37.8"	55	6.9	7.0	7.0	6.9	6.8	6.9	7.0	6.9	7.0	7.0	6.9	6.9	6.9	7.0	7.0	7.1	7.0
38.0"	62	6.9	6.9	6.9	6.8	6.8	6.9	7.0	6.8	6.9	6.9	6.8	6.8	6.8	6.8	6.9	7.0	7.0
38.2"	68	6.9	6.9	6.8	6.8	6.8	6.9	7.0	6.8	6.7	6.8	6.8	6.8	6.8	6.9	6.9	7.0	7.0
38.4"	74	6.9	6.9	6.8	6.7	6.8	6.8	6.9	6.8	6.7	6.7	6.8	6.8	6.9	6.8	6.8	6.9	7.2
38.6"	80	6.8	6.8	6.8	6.7	6.7	6.7	6.8	6.7	6.7	6.7	6.7	6.9	7.0	6.9	6.8	7.0	7.5
38.8"	86	6.8	6.8	6.8	6.7	6.6	6.6	6.7	6.7	6.7	6.6	6.7	6.9	7.1	7.0	7.1	7.3	7.9
39.0"	92	6.8	6.8	6.7	6.6	6.5	6.5	6.6	6.6	6.6	6.6	6.6	6.9	7.1	7.3	7.5	7.7	7.9

Longitude	4°37'	9.8"	9.5"	9.3"	9.0"	8.8"	8.5"	8.3"	8.0"	7.8"	7.5"	7.3"	7.0"	6.8"	6.5"	6.3"	6.0"
Latitude	Distance	79	83	88	93	97	102	106	111	116	120	125	130	134	139	143	148
36.0"	0	7.5	7.6	7.7	7.7	7.7	7.7	7.7	7.7	8.0	8.0	8.5	9.0	10.3	10.5	10.7	10.6
36.2"	6	7.5	7.6	7.7	7.6	7.5	7.4	7.3	7.5	7.7	8.1	8.6	9.5	10.2	10.5	10.6	10.6
36.4"	12	7.5	7.5	7.5	7.5	7.4	7.2	7.4	7.7	7.9	8.2	8.7	9.6	10.3	10.4	10.5	10.5
36.6"	19	7.4	7.4	7.3	7.3	7.1	7.8	8.0	8.0	7.9	9.3	9.0	9.6	10.0	10.2	10.4	10.3
36.8"	25	7.3	7.2	7.1	7.1	7.1	7.8	8.0	8.5	9.1	9.0	9.3	9.6	10.0	10.3	10.4	10.3
37.0"	31	7.2	7.1	7.1	7.2	7.5	8.0	8.5	8.9	9.1	9.3	9.6	9.6	10.1	10.3	10.5	10.4
37.2"	37	7.1	7.0	7.1	7.2	7.8	8.5	8.6	8.9	9.1	9.5	9.6	9.9	10.2	10.5	10.5	10.4
37.4"	43	7.0	7.0	7.2	7.4	8.0	8.1	8.0	8.2	9.2	9.6	9.9	10.3	10.5	10.4	10.4	10.4
37.6"	49	6.8	7.0	7.4	7.5	8.0	8.4	8.5	9.0	9.4	9.7	10.1	10.3	10.5	10.4	10.3	10.4
37.8"	55	6.9	7.0	7.5	8.0	8.5	8.7	8.8	9.0	9.6	9.8	9.9	10.2	10.4	10.3	10.2	10.2
38.0"	62	7.2	7.2	7.8	8.5	8.6	8.7	8.8	9.0	9.6	9.7	10.0	10.2	10.4	10.2	10.1	10.1
38.2"	68	7.4	7.7	8.0	8.0	8.2	8.0	8.9	9.0	9.8	9.9	10.1	10.2	10.3	10.2	10.1	10.1
38.4"	74	7.7	7.9	8.2	8.0	7.9	7.6	8.9	9.5	9.9	10.0	10.1	10.2	10.3	10.2	10.1	10.2
38.6"	80	8.0	8.2	8.4	8.0	8.0	8.0	8.9	9.5	10.1	10.1	10.2	10.2	10.3	10.3	10.2	10.3
38.8"	86	8.2	8.3	8.3	8.2	8.2	8.5	9.0	9.5	10.0	10.1	10.1	10.1	10.2	10.3	10.3	10.3
39.0"	92	8.2	8.3	8.3	8.4	8.4	8.5	9.0	9.5	10.0	10.0	10.0	10.1	10.2	10.3	10.4	10.4

Longitude	4°37'	5.8"	5.5"	5.3"	5.0"	4.8"	4.5"	4.3"	4.0"	3.8"	3.5"	3.3"	3.0"	2.8"	2.5"	2.3"	2.0"
Latitude	Distance	153	157	162	167	171	176	180	185	190	194	199	204	208	213	217	222
36.0"	0	10.6	10.5	10.4	10.4	10.3	10.3	10.4	10.5	10.6	10.7	10.7	10.7	10.8	10.8	10.9	10.9
36.2"	6	10.5	10.4	10.4	10.5	10.5	10.4	10.5	10.6	10.6	10.6	10.7	10.8	10.8	10.8	10.9	10.9
36.4"	12	10.3	10.2	10.3	10.6	10.6	10.6	10.5	10.6	10.6	10.6	10.6	10.8	10.9	10.8	10.8	10.9
36.6"	19	10.2	10.1	10.4	10.6	10.6	10.6	10.5	10.6	10.6	10.7	10.7	10.8	10.9	10.8	10.8	10.8
36.8"	25	10.3	10.2	10.3	10.5	10.5	10.6	10.5	10.6	10.6	10.8	10.9	10.9	10.9	10.8	10.8	10.9
37.0"	31	10.3	10.3	10.4	10.5	10.5	10.5	10.5	10.5	10.6	10.8	10.9	10.9	10.9	10.9	10.8	10.9
37.2"	37	10.4	10.3	10.3	10.4	10.5	10.5	10.5	10.5	10.6	10.8	10.9	10.9	11.0	11.0	10.9	10.9
37.4"	43	10.4	10.3	10.3	10.4	10.5	10.5	10.6	10.6	10.6	10.7	10.8	11.0	11.0	11.1	11.0	11.0
37.6"	49	10.3	10.3	10.3	10.4	10.5	10.6	10.7	10.7	10.7	10.8	10.9	11.0	11.1	11.2	11.0	11.0
37.8"	55	10.3	10.3	10.4	10.4	10.5	10.6	10.7	10.8	10.8	10.9	11.0	10.8	11.1	11.2	11.1	11.1
38.0"	62	10.3	10.3	10.4	10.5	10.5	10.6	10.7	10.8	10.9	11.0	11.1	11.0	11.2	11.3	11.1	11.2
38.2"	68	10.2	10.2	10.4	10.5	10.6	10.6	10.7	10.8	10.9	11.0	11.0	11.1	11.3	11.4	11.2	11.3
38.4"	74	10.3	10.2	10.3	10.4	10.5	10.6	10.7	10.8	10.9	10.9	10.9	11.0	11.2	11.4	11.3	11.4
38.6"	80	10.2	10.3	10.4	10.4	10.5	10.6	10.7	10.8	11.0	10.9	11.0	11.0	11.1	11.4	11.3	11.4
38.8"	86	10.3	10.4	10.4	10.5	10.6	10.7	10.8	10.9	11.1	11.0	11.0	11.0	11.1	11.3	11.4	11.5
39.0"	92	10.4	10.5	10.5	10.5	10.7	10.9	11.0	11.0	11.1	11.1	11.0	11.0	11.1	11.3	11.4	11.5

* Data points in the shaded boxes refer to the positions of the reported depth soundings and the remaining intermediate data points were estimated from contour diagrams constructed through the reported values.

Table A10.3. Change in water depth soundings (m) between two bathymetry surveys of Holyhead Harbour from 1985 to 1993.
(The positive values presented refer to the increase in sedimentation from 1985 to 1993).

Longitude coordinate (4°37')	7.8"	7.5"	7.3"	7.0"	6.8"	6.5"	6.3"	6.0"	5.8"	5.5"	5.3"	5.0"	4.8"	4.5"	4.3"	4.0"	3.8"	3.5"	3.3"	3.0"	2.8"	2.5"	2.3"	2.0"	
Longitude distance (m)	116	120	125	130	134	139	143	148	153	157	162	167	171	176	180	185	190	194	199	204	208	213	217	222	
Latitude distance (m)																									
Latitude coordinate																									
0m 53°19'36.0"	2.9	3.3	2.9	2.4	1.2	1.0	0.9	1.1	1.1	1.3	1.2	1.1	1.3	1.3	1.2	1.1	1.0	0.9	0.9	1.0	0.9	1.0	1.0	1.1	
6 53°19'36.2"	3.1	3.1	2.9	2.0	1.3	1.0	0.9	1.0	1.1	1.1	0.8	0.8	1.0	1.2	1.1	1.0	1.0	1.0	0.9	0.8	0.9	1.1	1.1	1.1	
12 53°19'36.4"	2.8	3.0	2.9	2.0	1.1	1.0	1.0	1.0	1.2	1.1	0.9	0.8	0.9	0.9	1.0	0.9	1.0	1.1	1.1	0.9	0.9	1.1	1.1	1.0	
18 53°19'36.6"	2.8	1.9	2.6	2.0	1.3	1.1	1.0	1.1	1.2	1.1	0.8	0.8	0.9	0.9	1.0	0.9	1.0	1.0	1.0	1.0	0.9	1.0	1.1	1.2	
25 53°19'36.8"	1.5	2.1	2.3	2.0	1.3	1.1	0.9	1.0	0.9	1.0	0.9	0.9	1.0	0.9	1.2	1.0	1.1	1.0	0.9	0.9	0.9	1.0	1.0	1.2	
31 53°19'37.0"	1.4	1.7	1.9	1.9	1.3	1.1	0.7	1.0	0.9	0.9	0.9	0.9	1.0	1.0	1.2	1.3	1.2	1.0	1.0	0.9	1.0	0.9	1.0	1.3	
37 53°19'37.2"	1.3	1.4	1.9	1.6	1.3	0.8	0.5	1.0	0.8	1.0	1.0	1.0	1.1	1.1	1.2	1.3	1.3	1.1	1.0	1.0	0.9	0.8	1.1	1.4	
43 53°19'37.4"	1.1	1.6	1.5	1.1	0.9	0.8	0.6	0.9	0.8	1.0	1.1	1.0	1.1	1.1	1.2	1.3	1.3	1.2	1.1	0.8	0.9	0.8	1.1	1.4	
49 53°19'37.6"	0.8	1.7	1.3	1.1	0.9	0.7	0.7	0.9	0.9	1.1	1.1	1.0	1.1	1.1	1.1	1.2	1.2	1.1	1.0	0.8	0.8	0.8	1.2	1.5	
55 53°19'37.8"	0.6	1.2	1.5	1.2	0.9	0.7	0.8	1.0	0.9	1.1	1.0	1.0	1.1	1.2	1.2	1.1	1.1	1.0	0.9	1.1	1.1	0.9	1.2	1.5	
62 53°19'38.0"	0.9	1.2	1.3	1.0	0.7	0.8	1.0	1.1	1.0	1.1	1.0	0.9	1.2	1.2	1.2	1.2	1.0	0.9	0.8	1.1	1.0	0.9	1.3	1.5	
68 53°19'38.2"	0.9	1.3	1.1	1.0	0.7	0.8	1.1	1.1	1.1	1.1	1.0	0.9	1.0	1.3	1.3	1.2	1.1	1.0	1.0	1.0	0.9	0.8	1.2	1.5	
74 53°19'38.4"	1.0	1.1	1.0	0.9	0.7	0.8	1.1	1.0	1.1	1.1	1.0	1.0	1.2	1.3	1.2	1.2	1.1	1.1	1.1	1.1	1.0	0.9	1.3	1.3	
80 53°19'38.6"	0.9	0.9	0.9	0.8	0.7	0.8	1.0	0.9	1.2	1.0	0.9	1.1	1.1	1.2	1.1	1.1	1.0	1.1	1.1	1.2	1.2	0.9	1.2	1.2	
86 53°19'38.8"	1.0	0.9	0.9	0.9	0.9	0.8	0.9	1.0	1.0	0.8	0.9	0.9	0.9	1.0	0.9	0.9	0.8	0.6	1.3	1.3	1.3	1.2	1.1	1.0	
92 53°19'39.0"	1.0	1.0	1.0	1.0	0.9	0.9	0.8	0.9	0.9	0.9	0.9	0.9	0.8	0.7	0.6	0.7	0.6	0.7	1.1	1.4	1.3	1.1	1.0	0.9	

* Shaded boxes refer to the reported depth soundings which closely overlapped (± 2 m GPS) from both the 1985 and 1993 surveys.

APPENDIX XI.

Table A11.1. Dry weight, wet weight, water content, wet sediment density (*i.e.* saturated unit weight), porosity (ϕ) and sediment diffusion coefficients (D_s) of the Holyhead sediments collected from the core barrels using the syringes with the cut-off luer end (approx. 5 cm³).

Depth (cm)	Total Wt. (g)	Dry Wt. (g)	Pore Water Volume (cm ³)	Wet Sediment Density (g cm ⁻³)	Porosity ϕ	D_s * (cm s ⁻¹)
Core A						
18	7.75	4.26	3.49	1.55	0.70	7.87 x 10 ⁻⁶
38	8.18	4.38	3.80	1.64	0.76	8.72 x 10 ⁻⁶
58	8.50	5.21	3.29	1.70	0.66	7.40 x 10 ⁻⁶
78	8.80	5.15	3.65	1.76	0.73	8.29 x 10 ⁻⁶
98	6.95	3.5	3.45	1.39	0.69	7.77 x 10 ⁻⁶
118	8.10	4.81	3.29	1.62	0.66	7.40 x 10 ⁻⁶
138	7.70	4.37	3.33	1.54	0.67	7.49 x 10 ⁻⁶
158	7.40	4.35	3.05	1.48	0.61	6.91 x 10 ⁻⁶
Core B						
10	8.21	4.33	3.88	1.64	0.78	8.97 x 10 ⁻⁶
30	8.67	4.87	3.80	1.73	0.76	8.72 x 10 ⁻⁶
50	8.90	5.09	3.81	1.78	0.76	8.75 x 10 ⁻⁶
70	8.73	5.16	3.57	1.75	0.71	8.07 x 10 ⁻⁶
90	8.91	4.89	4.02	1.78	0.80	9.45 x 10 ⁻⁶
110	8.07	4.27	3.80	1.61	0.76	8.72 x 10 ⁻⁶
130	8.61	4.89	3.72	1.72	0.74	8.48 x 10 ⁻⁶
150	8.14	4.47	3.67	1.63	0.73	8.34 x 10 ⁻⁶
Core C						
10	8.79	4.51	4.28	1.76	0.86	1.05 x 10 ⁻⁵
30	8.45	4.27	4.18	1.69	0.84	1.01 x 10 ⁻⁵
50	8.63	4.46	4.17	1.73	0.83	1.00 x 10 ⁻⁵
70	8.99	4.56	4.43	1.80	0.89	1.12 x 10 ⁻⁵
90	8.16	3.94	4.22	1.63	0.84	1.02 x 10 ⁻⁵
110	7.63	3.36	4.27	1.53	0.85	1.04 x 10 ⁻⁵
130	7.90	4.30	3.60	1.58	0.72	8.15 x 10 ⁻⁶
150	8.29	4.67	3.62	1.66	0.72	8.21 x 10 ⁻⁶
170	8.28	4.61	3.67	1.66	0.73	8.34 x 10 ⁻⁶
190	8.75	5.16	3.59	1.75	0.72	8.13 x 10 ⁻⁶
Core D						
6	9.02	4.56	4.46	1.80	0.89	1.13 x 10 ⁻⁵
26	8.91	4.6	4.31	1.78	0.86	1.06 x 10 ⁻⁵
46	9.20	4.81	4.39	1.84	0.88	1.10 x 10 ⁻⁵
66	8.11	3.78	4.33	1.62	0.87	1.07 x 10 ⁻⁵
86	8.76	4.59	4.17	1.75	0.83	1.00 x 10 ⁻⁵
106	9.51	5.68	3.83	1.90	0.77	8.81 x 10 ⁻⁶
126	9.37	5.73	3.64	1.87	0.73	8.26 x 10 ⁻⁶
146	8.43	5.31	3.12	1.69	0.62	7.05 x 10 ⁻⁶
Mean	8.44	4.64	3.84	1.69	0.76	8.95 x 10 ⁻⁶
SD	0.56	0.53	0.39	0.11	0.08	1.26 x 10 ⁻⁶

* $D_s = (D_o / (1 + n(1 + \phi)))$ where $n=3$, D_o = seawater diffusion coefficient at 15°C (Iversen & Blackburn 1981)

APPENDIX XI.

Table A11.2. Found and modeled methane concentrations for the Holyhead Harbour sediment cores. Showing the modeled effect of diffusion and depositional advection for a range of sedimentation rates (cm y⁻¹) on the methane profile above the point of methane saturation as well as the additional effect of first order methane removal rate terms, k1 (units = s⁻¹).

Depth (cm)	Measured Methane (mM)	Diffusion / Depositional Advection Modeled Data - Methane (mM)				Diffusion/Advection/Consumption Modeled Data - Methane (mM)		
		13.8 cm y ⁻¹	30 cm y ⁻¹	9.2 cm y ⁻¹	17.2 cm y ⁻¹	13.8 cm y ⁻¹ k1=2.5e-7	13.8 cm y ⁻¹ k1=8e-9	17.2 cm y ⁻¹ k1=2.5e-7
Holyhead Core A								
0		0.000	0.000	0.000	0.000	0.000	0.000	0.000
12		0.196	0.025	0.298	0.125	0.001	0.143	0.001
18	0.16	0.353	0.059	0.505	0.238	0.005	0.264	0.004
24		0.568	0.130	0.764	0.410	0.016	0.443	0.013
30		0.875	0.285	1.096	0.684	0.059	0.718	0.049
36		1.331	0.654	1.535	1.139	0.222	1.164	0.199
38	0.02	1.504	0.833	1.694	1.321	0.335	1.343	0.306
42		1.884	1.295	2.031	1.734	0.731	1.751	0.691
48.7	2.7	2.700	2.700	2.700	2.700	2.700	2.700	2.700
58	5.0							
Holyhead Core B								
0		0.000	0.000	0.000	0.000	0.000	0.000	0.000
6		0.190	0.049	0.251	0.141	0.006	0.159	0.006
10	0.14	0.350	0.104	0.448	0.269	0.015	0.295	0.015
12		0.442	0.142	0.556	0.345	0.022	0.375	0.022
18		0.776	0.317	0.928	0.638	0.072	0.675	0.072
24		1.216	0.647	1.379	1.060	0.227	1.096	0.227
30	0.01	1.787	1.247	1.919	1.652	0.702	1.680	0.702
32		2.023	1.562	2.129	1.912	1.036	1.934	1.036
36.9	2.7	2.700	2.700	2.700	2.700	2.700	2.700	2.700
50	7.8							
Holyhead Core C								
0		0.000	0.000	0.000	0.000	0.000	0.000	0.000
6		0.042	0.003	0.074	0.023	0.000	0.024	0.000
10	0.1	0.076	0.005	0.130	0.042	0.000	0.045	0.000
12		0.095	0.007	0.161	0.054	0.000	0.056	0.000
18		0.163	0.015	0.264	0.096	0.000	0.098	0.000
24		0.249	0.028	0.386	0.153	0.000	0.154	0.000
30	0.1	0.338	0.044	0.512	0.215	0.001	0.216	0.001
36		0.473	0.079	0.679	0.318	0.003	0.316	0.003
42		0.645	0.141	0.878	0.459	0.010	0.455	0.010
48		0.865	0.250	1.115	0.655	0.029	0.647	0.029
50	0.08	0.944	0.296	1.197	0.728	0.041	0.719	0.041
54		1.140	0.434	1.391	0.918	0.085	0.907	0.085
60		1.517	0.788	1.736	1.309	0.256	1.294	0.256
66		2.008	1.433	2.152	1.861	0.779	1.843	0.779
70	0.76	2.382	2.060	2.454	2.306	1.572	2.293	1.572
72		2.581	2.443	2.610	2.549	2.204	2.544	2.204
73.22	2.70	2.700	2.700	2.700	2.700	2.700	2.700	2.700
90.0	12.9							
Holyhead Core D								
0		0.000	0.000	0.000	0.000	0.000	0.000	0.000
6	0.01	0.066	0.007	0.103	0.041	0.000	0.043	0.000
12		0.148	0.019	0.223	0.095	0.000	0.098	0.000
18		0.250	0.039	0.363	0.167	0.001	0.170	0.001
24		0.363	0.064	0.513	0.248	0.002	0.250	0.002
26	0.01	0.398	0.072	0.561	0.273	0.003	0.275	0.003
30		0.504	0.106	0.688	0.358	0.006	0.358	0.006
36		0.697	0.187	0.908	0.522	0.016	0.519	0.016
42		0.943	0.325	1.168	0.746	0.046	0.738	0.046
46	0.02	1.168	0.499	1.386	0.968	0.098	0.954	0.098
48		1.280	0.595	1.493	1.081	0.138	1.065	0.138
54		1.671	1.005	1.851	1.493	0.386	1.475	0.386
60		2.162	1.696	2.271	2.048	1.077	2.035	1.077
65.4	2.7	2.700	2.700	2.700	2.700	2.700	2.700	2.700
66	2.8							